TEHNIČKI GLASNIK

TECHNICAL JOURNAL

TEHNIČKI GLASNIK / TECHNICAL JOURNAL – GODIŠTE / VOLUME 18 – SPECIJALNI BROJ / SPECIAL ISSUE SI1

PROSINAC 2024 / DECEMBER 2024 – STRANICA / PAGES 1-120

/

SVEUČILIŠTE SJEVER / UNIVERSITY NORTH – CROATIA – EUROPE

ISSN 1846-6168 (PRINT) / ISSN 1848-5588 (ONLINE)

ISSN 1846-6168 (Print) ISSN 1848-5588 (Online)

TEHNIČKI GLASNIK - TECHNICAL JOURNAL

Scientific-professional journal of University North

Volume 18 Special Issue si1
Varaždin, December 2024 Pages 1-120

Editorial Office:
Sveučilište Sjever / University North – Tehnički glasnik / Technical journal
Sveučilišni centar Varaždin / University Center Varaždin
Jurja Križanića 31b, 42000 Varaždin, Croatia
Tel. ++385 42 493 338, Fax.++385 42 493 336
E-mail: tehnickiglasnik@unin.hr
https://tehnickiglasnik.unin.hr
https://www.unin.hr/djelatnost/izdavastvo/tehnicki-glasnik/
https://hrcak.srce.hr/tehnickiglasnik

Founder and Publisher:
Sveučilište Sjever / University North

Print:
Centar za digitalno nakladništvo, Sveučilište Sjever

All manuscripts published in journal have been reviewed.
Manuscripts are not returned.

The journal is free of charge and four issues per year are published
(In March, June, September and December)
Circulation: 100 copies

Journal is indexed and abstracted in:
Web of Science Core Collection (Emerging Sources Citation Index - ESCI), Scopus, EBSCOhost Academic Search Complete, EBSCOhost – One Belt, One Road Reference Source Product, ERIH PLUS, CITEFACTOR – Academic Scientific Journals, DOAJ – Directory of Open Access Journals, Hrčak – Portal znanstvenih časopisa RH

Registration of journal:
The journal "Tehnički glasnik" is listed in the HGK Register on the issuance and distribution of printed editions on the 18th October 2007 under number 825.

Preparation ended:	Published (online):	Published (print):
November 20, 2024	November 25, 2024	December 30, 2024

ISSN 1846-6168 (Print), ISSN 1848-5588 (Online)
https://doi.org/10.31803/tj_18_2024_si1_preface_III-III

PREFACE

This Special Issue features twelve articles presented during the COBGI24 workshop (https://figcom3-ws-croatia2024.hgd1952.hr/), which focused on the challenges and opportunities in BIM and GIS integration. The event took place in Varaždin, Croatia, from June 18 to June 21, 2024. Organized by the Department of Geodesy and Geomatics at University North in collaboration with The Croatian Geodetic Society (https://www.hgd1952.hr/), the workshop was conducted under the auspices of the FIG (International Federation of Surveyors) Commission 3 (https://www.fig.net/organisation/comm/3/) and the BIRGIT Project (https://birgitproject.eu/).

The workshop served as a platform for participants to share and discuss innovative use cases and cutting-edge technologies related to BIM-GIS integration. Attendees included representatives from academia, industry, and national organisations worldwide, featuring distinguished keynote speakers, exhibitions, and presentations of advanced research and development. COBGI24 proved to be a productive venue for fostering advancements in technology, practice, and education, while facilitating new collaborations.

The focus of the COBGI 2024 workshop was on the utilization, analysis, and integration of 2D/3D digital modeling to enhance the effective and scalable management of built environments. Specifically, it addressed the challenges and opportunities associated with the integration of Building Information Modeling (BIM) and Geographic Information Systems (GIS). The workshop provided a forum for discussing the latest challenges and opportunities in BIM-GIS integration across various applications and services.

Participants had the opportunity to showcase recent research, developments, technologies, and policies, while also identifying emerging tools, trends, and services. Key topics covered during the workshop included:

- Geospatial data and geo-analytics
- Smart cities, digital twins, GIS, BIM, and SIM
- Indoor and outdoor mapping and navigation
- 3D modeling, analysis, and visualization, including VR and AR
- Geospatial planning, policies, and standards
- 3D data formats, standards, and interoperability.

The articles showcased in the COBGI24 workshop, and featured in this special edition, include:

- Prioritising Street Shade Intensification to Support Pedestrian Accessibility to Public Transport: A Data-driven Approach
- Assessment and Zoning of Areas by Risk Level of Snow Avalanches in Sharr Mountains
- Assessment and the Future Development of the Zagreb 3D City Model
- Developing of a Digital Twin for Urban Planning in an International Context
- Assessment of Solar Photovoltaic Potential of Building Rooftops Based on Multicriteria Spatial Analysis
- Navigating Urban Space: Unveiling Patterns in Walking Routes through Space Syntax in Kypseli Neighborhood (Athens)
- Selection of an Appropriate Extrinsic Camera Calibration Method for Handheld Mobile Mapping Systems
- Influence of 3D Barriers on Walkability for the Elderly in a German City
- BIM-GIS Integration for Interactive, Open and Low-Cost 3D Land Use Registration and Urban Neighbourhood Management
- Challenges and Opportunities for BIM-GIS Integration – BIRGIT Case Study
- Analyzing Depth Uncertainty of Near-Shore Bathymetric Survey Conducted by Single-Beam Echo Sounder
- Harnessing Remote Sensing Technologies for Successful Large-Scale Projects

The Special Issue is accommodating extra articles since the regular issues for 2024 have reached their limit, preventing the publication of articles accepted in that year. The articles selected at the COBGI24 workshop are not associated with these publications, as they explore different topics.

Dr. Danko Markovinović, Associate Professor
Guest Editor

Dr. Vlado Cetl, Full Professor
Guest Editor

Dr. Milan Kljajin, Full Professor with Tenure
Editor-in-Chief

XIX. International Urban Planning and Architectural Design for Sustainable Development Conference

August 07-08, 2025

Vancouver, Canada

XIX. International Urban Planning and Architectural Design for Sustainable Development is the premier interdisciplinary forum for the presentation of new advances and research results in the fields of Urban and Civil Engineering.

Today more than ever before it is extremely important to stay abreast of the changing landscapes of the Urban and Civil Engineering world. The multidisciplinary focus of this event aims to bring together presenters and attendees from different fields with expertise in various areas of Urban and Civil Engineering, providing an excellent opportunity to participate in the international exchange of ideas, current strategies, concepts and best practices, collaborations, and cooperation, offering a broader perspective and more enriching experience.
The program includes time allocated for networking, peer-to-peer discussions, and exploring the host city.

We invite the participation of leading academic scientists, researchers and scholars in the domain of interest from around the world to submit original research contributions relating to all aspects of:

- Urban Planning and Architectural Design for Sustainable Development
- Planning Approaches for Sustainable Development
- City planning, Development and management
- Landscape planning and design
- Urban design and urban infrastructure
- Accessibility in cityscape and development issues
- Waterfront developments
- Energy and the environment
- Community Participation
- Planning for risk and natural hazards
- Sustainable public transport systems
- Cultural development and awareness
- Balancing Heritage Conservation and Development
- Planning for public health
- Climate change and ecological planning
- Building Physics and Technology
- Architecture and Urban Design Education
- Sustainable design and configuration of sustainable cities
- Forms and aesthetics in architectural designs
- Sustainability and architecture
- Architectural design and urban design

https://waset.org/urban-planning-and-architectural-design-for-sustainable-development-conference-in-august-2025-in-vancouver?utm_source=conferenceindex&utm_medium=referral&utm_campaign=listing

ISSN 1846-6168 (Print), ISSN 1848-5588 (Online)
https://doi.org/10.31803/tg-20240828211854

Original scientific paper
Received: 2024-08-28, Accepted: 2024-10-25

Prioritising Street Shade Intensification to Support Pedestrian Accessibility to Public Transport: A Data-driven Approach

Or Aleksandrowicz*, Daniel Rosenberg, David Pearlmutter

Abstract: This article presents a new methodology for urban-scale prioritisation of shade-inducing operations by quantifying the gap between the use intensity of public transport stops and the solar exposure of the streets leading to them. By cross-referencing a high-resolution dataset of travel ticket validation with shade maps quantifying the average street shade provision, we were able to calculate a new metric, the Shading Priority Index, which quantifies the relative importance of adding street shading in each statistical zone. The method was applied to Tel Aviv-Yafo, a major city in Israel. The calculation of the **Shading Priority Index** at the scale of a statistical zone in the city made it possible to expose significant differences between each zone, both in passenger quantities and outdoor shading conditions in the routes leading to transportation stops, and to identify key weak points in the climate-related accessibility of pedestrians to public transport.

Keywords: big-data analysis; climatic urban policy; shade maps; urban human behaviour; urban microclimate

1 INTRODUCTION

Accessible and readily available public transport is perceived today as an essential component in securing urban quality of life and as one of the central goals of any urban sustainability vision. However, accessibility to public transport is often presented as depending mainly on the walking distance between users' starting points (e.g., places of residence or work) and transportation stops, alongside the availability of convenient physical infrastructure for walking [1-4]. This approach, while focusing on the network properties of public transport infrastructure and the morphological aspects of urban design, does not consider the need to secure comfortable thermal conditions along the footpaths leading to the stops.

Although several studies from recent years have examined the relationship between thermal comfort at bus stops and their use, these studies were limited to thermal comfort at the stops themselves and did not address the conditions along the walking routes leading to them [5-7]. In Israel and other hot-climate countries, it is known that the lack of outdoor shade can result in severe heat stress among pedestrians, as studies from Tel Aviv-Yafo [8] and Tempe, AZ [9] demonstrated. It is, therefore, expected that access routes to transportation stops that are more exposed to the sun would reduce the willingness to use public transport. A recent study from Boston, MA [10] has also suggested, based on a large dataset of pedestrian routes, that heat stress significantly affects the "perceived walking distance" and can thus negatively limit access to common points of interest like public transport destinations.

The evidence found in studies on urban climate indicates that the lack of "climatic accessibility" to public transport, i.e. the provision of comfortable climatic conditions along the routes to public transport stations and stops, should also be considered an impediment to public transport travel. Yet, until now, little attention has been given to methods that will enable us to highlight urban areas where the climatic accessibility to public transport is poor and prioritise actions for improving it based on standardised indices. This study was intended to provide an initial response to this gap by developing a method for prioritising improvements to the climatic accessibility of transportation stops based on urban-scale, high-resolution quantitative data.

2 METHODS

The goal of this study was to develop a metric that would facilitate the identification of the most extreme climatic vulnerabilities in a city's network of transportation stops. This metric uses large datasets of various inputs (geographic, climatic, and functional) that enabled us to quantify the intensity of use of urban transportation stops alongside the degree of exposure to solar radiation of the street network leading to them. The study focused on the city of Tel Aviv-Yafo, a city of about 475,000 residents (2023 figures, Israel's Central Bureau of Statistics) covering an area of 52 km^2 and the centre of Israel's main population conurbation (Gush Dan). The city's morphological complexity and its role as a central economic hub enabled us to calculate the metric for a variety of urban contexts that differ from each other in the spatial distribution of the transportation stops, the intensity of their use, the structure of the urban street network, and the level of exposure of the street network to solar radiation.

The study was based on the analysis and cross-referencing of two main databases: a national database of travel ticket validation at transportation stops that is maintained by Israel's Ministry of Transport (https://data.gov.il/dataset/tikufim_station_2022) and a zone shade map of Tel Aviv-Yafo. We produced the shade map according to a unique method we developed previously [11] by processing digital surface models and tree canopy mapping provided by the Survey of Israel. Using these two datasets, we calculated a new metric that quantified the importance of additional shading as a product of the average outdoor shading level of streets and the average daytime public transport passenger numbers in all the statistical areas of the city.

2.1 Travel Ticket Validation Dataset

Since 2022, Israel's Ministry of Transport has opened to the public a database containing data on public transport travel validation at every urban transportation stop in Israel. The source of the data is the online ticket validation system installed on all the public buses in Israel. The data is distributed as a table in a CSV format, in which the following fields are listed: unique stop ID number, stop name, period for which data was received, year, month number, and date number. For each day, the validation data is divided into seven unequal periods, allegedly representing peak and low times in the use of public transport, as follows: 00:00-03:59 ("night low"); 04:00-05:59 ("morning low"); 06:00-08:59 ("morning peak"); 09:00-11:59 ("daytime low 1"); 12:00-14:59 ("daytime low 2"); 15:00-18:59 ("evening peak"); and 19:00-23:59 ("evening low"). These somewhat rigid definitions do not represent the actual daily fluctuations in each city and were presumably adopted by the Ministry to establish a uniform common denominator for data from all over the country.

In this study, we used the complete ticket validation dataset for the year 2023, from which we extracted data from the stops located within the boundaries of Tel Aviv-Yafo. As part of the work process, we filtered out data from Fridays and Saturdays due to the partial public transport service on these days in Israel. Using the remaining data, we calculated **monthly and weekly averages of the total hourly number of passengers** in each city to examine daily and seasonal passenger trends. Since we wanted to develop an index relating to heat stress caused during the hot season's daytime hours, we further processed the data to calculate the **daytime average number of hourly passengers** in each statistical zone from 1 May to 31 August (four months, between 06:00-19:00). This metric makes it possible to assess and compare neighbourhood-level use of public transport during the hot season.

2.2 Urban Shade Maps

Urban shade maps are maps that depict the levels of outdoor shading conditions at a high resolution based on the calculation of a Shade Index (*SI*) that describes, on a scale from 0 to 1, the extent to which ground-level insolation is blocked during a typical summer day [11]. More specifically, the SI is based on calculating the **cumulative exposure** of the ground between 08:00 and 17:00 (daylight saving time) on 6 August, which is the middle day between the longest day of the year (21 June) and the autumn equinox (22 September) and represents the seasonal peak in local heat stress intensity. In that sense, the *SI* considers the variation in the intensity of global solar radiation throughout the day, comparing the blocked insolation at ground level at a certain location and the maximum insolation of an unobstructed horizontal surface at the same time and location. The higher the *SI* value, the higher the shading. This indicator considers shade produced by all elements in an urban environment: buildings, trees, and other shade-giving elements. It can be formulated as follows:

$$SI_{\mathrm{p}} = 1 - \left(\frac{Insolation_{\mathrm{p}}}{Insolation_{\mathrm{r}}} \right), \tag{1}$$

where SI_{p} is the Shade Index at a certain point, and $Insolation_{\mathrm{p}}$ and $Insolation_{\mathrm{r}}$ represent the intensity of incident solar radiation at that point and at an unobstructed reference point respectively. Roughly speaking, the level of SI can be evaluated as follows: below 0.1, acute shortage of shading; between 0.1 and 0.2, significant lack of shading; between 0.2 and 0.4, shading requires improvement; between 0.4 and 0.6, good shading; above 0.6, excellent shading.

For a high-resolution calculation of the SI in a city, we apply an enhanced process based on the insolation calculation module available in the Urban Multi-scale Environmental Predictor (UMEP) plugin [12] for QGIS. This tool uses high-resolution Digital Surface Model (DSM) and Digital Terrain Model (DTM) data to calculate horizontal insolation and requires the generation of separate DSMs for buildings and tree crowns. To extract the tree crown data from the input DSM, we used an urban crown contour mapping from 2022 that was produced by the Survey of Israel based on machine vision analysis of aerial photographs [13]. The input DSMs and DTM of Tel Aviv-Yafo that we used in this work were produced by the Survey of Israel in 2022.

To generate the shade maps, the input spatial data was processed at the resolution of 50 cm per pixel, resulting in a raw layer of SI values for each input pixel. Based on this layer, we then calculated an average SI value for the entire street area of each statistical zone in Tel Aviv-Yafo based on input land use vector layers provided by the municipality. The SI for each statistical area, therefore, represents the average level of shading throughout the entire street network contained within that statistical area. A city-scale shade map thus provides a good indication of the level of exposure to heat stress of public transport passengers during daylight hours in different parts of the city.

2.3 The Shading Priority Index

Based on the average hourly passengers and the SI values for the statistical zones, we calculated a Shading Priority Index (*SPI*) for each zone with the aim of using it to locate key areas in the city where concentrated activity is required to improve shading throughout their street network. This metric highlights areas where poor street shading conditions exist alongside a relatively high number of public transport users. A zone SPI (*SZ_SPI*) is calculated according to the following formula:

$$SZ\_SPI = \left(1 - SZ\_SI\right) \times \frac{SZ\_APh - APh_{\min}}{APh_{\max} - APh_{\min}}. \tag{2}$$

where *SZ_SI* is the zone's SI, *SZ_APh* is its average daytime hourly number of passengers (*APh*) during the hot season, $APh_{\max}$ is the highest *APh* among all statistical zones, and $APh_{\min}$ is the lowest. The *SZ_SPI* thus describes, on a scale of 0 to 1, the importance of improving the shading conditions in areas attracting a high number of public transport

passengers, with importance increasing as the value approaches 1.

3 RESULTS

The results were analysed in two stages: first, we calculated average hourly ticketing events at the city level, looking for general trends that could indicate whether the use of public transport is significant enough during all daytime hours. We assumed that if certain periods during the daytime show significantly low ridership, they may not be accounted for when prioritising shading actions. The second analysis stage consisted of calculating outdoor shade levels and the Shading Priority Index according to the abovementioned method and using it to map priority zones for increasing street shading.

3.1 Public Transport Passenger Trends

The city-scale analysis of the ticket validation dataset (Fig. 1) presents no significant seasonal changes in the quantities of public transport users throughout the year. However, a sharp decline in public transport rides occurred in October 2023, which can be attributed to the war that erupted in Israel on 7 October, resulting in a partial closure of workplaces and the education system. Additionally, in April and September, which are months of holidays and vacations in Israel, there was a slight decline in the weekly passenger averages. It can therefore be argued that the demand for public transport is more or less constant throughout the year, although there is a slight increase in the use of public transport during the hot season, starting in May. This hard demand is also apparent from the recurring daily pattern of passenger peaks and lows, which was similar throughout most of the year. In Tel Aviv-Yafo, the peak number of public transport passengers is between 15:00 and 19:00 and is relatively higher than in the other daily analysis periods. Nevertheless, it can be argued that passenger quantities were relatively high during all other daytime hours (06:00-15:00) when compared to the evening and night periods. This finding supported our decision to include all daytime hours (06:00-19:00) and not only the peak afternoon when calculating the Shading Priority Index since significant numbers of passengers still use public transport even outside the peak afternoon period.

3.2 Mapping Shade and Passenger Geographic Distribution

The Tel Aviv-Yafo zone shade map (Fig. 2) shows significant differences in street shading levels in different parts of the city. The dense street network in the city's historic centre is mostly well-shaded and generally provides very good climatic accessibility to transportation stops. At the same time, other central areas of the city suffer from a significant lack of shading, and this is especially evident in the area of the main central business district (CBD) along Begin Road, in the south-eastern parts of the city, as well as in the area of Tel Aviv University and the exhibition grounds ("Expo Tel Aviv").

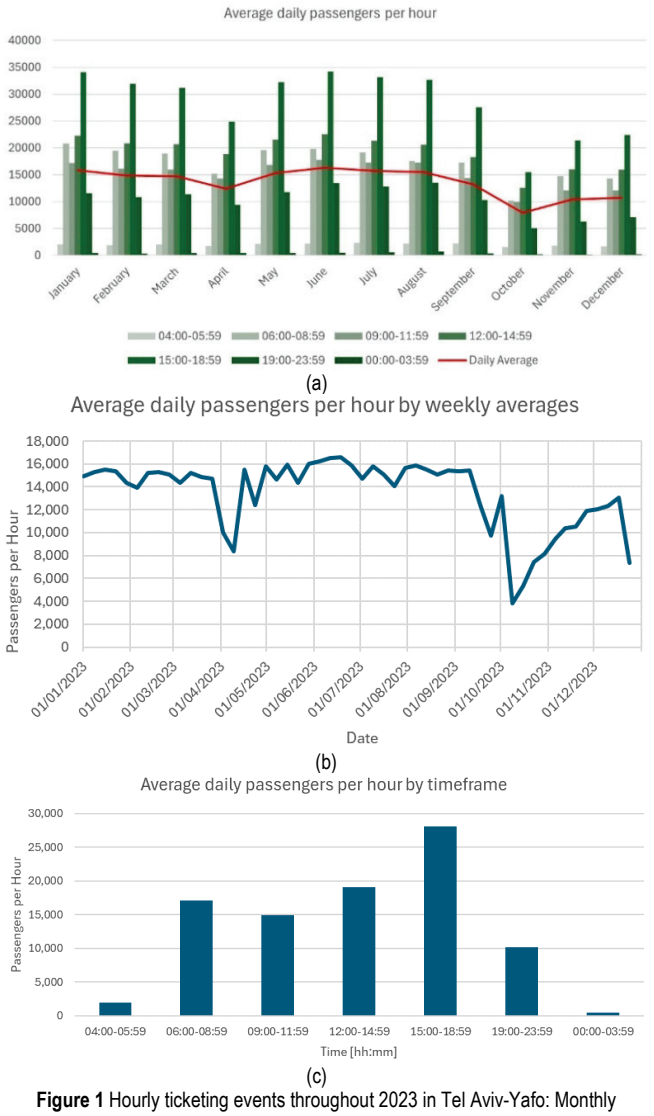

Figure 1 Hourly ticketing events throughout 2023 in Tel Aviv-Yafo: Monthly averages, divided into seven daily periods (a); weekly averages (b); and annual averages, divided into seven daily periods (c).

Mapping the average hourly number of daytime passengers in statistical zones (Fig. 3) reveals the effect of Tel Aviv-Yafo's four train stations on public transport use in the city. The average hourly passenger number during daytime from transportation stops in zones containing a train station was above 1,000, a number significantly higher than in most other parts of the city. These numbers do not include train rides but only urban bus rides. By comparing the shade and passenger mapping, it becomes evident that the zones attracting the highest numbers of passengers also suffer from low levels of street shading.

What seems to be visually apparent from comparing the shade and passenger maps becomes much more pronounced when calculating and mapping the *SPI* for each of the statistical zones (Fig. 4). The map highlights three distinct areas with the highest SPI, each consisting of several zones, and all of them located around the city's four train stations. Nevertheless, the index helps to differentiate between the shading priority of each of these areas, reflecting the centrality of the CBD area and the high need for shade in its

streets (*SPI* = 0.64 to 0.91) compared to the areas around the northern (*SPI* = 0.4) and southern (*SPI* = 0.38) train stations. The map also shows very low *SPI* values (less than 0.1) in most of the city's other statistical zones.

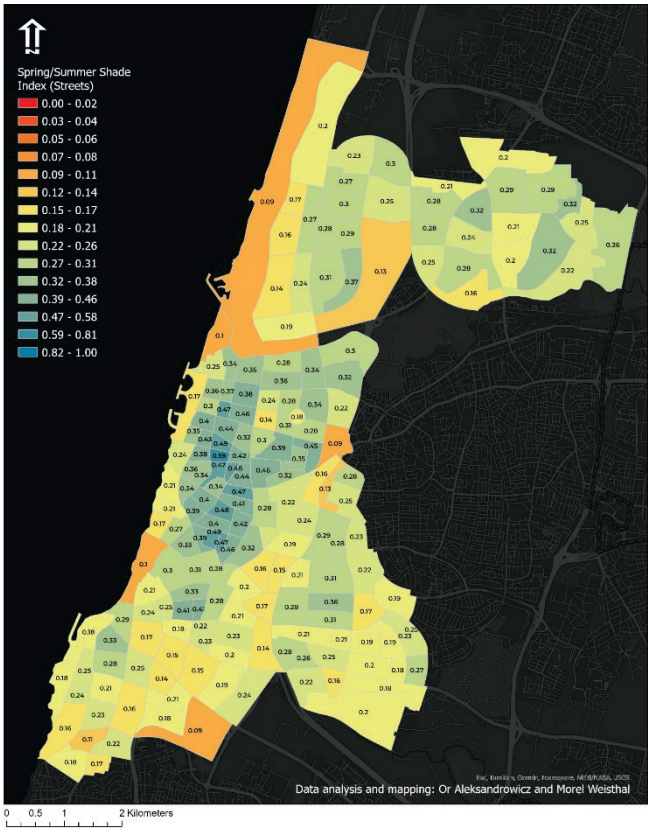

Figure 2 Shade map of statistical zones (average Shade Index in streets in each area) in Tel Aviv-Yafo, 2022. Data processing and mapping: Or Aleksandrowicz and Morel Weisthal.

4 DISCUSSION

Shade mapping based on a quantitative index like the SI can be regarded as the first step in allocating resources to outdoor shading improvements. However, in most cases, one cannot depend only on SI values to highlight urban areas where additional shading is particularly urgent and requires high prioritisation, especially in cities where many parts of the city suffer from a significant lack of shade. Prioritising shading actions usually depends on choices and preferences prevalent among the municipal planning and executive bodies, but these are rarely formulated based on quantitative evidence. Rather, they rely on accumulated experience and close familiarity with city life. However, data-driven prioritisation has stronger explanatory power, assuming we have the relevant data at hand, as well as the potential to direct actions in the most efficient and effective way.

The ticket validation dataset provided by the Ministry of Transport could significantly assist in adopting an evidence-based shading prioritisation policy since it reflects how certain populations use urban space. In the context of public transport, some of these populations are usually the most vulnerable to heat stress (children, the elderly) and, therefore, need closer attention with respect to additional shade provision. However, beyond that, it should be recognised that less vulnerable populations also use public transport daily and that policies which serve to increase their numbers can reduce the use of private vehicles in cities. Therefore, prioritising shading on the way to transportation stations is not only important for reducing exposure to heat stress and improving walkability but can also be seen as a complementary planning measure to encourage the transition to public transport and to pursue benefits ranging from improved health and safety to long-term environmental sustainability.

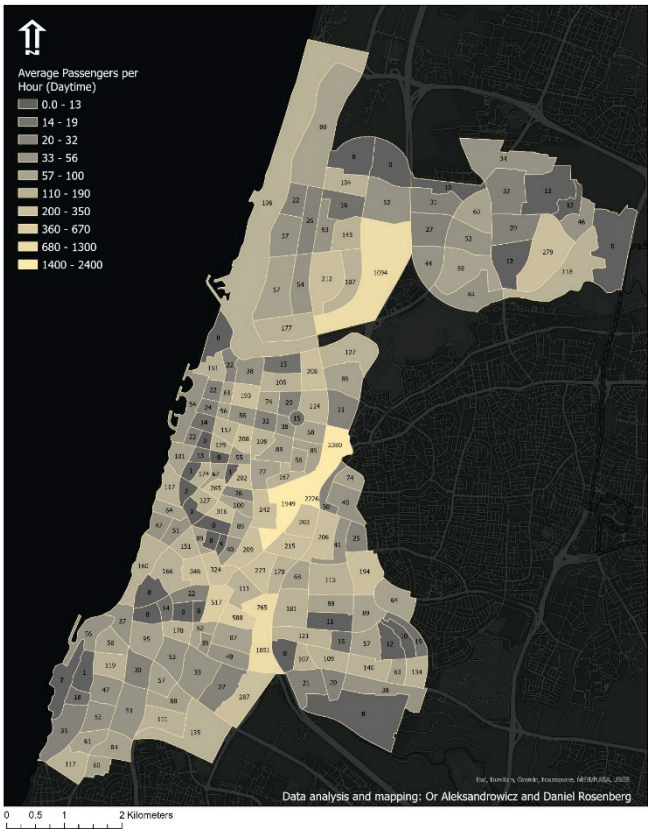

Figure 3 Map showing the average number of hourly daytime passengers from May to August in each statistical zone in Tel Aviv-Yafo (2023 data).

In this work, we proposed an index for prioritising shading operations that consider the number of passengers passing through the city's transportation stops alongside the degree of shading in the streets. In examining the mapping we produced, it is evident that it is possible to use this index to pinpoint a small number of areas in the city to which high priority should be given in shading operations. In this respect, the cross-referencing between mapping outdoor shade and calculating the average number of public transport passengers helps to distinguish between different degrees of importance that should be given to shading different parts of the city and to first direct efforts to areas where they are in the utmost need.

Some prioritisation of shading operations is always necessary since municipalities cannot simultaneously improve the shading situation in all parts of the city. A quantitative index calculated for prioritisation can only be effective when it helps highlight a relatively small number of

intervention sites. In this respect, the Shading Priority Index that we present here is up to the task because it highlights a relatively small number of areas for action. At the same time, in Tel Aviv-Yafo, the concentration of exceptionally high passenger rates in a small number of areas that are also poorly shaded makes the distinctions revealed by applying the SPI more clear-cut than they would be in cities with a lesser confluence of these two factors.

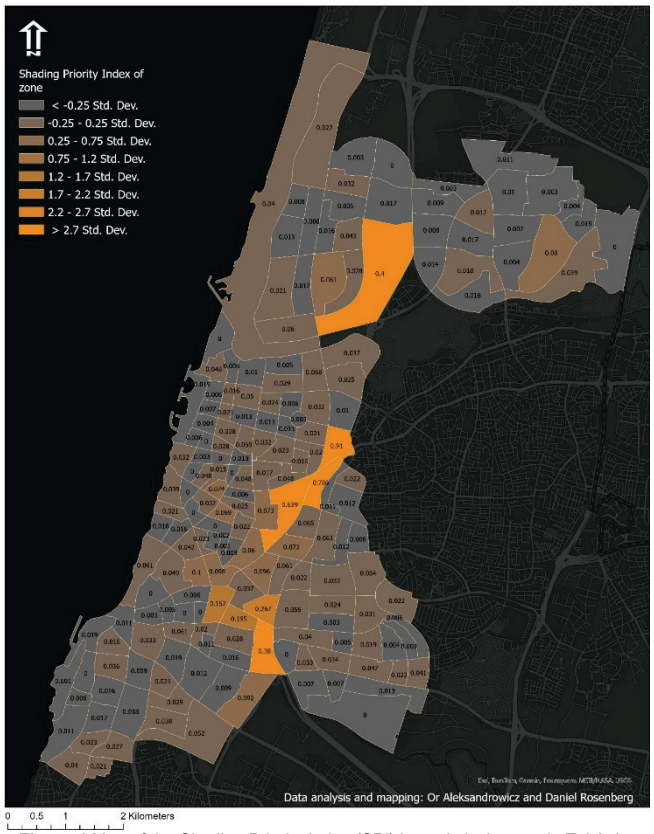

Figure 4 Map of the Shading Priority Index (SPI) in statistical zones in Tel Aviv-Yafo. The three zones with the highest SPI (visible in orange) are adjacent to the city's four main train stations: University Station in the north, Central and Hashalom Stations in the centre, and Hahagana Station in the south.

5 CONCLUSION

This study introduces a method and metrics for quantitatively assessing outdoor shading in streets and prioritising actions to improve shading conditions while considering the geographic distribution of public transport passenger flows during the hot season. These metrics make it possible to conduct a broad assessment of the degree of climatic accessibility of public transport in a city. The proposed Shade Priority Index makes it possible to identify a city's climatic vulnerabilities in public transport access while highlighting the need for a granular level of analysis and mapping to extract insights on the climatic management of urban spaces.

The calculation of the new metric presented in this study combines the analysis of two types of public datasets: a high-resolution, three-dimensional geographic mapping of the urban area from which urban shade maps can be generated and high-resolution ticket validation data at transportation stops. From the ticket validation dataset, it was possible to learn, on the one hand, about substantial differences in passenger numbers during peak and low times and, on the other hand, to conclude that most trips on urban public transport take place throughout the daytime, even during the hot season. This conclusion emphasises the need to secure shading along pedestrian routes to transportation stops.

The mapping we produced during the study also shows that the method we present here can be applied relatively easily in other cities and urban areas where coordinated shading operations are required. Widespread implementation of this method in other cities may also enable decision-makers and planners to identify recurring vulnerabilities in the climatic accessibility to public transport and to conduct a comparative examination of its levels between cities. Cross-referenced with spatial socioeconomic indicators, the index developed in this study may also help expose gaps in climatic accessibility to public transport that particularly affect the access of disadvantaged populations to this public resource.

Acknowledgement

This study was financially supported by the Environment and Sustainability Research Center at The Open University of Israel.

6 REFERENCES

[1] Alshalalfah, B. W. & Shalaby, A. S. (2007). Case Study: Relationship of Walk Access Distance to Transit with Service, Travel, and Personal Characteristics. *Journal of Urban Planning and Development, 133*(2), 114-118. https://doi.org/10.1061/(ASCE)0733-9488(2007)133:2(114)

[2] Shaaban, K., Siam, A., Badran, A. & Shamiyah, M. (2018). A simple method to assess walkability around metro stations. *International Journal of Sustainable Society, 10*(1), 1. https://doi.org/10.1504/IJSSOC.2018.092651

[3] Sukor, N. S. A. & Fisal, S. F. M. (2020). Safety, Connectivity, and Comfortability as Improvement Indicators of Walkability to the Bus Stops in Penang Island. *Engineering, Technology & Applied Science Research, 10*(6), 6450-6455. https://doi.org/10.48084/etasr.3849

[4] Taplin, J. H. & Sun, Y. (2020). Optimizing bus stop locations for walking access: Stops-first design of a feeder route to enhance a residential plan. *Environment and Planning B: Urban Analytics and City Science, 47*(7), 1237-1259. https://doi.org/10.1177/2399808318824108

[5] Dzyuban, Y., Hondula, D. M., Coseo, P. J. & Redman, C. L. (2022). Public transit infrastructure and heat perceptions in hot and dry climates. *International Journal of Biometeorology, 66*(2), 345-356. https://doi.org/10.1007/s00484-021-02074-4

[6] Electricwala, F. & Kumar, R. (2016). Impact of green shading on urban bus stop structure. *Proceedings of the 2nd International Conference on Computational Intelligence and Communication Technology, CICT 2016*, 615-622. https://doi.org/10.1109/CICT.2016.128

[7] Lanza, K. & Durand, C. P. (2021). Heat-moderating effects of bus stop shelters and tree shade on public transport ridership. *International Journal of Environmental Research and Public Health, 18*(2), 1-15. https://doi.org/10.3390/ijerph18020463

[8] Aleksandrowicz, O. & Pearlmutter, D. (2023). The significance of shade provision in reducing street-level summer heat stress

in a hot Mediterranean climate. *Landscape and Urban Planning, 229*, 104588. https://doi.org/10.1016/j.landurbplan.2022.104588

[9] Middel, A., Alkhaled, S., Schneider, F. A., Hagen, Bj. B. & Coseo, P. (2021). 50 grades of shade. *Bulletin of the American Meteorological Society, 102*(9), 1-35. https://doi.org/10.1175/BAMS-D-20-0193.1

[10] Basu, R., Colaninno, N., Alhassan, A., & Sevtsuk, A. (2024). Hot and bothered: Exploring the effect of heat on pedestrian route choice behavior and accessibility. *Cities*, 155, 105435. https://doi.org/10.1016/j.cities.2024.105435

[11] Aleksandrowicz, O., Zur, S., Lebendiger, Y. & Lerman, Y. (2020). Shade maps for prioritizing municipal microclimatic action in hot climates: Learning from Tel Aviv-Yafo. *Sustainable Cities and Society, 53*, 101931. https://doi.org/10.1016/j.scs.2019.101931

[12] Lindberg, F et al. (2018). Urban Multi-scale Environmental Predictor (UMEP): An integrated tool for city-based climate services. *Environmental Modelling & Software, 99*, 70-87. https://doi.org/10.1016/j.envsoft.2017.09.020

[13] Shnaidman, A., Aleksandrowicz, O., Renn-poni, D., Hoze, M. & Weisthal, M. (2023). Geo data-based policymaking: National Tree Canopy Cover Example. *FIG Working Week 2023*.

Authors' contacts:

Or Aleksandrowicz, Assistant Professor
(Corresponding author)
Technion – Israel Institute of Technology,
Technion City, Haifa 3200003, Israel
oraleks@technion.ac.il

Daniel Rosenberg, Research Fellow
Technion – Israel Institute of Technology,
Carmel Haifa 293982, Israel

David Pearlmutter, Professor,
Ben-Gurion University of the Negev,
1 Ben Gurion Blvd., Be'er Sheva 8443944, Israel

ISSN 1846-6168 (Print), ISSN 1848-5588 (Online)
https://doi.org/10.31803/tg-20240909221359

Original scientific paper
Received: 2024-09-09, Accepted: 2024-11-12

Assessment and Zoning of Areas by Risk Level of Snow Avalanches in Sharr Mountains

Bashkim Idrizi, Fitore Bajrami Lubishtani*, Elone Zeqiri

Abstract: In the past decades, snow avalanches on Shar mountain have occurred continuously, which in certain places have led to undesirable consequences. The assessment and zoning of the areas with a level of risk in the case of Shar Mountain was carried out by applying MDA-AHP and Fuzzy Logic methods, while the analysis of the accuracy of the final obtained results were performed by applying the ROC method. The study area was classified in five categories, as areas with very low ($Z = 0$), low ($0 < Z < 0.2$), moderate ($0.2 < Z < 0.5$), high ($0.5 < Z < 0.7$), and very high ($Z > 0.7$) avalanche release potential zones, recorded in a developed geodatabase, as well as shown in two maps with zoned areas by risk level of snow avalanches in Sharr Mountains area, that are intended to be used as an open geospatial database by all stakeholders.

Keywords: Analytic Hierarchy Process (AHP); Avalanche release potential; Fuzzy Logic (FL); Multicriteria Decision Analysis (MDA); Receiver Operating Characteristics method (ROC); Sharr Mountains; Snow avalanche

1 INTRODUCTION

Natural disasters are events that negatively affect human life and well-being. They are classified as natural as they are generally caused by climatic phenomena, biological factors, geomorphological processes, or spatial phenomena. Their cause can be directly or indirectly the man himself with his activities, but which are minor in relation to the above factors. Natural disasters are generally unpredictable, with varying intensities and effects, which can strike at any moment, causing significant loss of human, animal, and material life. The person in this situation can influence their warning and prevention if possible.

Avalanches are snow masses that are released and move from mountain slopes in the direction of falling terrain. Avalanches are a significant natural hazard that affects road infrastructure, settlements and threaten the lives of people and animals, mainly in mountainous terrain. They occur because of the interaction of the snow layer, meteorological conditions, and topographic surface. These three factors are referred to as the avalanche triangle [1]. The mean avalanche victims are 250 per year [2]. For the tendency of a snow avalanche, there must be favorable meteorological conditions and terrain which meets the characteristics for the release of a snow avalanche. With the interconnection of these factors which include the physical component (theory of friction and movement of bodies), comes the potential for the release of an avalanche. By defining a model of snow avalanche potential, geographic terrain zoning can be done. In environments with snow avalanche discharge potential, the most influential factor within the avalanche triangle is the terrain factor. Among the components that characterize the terrain factor are slope required for sliding, rugged terrain, ground cover, distances from ridges, presence of gorges, relief forms (concavity and convexity), slope orientation, altitude, and many factors others with lesser influence.

The extent of an avalanche is characterized by three spatial zones:

• Initial area – that represents the area in which the avalanche begins to detach from the body in which it is superimposed. If the avalanche is of the slab type, it initially creates the refractive line, which simultaneously forms the upper avalanche boundary line.

• Movement area - represents the area in which the avalanche develops the highest speed of movement, the route of which is mainly determined by the relief. The boundary can be limited or unlimited depending on the terrain, for example: if the avalanche moves along the gorges, then the boundary is easily defined, but if the avalanche moves along the open slopes, then the boundary is indefinable for longer periods and may change depending on the amount of snow, speed, current vegetation, and many other factors.

• Deposit area - represents the area in which the avalanche ends or is deposited, which are usually areas with a smaller slope where the terrain "opposes" the direction of movement of the avalanche.

A snow avalanche in its formation has three main components, which with the interconnection between them create favorable conditions for the initiation of a snow avalanche, and they are:

- Topographic component,
- Meteorological component, and
- Physical component.

The only parameter from the above which can be taken as immutable is the relief. We can take this as such from the broader point of view because even the relief can't be said to be immutable as we know that the relief undergoes constant changes, but which are not observed in the short term. However, for the analysis, we are dealing with, compared to other parameters that are constantly changing, but at different time intervals, the relief will be part of the static components and will be presented through the digital elevation model (DEM) integrated through DTA (Digital Terrain Analysis) in GIS software.

Determining meteorological conditions and their impact [3] on avalanches requires a statistical study covering a period of about 30 years, as well as a review of meteorological conditions of all avalanche activities from the past to the moment they occurred. If such statistical data exist, for each climatic factor can be defined the so-called "zero line", which means the most favorable conditions for

avalanches. In every winter season, after every snowfall, the climatic conditions can be identified and compared to the "zero line". After that, actions can be taken in different parts of the world with experiences in avalanches, such as closing roads which are high risk, snowfall in areas which are identified as areas with high snow avalanche potential or other actions depending on the need of that area.

2 MATERIALS AND METHODS

2.1 Study Area

For the study of snow avalanches in the framework of this paper, the area has been selected, the parameters of which have the potential for snow avalanches. The selected area is the geographical area of the Sharr Mountains. These mountains are located in Southwestern Europe, specifically in the south-southeast of the Republic of Kosovo, northwest of North Macedonia, and northeast of the Republic of Albania. This study area occupies an area of 1162 km^2 in the territory of the Republic of Kosova and 841 km^2 in the territory of the Republic of North Macedonia, while the whole the study area of Sharr Mountains is 2003 km^2.

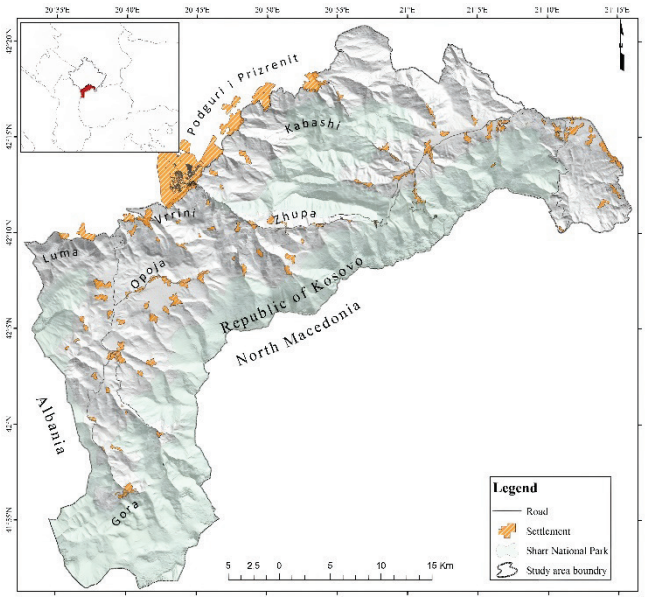

Figure 1 Map of the study area of Sharr Mountains in Kosova [4]

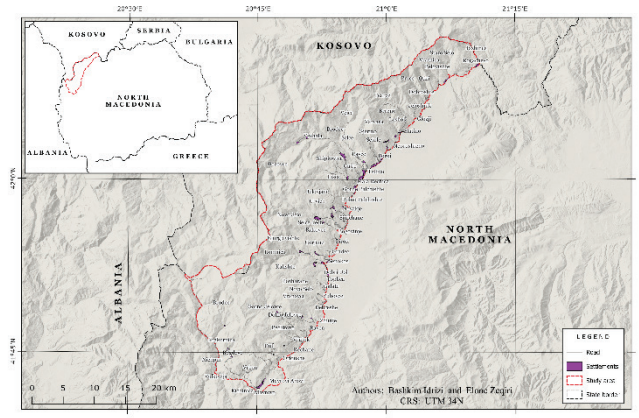

Figure 2 Map of the study area of Sharr Mountains in North Macedonia

Sharr Mountains in both side of border, in Kosovo and North Macedonia is already national park with special lows for its protection as natural heritage.

2.2 Topographic and Meteorological Conditions of Sharr Mountains

The altitude of the study area varies from 292 m in Kosovo side up to 2747 m in "Titov Vrv" highest point of Sharr Mountains in North Macedonia, which according to the classification of mountain by European Avalanche Warning Services – EAWS [5], Sharr Mountains are classified as high mountains, where the snow avalanches of all types can occur.

In the Kosovo side there are two meteorological stations, while in North Macedonia there are six meteorological stations of which one is in the center of area (in Popova Shapka / Kodra e diellit) and five are in the border between Sharr Mountain and the Pollog field.

Extreme recorded temperature value in the study area is –34 °C, the mean temperature in high areas with more than 1200 m is –3 °C, while the length of the period with low temperatures during winter season is up to 4 months. Sunny days in the study area range from 220 to 280 days, while winds reach speeds from 1 to 18 m/s with about 22% winds that comes from the northern direction.

The level of snow in mountainous areas reaches 1.6 m and 2 m in higher terrains, while the extreme recorded highest snow value is 3 m. The duration of maximal snowfall is 117 days.

The mean annual air humidity is 76%, in which the extremes range from 83% maximum in November and 64% minimum in August.

Such topographical and meteorological conditions are very suitable for generating a thick snow cover in the study area of Sharr Mountains, as very important precondition for snow avalanches.

2.3 Methods for Calculation of Potential Snow Avalanche Areas

2.3.1 Fuzzy Logic Method

During complex modeling, which are not defined according to a formula, and in which relations of diffuse categories prevail, due to large parameters number and the complex nature of the processing, a considerable degree of uncertainty expert decision-making contains. Such issues cannot be resolved through a classical approach. Zadeh on year 1965 [6] introduced a Fuzzy Logic methodology, in which the values in range from 0 to 1 reflect the degree of membership security. The process of transforming the initial input values on a scale of 0 to 1 is called the fuzzification process (μ).

$$\mu(C_{ij}) = \frac{FR_{ij} - Min(FR_{ij})}{Max(FR_{ij}) - Min(FR_{ij})} \cdot \left[Max\left(\mu(C_{ij})\right) - Min\left(\mu(C_{ij})\right) \right] + Min\left(\mu(C_{ij})\right) \quad (1)$$

where μ (C_{ij}) is the degree of class membership within the factor and *FR* is frequency of occurrence of the phenomenon.

2.3.2 Multicriteria Decision Analysis (MDA) - The Analytic Hierarchy Process (AHP)

The Analytic Hierarchy Process (AHP) is a multi-criteria decision-making approach that has been successfully implemented for a variety of decision-making situations and was introduced and developed by Thomas Saaty in 1980. It is the pairwise comparison method used for objective-related criteria. These pairwise comparisons are performed for all relevant factors within the analysis.

Estimates for each class of factors/criteria for spatial analysis of avalanches can be based on locations with avalanche activity as well as judgments of avalanche experts. After evaluating the classes for each factor, the weights for each factor are assigned hierarchically using the pairwise comparison matrix and the evaluation is done using the basic Saaty comparison scale ranging from 1 to 9. Value 1 expresses "equal importance" between a comparative pair and a value of 9 is given to those factors that are of much higher importance within the comparative factors.

$$CR = \frac{CI}{RI} \tag{2}$$

$$CI = \frac{\lambda_{\max} - N}{N - 1} \tag{3}$$

where: *CR* is consistency index, *RI* the common index of the AHP method, which has predefined values, but whose value depends on the size of the comparison matrix (Tab. 1), λ characteristic scalar value, and *N* the order of the matrix.

Table 1 Common Consistency Index [7]

N	1	2	3	4	5	6	7	8
RI	0	0	0.58	0.90	1.12	1.24	1.32	1.41
N	9	10	11	12	13	14	15	
RI	1.45	1.49	1.51	1.53	1.56	1.57	1.59	

In addition to the interrelated factors, the AHP method can be met with some strict criteria, for example in areas that are covered with dense forests, it is known that due to their existence in the same area there can be no snow avalanche potential and in these cases, we can operate with the elimination method through Boolean actions which strictly exclude these areas in the margin of areas with potential [8].

$$Z = \sum_{i=1}^{n} (w_i x_i) \prod c_j \tag{4}$$

2.4 Data for Determination of Avalanche Zones

Precise determination of avalanche zones for larger spatial areas is difficult to accomplish and therefore always tends to determine potential. It is divided into four phases, namely the input phase, the processing phase, the output phase, and the verification phase. The first phase is composed of input data, which are divided into two main parts, on the one hand, the data from the avalanche history, and on the other hand the data on the factors that are part of the second phase. In the second phase, all the important factors in defining the areas with avalanche a potential re determined. The third stage is obtaining results, and the last stage is verifying this result based on a comparative method.

Terrain Slope - Primary factor within the topographic component is the slope of the terrain. Theoretically, the release of an avalanche cannot begin without the presence of a terrain inclination angle, and according to Maggioni (2004) the areas with the potential to start an avalanche are those with a slope of 30°-60° [9].

Terrain orientation (aspect) and solar radiation - The orientation of the terrain, respectively the mountain slopes is directly related to the movement of winds and solar radiation. Knowing the geographical position of the study area, the positioning of the mountain slopes is a factor in the absorption of solar radiation from the earth's surface.

Topography is a key factor determining the spatial variability of irradiation. Latitude and longitude, slope and orientation of slopes, are elements that affect the amount of irradiation received in different places. Total solar irradiation can be determined based on direct sunlight on the surface, distorted radiation (due to obstructions such as clouds, smog, etc.), and reflected radiation (with albedo 0.9 for snow-covered surfaces), calculated with the formula:

$$\begin{aligned} {}_s g = {} & S_0 \tau^m \cos i + S_0 (0.271 - 0.294\tau^m) \sin\alpha \cdot \cos^2\left(\frac{\beta}{2}\right) + \\ & + r S_0 (0.271 - 0.706\tau^m) \sin\alpha \cdot \sin^2\left(\frac{\beta}{2}\right) \end{aligned} \tag{5}$$

where: ${}_s g$ is the total irradiation on sloping surface (Wm^{-2}), S_0 solar radiation (on certain days of the year), τ^m transmission of radiation from the atmosphere, i is the angle between the normal to the surface and the sunlight, a is the solar angle (solar altitude), and β is the terrain slope. Irradiation is calculated for the period of: beginning of February.

The relief altitude - The altitude factor as a geographical component has a great correlation with the meteorological factors because, with the increase of the relief altitude, the climatic conditions also change. The greater the amount of snow, the greater its deposition, which increases the possibility of avalanches, while the lower temperatures enable greater stability of the snow structure.

The relief concavity and convexity - The relief forms are very diverse where besides the canals, ridges, galleries, we also distinguish mainly rounded shapes in the form of valleys or hills. These shapes are otherwise called convex and concave. Within these two types, we distinguish many subtypes according to the transverse and longitudinal sides of the terrain. Transverse curvature is the degree of variability of terrain orientation along a contour lines, whereas longitudinal curvature is the degree of variability of terrain along a flow line. Gleason [11] and McClung [10] concluded

that avalanches are more common in initial areas with concave transverse curvature.

Mountain ridges - It is important to determine as they affect the movement of snow due to wind transport and its deposition behind the ridges. At the same time, the ridge plays the role of a shield from the solar radiation, as well as from the hot winds which hit the front part of the mountain. According to a study by Gauer [12] where measurements were made on both sides of the mountain ridge, it turned out that about 20-30% more snow was deposited on the side on which the ridge served as a shield against the wind than on the flat ground.

Land Cover - In general, avalanches can start on any slope with a certain inclination if a dense forest is not available to prevent the onset of the avalanche.

The terrain ruggedness - It plays an important role in the avalanche release potential, as terrains with greater ruggedness are obstacles or forces which counteract the pressure of the snow layer. The ruggedness of the terrain is affected by the layers of snow as well as its amount. If a terrain has a certain ruggedness, after the snowfall and the creation of a snow bed, that terrain will no longer have the same ruggedness after the formation of this snow bed. The topographic ruggedness index (*TRI*) express the amount of height difference between neighboring cells of a DEM and is determined based on the digital relief model and that according to the mathematical formula $TRI = (\sum(z_i - z_n)^2)^2$, where z_i represents the central cell for which it is defined TRI, and z_n represents the neighboring cell ($i = 1, 2, \ldots, 8$) [13].

The air and soil humidity - With the presence of humidity, the structure of snow undergoes deformations, the particles of which stick and create weight. We distinguish the presence of humidity at the top, bottom, and inside the snow space. When water penetrates under the snow layer due to melting or eventually due to rainfall that penetrates under it, it has the effect of reducing the frictional force between the snow layer and the layer in which this snow layer is located. The humidity of the soil surface depends on its very shape. Non-accumulative forms of relief always tend to be dry in terms of soil moisture, while the accumulative ones are to be wet, this is because the water streams that can form at the bottom of the snow bed target the latter. Index of soil moisture is not limited only by the topographic component, but since we do not have measurable data on soil moisture, we have limited its definition only to the topographic surface, which means that it is static and can be useless in cases when the soil moisture is assessed according to time variability. The wetness indexing is determined based on the formula $TWI = \ln(A/\tan\beta)$, where A represents the specific areas of the watershed, whereas β represents the terrain slope.

Exposure to the wind - Determining wind direction is a very important but quite delicate element, as wind dynamics are quite large. The two key wind elements that are important to this study are its ability to carry snow particles, as well as its strength to help initiate a snow avalanche. The first and most important element can be evidenced in the newly fallen snow which is compact and dry. Usually, the areas most exposed to the wind are mountain slopes, where the nearest pits or concave areas are subject to the accumulation of that snow carried by the wind. Snow deposition in the part of the ridge located behind the exposed slope, increase of up to four times [14]. In these positions, the snow depth marks the highest values of 2 up to 40 m distance from the ridgeline.

Snowfall - Snowfall in the existing snow layer is quite essential as it increases the weight of the snow slab, which can lead to a critical and favorable phase to increase the avalanche potential of the volatile layers. For large (catastrophic) avalanches, new snow is the main predictor [15]. Accumulation (layering) of new snow with a depth of 1 m during 3 days of rainfall is considered critical for the onset of an extreme avalanche, while with a depth of 30-50 cm, critical for the release of an ordinary avalanche [16]. If the snow load is larger than 2.5 cm/h, it will affect the instability of the weak layer which is expressed according to the stability index [17].

Air temperature - It effects on snow stability in different ways, where the degree of change is significant. Rising temperatures during snowfall and at fast intervals immediately after rainfall, contribute to instability. Time changes in air temperature has direct influence on the surface layers, while the weak layer is relatively unaffected by the air temperature due to the low thermal conductivity of snow [18].

2.5 Data Classification and Contribution to Snow Avalanches

Bucaj [4] in his master thesis research supervised by prof Bashkim Idrizi, has adopted the special methodology and standards for spatial modeling of areas with avalanche potential in Sharr Mountains, based on criteria of Fuzzy Logic and MDA/AHP methods, previous similar analyses for other cases of avalanches in other areas, as well as the specific topographic and meteorological conditions of Sharr Mountain. In next diagram (Fig. 3), the methodology with data classification and classes contribution to snow avalanches in a case of Sharr Mountains study area is given.

At the top of Fig. 3 are shown six datasets as contents of developed geodatabase within this research study. Three of them (orthophotos, topographic maps and photos) are part of the historical avalanche inventory, as necessary input data for output results evaluation. Other datasets (DEM, landcover and winds) are part of the data to be used for performing spatial analysis for detecting potential snow release areas. Based on the list of criteria for spatial analyses, core data from three datasets were used for processing necessary layers of terrain slope, terrain orientation (aspect), hypsometry (elevation), plan curvature, profile curvature, topographic wetness, topographic roughness, solar radiation and land cover.

Developed data stored in nine layers needs to be reclassified to be able for use in both Fuzzy Logic and MDA/AHP methods. For this reason, slope data was classified into five categories (<25, 25-30, 30-50, 50-60, and > 60%), aspect data in nine categories (347.5-22.5, 22.5-67.5, 67.5-112.5, 112.5-157.5, 157.5-202.5, 202.5-247.5, 247.5-292.5, 292.5-337.5°, and "plan" areas with slope 0%), hypsometry in four categories (<900, 900-1400, 1400-2200, and >2200 m), then plan curvature (<–0.2, –0.2-0.2, and

>0.2), profile curvature (<–0.2, –0.2-0.2, and >0.2), topographic wetness (<5, 5-10, and >10) and topographic roughness (>15, 15-25, and >25) per three categories, solar radiation data in four categories (<30, 30-60, 60-90, and >90), while land cover layer in fourteen categories (settlement, industrial commercial area, arable land, pastures, heterogonous agricultural land, deciduous forests, coniferous forest, mixed forest, natural/herbal pastures, herbaceous soil/shrubs, rare shrubs and forests, area with rare vegetation, burned area, and aquatic land). Such reclassified data layers are source data for performing analyses with MDA/AHP and Fuzzy Logic methods, as it is shown in figure 3.

Fuzzy Logic method applies determining the avalanche frequency ratio and fuzzification/fuzzy membership process, while MDA/AHP method applies comparative pair matrix of the classes of each factor, and hierarchical weighing. Two separate maps of areas with avalanche potential based on the developed datasets by using both methods are main outputs of this model on determination of areas with avalanche release potential.

Defined methodology in Fig. 3 ends with evaluation of results through the ROC method based on maps of areas with avalanche potential as main research outputs and historical avalanche inventory.

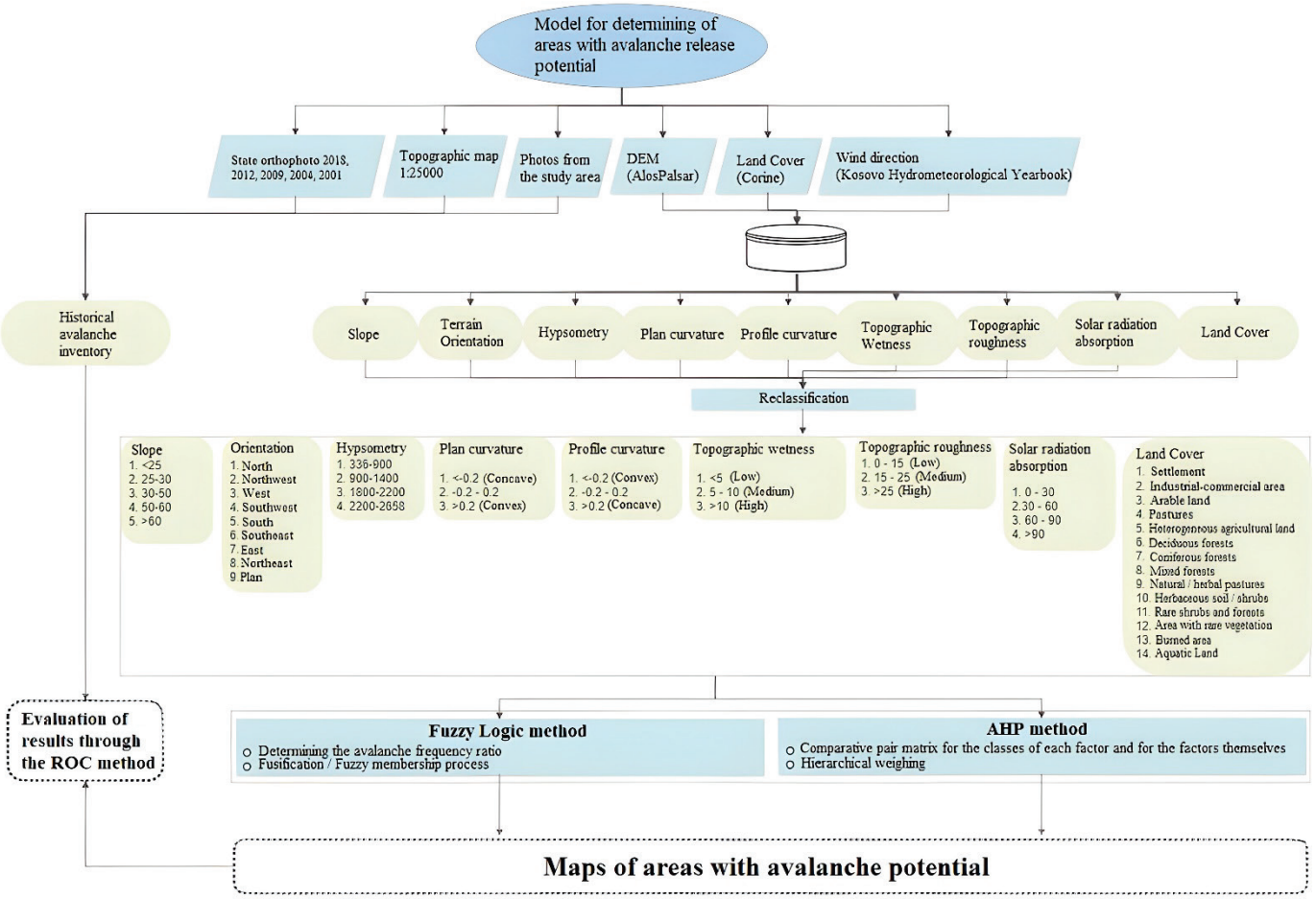

Figure 3 Model on determination of areas with avalanche release potential [4]

2.6 Source Data for Calculations of Potential Areas with Avalanche Release in Sharr Mountains

In this research, the biggest focus is on the topographic component but related to the meteorological, and not to the physical component, due to lack of data and lack of measurements on the structure of snow, density, thickness, distance from layer to layer and identification of icy layers between them.

Great importance was paid to the spatial resolution of the DEM, as its scale is directly related to its derivatives. In geographical areas in which the snow stability can't be longer than one year, we can say that high-resolution DEM can be used as any detail of the relief would contribute to the parameter of soil ruggedness and therefore the DEM resolution for the respective destination must also be selected. However, if the spatial analysis is done for a geographical area in which snow is continuously present and has permanent stability, then the snow-covered surface is smoother, and the ruggedness of the soil cannot be obtained as in a DEM with a resolution of up. In these cases, lower resolution DEMs are chosen so that the terrain is reflected more smoothly.

In next Tab. 2, a list of used topographic and meteorological data sources for performing spatial analyses

for determination of snow avalanche release potential areas in Sharr Mountains is given [20-28].

Table 2 List of source data.

Data type	Data source	Technical details
Topographical data		
DEM	Alos Palsar Satellite	Spatial resolution: 12.5 m
Land cover	Corine	Spatial resolution: 100 m Categories: 47
Satellite image	Sentinel 2 MSI	Spatial resolution 10 m, 20 m and 60m Bands: 12
Satellite image	Landsat 8 OLI & TIRS sensors	Spatial resolution 30 m, 15 m, 60 m and 100 m Bands: 11
Satellite image	Landsat 5 TM	Spatial resolution 30 m and 120 m Bands: 7
Satellite image	Google earth	Spatial resolution 1 m
Meteorological data		
Winds	Global wind atlas	Spatial resolution 250 m
Temperature	Meteorological stations	List of data in excel file
Rain	Meteorological stations	List of data in excel file
Solar radiation	Global solar atlas	Spatial resolution 250 m

3 RESULTS DISCUSSIONS

3.1 GIS Database for Determination of Avalanches Release Potential areas of Sharr Mountains

Based on the model on determination of areas with avalanche release potential (Fig. 3), all source data have been preprocessed to adopt to the technical and content model requirements, as well as to be harmonized all layers between them. From source DEM with 12.5 m spatial resolution, new raster layers for terrain slope expressed in percentage (%), aspect (terrain orientation) of terrain expressed in degree based on the North direction as an initial value, profile terrain curvature, plan terrain curvature, terrain ruggedness index, and topographic wetness index have been created.

Since the CRS (Coordinate Reference System) and geometrical components (spatial resolution, point of origin and orientation) of all sources and developed raster data are different to each other, the data harmonization process [19] preceded as final step for establishing spatial database for determination of avalanches release potential areas in Sharr mountains. In next Fig. 4, the database structure is given.

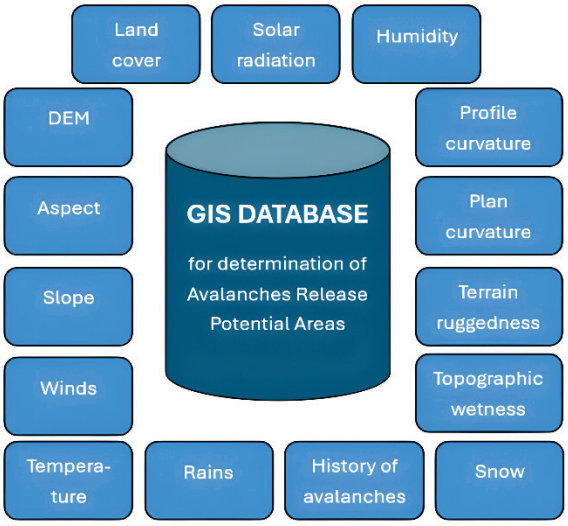

Figure 4 GIS database structure for determination of Avalanches Release Potential areas

3.2 Determination of Avalanches Release Potential Areas of Sharr Mountains with Fuzzy Logic Method

The Fuzzy Logic method first incorporates data from the avalanche history, and that the main locations of snow avalanches, although as very scarce data, but quite important. The avalanche frequency in each class of each contributing factor was then determined. During the fusion process, each class received the appropriate credits in relation to the frequency of avalanche occurrences from the snow avalanche inventory. Following the process of factor fusion, results of areas with the potential for avalanches are calculated. In next Tab. 3 the values of calculation of fuzzy membership for each category of input data, based on the criteria defined by [4] and shown in diagram in Fig. 3, are calculated.

Table 3 Fuzzy Logic determining the membership rate of each factor based on avalanche occurrences

Factor	Class	Nr. of class	% of avalanche areas	Fuzzy Membership	% of avalanche areas	Fuzzy Membership
			Kosova		North Macedonia	
Slope	<25	1	0.00	0.00	66.16	1.00
(%)	25-30	2	0.97	0.01	16.03	0.24
	30-50	3	99.02	1.00	17.45	0.26
	50-60	4	0.00	0.00	0.30	0.00
	>60	5	0.00	0.00	0.07	0.00
		∑	100		100	
			Kosova		North Macedonia	
Altitude	<900	1	0.00	0.00	12.38	0.47
(m)	900-1400	2	0.00	0.00	26.12	1.00
	1400-1800	3	0.00	0.00	19.25	0.74
	1800-2200	4	30.09	0.43	19.09	0.73
	2200-2747	5	69.90	1.00	23.16	0.89
		∑	100		100	
			Kosova		North Macedonia	
Profile	< -0.2 convex	1	32.03	0.79	34.96	1.00
curvature	(-0.2) – 0.2	2	27.66	0.68	30.00	0.86
	>0.2 concave	3	40.29	1.00	35.04	1.00
		∑	100		100	

			Kosova		North Macedonia	
Plan	< -0.2 concave	1	60.19	1.00	33.91	0.97
curvature	(-0.2) - 0.2	2	17.96	0.29	31.26	0.90
	>0.2 convex	3	21.84	0.36	34.83	1.00
		∑	100		100	
			Kosova		North Macedonia	
Terrain	<15 low	1	100.00	1.00	99.86	1.00
ruggedness	15-25 medium	2	0.00	0.00	0.12	0.00
	>25 high	3	0.00	0.00	0.02	0.00
		∑	100		100	
			Kosova		North Macedonia	
Topographic	<5 low	1	65.53	1.00	0.01	0.00
wetness	5-10 medium	2	34.46	0.52	75.40	1.00
	>10 high	3	0.00	0.00	24.59	0.33
		∑	100		100	
			Kosova		North Macedonia	
Solar	<30	1	70.38	1.00	0.41	0.01
radiation	30-60	2	16.50	0.23	17.29	0.22
absorption	60-90	3	13.10	0.18	78.55	1.00
	>90	4	0.00	0.00	3.74	0.05
		∑	100		100	
			Kosova		North Macedonia	
Land cover	Settlement	1	0.00	0.00	0.71	0.02
	Industrial-commercial area	2	0.00	0.00	0.00	0.00
	Arable land	3	0.00	0.00	0.00	0.00
	Pastures	4	0.00	0.00	0.83	0.02
	Heterogeneous agricultural land	5	0.00	0.00	1.18	0.03
	Heterogeneous agricultural land	6	0.00	0.00	6.81	0.16
	Deciduous forests	7	0.00	0.00	30.90	0.72
	Coniferous forests	8	0.00	0.00	0.71	0.02
	Mixed forests	9	0.00	0.00	2.79	0.06
	Natural / herbal pastures	10	33.01	0.89	43.04	1.00
	Herbaceous soil / shrubs	11	30.09	0.81	2.33	0.05
	Rare shrubs and forests	12	0.00	0.00	8.93	0.21
	Area with rare vegetation	13	36.89	1.00	1.22	0.03
	Burned area	14	0.00	0.00	0.00	0.00
	Aquatic Land	15	0.00	0.00	0.54	0.01
		∑	100		100	
			Kosova		North Macedonia	
DEM Aspect	(degree)					
Plan	slope 0%	1	0.97	0.02	0.00	0.00
North	337.5-22.5	2	35.92	1.00	8.15	0.38
Northeast	22.50-67.5	3	22.81	0.63	12.91	0.60
East	67.5-112.5	4	2.42	0.06	17.62	0.82
Southeast	112.5-157.5	5	0.00	0.00	21.45	1.00
South	157.5-202.5	6	0.00	0.00	16.91	0.79
Southwest	202.5-247.5	7	0.00	0.00	11.07	0.52
West	247.5-292.5	8	15.04	0.41	6.08	0.28
Northwest	292.5-337.5	9	22.81	0.63	5.80	0.27
		∑	100		100	

Table 4 Multicriteria Decision Analysis (MDA) - the analytic hierarchy process (AHP) determining the membership rate of each factor based on avalanche occurrences

	Slope	Altitude	Plan curvature	DEM Aspect	Profile curvature	Land cover	Solar radiation absorption	Topographic wetness	Terrain ruggedness
Slope	1	0.5	0.5	0.33	0.25	0.33	0.2	0.2	0.2
Altitude	2	1	2	0.33	0.33	1	0.25	0.25	0.25
Plan curvature	2	0.5	1	0.333	0.5	2	0.25	0.2	0.2
DEM Aspect	3	3	3	1	0.5	3	0.2	0.2	0.25
Profile curvature	4	3	2	2	1	3	0.333	0.25	0.333
Land cover	3	1	0.5	0.333	0.333	1	0.25	0.2	0.25
Solar radiation absorption	5	4	4	5	3	4	1	0.5	1
Topographic wetness	5	4	5	5	4	5	2	1	2
Terrain ruggedness	5	4	5	4	3	4	1	0.5	1
Weights	**0.255**	**0.148**	**0.162**	**0.097**	**0.071**	**0.171**	**0.035**	**0.026**	**0.035**

3.3 Determination of Avalanches Release Potential Areas of Sharr Mountains with Multicriteria Decision Analysis (MDA) - the Analytic Hierarchy Process (AHP) Method

In addition to the first method, the AHP method is used as the second method of determining potential areas. This method, as stated above, is based on expert judgments in setting weights for each factor and factor class, where

subjective judgments based on rationality are also expressed. The Consistency Ratio (*CR*) of the matrix in pairs after setting the values shown in Tab. 4 was 0.052, indicating that the cumulative judgments derived from the matrix in the pair are satisfactory. In Tab. 4, the weighting was performed for the classes of each factor for the case of determining the potential areas with snow avalanche release, which then was executed based on calculated values in GIS by using Eq. (4) whereas Boolean data were used data on land coverage and terrain slope.

3.4 Four Level Classification of Avalanches Release Potential Areas of Sharr Mountains

The avalanche release potential zones are classified in four categories, as areas with low potential ($Z < 0.2$), moderate ($0.2 < Z < 0.5$), high ($0.5 < Z < 0.7$), and very high ($Z > 0.7$), using the Jenks optimization method [29, 30, 31, 32, 33]. In a case of analyses for the North Macedonian side of Sharr Mountains, additional category very low with value ($Z = 0$) is used. Next four maps, separately for Kosova and North Macedonia by using both analyzing methods of Fuzzy Logic and MDC-AHP, shown the study area classified based on the potential category calculated for each sell in spatial resolution of 12.5 m.

3.5 Verification the Accuracy of Determined the Avalanches Release Potential Areas of Sharr Mountains

After determining the locations with avalanche potential, simultaneously with the result, accuracy of the model was verified. A proper verification can be performed by making a comparison between the results obtained from performed analysis and the historical inventory of snow avalanches by using the ROC – Receiver Operating Characteristics method [35]. In next Tab. 5, the results of four results with the Area Under the Curve (AUC) value are given.

Table 5 AUC values obtained from the verification process.

	Fuzzy Logic	AHP
Kosova side	0.993	0.986
North Macedonia side	0.989	0.991

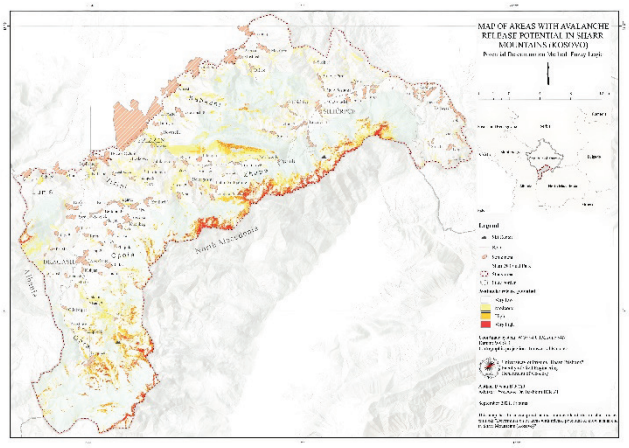

Figure 5 Map of potential snow avalanche release area determining the potential according to Fuzzy Logic method for Sharr Mountains in the side of Kosova [4]

The ROC analysis gave satisfactory results, close to each other and acceptable for such a spatial analysis.

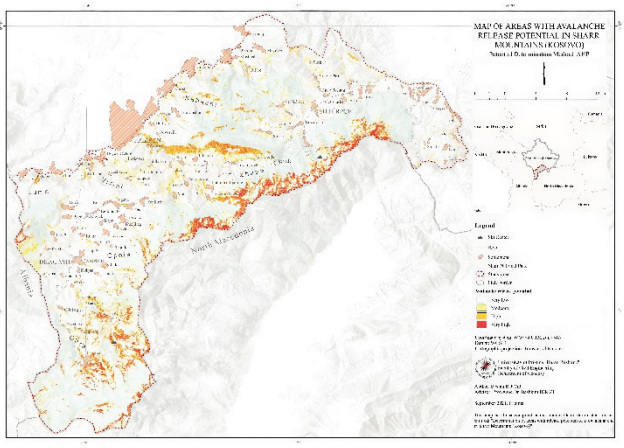

Figure 6 Map of potential snow avalanche release area determining the potential according to Fuzzy Logic method for Sharr Mountains in the side of North Macedonia

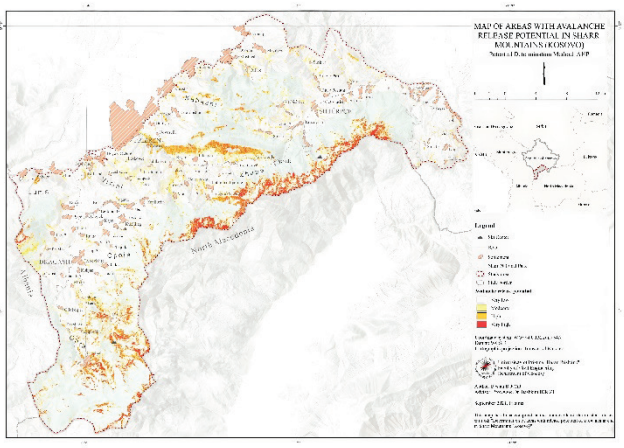

Figure 7 Map of potential snow avalanche release area determining the potential according to MDA-AHP method for Sharr Mountains in the side of Kosova [4]

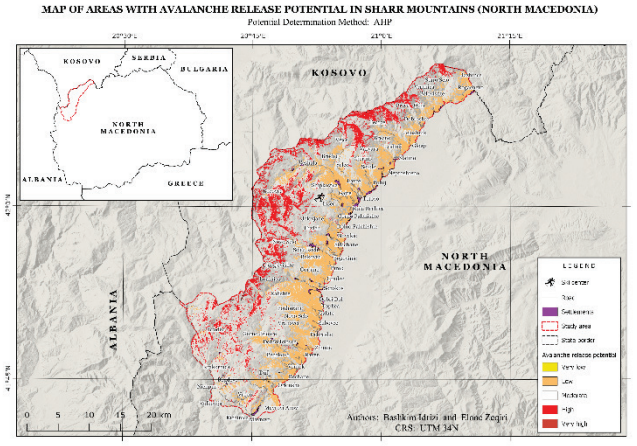

Figure 8 Map of potential snow avalanche release area determining the potential according to MDA-AHP method for Sharr Mountains in the side of North Macedonia

4 DISCUSSIONS

The methodology applied in this research consider relevant topographical, meteorological and physical components, by data classification, using processing algorithms of MDC/AHP and Fuzzy Logic methods, and automatic implementation in GIS platform. Our novel approach for assessing and zoning areas by risk level of snow avalanche is valid at large scales with a high level of accuracy, by adopting criteria in correlation with the microregional data for the study area. Establishing such a system as official at the national level will have positive impact in better spatial planning, and prevention from snow avalanches as natural hazards.

Developed methodology from a narrow and detailed point of view in the next period should be extended by using real-time data, GIS spatial analyses and machine learning technology, in relation to digital meteorological stations.

5 CONCLUSIONS

The results show that the area of Sharr Mountains is affected by avalanches, the danger of which should be accurately determined, by using more meteorological data on snowfall, temperature, and additional data about the speed and direction of the wind, given by the local meteorological stations instead the global databases [34]. Such data should include the longest possible time interval to obtain the extreme values of all factors, as well as to make the connection with the historical avalanches at a moment when they occurred. The avalanche hazard levels could be determined for each surface which has resulted as a potential surface separately.

Spatial analysis of natural disasters through GIS, helps all areas of interest in decision making as GIS in addition to the potential in the analysis allows the visualization of parameters or factors, so the assessment by experts will be easier and closer to reality. The obtained result within this research shows a satisfactory and quite good relationship between the map of areas with avalanche potential and avalanche location data from the history of events. Within the Fuzzy Logic model, the model can be easily revised and modeled, modifying the membership functions for different study areas, while in the AHP model care must be taken in the values of the evaluation weights, as this depends on the selected study area.

6 REFERENCES

[1] Fredston, J. & Fesler, D. (1994). *Snow Sense: A Guide to Evaluating Snow Avalanche Hazard*. Alaska Mountain Safety Center, pp. 116.

[2] Meister, R. (2002). Avalanches: Warning, rescue and prevention. *Avalanche News*, 62.

[3] Izeiroski, S., Idrizi, B., Lutovks, M. & Kabashi, I. (2018). GIS-based Multi Criteria Analysis of site suitability for exploatation of renewable energy resources. *Proceedings of the 7th International Conference on Cartography and GIS.*

[4] Bucaj, B. (2021). Determining the surfaces with avalanche discharge potential in the Sharri Mountains (Kosovo). *Master thesis*. University of Prishtina. Prishtina. Kosovo.

[5] EAWS - European Avalanche Warning Services. (2021). European avalanche size classification, http://www.avalanches.org

[6] Zadeh, L. (1965). Fuzzy sets. *Information and Control*, 338-353. https://doi.org/10.1016/S0019-9958(65)90241-X

[7] Saaty, T. L. (1980). *The Analytical Hierarchy Process*. McGraw-Hill: New York, NY, USA.

[8] Duc, T. T. (2006). Using GIS and AHP technique for land-use suitability analysis. *International Symposium on Geoinformatics for Spatial Infrastructure Development in Earth and Allied Sciences 2006*.

[9] Maggioni, M. (2004). *Avalanche release areas and their influence on uncertainty in avalanche hazard mapping*. Zurich.

[10] McClung, D. M. (2001). Characteristics of terrain, snow supply and forest cover for avalanche initiation caused by logging. *Annals of Glaciology*, 223-230. https://doi.org/10.3189/172756401781819391

[11] Gleason, J. A. (1995). Terrain parameters of avalanche starting zones and their effect on avalanche frequency.

[12] Gauer, P. (1999). Blowing and Drifting Snow in Alpine Terrain: A Physically Based Numerical Model and Related Field Measurements. https://doi.org/10.3189/1998AoG26-1-174-178

[13] Riley, S. J., DeGloria, S. D. & Elliot, R. (1999). A terrain ruggedness index that quantifies topographic heterogeneity. *Intermountain Journal of Sciences, 5*(1-4), 23-27.

[14] Doorschot, J., Raderschall, N. & Lehning, M. (2001). Measurements and one-dimensional model calculations of snow transport over a mountain ridge. *Ann. Glaciol., 32*, 153-158. https://doi.org/10.3189/172756401781819616

[15] Fohn, P., Stoffel, M. & Bartelt, P. (2002). Formation and forecasting of large (catastrophic) new snow avalanches. *Proceedings of the ISSW 2002*, edited by Stevens J. R., 141-148, Int. Snow Sci. Workshop Can., B. C. Minist. of Transp., Snow Avalanche Programs, Victoria, B. C., Canada.

[16] Schweizer, J., Jamieson, J. B. & Schneebeli, M. (2003). Snow avalanche formation. Reviews of Geophysics, 41(4). https://doi.org/10.1029/2002RG000123

[17] Conway, H. & Wilbour C. (1999). Evolution of snow slope stability during storms. *Cold Reg. Sci. Technol., 30*(1-3), 67-77. https://doi.org/10.1016/S0165-232X(99)00009-9

[18] Sturm, M., Holmgren, J., Konig, M. & Morris, K. (1997). The thermal conductivity of seasonal snow. *J. Glaciol., 43*(143), 26-41. https://doi.org/10.3189/S0022143000002781

[19] Idrizi, B., Sulejmani, V. & Zimeri, Z. (2018). Multiscale map for three levels of spatial planning databases for the municipality of Viti in Kosova. *Proceedings of the 7th International Conference on Cartography and GIS. Vol. 1*, 577-585.

[20] https://globalwindatlas.info/en (Accessed on May 2024)

[21] https://globalsolaratlas.info/download/north-macedonia (Accessed on May 2024)

[22] https://earthexplorer.usgs.gov (Accessed on May 2024)

[23] https://land.copernicus.eu/en/products/corine-land-cover/clc2018 (Accessed on May 2024)

[24] https://earth.google.com (Accessed on May 2024)

[25] https://earthobservatory.nasa.gov/global-maps/GPM_3IMERGM (Accessed on May 2024)

[26] https://cloudatlas.wmo.int/en/snow.html (Accessed on May 2024)

[27] https://atlas.climate.copernicus.eu (Accessed on May 2024)

[28] https://map.worldweatheronline.com (Accessed on May 2024)

[29] Xu, C. Xu, X. Dai, F. Xiao, J. Tan, X. & Yuan, R. (2012). Landslide hazard mapping using GIS and weight of evidence model in Qingshui River watershed of 2008 Wenchuan earthquake struck region. *Earth Sci 23*. https://doi.org/10.1007/s12583-012-0236-7
[30] Yilmaz, B. (2010). Application of GIS-based fuzzy logic and analytical hierarchy process (AHP) to snow avalanche susceptibility mapping, North San Juan, Colorado.
[31] Selçuk, L. (2013). An avalanche hazard model of Bitlis Province, Turkey, using GIS based multicriteria decision analysis. https://doi.org/10.3906/yer-1201-10
[32] Pourghasemi, H. R., Moradi, H. R., Aghda, S. M., Gokceoglu, C. & Pradhan, B. (2012). GIS-based landslide susceptibility mapping with probabilistic likelihood ratio and spatial multi-criteria evaluation models (North of Tehran, Iran). https://doi.org/10.1007/s12517-012-0825-x
[33] Kumar, S., Snehmani, Srivastava, P. K., Gore, A., & Singh, M. K. (2016). Fuzzy–frequency ratio model for avalanche susceptibility mapping. *International Journal of Digital Earth, 9*(12), 1168-1184. https://doi.org/10.1080/17538947.2016.1197328
[34] Idrizi, B. (2006). Developing of Globally Homogeneous Geographic Data Set through Global Mapping Project. *Kartografija i geoinformacije, 5*(6), 90-101. https://hrcak.srce.hr/6371
[35] https://online.stat.psu.edu/stat504/lesson/7/7.4 (Accessed on May 2024)

Authors' contacts:

Bashkim Idrizi, Prof. Dr.
University of Prishtina "Hasan Prishtina",
Str. "George Bush", No. 31, 10 000 Prishtina, Republic of Kosovo
+38975712998, bashkim.idrizi@uni-pr.edu

Fitore Bajrami Lubishtani, Prof. Dr.
(Corresponding author)
University of Prishtina "Hasan Prishtina",
Str. "George Bush", No. 31, 10 000 Prishtina, Republic of Kosovo
fitore.bajrami@uni-pr.edu

Elone Zeqiri, MSc.
University of Prishtina "Hasan Prishtina",
Str. "George Bush", No. 31, 10 000 Prishtina, Republic of Kosovo
elone.zeqiri@student.uni-pr.edu

ISSN 1846-6168 (Print), ISSN 1848-5588 (Online)
https://doi.org/10.31803/tg-20240909232934

Original scientific paper
Received: 2024-09-09, Accepted: 2024-10-25

Assessment and the Future Development of the Zagreb 3D City Model

Vlado Cetl*, Darko Šiško, Hrvoje Matijević, Danko Markovinović

Abstract: The first 3D model of the city of Zagreb was developed in 2008. Since then, the model has been improved and updated. Today, it is used for various purposes in the city planning and management. It is also publicly available to citizens through the ZG3D Web application. In this paper, an assessment of the existing 3D model is provided by considering different factors (i.e. consistency between models, standardization, data quality, data interoperability, data maintenance/governance, and use cases) that need to be tackled in order for the 3D city model to be further improved and used towards the creation of the digital twin and ultimately to support the smart city concept. The assessment considered some general criteria and also the 3D City Index assessment tool developed by the Urban Analytics Lab, National University of Singapore (NUS). The assessment results show that the existing model is used for various purposes, but to evolve towards a true digital twin, it must be improved.

Keywords: 3D city model; assessment; city of Zagreb

1 INTRODUCTION

In today's digital age, analogue maps are increasingly being replaced by 3D digital models that have become the basis for planning and managing space, especially in urban areas. Digital city twins and smart cities need 3D city models as a basis for further development. Thanks to surveying and ICT developments, 3D models are already mainstream in many cities around the world. Their usage is evident in many different areas. New challenges arise with the smart city concept. There, the 3D city model is not enough, but rather a digital twin that integrates static 3D city models with different sensors.

3D city models are available in two different representations. Semantic 3D models (information models) and 3D mesh models. The two have established themselves as valuable tools for the digital description of the physical environment. Their characteristics, usage scenarios, and production methods are, however, different. There are also use cases when both model types can be complementary [12].

3D city model provides numerous potential advantages and benefits in the maintenance of city infrastructure, including simpler and more efficient management, reduction of redundancy, easier access to relevant information, easier communication, etc. [21].

The City of Zagreb also followed this trend through the development of the initial 3D model in 2008 [1, 2]. Since then, the initial 3D model has been updated several times, which was mostly done at certain city locations of interest [3, 4].

The city of Zagreb, like other major cities, is complex and requires a lot of effort to measure and model it. Therefore, usually, only a part of a city (e.g. a building or a group of buildings) is measured and modelled at one time. Moreover, any single act of measuring and modelling a city is not enough, because cities are never completed, but continue to expand and develop. Given the needs of modern cities, existing 3D models are not sufficient because they most often represent static models. The development of the Internet of Things (IoT) imposes the need to integrate a static 3D model with various sensors and create a dynamic environment that can meet the increasing needs and challenges of cities for sustainable real-time management. The biggest challenge urban management teams face today in data-driven processes is to extract value from the ever-increasing volume, frequency of change, and diversity of data, also known as Big data).

Stoter et al. [5] state several basic challenges regarding 3D data models:

- consistency between models
- standardization
- data quality
- data interoperability
- data maintenance/governance
- from utopian pilots to real-world use cases.

All listed challenges need to be tackled in order for 3D city models to be used for sustainable urban environments.

Existing studies usually validate some aspects of 3D models such as geometry [15], compliance with standards [16], [17], and application requirements [18]. Also, metadata for describing 3D models [19] and data openness [20], [22] are in focus.

In this paper, an assessment of the existing Zagreb 3D city model is provided by considering above mentioned challenges [5]. The assessment was done as a combination of different factors including previous studies [7], other data sources (e.g. cadastral data), 3D city index [6] which is a very comprehensive and relevant tool, and also insights from the city employees who are in charge of the data, but also data users.

2 ZAGREB 3D CITY MODEL

The Zagreb 3D city model is under the responsibility of the City Office for Economy, Environmental Sustainability and Strategic Planning [13]. The office is in charge of data maintenance, as well as data sharing and publishing.

2.1 The Existing Model

The initiative for the creation of a 3D model came in 2008 from the private company Geofoto LLC from Zagreb. The idea was to create a digital terrain model (DTM), a 3D

building model and a true orthophoto map. Geofoto conducted aerial photography in September 2008, taking 4,000 shots (Ground Sample Distance = 8 cm) with 80% overlap within the array and 60% between the arrays. The model was created by using photogrammetric mapping of roof lines, along with DTM, aero-photo and real ortho-photo shots. A physical model of the city with 3D printing technology was also made [8]. The most of the 3D model was made at the level of detail LOD 2 [9].

The city office responsible for spatial planning took over the 3D model only a few years later, due to slow and complicated public procurement procedures. At the time of the takeover, the city had two main objectives: to assess the data quality and its fit for purpose in the city planning. In addition, the plan included the development of an online application for reviewing and using the 3D city model. In 2014, the Faculty of Geodesy at the University of Zagreb made a quality test of the 3D model. The project included the following [2]:

- Data analysis of the existing 3D model
- Quality assessment of existing 3D model data in accordance with HRN EN ISO 19157:2014 Geoinformation - Data quality (integrity, logical consistency, positional and altitude accuracy, thematic accuracy, temporal quality, usability).
- Transformation of data into the official coordinate system and cartographic projection of the Republic of Croatia
- Harmonization of data according to INSPIRE (Infrastructure for Spatial Information in Europe) data specifications (Buildings and Heights)
- Data testing in AutoDesk and ESRI software packages
- Creating 3D displays - visualization for the areas of 15 strategic city projects (shadow displays, minimum 4 for each area)
- Analysis of the volume of buildings for the areas of strategic city projects
- Guidelines for updating and creating a web application for using 3D model data
- Guidelines for the integration of 3D model data into the Zagreb Spatial Data Infrastructure.

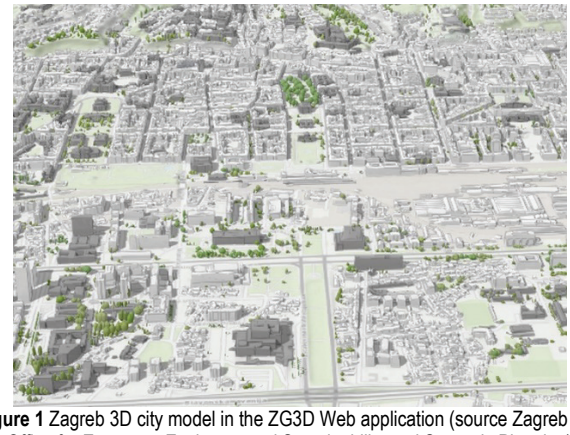

Figure 1 Zagreb 3D city model in the ZG3D Web application (source Zagreb City Office for Economy, Environmental Sustainability and Strategic Planning)

Overall the results showed that data was incomplete and inconsistent. For the purpose of wider application, the company GDi, created the Web application ZG3D in 2016 (Fig. 1).

The application contains 3D building data in combination with other 3D and 2D data layers in the areas of urban planning, architecture, topography, geotechnics, public green spaces, heritage protection, urban renewal and statistics [10].

2.2 Applications of the existing model

There are many areas in which the existing model is already in use or is planned to be used [3].

In July 2022, the Energy Info Centre of the City of Zagreb platform was presented. The platform enables the calculation of basic parameters of solar power plants integrated into single-family houses, i.e. multi-dwelling buildings, and the basic data used are the 3D model data (Fig. 2).

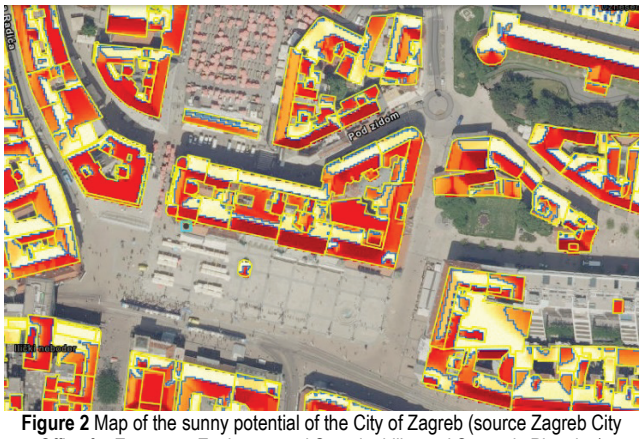

Figure 2 Map of the sunny potential of the City of Zagreb (source Zagreb City Office for Economy, Environmental Sustainability and Strategic Planning)

The 3D model is also recognized as one of the fundamental sources for the post-earthquake reconstruction after the earthquake in 2020. A lot of projects for the reconstruction of public buildings are carried out by using Web GIS solutions with online ZG3D application integration.

2.3 Data Assessment

Data assessment in this research was made in 2024 as a continuation of previous studies (Fig. 3).

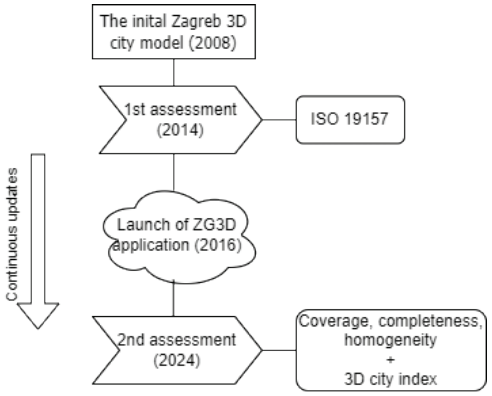

Figure 3 Methodology (source authors)

The initial 3D model was created in 2008 only for the urban area, but the data update over the years was slow and based on a fragmented project approach. There were several reasons, the lack of resources and the usage of 3D collected data from different projects in the city area. The updates were made mostly using LiDAR and aero-photogrammetry data from 2012, and unmanned aerial vehicle images in 2016, 2019 and 2020. The existing model is semantic in mostly LOD 2 and for some areas LOD 1. Fig. 4 shows the current coverage of the 3D model.

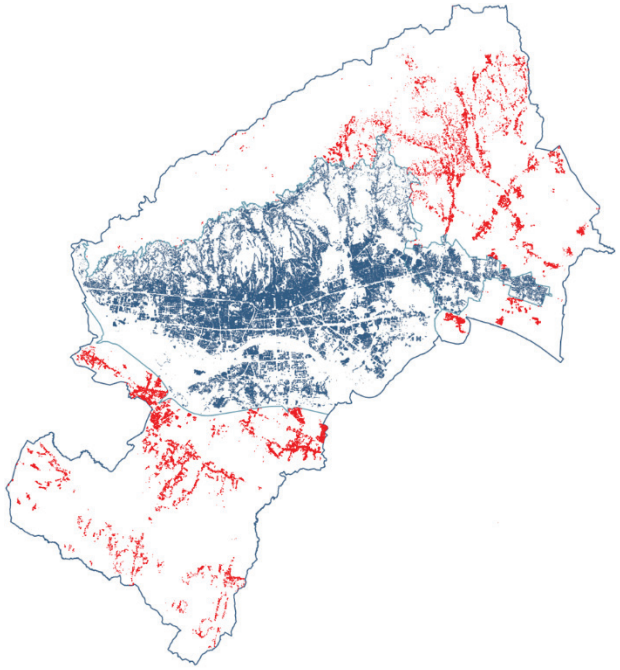

Figure 4 Zagreb 3D city model coverage (source Zagreb City Office for Economy, Environmental Sustainability and Strategic Planning)

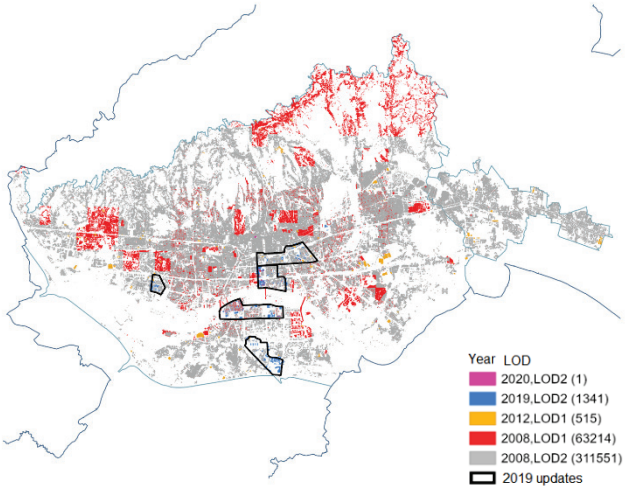

Figure 5 Zagreb 3D city model 3D model coverage by the year of recording and level of detail (LoD) (source Zagreb City Office for Economy, Environmental Sustainability and Strategic Planning)

The coverage with a 3D model is approximately 37 % of the whole administrative area of the City of Zagreb. The 3D model contains an estimated 80% of buildings (the blue part) compared with cadastral map data.

The existing 3D model data are still largely outdated and inhomogeneous despite updates in recent years (Fig. 5).

Fig. 6 and Fig. 7 show the out-of-dateness and inhomogeneity of the data of the 3D model in more detail.

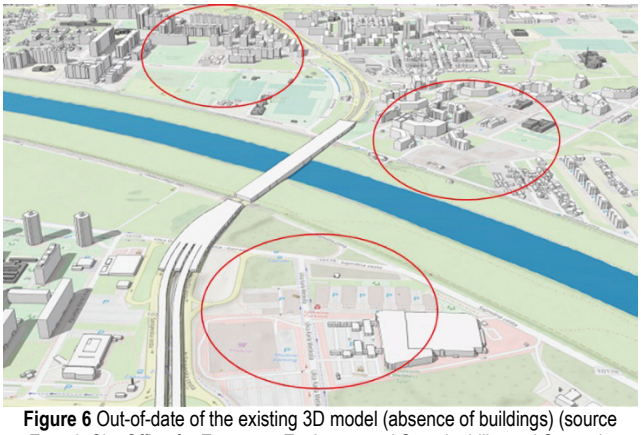

Figure 6 Out-of-date of the existing 3D model (absence of buildings) (source Zagreb City Office for Economy, Environmental Sustainability and Strategic Planning)

Figure 7 Inhomogeneity of the existing 3D model (different LoDs) (source Zagreb City Office for Economy, Environmental Sustainability and Strategic Planning)

After the initial assessment, the 3D City Index Assessment [6] developed by the Urban Analytics Lab [14] was used for the more comprehensive assessment of the existing 3D model.

The 3D city index is a holistic and comprehensive framework containing 4 categories. It includes 47 criteria for identification of the main features of 3D city models, enabling their assessment and comparison, as well as for suggesting usability. The implementation of the framework enables a comprehensive and structured understanding of the landscape of semantic 3D geospatial data, as well as a double assessment of the collection of open 3D models of cities.

Additional benefits of this framework are reflected in the standardisation of 3D data characterisation: monitor developments and trends in 3D modelling of cities and enable findability of the fit-for-purpose datasets to all interested users to satisfy their needs. The framework is designed for continuous measurement of datasets and can also be applied to other instances in the spatial data infrastructure.

The 3D City Index contains the following categories:

1) Data Portal
2) Basic Information
3) Thematic Content
4) Attribute Content.

In each category, there is a set of criteria to comprehensively highlight different viewpoints [11].

The maximum total score can be 47 points based on the 4 categories (Tab. 1):

1) The Data Portal category is scored with max. 6 points.
2) Basic Information category is scored with max. 15 points.
3) Thematic Content category is scored with max. 11 points.
4) The Attribute Content category is scored with max. 15 points.

Better scores of course reflect better performance. The framework is generic and flexible by allowing users to adapt it to specific use cases or geospatial context. To obtain a standardised comparison, the scoring system tries to give a result from two aspects. One is an overview of the measures of the included 3D models by comparing their performance, and the second is a study of the properties of datasets within each category. Users can select the relevant parts in the dataset.

The Zagreb 3D city model was scored with a total of 26 points [7] (Tab. 1), which places it relatively high on the current list of scoring cities between, for example, Helsinki with 32 points and Vienna with 24 points.

Table 1 Zagreb 3D city index assessment

Category	Criteria	3D model of the City of Zagreb
Data portal	1C1 - Does the dataset have a dedicated website?	YES
	1C2 - Is there a web browser in 3D?	YES
	1C3 - Is there near real-time information in the viewer?	YES
	1C4 - Is it available in local language?	YES
	1C5 - Is it available in English?	NO
	1C6 - Is there a way to leave feedback?	YES
Background information	2C1 - Is this a semantic 3D (information) model?	YES
	2C2 - Is it a 3D mesh model?	YES
	2C3 - Can it be downloaded?	YES
	2C4 - Is it free?	YES
	2C5 - Can it be downloaded without registration?	NO
	2C6 - Is it available for download in more than one format?	YES
	2C7 - Is it generated using open data standards?	NO
	2C8 - Is it openly licensed?	NO
	2C9 - Does it provide metadata?	YES
	2C10 – Has it been published recently (in the last 5 years)?	NO
	2C11 - Is it up to date?	YES
	2C12 - Is there a plan to update?	YES
	2C13 - Does it preserve historical datasets?	NO
	2C14 - Does it include more than one level of detail (LoD)?	YES
	2C15 - Does it cover the entire administrative unit?	NO
Thematic content	3C1 - Are buildings modelled with semantic differentiated surfaces?	YES
	3C2 - Does it contain bridges?	YES
	3C3 - Does it contain land use?	YES
	3C4 - Does the terrain contain?	YES
	3C5 - Does it contain roads?	NO
	3C6 - Does it contain tunnels?	NO
	3C7 - Does it contain lines?	NO
	3C8 - Does it contain urban equipment?	NO
	3C9 - Does it contain vegetation?	YES
	3C10 - Does it contain individual trees?	YES
	3C11 - Does it contain water bodies?	YES
Attribute content	4C1 - Does it contain a postal code?	YES
	4C2 - Do buildings have a texture?	NO
	4C3 - Does the building ID contain?	NO
	4C4 - Does it have a year of construction?	NO
	4C5 - Does it contain the address of the buildings?	NO
	4C6 - Does it contain a building function?	YES
	4C7 - Does it contain the height of the buildings?	YES
	4C8 - Does the volume of buildings contain?	YES
	4C9 - Does it contain a catholicity?	NO
	4C10 - Does it contain a wall surface?	YES
	4C11 - Does it contain a roof surface?	NO
	4C12 - Does it contain a type of roof?	NO
	4C13 - Does it contain the surface of the terrain under the building?	NO
	4C14 - Does it contain gross floor area?	NO
	4C15 - Does it contain building materials?	NO

Such a status confirms the assumption of a quality concept and the correct development of the 3D model project of the City of Zagreb so far. However, it is necessary to bear in mind the shortcomings of the existing 3D model in terms of non-coverage, inhomogeneity and out-of-date existing data, which ultimately results in the necessary and unquestionable need for its further development and updating.

3 DISCUSSION

To improve the existing 3D model and create a digital twin for further development a set of guidelines is proposed.

When defining the guidelines, all the facts listed in the previous chapters were used, including the state of the art, regulations, theory, foreign experiences, characteristics of the existing model and the need for its application.

I) Selection of 3D model types:

- It is recommended to create a semantic 3D model of the level of detail LOD 2.2 for the entire city administrative area.
- It is recommended to create a network photo realistic 3D model for the area of protected building units and individual protected buildings outside protected units, as well as other significant buildings (investments, tourist significant buildings, etc.).

II) Priorities:

- It is recommended to create a semantic 3D model of the level of detail LOD 2.2 for the area not previously covered by the 3D model of the City of Zagreb (63% of the administrative area, approx. 20% and 40,000 buildings, respectively).
- It is recommended to create a semantic 3D model of the level of detail LOD 2.2 for all complete areas where in the existing model the data are at the level of detail LOD 1 (approx. 40,000 buildings).
- When updating, it is necessary to assess the state of the existing 3D model in a particular area, and accordingly maintain or delete the existing models. In doing so, it is necessary to consider the geometric accuracy and fidelity of the model, as well as recommendations on linking with official registers.
- It is recommended to carry out the update according to predefined milestones, and include the updated data as soon as possible in existing applications and applications, providing information on the up-to-date of the data.

III) To update the existing 3D model, it is proposed to use the data of multisensor imaging of the Republic of Croatia:

- It is recommended to use LiDAR data for the City of Zagreb as well as other products (DOF5, DMR and DMP) from multisensor imaging of the Republic of Croatia (SGA) to create a semantic 3D model of the level of detail LOD 2.2. This data can be used directly to update and complement the existing model with missing objects.
- It is recommended to use existing data sources (terrestrial and aero-photogrammetric UAV imaging) if they exist, or to conduct a new data collection (recommendation aero-photogrammetric UAV and/or LiDAR imaging) to create an online photo-realistic 3D model.

IV) Link the 3D model to the official registers:

- It is recommended to align the semantic model with the cadastral parcels of the real estate cadastre (land), according to the principle that one model of the building is located on a floor plan on one or possibly more cadastral parcels.
- It is recommended to align the semantic model with the official address model of the Regional Register of Spatial Units of the City of Zagreb
- It is recommended to align the semantic model in the future with the building register when it officially begins to be produced for the City of Zagreb.

V) Formats:

- It is recommended to convert all existing data once that will not be updated to CityGML 2.0 format and put such data to open use.
- It is recommended to convert new or updated data to CityGML 2.0 format and put such data to open use.

VI) Technology:

- It is recommended to use the ESRI technology platform because it enables the correct technical development of the model, and at the same time it is used as a basic GIS platform for the city administration.

VII) Recommendations for further maintenance and updating of data:

- It is recommended to maintain the new (or improved) model regularly, ideally when completing the construction of individual buildings, after the issue of a use permit or registration in the cadastre. Implementation requires the establishment of a clear procedure, work process, stakeholders and financial resources.
- It is recommended to update the complete model periodically, in accordance with the development of new official LiDAR and aero-photogrammetry imaging, or based on imaging specifically ordered for the purpose of updating the model.
- It is recommended to provide funding for model updates from sources outside the city budget (EU and national funds and projects). Funding is possible through projects using 3D models as a data source, analytics or visualisation technology and platform.

VIII) Recommendations for the development of a digital twin:

- When updating the existing 3D model, it is recommended to expand the model in thematic terms by including transport and energy infrastructure, and other content that is missing in the existing model and exists in the real world.
- It is recommended to connect the new (or improved) 3D model with various sensors in real-time (traffic, lines, environmental monitoring, etc.) which will support the monitoring and functioning of the city in real-time. Additionally, carry out accuracy and reliability analyses of the data collected so far.

4 CONCLUSION

This paper aimed to investigate if the existing Zagreb 3D city model fits the new challenges towards the digital twin and ultimately the smart city concept. The model was assessed by using different criteria. The general ones like completeness, coverage, homogeneity and up-to-dateness showed that there are serious gaps in the existing model. The further assessment used the 3D city index. The overall score shows that the existing model is not bad but however, needs improvement and future developments.

Based on the assessment results a set of recommendations (guidelines) is proposed. The guidelines

for further development and improvement cover the topics of choice of model type, priorities for updating, input data sources, technology, data format, further update, digital twin development, and application in smart city development.

By following the proposed guidelines, the existing Zagreb 3D city model could be significantly upgraded and improved to evolve towards the real digital twin.

Acknowledgment

The research was partially supported by University North, Croatia, Scientific project UNIN-TEH-24-1-16 "The role of geodesy and geomatics in the development of smart spaces (2024)".

5 REFERENCES

[1] Novaković, I., Ivan Bačić-Deprato, I., Franić, S. & Tonković, T. (2009). Izrada trodimenzionalnog modela Grada Zagreba. *Zbornik radova II. Simpozija ovlaštenih inženjera geodezije*, Opatija, 111-120. (in Croatian)

[2] Jurakić, G., Cetl, V. & Stančić, B. (2015). Testing the data quality of existing 3D model of the city of Zagreb. *Conference Proceedings of the 15th International Multidisciplinary Scientific GeoConference SGEM 2015 - Volume 2.* Retrieved from http://sites.umuc.edu/library/libhow/apa_examples.cfm

[3] Šiško, D., Cetl, V., Gavrilović, V. & Markovinović, D. (2022). Application of 3D City Model in Spatial Planning of the City of Zagreb. *Proceedings of XXVII FIG Congress*. Retrieved from https://www.fig.net/resources/proceedings/fig_proceedings/fig2022/papers/ts02g/TS02G_sisko_cetl_et_al_11603.pdf

[4] Šiško, D., Cetl, V. & Gavrilović, V. (2023). Spatial planning in the city of Zagreb. *GIM international magazine, 37*(4+5), 14-17.

[5] Stoter, J. E., Arroyo Ohori, G. A. K., Dukai, B., Labetski, A., Kavisha, K., Vitalis, S. & Ledoux, H. (2020). State of the Art in 3D City Modelling: Six Challenges Facing 3D Data as a Platform. *GIM International: the worldwide magazine for geomatics*. Retrieved from https://www.gim-international.com/content/article/state-of-the-art-in3d-city-modelling-2Reitzes

[6] See 3D City Index assessment tool, https://ual.sg/project/3d-city-index/

[7] Cetl, V. & Matijević, H. (2023). Design of the Zagreb Digital city twin project, *Study*, University North, Department of Geodesy and Geomatics.

[8] Novaković, I. (2011). 3D Model of Zagreb. GIM International. https://www.gim-international.com/content/article/3d-model-of-zagreb

[9] See City GML, https://www.ogc.org/standard/citygml/

[10] ZG3D: 3D model of the City of Zagreb, https://zagreb.gdi.net/zg3d/

[11] Lei, B., Stouffs, R. & Biljecki, F. (2022). Assessing and benchmarking 3D city models, *International Journal of Geographical Information Science*. https://doi.org/10.1080/13658816.2022.2140808

[12] Willenborg, B., Pültz, M. & Kolbe, T. H. (2018). Integration of Semantic 3D City Models and 3D Mesh Models for Accuracy Improvements of Solar Potential Analyses. *Int. Arch. Photogramm. Remote Sens. Spatial Inf. Sci., XLII-4/W10*, 223-230. https://doi.org/10.5194/isprs-archives-XLII-4-W10-223-2018

[13] See https://zagreb.hr/gradski-ured-za-gospodarstvo-ekolosku-odrzivost-i-/175274

[14] See Urban Analytics Lab, https://ual.sg/

[15] Wagner, D., Alam, N., Wewetzer, M., Pries, M. & Coors, V. (2015). Methods for geometric data validation of 3D city models. Int. Arch. Photogramm. *Remote Sens. Spatial Inf. Sci., XL-1-W5*, 729-735. https://doi.org/10.5194/isprsarchives-xl1-w5-729-2015

[16] Biljecki, F., Ledoux, H., Du, X., Stoter, J., Soon, K. H. & Khoo, V. (2016). The most common geometric and semantic errors in CityGML datasets. *ISPRS Annals of Photogrammetry, Remote Sensing & Spatial Information Sciences, IV-2*/W1, 13-22. https://doi.org/10.5194/isprs-annals-IV-2-W1-13-2016

[17] Ledoux, H., Arroyo Ohori, K., Kumar, K., Dukai, B., Labetski, A. & Vitalis, S. (2019). CityJSON: A compact and easy-to-use encoding of the CityGML data model. *Open Geospatial Data, Software and Standards, 4*(1), 1-12. https://doi.org/10.1186/s40965-019-0064-0

[18] Tang, L., Ying, S., Li, L., Biljecki, F., Zhu, H., Zhu, Y., Yang, F. & Su, F. (2020). An application-driven LOD modeling paradigm for 3D building models. *ISPRS Journal of Photogrammetry and Remote Sensing*, 161, 194-207. https://doi.org/10.1016/j.isprsjprs.2020.01.019

[19] Labetski, A., Kumar, K., Ledoux, H. & Stoter, J. (2018). A metadata ADE for CityGML. *Open Geospatial Data, Software and Standards, 3*(1). https://doi.org/10.1186/s40965-018-0057-4

[20] Shannon, J. & Walker, K. (2018). Opening GIScience: A process-based approach. *International Journal of Geographical Information Science, 32*(10), 1911-1926. https://doi.org/10.1080/13658816.2018.1464167

[21] Biljecki, F., Stoter, J., Ledoux, H., Zlatanova, S. & Çöltekin, A. (2015). Applications of 3D city models: State of the art review. *ISPRS International Journal of GeoInformation, 4*(4), 2842-2889. https://doi.org/10.3390/ijgi4042842

[22] Komadina, A. & Mihajlović, Ž. (2022). Automated 3D Urban Landscapes Visualization Using Open Data Sources on the Example of the City of Zagreb. *KN J. Cartogr. Geogr. Inf*. 72, 139-152. https://doi.org/10.1007/s42489-022-00102-w

Authors' contacts:

Vlado Cetl, Prof.
(Corresponding author)
University North,
Ul. 104. brigade 3, 42000 Varaždin, Croatia
vcetl@unin.hr

Darko Šiško, PhD
City of Zagreb,
Park Stara Trešnjevka 2, 10000 Zagreb, Croatia
darko.sisko@zagreb.hr

Hrvoje Matijević, Prof.
University North,
Ul. 104. brigade 3, 42000 Varaždin, Croatia
hmatijevic@unin.hr

Danko Markovinović, Prof.
University North,
Ul. 104. brigade 3, 42000 Varaždin, Croatia
dmarkovinovic@unin.hr

ISSN 1846-6168 (Print), ISSN 1848-5588 (Online)
https://doi.org/10.31803/tg-20240910101801

Original scientific paper
Received: 2024-09-10, Accepted: 2024-10-25

Developing of a Digital Twin for Urban Planning in an International Context

Darko Šiško*, Vlado Cetl, Hrvoje Matijević

Abstract: The digital twin, adapted to the needs of urban planning and monitoring systems, is the subject of research and development in the academic, commercial and public sectors. The article provides international context in conceptual and practical implementation through their maturity level, scope, purpose, structure, input, processing features and output. The City of Zagreb is presented as an example of the implementation of GIS and 3D city models in urban planning, with activities towards a digital twin city. Based on research and local specifics, the concept of a digital city twin was proposed for the needs of urban planning, and future challenges were identified.

Keywords: digital twin; City of Zagreb; international context; urban planning

1 INTRODUCTION

The digital twin, adapted to the needs of urban planning and monitoring systems, is the subject of research and development in the academic, commercial and public sectors. To develop such a complex tool for urban planning, many aspects need to be explored and fulfilled.

Urban planning and monitoring systems traditionally use a wide variety of spatial data sets. Data management, analysis and creation have evolved from analogue techniques to 2D GIS and 3D city models. The next step is to build digital twins for urban planning. This can be achieved by integrating digital twins with official and real-time data and by introducing improved analytical and simulation models into them.

The digital twin city is an actual topic of many world's researchers in different aspects of purpose, structure, technology, data sources and tools. However, existing case study comparisons tend to be general and not specifically focused on the topic of urban planning and monitoring. Digital twin for urban planning and monitoring is a specific type of digital twin with specific research and development challenges and questions, considering 3D city model type and quality, government data integration, need for live data, data visualization issues, simulation issues, planning functionalities and tools.

This paper provides an overview of historical and current research on the topic, from the need for spatial data in urban planning, to the role of 3D models, and finally the transformation into digital city twin.

Selected international digital city twin projects and initiatives are used as a background to define the characteristics of a generic digital city twin for urban planning.

The new Zagreb digital twin was proposed on the basis of a generic model, existing achievements in the use of 3D city models for urban planning, and local specificities.

2 SPATIAL DATA FOR URBAN PLANNING

The basis for urban planning and monitoring system are quality and up-to-date spatial data and information, managed by geoinformation systems and technologies. In urban planning systems, spatial data on city's present and past is used to transform goals and objectives of society into formal urban plans and documents. Urban monitoring systems uses real-time spatial data to monitor and supervise practical implementation of urban plan regulations [1] (Fig. 1).

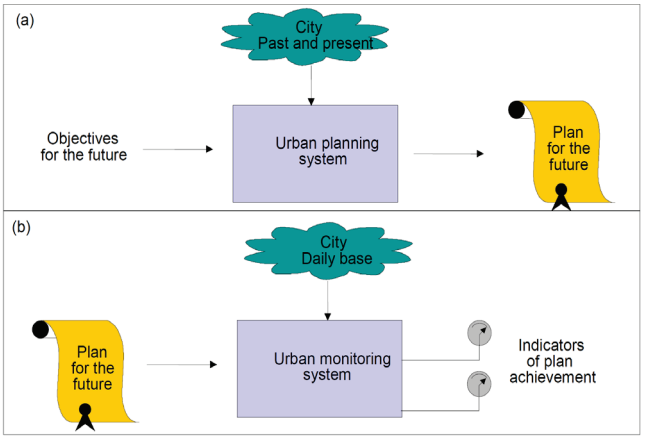

Figure 1 Urban planning and urban monitoring system [1]

The process is also seen as a spatial planning cycle, which consists of [2] (Fig. 2):

1) spatial policies
2) implementation
3) monitoring and evaluation.

According to [3], spatial information analysis and spatial planning are part of a wider land management system. Society's needs and spatial information are the basis for decision-making on the general goals of land development. These goals are the input for the spatial planning system, followed by implementation measures and monitoring of practical results.

Urban planning uses a wide range of spatial data and information during the analytical phase. These data come from several professional areas, e.g. [4, 5]:

- topography
- hydrology
- geology

- climate
- vegetation
- infrastructure
- land use
- land cover
- demography
- economy
- housing, etc.

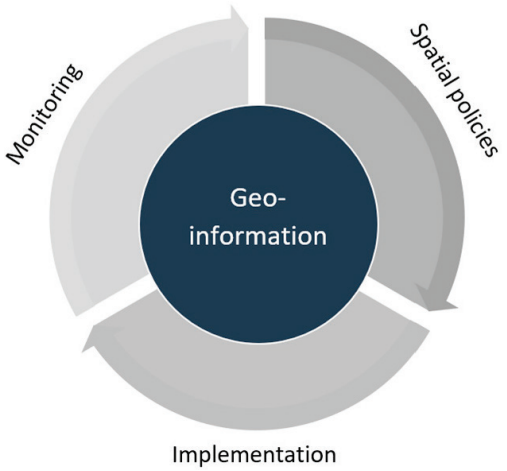

Figure 2 Geoinformation and spatial planning cycle [2]

In a narrower sense, the urban planning and monitoring system focuses on creating and implementing of land use plans and monitoring of land use changes.

3 THE ROLE OF 3D MODELS AND DIGITAL TWINS IN URBAN PLANNING

With the development of geospatial technologies in the collection, processing and visualization of spatial data, the next step was the creation and use of 3D models of cities in urban planning. The main advantages of the use of 3D models were new visualization and analytical tools, such as [6]:

- overlay of 3D model and 2D land use maps
- 3D visualization of urban plan regulation scale
- 3D visualization of proposed buildings purpose
- 3D visualization of urban greenery structure
- 3D measurements and quantifications
- shadow analysis
- line of sight analysis
- 3D visualization of statistical data
- photo visualization etc.

The transformation from traditional cities to smart cities has brought forward new urban development requirements that can be supported by emerging technologies. The emerging field of City Digital Twins has advanced with the help of digital infrastructure and technologies connected to the Internet of Things (IoT) [7]. The collection of spatial data and the creation of a 3D city model are recognized as two initial phases (out of six) in the development of a complete digital city twin [7, 8] (Fig. 3).

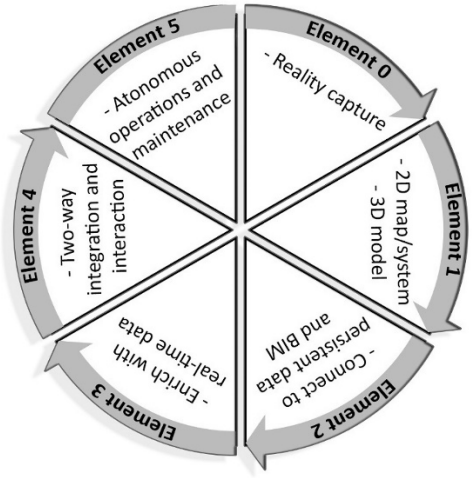

Figure 3 Digital twin maturity levels (elements) and descriptions [7]

In the scientific and cultural debate of the discipline of urbanism, the concept of the digital twin applied to cities, sustainable urban policy development and governance is currently one of the most discussed and cutting-edge topics [9], although the topic has been experimented mainly in scientific fields of geomatics and information technology.

The field of urban planning needs specific spatial tools for urban change detection and optimization of impact of new development projects on existing urban environment. Digital city twin is viewed as a virtual 3D environment designed for urban monitoring, collaboration between different stakeholders, and practical research. Its aim is to help create cities that are more flexible, healthier, and more livable.

Digital twin characteristics are highly dependent on their use (i.e., users, lifecycle stage and application) and share few similarities, with digital model of the physical city as the foundation for other thematic modules [10].

Urban planning and asset management are recognized as the main users of the basic digital city twin model, while other main thematic modules are:

- urban mobility
- water management
- energy management
- environment and climate.

Table 1 Example of functional and physical layers of modules for urban planning and urban mobility in the modular digital city twin concept, according to [10]

Module	Urban planning	Urban Mobility
Service / actuation layer	Urban planning, asset management	Mobility management, road infrastructure, noise monitoring
Simulation layer	3D visualization	Simulation, logic operation, machine learning
Digital modelling layer	City information model	Mobility simulation model
Data acquisition layer	Terrestrial/aerial imagery, cadastre, geodata, asset database	Video surveillance, microphones, public transport database
Physical layer	City	Private mobility, public transport, road infrastructure

Tab. 1 shows the example of functional and physical layers of digital twin for urban planning and asset management module (user of basic digital twin model) and mobility management module (one of main thematic modules), according to [10]. Intended users of the system are public administration, citizens, asset owners, asset managers and researchers.

4 DIGITAL CITY TWINS IN INTERNATIONAL CONTEXT

Benchmarking of international digital city twin projects and initiatives is used as background for development of the concept of new digital city twin for urban planning. Methodology and data are based on tree relevant international studies and experiences [7, 9, 10].

Masoumi et al. from 2023 [7] compared 10 case studies from existing literature on digital twins in Europe, Asia, North and South America. Main research topics were purpose, technologies, data type and further development.

Caprari et al. from 2022 [9] analysed scientific articles on 23 digital twin projects in urban planning context from Europe, North America, Asia and Oceania. For selected 5 cities the comparison questions were digital twin type, scale, purpose, technologies, experiments, strengths and weaknesses (Tab. 2).

Ferré-Bigorra et al. from 2022 [10] made a review of 22 research papers and conference abstract on digital twins for the cities in Asia, Europe, Africa, North America and Oceania. The research was based on several indicators organized in thematic groups: application data, input data, processing data and output data.

In these studies, urban planning is recognized as one of the main beneficiaries of digital twin cities. According to [7], urban planning is the most common application by keyword search (Fig. 5), while in [10] urban planning is recognized as the second most frequent, after city management and maintenance.

Table 2 Example of comparison of digital twins used for urban planning issues, according to [9]

	Cambridge	Zurich, Dublin, Helsinki	Singapore
Type	Static and managerial	Dynamic-evolutive	Dynamic-evolutive
Scale	Supra-municipal	City, sub-areas, district	City-State
Purpose	Multi-level platform for cooperation between different planning levels	Data-driven preventive assessment, scenarios in sustainable urban development	Decision support platform
Technology	GIS-processing	GIS-BIM, Laser Scanner, UAV, IoT,	GIS-BIM, Satellite imagery, Lidar, Deep and machine learning, AI

When it comes to [9], urban planning is the main focus of the study, with detailed subtopics such as cooperation between different planning levels, scenarios for support in sustainable urban development policies, democratisation of decision-making processes and decision support platform.

Based on research topics and case studies, main characteristics of digital twin relevant for urban planning were selected as follows:

1) **Maturity level**. 3 or more, integrated 2D, 3D and real-time data, two-way interaction
2) **Scale**. City (administrative), sub – areas, projects
3) **Purpose**. Planning support, decision support, multi stakeholder collaboration, scenarios, citizen involvement, data integration
4) **Structure**. Modular system, common digital twin platform and urban planning module as one of connected thematic modules for specific purposes
5) **Input data**. 3D city model, government data, GIS, real-time sensors, urban planning data
6) **Processing features**. 3D visualization, urban simulations
7) **Output**. 3D application, dashboard, AR/VR

Besides the recommended characteristics, practical implementation of digital city twin for urban planning have to include local specificities and user needs.

5 3D CITY MODEL IN URBAN PLANNING OF THE CITY OF ZAGREB

Since 2008, the City of Zagreb has been developing a semantic 3D city model. The spatial planning department was identified as the primary user and developer of the project, with additional users found in areas such as emergency management, environmental protection, energy, and heritage conservation [11, 12].

This 3D city model has been used in Zagreb's spatial planning for tasks like master and detailed planning, architectural competitions, and development within the city's protected core. In land use planning, the model helps planners verify proposed building regulations against existing conditions, making adjustments based on the heights and volumes of current structures. Additionally, the combination of land use maps and digital terrain models (DTM) aids in planning hilly or mountainous areas, taking into account terrain constraints and landslide risks.

In detailed urban planning, the 3D city model serves as a tool for assessing existing structures and for creating and presenting building regulations to the public. It allows 3D building outlines to be visualized, showing the potential future size and dimensions of buildings in a virtual environment, making it easier for both local residents and city officials to understand proposed developments (Fig. 4).

Architects were among the first to use 3D data, especially for illustrating how proposed buildings would impact their surroundings. Previously, these visualizations were created by estimating building heights and shapes without precise spatial references.

The introduction of 3D city models provided architects with these missing elements, along with the ability to integrate various spatial data. After Zagreb introduced its 3D model, architects began using it for analysis and visualization

in architectural competitions and for designing new structures in the city center (Fig. 5). This approach allows for more accurate spatial solutions and better-informed urban planning decisions.

Figure 4 3D interpretation of detailed urban plan overlapping 3D city model [11]

The city also plans to upgrade the 3D model to support the development of a digital city twin. The study was made in cooperation with University North, Croatia [13], with guidelines considering model types, data update methods and priorities, data sources, data integration, data formats, software technology, smart city and digital twin issues.

The latest update of the LoD 2.2 model is based on official LiDAR survey of the Republic of Croatia from 2022, and will be used as a starting point for further improvements.

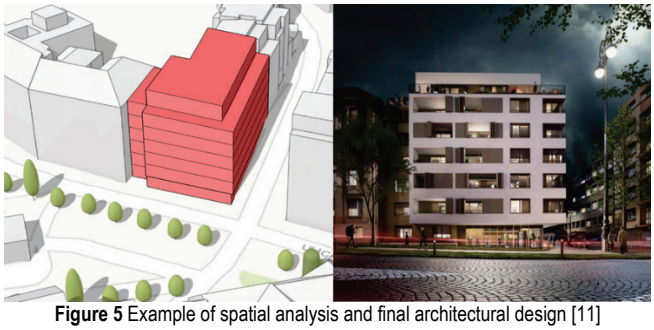

Figure 5 Example of spatial analysis and final architectural design [11]

6 DEVELOPMENT OF ZAGREB DIGITAL TWIN

The City of Zagreb has started activities on the development of a comprehensive digital city twin. The initiative came as the next step after GIS and 3D model implementation in the city administration, and also influenced by development of Smart City concept and practical project implementations.

Three different city administrative units were recognized as stakeholders in comprehensive digital city twin project:

- Department for GIS and urban analytics
- Department for development of smart city
- Service for city IT infrastructure.

The role of the GIS and urban analytics department is to develop and update the 3D model of the city and all key GIS databases. In addition, their important role is the development of generic visualization and analytical features of the system. The Department for Smart Cities should define the strategic position of the digital twin in the overall strategy and activities of the smart city and coordinate the users of the digital twin within the city administration and beyond. The IT service must provide the entire IT infrastructure, with a special focus on the integration and harmonization of data sources in real time.

The City plans to develop common digital twin platform and thematic modules for specific administrative and professional needs. Based on research and previous experiences, some of the key topics were identified as city planning, environment protection, energy management, climate, urban mobility and emergency management. Besides that, modular approach gives opportunity for other thematic fields to join the project in the future.

Zagreb digital city twin platform is based on 3D city model, connected to all relevant data – city and national SDI services, national government registers, real-time data from smart city sensors and other thematic data for different uses (Fig. 6). Common digital twin platform has to provide basic 3D visualization and analytical features, while specific visualization, analytical, simulation and workflow features are planned to be developed as part of thematic modules.

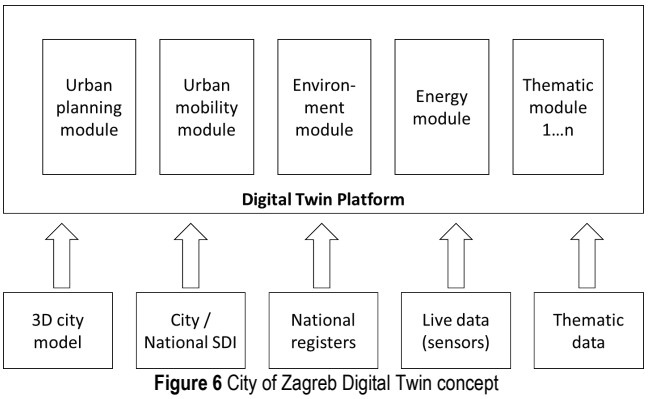

Figure 6 City of Zagreb Digital Twin concept

Urban planning module is expected to be one of the first to be implemented, considering rich experience in using 3D model and GIS databases in that professional area. Except the user needs, modelling this thematic module must be in line with the development of national digital urban planning tools, e-Plans and e-Plans editor [14]. Urban planning module is expected to have several user groups:

- urban planners
- city administration
- architects and engineers
- academia
- civil society
- citizens.

Final visualization and analytical features of the model still must be considered and discussed with final users, and basically will include:

- 3D city model visualizations
- data and information integration
- simulations of urban plan regulations
- land use change detection
- monitoring of spatial development.

Considering the planned user groups, their needs and basic analytical features, data themes were identified, together with their sources and needed update cycles (Tab. 3).

Table 3 Data themes, update cycles and sources for urban planning module of digital city twin

Data theme	Update cycle	Source
3D semantic model, LoD 2.2	Annual, change detection	LiDAR 2022, UAV surveying
3D photorealistic model	Annual, change detection	UAV surveying
Land use	Planning cycle	Land use maps
3D detailed urban plans	Planning cycle	Detailed plans maps
Architectural competitions	Competitions cycle	Architectural plans
Land parcels	Daily	National register
Planned buildings	Daily	National register
Urban greenery	Daily	City green cadastre
Population distribution	Census / Daily	Census / National register
Thematic GIS layers	Daily	City and National SDI

Special attention should be paid to the 3D model of the city, because it is a prerequisite for most visualizations and analytical features. Periodic updating from national LiDAR surveys is a potential solution, with an alternative approach in change detection from cadastral records and annual updating for selected locations using UAV imagery.

Although real-time data is usually a core part of any digital twin city, none of the smart city sensors have been identified as essential for the urban planning module.

In addition to the topic of real-time data, the main challenges identified at the moment are issues related to urban simulation features, the relationship between the digital twin and the formal urban planning process, and VR/AR visualizations.

7 CONCLUSION

The urban planning and monitoring system is a traditional and important user of spatial and non-spatial data, as well as an important initiator and stakeholder in the development of new smart spatial technologies such as the digital city twin.

The topic of digital twins of cities and urban areas is the subject of many researchers around the world. Academic studies of several researches and projects of digital city twins show the complexity of the topic and different approaches in practical implementations in different cities and different users.

One of the conceptual solutions is to organize a digital city twin as a modular system with a common information platform and several thematic modules. Elements of such a concept include maturity level, scope, purpose, structure, input, processing features, and output.

The City of Zagreb is an example of the implementation of GIS and 3D city models in urban planning, with practical projects of general and detailed planning, architectural competitions and interpolations in protected areas. The city administration is working on upgrading the 3D model of the city for the needs of the future digital city twin.

Based on relevant research and local specifics, the concept of a digital city twin was proposed for the needs of urban planning. The main stakeholders of the project are the city departments for GIS, smart city and IT infrastructure. Key users and visualization and analytical features are defined, as well as a list of data topics, update cycles and data sources.

Developing a digital city twin for urban planning is a complex process with several challenges. Issues of updating 3D city models, using real-time data, visualization and simulation features, and the relationship with the formal urban planning process are still topics for academic research and government consideration.

Acknowledgment

The research was partially supported by University North, Croatia, Scientific project UNIN-TEH-24-1-16 "The role of geodesy and geomatics in the development of smart spaces (2024)".

8 REFERENCES

[1] Laurini, R. (2001). *Information Systems for Urban Planning: A Hypermedia Co-operative Approach*. Taylor and Francis, London

[2] Louwsma, M. & Şahinkaya Özer, C. (2022). Spatial Planning and Geospatial information. *Geospatial Data in the 2020s, Transformative Power and Pathways to Sustainability, FIG Publication No 78,* 21-33, https://fig.net/resources/publications/figpub/pub78/Figpub78.pdf

[3] Larsson, G. (1997). *Land management – Public Policy, Control and Participation*. The Swedish Council for Building Research, Stockholm.

[4] Prinz, D. (1980). *Städtebau, Band 1: Städtebauliches Entwerfen*. Kohlhammer, Stuttgart. (in German)

[5] Marinović-Uzelac, A. (2001.). *Prostorno planiranje*. Dom i svijet, Zagreb. (in Croatian)

[6] Jonas, D. (2014). Utilising the Virtual World for Urban Planning and Development. *FIG Congress 2014*, https://www.fig.net/resources/proceedings/fig_proceedings/fig2014/papers/ts10h/TS10H_jonas_7036.pdf

[7] Masoumi, H., Shirowzhan, S., Eskandarpour, P. & Pettit, C., J. (2023). City Digital Twins: their maturity level and differentiation from 3D city models. *Big Earth Data, Volume 7, 2023 - Issue 1, Taylor & Francis Online,* 1-36. https://doi.org/10.1080/20964471.2022.2160156

[8] Evans, S., Savian, C., Burns, A. & Cooper, C. (2019). Digital twins for the built environment: An introduction to the opportunities, benefits, challenges and risks. *The Built Environment Panel of the Institution of Engineering and Technology (IET)*, https://www.theiet.org/media/8762/digital-twins-for-the-built-environment.pdf

[9] Caprari, G., Castelli, G., Montuori, M., Camardelli, M. & Malvezzi, R. (2022): Digital Twin for Urban Planning in the Green Deal Era: A State of the Art and Future Perspectives. *Sustainability 2022, 14, 6263*. https://doi.org/10.3390/ su14106263

[10] Ferré-Bigorra, J., Casals, M. & Gangolells, M. (2022): The adoption of urban digital twins. *Cities, Volume 131, December 2022*, *103905*. https://doi.org/10.1016/j.cities.2022.103905
[11] Šiško, D., Cetl, V., Gavrilović, V. & Markovinović, D. (2022). Application of 3D City Model in Spatial Planning of the City of Zagreb. *FIG Congress 2022*, https://www.fig.net/resources/proceedings/fig_proceedings/fig2022/papers/ts02g/TS02G_sisko_cetl_et_al_11603.pdf
[12] Šiško, D., Cetl, V. & Gavrilović, V. (2023). Spatial planning in the city of Zagreb. *GIM International, Issue 4+5 2023, Volume 37*, https://www.gim-international.com/content/article/spatial-planning-in-the-city-of-zagreb
[13] Cetl, V. & Matijević, H. (2023). *Izrada koncepcije projekta Zagreb Digital city twin.* Sveučilište Sjever, Varaždin. (in Croatian)
[14] Habrun, S. (2022). Aktualnosti iz Informacijskog sustava prostornog uređenja - ususret prostornim planovima nove generacije. *13. NIPP i INSPIRE dan*. https://www.nipp.hr/UserDocsImages/dokumenti/skupovi/13/1_Habrun_DanIPP2022_Habrun_OCR.pdf?vel=3919908 (in Croatian)

Authors' contacts:

Darko Šiško, PhD
(Corresponding author)
City of Zagreb,
Park Stara Trešnjevka 2, 10000 Zagreb, Croatia
darko.sisko@zagreb.hr

Vlado Cetl, Prof.
University North,
Ul. 104. brigade 3, 42000 Varaždin, Croatia
vcetl@unin.hr

Hrvoje Matijević, Prof.
University North,
Ul. 104. brigade 3, 42000 Varaždin, Croatia
hmatijevic@unin.hr

ISSN 1846-6168 (Print), ISSN 1848-5588 (Online)
https://doi.org/10.31803/tg-20240910121606

Original scientific paper
Received: 2024-09-10, Accepted: 2024-11-12

Assessment of Solar Photovoltaic Potential of Building Rooftops Based on Multicriteria Spatial Analysis

Natasha Malijanska Andreevska*, Gjorgji Gjorgjiev, Emilija Bozhinov

Abstract: This paper presents a methodology using Geographic Information Systems (GIS) to assess the photovoltaic potential of building rooftops by applying available data in North Macedonia. Applied to a case study, the method encompasses a high-resolution 3D model from LiDAR data to accurately represent rooftop surfaces and terrain. The approach includes generating a Digital Surface Model (DSM), analysing rooftop slopes and aspects, calculating solar radiation, and identifying suitable rooftops. It was concluded that out of 628 buildings, an area of 73 544 m², about 62% of the total rooftop area, is suitable for photovoltaic system installation. The potential electricity production from each building varies from 4 MWh to 1000 MWh annually and can be estimated at a total of 11 329 MWh from all suitable rooftops within the study area. The proposed method enables a large-scale valuation of suitable roof surfaces for photovoltaic system installation.

Keywords: building rooftops; GIS; LiDAR; solar potential; spatial models

1 INTRODUCTION

In recent decades, the world has undergone rapid urbanization, technological advancement, and industrial growth. While these developments have brought many benefits, they have also resulted in increased electricity consumption and increased atmospheric pollution. According to a United Nations report [1], although cities cover only 3% of the Earth's surface, their contribution is up to 80% of global energy consumption and 75% of greenhouse gas emissions. Rapid urban development and the electricity demand represent a complex challenge that requires innovative solutions, finding new ways to sustainably satisfy this demand, without negative impact on the environment or the economy. One of the potential solutions for addressing this challenge is focusing on the use of renewable sources of energy. Among them, solar energy is the most promising one.

In urban areas, where solar energy is generally one of the more accessible renewable energy sources, building rooftops is considered one of the most suitable locations for installing a photovoltaic system for electricity production. However, it is important to note that not all roof surfaces are equally suitable for installing a photovoltaic system. The identification of suitable building rooftops in terms of their solar potential and estimation of the amount of electricity that could be produced if there is a photovoltaic system installed can be performed using multicriteria spatial analysis utilizing GIS.

In recent years, innovations like advanced data analysis have made it possible to realistically evaluate the prospects of deploying rooftop solar photovoltaic systems. Gagnon et al. (2016) studied the solar capacity and photovoltaic potential over the entire USA in detail by estimating the solar resources both in terms of amount and geographical distribution. The author's findings highlighted sustainable energy production from urban Rooftops and stressed the regional differences in solar potential across the country by showing notable scope for photovoltaic deployment [2].

Palmer et al. (2018) developed a GIS-based methodology employing LiDAR and photogrammetry data to investigate the rooftop-portion of urban areas that can be devoted to photovoltaic installations. This allows for the spatial analyses of rooftops by reinforcing the scale's components such as slope, orientation, and shading and therefore supporting on estimation of the solar energy production potential [3].

Huang et al. (2022) went further by utilizing GIS methodologies when carrying out a case study in Japan, that compared solar potential on rooftops applying remote sensing and solar radiation datasets. The comparison made it clear that it is necessary to use diverse sources of information for better accuracy of solar potential resources. Huang et al have shown that in places with immense rooftop infrastructures (which are often the case in urban environments), combining imagery with solar radiation data, can improve the assessment's accuracy of how much solar energy can be collected [4].

In a recent study, Kozlovas et al. (2023) examined the feasibility, both technical and economic, of the respective rooftops with photovoltaic units in cities of Lithuania. Their study involved a self-determined search encompassing the cost of installing solar photovoltaic units, energy conservations and returns on investments, thus enhancing research on economic aspects of rooftop solar resources. Kozlovas et al. argued that besides factors related to the building, the level of economic is also important when looking for the factors that would increase the use of rooftop photovoltaic systems. This combination of the two parameters provides decision-makers a better idea about the case in hand regarding deployment of photovoltaic technologies [5].

Assessing photovoltaic potential of building rooftops is highly dependent on the available data sources, and consequently, the applied methodology needs to be adapted accordingly. Today many recent or ongoing research are focusing on this topic trying to incorporate different parameters coming out from many different data sources. In

general, four potentials can be incorporated into the estimation model: physical, geographical, technical, and economic potential [6].

Depending on the level of requested assessment accuracy, different types of data could be incorporated. Spatial data used in the assessments can go from statistical data for assessing types of buildings and roof characteristics, all the way to LiDAR scanning or photogrammetry-based data for modelling the position, type, and orientation of the building rooftops.

Large-scale assessment usually is based on statistical data where roof types and roof surfaces are statistically calculated. Calculations of the needed parameters are based on other available data such as the size of the municipality, number of inhabitants, building types, etc. [7]. Further on, additional spatial data such as satellite images, airborne images, and land use data combined with other relevant statistical data is used to provide better estimation results [8]. As details are increasing the assessment accuracy is higher and better. For higher accuracy assessment, usually on smaller target areas, 3D City models are used with LoD not less than 2, or LiDAR data to provide higher detailed model of building rooftops [9, 10].

2 METHODOLOGY

The purpose of this paper is to evaluate the solar photovoltaic potential of building rooftops, by applying GIS technology and available spatial data in the Republic of North Macedonia. The main objective is to estimate the photovoltaic potential for individual rooftops on each building, as well as to determine the total photovoltaic potential across all buildings in the study area that are suitable for installing photovoltaic systems. The research was conducted as a case study in a particular urban area, in which a three-dimensional model had been developed. This included topographic features of the terrain, together with a three-dimensional surface model that represented morphological characteristics of the building's rooftop surfaces.

Assessment methods and approaches for determining rooftop photovoltaic potential vary, most of them rely upon a common foundation: the use of a digital surface model to execute the assessment. The DSM contains crucial information on elevation, not only of the buildings themselves but also of surrounding objects, which once more is an essential ingredient in arriving at a reasonably accurate estimate of solar energy.

As already mentioned in the introduction, most of the methodologies proposed to estimate the photovoltaic potential take into consideration four categories of potential: physical, geographical, technical, and economic potential [11]. Each of the above contributes to a holistic view of solar energy potential, but their usefulness varies depending on the study or area under consideration.

In the specific approach adopted in this research, emphasis is placed on physical and geographical potentials, as these two have a direct and significant impact on the initial stages of estimating photovoltaic feasibility.

Physical potential refers to the total amount of solar radiation that reaches a given area over a specific period. It considers factors such as latitude, weather conditions, and the amount of sunshine received throughout the year. This potential provides a raw estimate of how much energy can be captured in the absence of obstacles. It is crucial for determining how much solar energy can be generated under ideal conditions, setting the baseline for further analysis.

Geographical potential, on the other hand, involves a more detailed spatial assessment. It focuses on the physical characteristics of the rooftop and its surroundings. This includes the shape, orientation, and slope of the roof, as well as the height and proximity of surrounding buildings, trees, or other structures that might obstruct sunlight. These elements influence how much of the solar energy calculated in the physical potential can actually be captured by photovoltaic panels. In urban environments, this factor is particularly important due to the potential for shadowing from neighbouring structures, which can significantly reduce the efficiency of solar panels.

By focusing primarily on physical and geographical potentials in this research, a more accurate estimation of photovoltaic potential can be achieved, especially in densely populated or built-up areas. Once the physical potential provides the theoretical energy input, the geographical potential allows for adjustments based on real-world conditions, ensuring that the final estimates reflect both the available sunlight and the practical limitations of the built environment.

Technical and economic potentials, although crucial in a broader energy planning context, are considered secondary in this particular study. Technical potential typically addresses the efficiency of solar panels and the feasibility of installation, while economic potential considers cost-benefit analyses and return on investment. These factors are often applied after the physical and geographical potentials have been thoroughly assessed to fine-tune the feasibility and scalability of solar installations.

To achieve the highest possible DSM accuracy as a necessity for accurate assessment of photovoltaic potential, the three-dimensional model of the urban area could be generated using a LiDAR point cloud data. The LiDAR point cloud enabled the development of a high-resolution 3D model, which is vital for accurately capturing the characteristics of building roof surfaces, necessary to obtain the most reliable information about the solar photovoltaic potential of the building. In this context, Palmer et al. (2018) suggested a new method for identification of suitable rooftop areas based on LiDAR data by applying criteria related to slope, aspect, and minimum suitable rooftop area, but doesn't go further in estimating potential electricity production from the suitable roof surfaces [3].

In this research the methodology for assessment of the solar photovoltaic potential of the roof surfaces was established based on multicriteria spatial analysis, integrating a three-dimensional urban area model, building footprints, and solar radiation data. This approach is conceptually close to the applied Method 1 in the study by Huang et al. (2022) where high-resolution DSM is used for identification of

suitable roof surfaces and estimation of potential electricity production [4]. This comprehensive approach allowed for a more accurate and detailed evaluation of each building solar energy potential by considering multiple factors that influence photovoltaic performance.

The process of assessment of solar photovoltaic potential of buildings consists of five consecutive steps:

1) Creation of Digital Surface Model (DSM) and extraction of building footprints,
2) Providing model for slope and aspect of roof surfaces,
3) Creating model of solar radiation for each roof surface,
4) Identifying appropriate roofs for installation of photovoltaic systems,
5) Assessment of solar photovoltaic potential of each building.

The **first step** of the process generates two key outcomes. The first outcome is the creation of a DSM, which is derived from the point cloud by utilizing only the first return points from the LiDAR beam. The DSM captures the highest elevation points on the surface, whether from buildings, vegetation, or terrain features. By providing a detailed representation of the surface's highest points, the DSM delivers valuable data for subsequent analyses, such as solar potential or shading effects. The second outcome is the building footprint extracted from the LiDAR point cloud data. These building footprints are basic inputs since they provide the bases for analysing rooftop photovoltaic potential. This potential is computed by means of roof geometry, but it is bounded within the areas set by the polygons representing building footprints. This ensures that only relevant portions of the Digital Surface Model (DSM) are considered in certain steps of the analysis.

The **second step** focuses on generating detailed data about the rooftop geometry, which is crucial for accurately assessing the photovoltaic potential of a building. Two key geometric factors, slope and aspect, play a significant role in determining how much solar radiation a roof can receive.

The slope of the roof defines the angle of incidence that the sunbeams have with the surface, the amount, and the period they are exposed to. A well-angled roof maximizes the capture of solar energy, therefore becoming more efficient in electricity production. On the contrary, a too-steep roof reduces the total solar gain.

The aspect of the roof includes the orientation, whether it is facing north, south, east, or west, which in turn decides upon the exposure of the roof to sunlight during the day and throughout the seasons of the year. In the northern hemisphere, south-oriented roofs have maximum sunshine, therefore, they are ideal for photovoltaic systems. East and west-facing roofs also present possibilities, though not as good as those oriented to the south, while north-facing surfaces receive considerably less solar radiation.

By accurately calculating the slope and aspect of each rooftop, this step enables a precise estimation of solar potential, ensuring that the placement of photovoltaic panels is optimized for maximum energy efficiency.

In the **third step**, the solar radiation at rooftop surfaces needs to be computed. An algorithm based on Rich et al. [12, 13, 14], Rich et al. 1994, Fu and Rich 2000, 2002 is employed for calculating the solar radiation, which integrates various factors to estimate how much solar energy a surface receives. These include the following:

1) Digital Surface Model: It provides the surface elevation and slope and aspect created in step two.
2) Sun position - The model simulates the movement of the sun during both the daily and yearly cycles and takes into account all variations in solar altitude and azimuth in a rough approximation of how much sunlight actually reaches the surface at given day and time of year.
3) Atmospheric Condition: This is a rough approximation of the amount of cloud cover, moisture, and scattering in the atmosphere. It subtracts from the calculated quantity the sun lost through the mentioned conditions.
4) Shading: Here, the model considers DSM to yield the shading from surrounding features that reduce solar exposure, such as hills or buildings.
5) Radiation Types: The model differentiates between direct, diffuse, and reflected radiation in developing an elaborate estimation of solar energy potentials.

These factors are combined to produce an estimation of solar radiation (W/m²). The output of the step three is a solar radiation raster that registers the amount of solar radiation at each pixel.

The **fourth step** deals with selection of suitable roof surfaces for electricity production. All roof surfaces have different potentials for electricity production, depending on factors like slope, aspect, and exposure to solar radiation. The identification of suitable roof surfaces for electricity production involves elimination of roof surfaces that do not meet specific criteria. The selection process includes the following criteria groups:

- *Elimination of excessively steep surfaces:* Such roofs that are steeply angled are not fit for installation of solar panels. Shading often result from their nature and the angle is quite high to expose fully sunshine on the solar panels.
- *Exclusion of areas with insufficient solar radiation:* Roof surfaces receiving poor solar irradiance, whether because of the effect of shading by nearby objects or orientation, will not be suitable for electricity generation.
- *Removal of north-facing surfaces:* In the Northern Hemisphere cases, north-facing roofs receive hardly any sunlight and so are usually inefficient for solar energy generation.

After filtering out all unsuitable roof surfaces, the remaining suitable surfaces are identified, and a raster model is generated, consisting solely of pixels that meet the predefined criteria. This raster represents the areas with optimal conditions for solar energy production.

The **fifth step** as a final one is providing the assessment of solar potential for each building in the model. The solar potential per building is determined by first grouping all pixels identified as suitable within a specific building and calculating both the total area they occupy and the mean solar radiation value (in kWh/m²) from each cell in the raster model within that particular building footprint. The size of the suitable roof area is one of the main factors in consideration for the assessment of the building's suitability for installing photovoltaic panels.

Roofs with suitable area less than the defined minimum in square meters are considered too small for installation of

photovoltaic panels from economical aspect and have been excluded from further analysis. For the rest of the buildings, with suitable roof areas above the minimum defined area, total solar radiation is calculated for every single building.

The total solar radiation per building is expressed in megawatt-hours per square meter (MWh/m²) and is calculated using the following formula:

$$\text{Solar radiation per building} = (\text{Suitable area} \times \text{Mean solar radiation})/1000$$

To estimate the potential electricity production, the total solar radiation is converted using the following formula:

$$\text{Electricity production potential} = \text{Total solar radiation per building} \times 0.16 \times 0.86$$

In this calculation, the energy production depends not only on solar radiation but also on the efficiency of the solar panels and the system's performance ratio. According to the US Environmental Protection Agency (EPA), a conservative estimate for solar panel efficiency is 16%, meaning that 16% of the incoming solar energy is converted into electricity. Additionally, the performance ratio of 86% reflects the system's ability to retain and store 86% of the electricity generated as it passes through the installation [15].

These values are used to provide an accurate estimation of the building's potential for solar electricity production, factoring in both the available roof area and the efficiency of the technology in place.

3 CASE STUDY

To test the proposed methodology, a research area was selected, focusing on a section of the central part of the town of Strumica. The town is situated in the southeastern Republic of North Macedonia, in the western part of the Strumica Valley, at 41° 26' N latitude and 22° 38' E longitude, at an average elevation of 230 meters above sea level.

Strumica is well-known for its long periods of sunshine and high light intensity, factors that enhance its solar energy potential. On average, the region experiences approximately 230 sunny days per year, or around of 2,377 hours of sunshine annually, making it an ideal candidate for solar energy studies.

The selected research area, covering 38 hectares in the city centre, was chosen with the aim of assessing the solar photovoltaic potential of building rooftops. This area includes buildings with various heights, sizes, and types such as: individual and collective residential buildings, public and commercial buildings, a shopping centre, schools, a kindergarten, a hospital, and many more. These buildings are characterized by various geometries and roof types, with different slopes and orientations of the roofs, which is considered one of the important factors when studying the solar potential of roofs.

The research area also includes vegetation of different types and heights, providing an opportunity to assess the impact of greenery and tall trees on the solar photovoltaic potential of nearby rooftops.

LiDAR point cloud data served as the primary source for building extraction, the creation of a Digital Surface Model (DSM), and subsequent analyses. This LiDAR data was acquired through aerial scanning during the 2019–2020 period and was provided by the Agency for Real Estate Cadastre of North Macedonia. The parameters of used point cloud are given in Tab. 1.

Table 1 Characteristics of LiDAR point cloud

Parameter	Value
LiDAR sensor	RIEGL VQ-1560i S.N. S2223066
Height of flight	1400 m
Scanning angle	± 20°
Distance between points	0,3 m
Minimal point density	5 points/m²
Average point density	10 points/m²
Hight accuracy	0,1 m

The first step in the analysis is the creation of a Digital Surface Model (DSM). A raster surface model with a spatial resolution of 0.5 meters was generated. Although raster models with higher resolutions can define surface features with greater precision, they are more computationally intensive to process.

In this study, a spatial resolution of 0.5 meters was selected as the optimal balance between accuracy and efficiency. This resolution was chosen because LiDAR point cloud data has a point spacing of approximately 0.3 meters. Even though a higher resolution would provide more surface details, the chosen resolution was considered as satisfactory since it preserves enough details while minimizing processing time.

The second step involved detecting building footprints. To create a building footprint model, a classified LiDAR point cloud with a class "Building" was required, and an automatic classification approach was applied. During the automatic classification, points corresponding to flat roof characteristics were identified with a moderate tolerance for irregularities. The classification conditions were set as follows:

- Minimum roof height: The lowest height from which points on the roof would be detected (set to a minimum of 2 meters).
- Minimum roof area: Only roofs with a surface area of at least 10 m² were included.

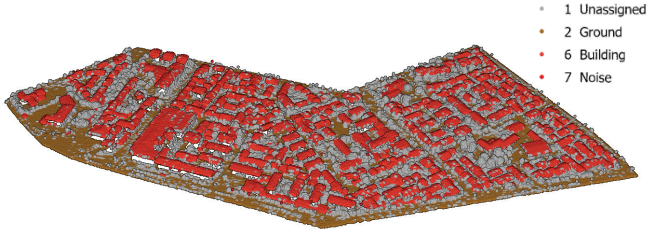

Figure 1 Classified LiDAR point cloud of the study area

After the automatic classification of the class "Building", a raster model of the buildings was created. This raster model, with a resolution of 0.5 meters, was then converted to

vector format to create polygons representing the building footprints.

Figure 2 Buildings as raster data combined with orthophoto image

The position and shape of the automatically created polygons were visually cross compared with high-resolution orthophoto images. This showed that it corresponds well with the real position and actual geometry of the buildings. As this has been an automatic processing of data, some irregularities existed, like empty spaces within the polygons or uneven edges of polygons. To fix this, a regularization process that straightens the sides of polygons and creates right angles, where appropriate, was applied. For small empty spaces in the polygons below threshold, these were removed, though some empty space was retained if it represented an actual building feature.

After this additional automatic processing, a manual correction phase followed. This involved comparing the generated polygons with the digital surface model, satellite imagery, and Google Street View photos. Manual adjustments were made, particularly for attached buildings, ensuring that separate polygons were created for each building.

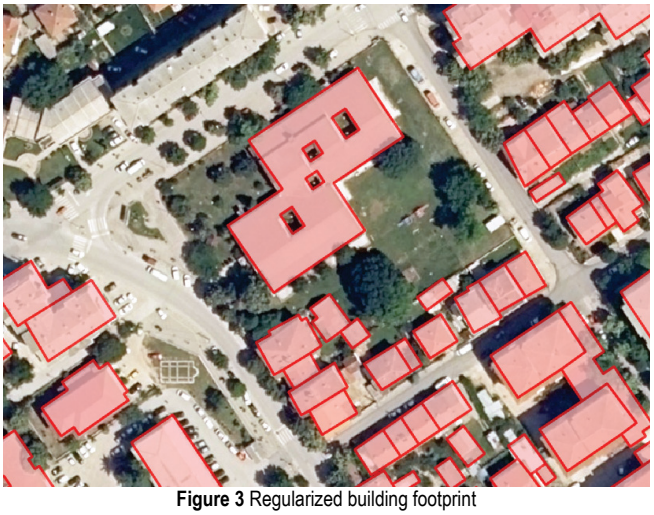

Figure 3 Regularized building footprint

At the end of this step, a 3D model of the urban area was produced, clearly showing the buildings within the research area, providing a solid foundation for further analysis.

Figure 4 3D model of buildings within study area

Based on the digital surface model, digital models of roof slope and orientation were generated for the buildings. These spatial models were created with an optimal resolution of 0.5 meters.

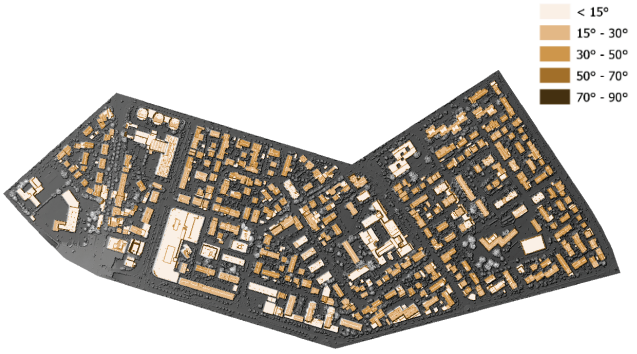

Figure 5 Building rooftop slope

The digital slope model assigns a value to each pixel representing the roof's inclination, ranging from 0° (completely flat) to 90° (vertical). Lighter colours indicate flatter surfaces, while darker colours correspond to steeper slopes. The digital orientation model, on the other hand, assigns a value to each pixel that indicates the direction the roof surface faces, with 0° representing true north and 180° representing true south.

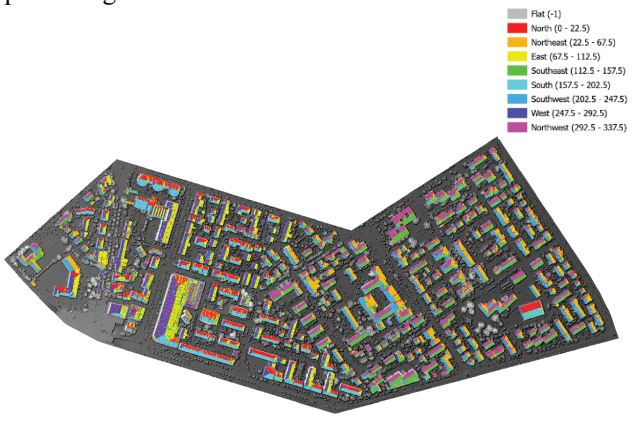

Figure 6 Building rooftop aspect

To estimate the solar photovoltaic potential, a digital solar radiation model was created for each building's roof. This model is based on the digital surface model and incorporates data on obstacles, roof slope, and orientation. The solar radiation calculation uses an advanced algorithm that accounts for the sun's position throughout the year and different times of day, as well as obstacles like nearby trees or buildings that can block sunlight. The model also considers the slope and orientation of the surface. Additional parameters include the time interval for the calculation and the number of directions to the sky to detect shadows and visible areas. Each pixel in the resulting raster model contains a value representing the amount of solar radiation, measured in watt-hours per square meter (Wh/m²) or kilowatt-hours per square meter (kWh/m²).

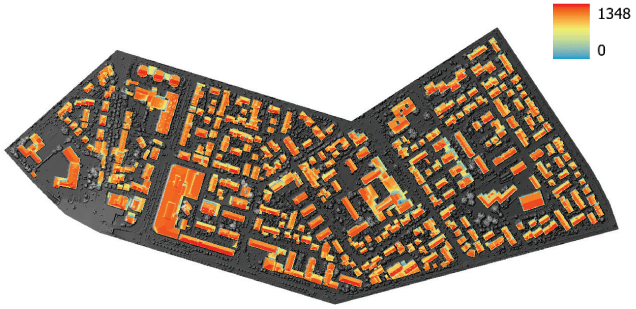

Figure 7 Building rooftop solar radiation

After generating all necessary spatial data, the following criteria have been used to identify roof surfaces that are suitable for the installation of solar photovoltaic systems:

- Slope: The slope of the roof surface should be less than 45°.
- Solar Radiation: The annual incident solar radiation received should be more than 800 kWh/m².
- Aspect: The roof surfaces shouldn't be oriented to the north except flat roofs whose inclination is less than 10°.

To qualify as suitable for solar photovoltaic installation, a building must have at least 30 m² of roof area that meets these conditions. For buildings that meet the criteria, the average annual solar radiation is calculated. The total annual available solar radiation for every building is calculated by multiplying the suitable roof area with the average solar radiation.

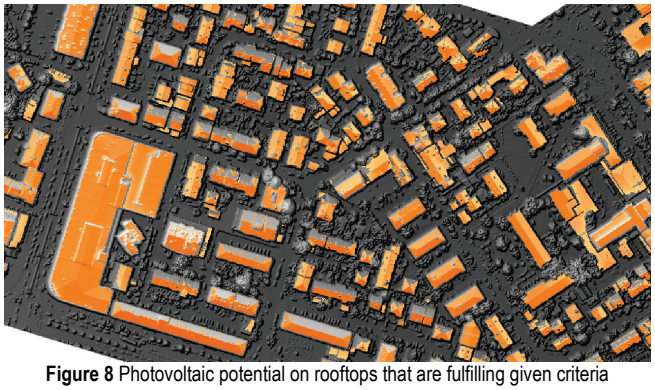

Figure 8 Photovoltaic potential on rooftops that are fulfilling given criteria

Finally, to estimate the solar photovoltaic potential for each building, the following three values are taken into consideration: the roof area that is considered suitable, the conversion efficiency of solar energy to electricity, and any losses incurred by the photovoltaic system equipment. The photovoltaic potential is calculated for each building as well as collectively for all buildings within the study area.

4 RESULTS

Based on the analysis of the urban area selected as a case study, building footprints were extracted for 628 buildings, covering a total area of 119 079 m². The smallest building has an area of 17 m², while the largest building is 6932 m².

Out of these 628 buildings, 529 were identified as suitable for the installation of photovoltaic systems, after applying the conditions for roof suitability. The total roof area suitable for solar photovoltaic installation is 73 544 m², representing 62% of the total rooftop area analysed.

Although the number of suitable buildings is reduced compared to the total number analysed, most of the excluded buildings were small auxiliary structures with minimal roof space. These buildings are typically low in height and situated close to other buildings, resulting in significant shading of their rooftops.

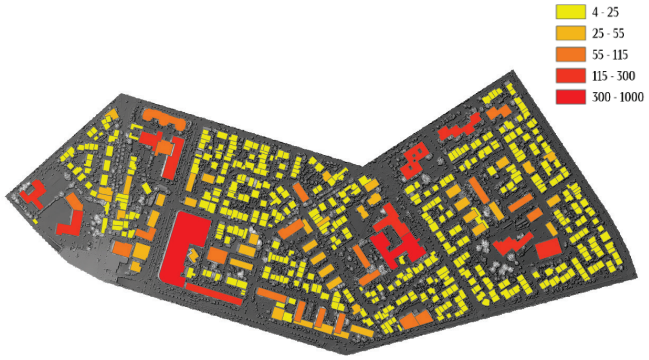

Figure 9 Photovoltaic potential (MWh) per year

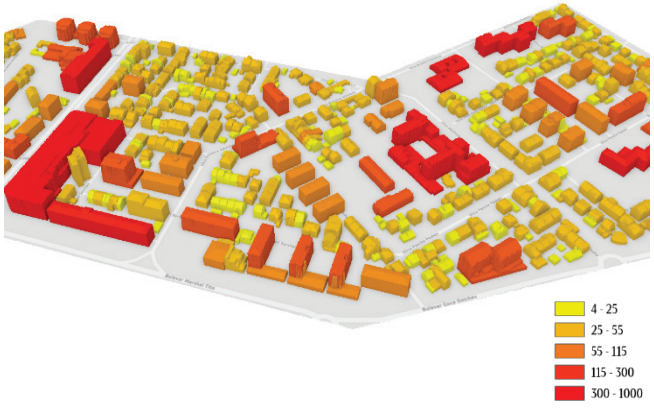

Figure 10 3D model of the case study area coloured by estimated photovoltaic potential

On the other hand, most of the individual, collective housing, and public buildings, like schools, the shopping centre, and the city hospital, were highlighted to have large parts of their rooftop area suitable for installing a

photovoltaic system. These buildings have a high potential in terms of electricity production.

The potential electricity production per building ranges from 4 MWh to 1000 MWh annually, with larger and taller buildings generally producing more electricity. If photovoltaic systems were installed on all suitable rooftops in the study area, the total potential electricity generation would amount to 11 329 MWh per year.

The largest building in the study area is a shopping centre with a flat roof. It has a suitable roof area of 6198 m² and an estimated electricity production potential of nearly 1000 MWh per year. The entire rooftop was determined suitable for photovoltaic installation, because of its flat design, height, and low shadow coverage, making it an ideal candidate for maximizing solar energy production.

5 CONCLUSION

The integration of LiDAR data, spatial modelling, and Geographic Information Systems (GIS) allows for a highly sophisticated and efficient analysis of optimal locations for solar photovoltaic system installations.

This approach takes into consideration all critical spatial factors affecting the solar energy potential of rooftops, such as roof slope and orientation, shading from nearby objects, and solar exposure throughout the year. In this case study, out of 628 analysed buildings, 529 buildings were selected to be suitable for the installation of photovoltaic systems, covering 73 544 m², or 62% of the total rooftop area, with an impressive electricity production potential. Notably, larger structures such as individual buildings, residential buildings, schools, shopping centres, hospitals were found to have rooftop areas capable of producing between 4 MWh and 1000 MWh annually, with a cumulative potential of 11 329 MWh across all suitable rooftops.

LiDAR data provides the precise input necessary for creating spatial models that assess the solar photovoltaic potential of building rooftops. These models, developed through the established methodology, are used to determine the feasibility and effectiveness of installing solar photovoltaic systems for electricity generation. Since LiDAR data of the entire territory of the Republic of North Macedonia is available, this methodology is implementable on every part of the country.

Such high-resolution spatial data availability allows the estimation of photovoltaic potential not only of large urban areas but also of single residential or commercial buildings. This flexibility can ensure that the methodology will be used to maximize energy production by solar photovoltaic installations across various building types and regions.

This approach raises the level of awareness of all stakeholders in regard to property owners, investors, and authorities at the local government level by assessing the potentials of each individual building for solar photovoltaic system installation. The detailed, data-driven assessment can further encourage more participation in the adoption of solar energy to achieve national and local renewable energy goals. These can also serve as a basis for policy development in motivating or incentivizing sustainable energy investments or providing information for urban planning strategies toward clean energy access.

6 REFERENCES

[1] United Nations Department of Economic and Social Affairs. World Urbanization Prospects – The 2018 Revision. New York: United Nations. (2015). Available online: https://population.un.org/wup/Publications/Files/WUP2018-Report.pdf (accessed on 16 January 2024).

[2] Gagnon, P., Margolis, R.M., Melius, J., Phillips, C. & Elmore, R. (2016). Rooftop Solar Photovoltaic Technical Potential in the United States. https://doi.org/10.2172/1236153

[3] Palmer, D., Koumpli, E., Cole, I., Gottschalg, R. & Betts, T.R. (2018). A GIS-Based Method for Identification of Wide Area Rooftop Suitability for Minimum Size PV Systems Using LiDAR Data and Photogrammetry. *Energies, 11*(12), 3506. https://doi.org/10.3390/en11123506

[4] Huang, X., Hayashi, K., Matsumoto, T., Tao, L., Huang, Y. & Tomino, Y. (2022). Estimation of Rooftop Solar Power Potential by Comparing Solar Radiation Data and Remote Sensing Data - A Case Study in Aichi, Japan. *Remote. Sens., 14*(7), 1742. https://doi.org/10.3390/rs14071742

[5] Kozlovas, P., Gudzius, S., Ciurlionis, J., Jonaitis, A., Konstantinaviciute, I. & Bobinaitė, V. (2023). Assessment of Technical and Economic Potential of Urban Rooftop Solar Photovoltaic Systems in Lithuania. *Energies, 16*(14), 5410. https://doi.org/10.3390/en16145410

[6] Fakhraian, E., Forment, M. A., Dalmau, F. V., Nameni, A. & Guerrero, M. J. (2021). Determination of the urban rooftop photovoltaic potential: A state of the art. *Energy Reports, 7*(3), 176-185. https://doi.org/10.1016/j.egyr.2021.06.031

[7] Schallenberg-Rodríguez, J. (2014). Photovoltaic Techno-Economical Potential on Roofs in the Canary Islands. Journal of Sustainable Development of Energy, Water and Environment Systems, 2(1), 68-87. https://doi.org/10.13044/j.sdewes.2014.02.0007

[8] Singh, R. & Banerjee, R. (2015). Estimation of rooftop solar photovoltaic potential of a city. *Solar Energy, 115*, 589-602. https://doi.org/10.1016/j.solener.2015.03.016

[9] El-Hosaini, H. (2015). Locating and Positioning Solar Panels in a 3D City Model: A Case Study of Newcastle, UK. https://doi.org/10.1553/giscience2015s147

[10] Willenborg, B., Pültz, M. & Kolbe, T. H. (2018). Integration of semantic 3D City Models and 3D Mesh Models for accuracy improvements of solar potential analyses. Int. Arch. Photogramm. *Remote Sens. Spatial Inf. Sci.*, XLII-4/W10, 223-230. https://doi.org/10.5194/isprs-archives-XLII-4-W10-223-2018

[11] Sredenšek, K., Stumberger, B., Hadžiselimović, M., Mavsar, P. & Seme, S. (2022). Physical, Geographical, Technical, and Economic Potential for the Optimal Configuration of Photovoltaic Systems Using a Digital Surface Model and Optimization Method. *Energy, 242*, 122971. https://doi.org/10.1016/j.energy.2021.122971

[12] Fu, P. & Rich, P. M. (2002). A Geometric Solar Radiation Model with Applications in Agriculture and Forestry. *Computers and Electronics in Agriculture, 37*(1-3), 25-35. https://doi.org/10.1016/S0168-1699(02)00115-1

[13] Rich, P. M., Dubayah, R., Hetrick, W. A. & Saving, S. C. (1994). Using Viewshed Models to Calculate Intercepted Solar Radiation: Applications in Ecology. *American Society for Photogrammetry and Remote Sensing Technical Papers*.

[14] Rich, P. M. & Fu, P. (2000). Topoclimatic Habitat Models. *Proceedings of the Fourth International Conference on Integrating GIS and Environmental Modeling*.

[15] United States Environmental Protection Agency. Green Power Equivalency Calculator-Calculations and References. Available online: https://www.epa.gov/greenpower/green-power-equivalency-calculator-calculations-and-references (accessed on 25 January 2024).

Authors' contacts:

Natasha Malijanska Andreevska
(Corresponding author)
Ss. Cyril and Methodius University,
The Faculty for Civil Engineering,
bul. Partizanski odredi bb, 1000 Skopje, North Macedonia
e-mail: malijanska@gf.ukim.edu.mk

Gjorgji Gjorgjiev
Ss. Cyril and Methodius University,
The Faculty for Civil Engineering,
bul. Partizanski odredi bb, 1000 Skopje, North Macedonia
e-mail: gorgi.gorgiev@gmail.com

Emilija Bozhinov
Agency for Real Estate Cadastre of the Republic of North Macedonia,
St. Trifun Hadzijanev 4, 1000 Skopje, North Macedonia
e-mail: emilija.bozhinov@gmail.com

ISSN 1846-6168 (Print), ISSN 1848-5588 (Online)
https://doi.org/10.31803/tg-20241013222733

Original scientific paper
Received: 2024-10-13, Accepted: 2024-11-20

Navigating Urban Space: Unveiling Patterns in Walking Routes through Space Syntax in Kypseli Neighborhood (Athens)

Kyriakidis Charalampos*, Apostolopoulos Konstantinos, Papadima Anna, Sideris Athanasios, Potsiou Chryssy, Bakogiannis Efthimios

Abstract: This paper explores pedestrian mobility patterns in Kypseli, a dense and socio-economically diverse neighborhood in Athens, Greece, that it is considered as a typical Greek residential area, in terms of its built environment and road network characteristics. The research method included crowdsourced geospatial data overlayed on cadastral maps, and semi-structured interviews with residents and visitors to understand the routes they usually take, the routes they could take, and the routes they would like to take. The study also applied space syntax analysis, using angular integration and choice tools, to assess how the urban layout impacts the pedestrian flow. Findings showed that the walking routes are primarily influenced by safety, accessibility, and pavement width, with well-connected streets and streets with intense mixed land-use. The study highlights the importance of urban design and land management in promoting the perceived walkability. It also recommends enhancing pedestrian spaces to create more sustainable, livable, and socially inclusive cities to support the implementation of the Sustainable Development Agenda 2030 SDG 11.

Keywords: Athens; crowdsourcing; SDGs; semi-structured interviews; space syntax; sustainable mobility planning

1 INTRODUCTION

Since urban mobility has grown during the last decades [1], integrated strategic planning -that combines traffic planning with urban policies - consists of a topical issue at the global level and seems to be one of the main pillars of modern spatial planning policy [2]. Through the Agenda 2030, which promotes sustainable economic development by reducing negative impacts on the environment and society, the importance of integrated sustainable planning, good land administration and management is even more evident. Two of the seventeen goals are mainly related to this topic: Goal 11 about sustainable cities and communities and Goal 13 about climate action [3].

Apart from the global policy through the United Nations, the European Union adopts sustainable urban mobility planning [4] to create environmentally friendly and "compact" cities that will encourage alternative means of transport such as walking [5]; this is the reason why planners do not focus only in making cities more walkable, in terms of infrastructure, but also urge people walking by making public spaces safer and more comfortable for citizens. To achieve this goal, planners consider multiple factors and parameters that affect walking, as it came into the fore through research. Such a series of factors include not only the mere provision of pavements [6] and pedestrian crossings but also the ideal geometric characteristics of the pavements that should be preserved in a good situation [7] without obstacles (i.e., illegally parked cars), adequate street lighting, planting [8] and clear signage [9]. Along with the above, mixed land-use [8], pedestrian networks continuity, geometric characteristics of streets [10] and social characteristics of public spaces [6] may also be considered as crucial parameters affecting people to feel comfortable while they walk and, thus, they act as factors enhancing walking.

All of these parameters contribute in creating a secure environment, particularly for vulnerable groups like children and elders. Additionally, the inclusion of green spaces, shaded pathways, and street furniture enhances the physical comfort of walking, making the walking experience more enjoyable [8] and urging people to remain in public space.

With all the above in mind, it could be understood that some public spaces that have been designed based on specific criteria that respond to the aforementioned parameters may be more walkable and, thus, more popular. When such design standards are not followed, public spaces = fall behind in terms of walkability, although there may be spots with architectural interests and good social characteristics.

This topic has not been extensively studied. Despite the fact that in Greece a lot of research has been conducted during the last ten years for promoting urban walkability in the context of sustainable mobility, no sufficient research has been implemented on this specific topic. In response, this study aims to address this challenge through a comprehensive analysis of mobility patterns in typical residential areas in Greek cities. Kypseli, a residential area of Athens, Greece close to the historic centre, was selected to be examined in the context of a case study analysis. The research question was focused on the criteria affecting people to select the routes they usually follow within the neighborhood. Moreover, it was crucial to identify whether the routes people follow differ from the ones they would prefer to follow or even those they could follow. The methodology applied, is presented in Section 3, and is focused on map-based surveys implemented during interviewing, in the field. Based on the results, explained in Section 4, conclusions (Section 5) came to the fore not only for Kypseli but also for typical Greek cities, through generalization of the research outcomes. These conclusions are discussed in light of the literature review that is briefly pointed out in Section 2.

2 LITERATURE REVIEW

Over the years, urban land managers and planners have seen cities through different lens; either through a visual-aesthetic tradition, or through a social-usage one, while now, the place-making tradition seems to be the most popular approach [11]. But even among researchers whose perception seems to be the same, differences are found in terms of their objectives and the methodologies applied. A typical example

is the different approaches of Lynch, Jacobs, and Alexander (social-usage tradition). Jacobs mainly focuses on social factors that create sense of safety, while Lynch examined urban space with the use of environmental images and Alexander focused on structural elements that produce specific patterns [12]. In Lynch and Alexander's approaches, urban space is understood through descriptions of its form that are classified into typologies [13]. Such approaches may be included into typo-morphology that was evolved by a more qualitative logic into a more quantitative one, over the years and through the evolution of research - even in the case of terminology applied [14] - across different countries.

However, nowadays, quantitative analytical methods tend to dominate in this field. The work of Wang et al. [15], who developed a method of feature analysis in order to quantitatively generate applicable design schemes, is one of such typical cases. Stojanovski [16] also combined typo - morphological analysis and statistics to show the various urban form factors affecting neighbourhood typology. Furthermore, another quantitative perception is the research work conducted by Bobkova, et al. [17] about the plot types across different European cities.

However, space syntax was one of the methodologies that arose a new perception in understanding cities. It provides a mathematical framework to integrate and re-evaluate both social and structural dimensions. In his work, Hillier [18] differentiates intrinsic and extrinsic spatial properties. The latter govern the relationships among spatial units, shaping the configurative rules of space [19]. From this perspective, topological considerations become particularly significant. These extrinsic properties not only influence the physical form of the built environment but also its potential function. While extrinsic spatial properties are concerned with underlying, invisible structural connections, intrinsic properties pertain to visible characteristics, such as geometry, patterns, and textures. These intrinsic attributes play a crucial role in expressing social meaning through the physical form of the built environment [6].

According to Hillier [20], extrinsic spatial properties are found in all built environments; the same happens in activities taking place in these spaces that characterize its functions. As a result, he supported that the spatial structure of a city affects shaping economic and social life in cities [6]. This is more evident in case of economic activities that are primarily driven by the implicit goal of profit maximization. In case of social activities, this relationship seems to be sicker, as cultural and societal contexts affect them. However, space syntax is considered as a tool of prediction of human activity [21] it gives the opportunity to esteem urban spaces with high - not only current but also potential-pedestrian flows [22] and, as a result, the areas that are characterized by centrality [6, 21].

As space syntax has a strong empirical validation and a high level of accuracy in predictions, it is applied to a broad spectrum of built environments, thereby enhancing and advancing the formulation of descriptive theories related to urban space. In this research, space syntax has been applied in order to correlate physical attributes with the degree of walkability. In Section 3, a description of the steps followed to answer the research question set in Section 1.

3 METHODOLOGY

3.1 Aims and Objectives

The primary focus of this study is to identify the components of urban space and the pedestrian flows expressed in it. It is essential to emphasize that the study specifically examines the walkability of pedestrians, as walking is essential for fulfilling daily needs and is a fundamental aspect of sustainable mobility. Our approach to study walking routes in Kypseli combines interviews with the analytical tools of space syntax. This method allows us to gain both qualitative insights from the interviewees and quantitative spatial analysis to better understand movement patterns in the study area.

3.2 Study Area

As it was mentioned above, Kypseli has been selected to be examined as it is a central area (built according to the Athenian modernistic architecture patterns and it is characterized by building density, socio-economic diversity [23] and touristification [24]. The coexistence of various population groups is important as it affects the character of the area and consequently, the way residents travel across Kypseli.

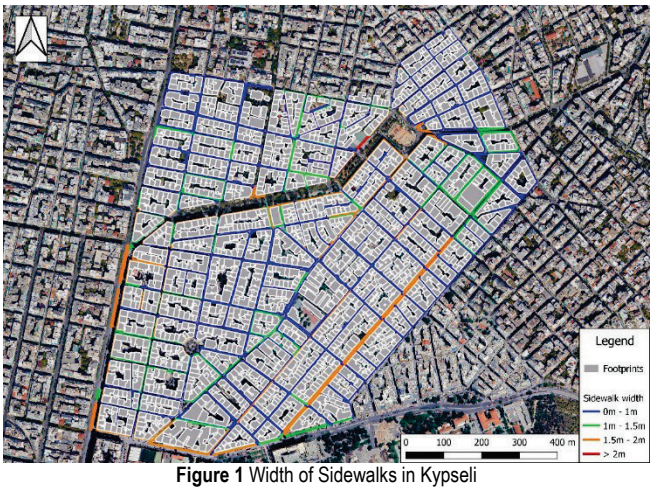

Figure 1 Width of Sidewalks in Kypseli

The scales of the policies applied in Kypseli are multiple. There are policies that focus on Kypseli as a neighbourhood, and policies that perceive Kypseli as a sector of the Municipality of Athens. As a result, Kypseli is influenced by strategic directions for the centre of Athens, which have a metropolitan character.

In terms of urban environment, a key characteristic and potential mobility problem in Kypseli is the existence of pavements of a very narrow width. This fact creates a strong disproportion between buildings and pavements.

3.3 Data Collection

The methodology applied to answer the research question posed is divided into two parts. In the first one, geospatial information (land uses, road space geometry,

pavement width, plantings, and urban equipment) was collected by local residents and undergraduate students in the School of Rural, Surveying and Geoinformatics Engineering of National Technical University of Athens, who participated in the project as volunteers. The geospatial data collection methodology that was followed has been developed in a previously published research and its accuracy has been tested and proved as adequate [3]. In addition to the collection of the footprint of the buildings, relevant information is also collected about the prevailing use of each building. All necessary data was collected remotely online using Google Earth and StreetView, as well as open data derived from the Hellenic Cadastre. However, in cases where it was difficult to distinguish these features, fieldwork was also useful.

Concerning the data collection process, it should be clarified that, at an initial stage, the recordings were made individually by each volunteer in a predetermined area and after proper editing they were combined into a unified database.

Next, 188 semi-structured personal interviews were conducted (Tab. 1), during late January - early March 2022. Totally, 142 residents and 46 visitors participated in this activity as they agreed to be interviewed; the snowball method has been used in order for the interviewees to be found.

Table 1 Interviewers' demography

Relation to the area		Biological sex		Age Groups	
Residents	76%	Female	43%	18-29	55%
Visitors	24%	Male	57%	30-44	45%

The main topics of the interview were about (a) the routes they usually walk, (b) the routes to which they can walk and (c) the preferable routes (Fig. 3). Due to the fact that interviews have been scheduled to take place on-street, it was not easy to last too much. Most of them lasted less than 8 minutes and only 9 exceeded 20 minutes. Subsequently, the appropriate maps were created where the results of the interviews were illustrated.

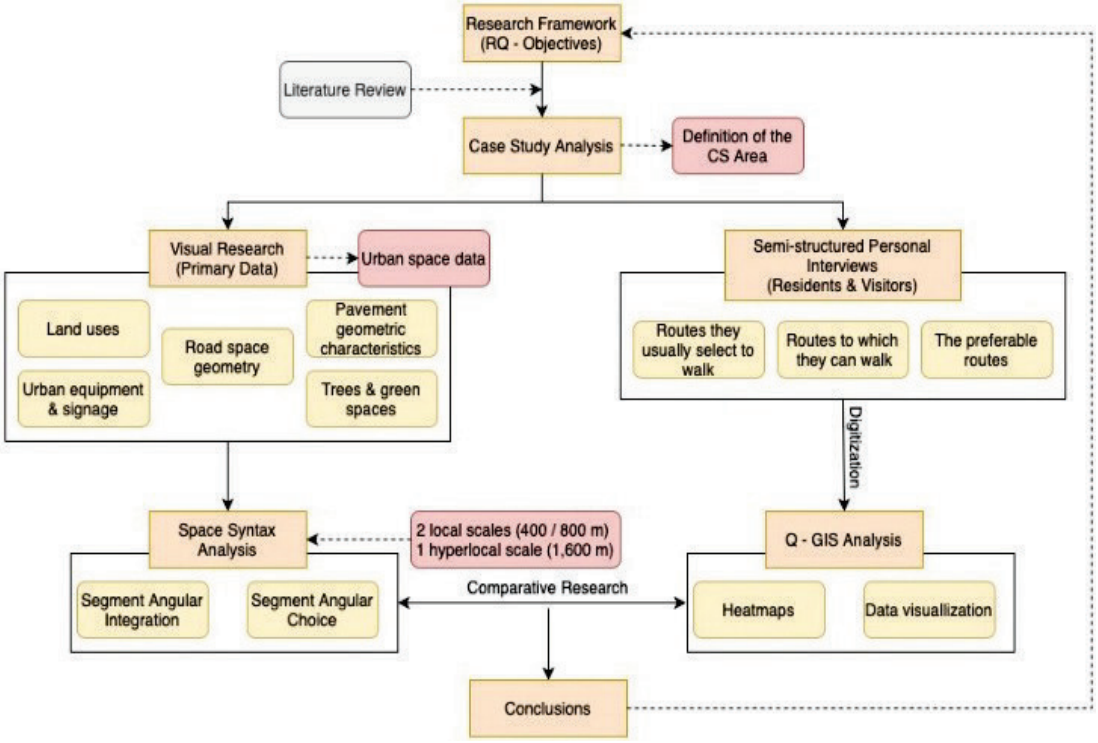

Figure 2 Methods applied

Then, analysis through space syntax methodology was applied [13]. As it was noted, space syntax analysis focuses on how the geometry and topology (connectivity) of the urban network affects the movement flows, land use and ultimately human activity in a city [25]. In the space syntax analysis the most important tools for identifying potential movements and important routes in the urban network, are segment angular integration (the quantification of the accessibility of a site in relation to the urban system to which it belongs) and segment angular choice (the quantification of the possibility of unfettered movement through a site in relation to the urban system to which it belong) [26].

Taking into account that real-world movement patterns have shown that citizens move in space by "reading" the angular geometry of the network rather than simply physical distances [27] and also that "angular resolution is highly responsive to spatial navigation and orientation, as users are more likely to minimize perceived distance when in an unfamiliar environment" [28], in this research, 3 different radius have been calculated (Figs. 4-9): 2 local ones (400 m, 800 m) and 1 hyperlocal one (1600 m). The choice of rays is based on the logic of the 15-minute city model. In particular, for a radius of 400 m, the angular deviations from each node to all others have been calculated (respectively for each

radius) only within this radius. Therefore, by applying the radius during structural analysis, it is possible to analyze the city at different scales for the local and supra-local relations that emerge in the urban network.

Through comparative research, the outcomes came from both methodological types are correlated in order for conclusions to be drawn, not only for the study area, but also for residential areas in Greek cities, as a generalization.

4 RESULTS

In the following images, the results of our research are presented. Firstly, the final map with all the routes derived from the interviewees (Fig. 3). Visualization is also seen under the light of statistics about the time spent, the reason for moving, and the time spent walking in the area (Tab. 2). As it is pointed out in Tab. 2, most of the participants tend to walk for more than an hour, in each autonomous trip. Their majority supported that, on a daily basis, just one or two trips are implemented; either for amusement and exercise or for work. Afternoon is the most popular time of the day for walking in Kypseli, as 33% of the interviewers prefer this time zone. Probably, 25% of the people who walk, in the morning times, on a daily basis, are those who go to their work, on foot (partly or totally). The majority of the afternoon walkers (8%) are probably urged to walk for leisure.

Initially, the results between the three types of routes revealed moderate differences (Fig. 3) – this was attributed to two key characteristics of a city that are indicators of road safety and the quality of road networks: lighting and pavement width. Therefore, the majority of the residents are choosing the best route, taking into account two main qualities: safety as well as accessibility.

Table 2 Statistics about each autonomous trip

Time Spent per Walk				
Variable prices	>1 hour	1-2 hours	2-3 hours	>3 hours
Percentage	10%	30%	40%	20%
Preferred Time to Walk				
Variable prices	Morning	Noon	Afternoon	Evening
Percentage	25%	25%	33%	17%
Reason for Moving				
Variable prices	Leisure	Work	Child at school / Walk with child / School	Sports	Shopping
Percentage	37%	30%	15%	8%	10%

Furthermore, by contrasting the routes derived from interviewing, it was noticed that a large part of them were identical. This was also expected from the interview stage as many of the participants reported that the routes they take are identical to the routes they could take and the routes they would like to take. This shows that most participants have inevitably adapted their routes in an optimal way, both in terms of meeting their needs (shopping, work, etc.) and in terms of the aesthetic choice of these routes. The already developed city, in terms of urban form, has indirectly defined its routes.

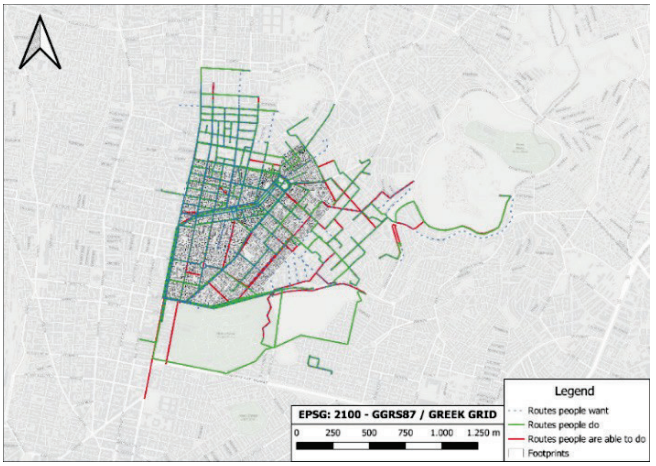

Figure 3 Routes derived by the interviews

Small differences can be found in the routes they take and the routes they want to take. These differences are found on the narrow roads in the north-western part of the study area. In particular, interviewees seem to wish to follow these routes but do not choose them in their daily lives. This is most likely related to the limited width of the sidewalks, the high height of the surrounding buildings and the lack of lighting compared to other areas. For the selection of a route, it was observed that most routes are located on streets across which mixed land uses are developed, as well as on those in which the largest sidewalk widths is observed; urban equipment also plays a significant role. This observation was also expected, as the built environment has also been shown to have a significant effect on walkability and environmental quality for those who walk [29].

Figure 4 Angular Choice 400 m (Source: Research Team Elaboration)

In a second stage, when the routes were compared with the results of the space syntax analysis, it was not observed direct correlation between them, proving Pafka's claim [30], according to whom, integration, although it is a useful tool in terms of identifying morphogenetic tendencies in a large scale, however, it may be misleading as a means of measurement of walkable access, at a neighborhood scale. More specifically, greater emphasis is placed on the angular integration measure, which highlights the accessibility of a

space in relation to the urban system to which it belongs. Therefore, the roads on which interviewees move are not always as integrated as it may be expected, according to the editorial analysis of the local 400 and 800-meter radius (Fig. 10). In contrast, the roads they move are more closely converged with the 1600-meter radius integration; this is a hyper-local radius and is more associated with car travel than pedestrian travel. Finally, although they are not highlighted through the space syntax analysis but only through the routes, it is observed that the pedestrian streets, such as Fokionos Negri and Agias Zonis, are usually preferred by pedestrians for their movements either as a destination or for transit. This is probably because these streets combine the presence of urban amenities with a variety of land uses, such as commercial shops and residential. Finally, another street in which preferable routes were found is Patision Street. It is mainly preferred for commuting as many people move in there because of the existence of public transportation stops, the wide pavements, and the extensive commercial activity.

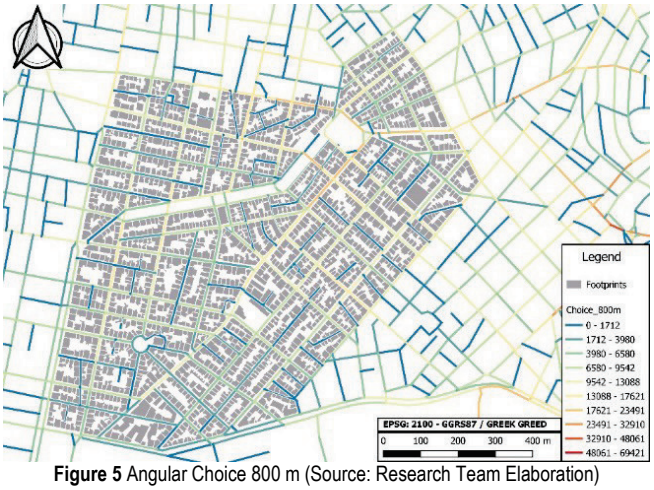

Figure 5 Angular Choice 800 m (Source: Research Team Elaboration)

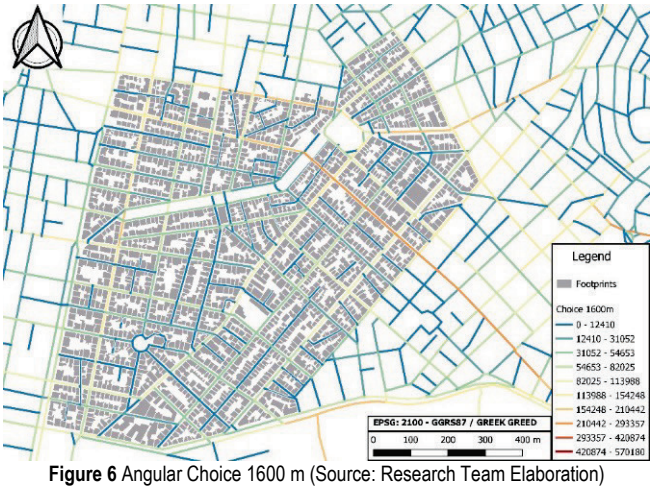

Figure 6 Angular Choice 1600 m (Source: Research Team Elaboration)

Based on the angular integration tool, which has been applied in the context of space syntax analysis and highlights the accessibility of a space in relation to the urban system to which it belongs, it was concluded that the study area, in total, is not well integrated with the neighboring ones. Such an observation was obvious for the case that the analysis was conducted by using 1600 m as a measurement basis (Fig. 9). In the rest of the cases in which the angular integration tool was applied on a local scale, it was concluded that a big part of the area is integrated to the neighboring ones. This observation has to do with urban form not only of the study area but also of the wider one; Pedion of Areos Park seems to be the main reason why this observation takes place. According to Fig. 9, the eastern as well as the northern part of the area is less integrated in relation to the rest part. Another reason explaining this differentiation is the existence of important streets in the western part of the area that plays a crucial role in connecting city centre to the northern part of the Municipality of Athens: Pattison Ave. and 3rd of October Ave. In the same figure, Drosopoulou Street, which is a quite important road artery for the function of Kypseli, is also highlighted as a quite integrated axis.

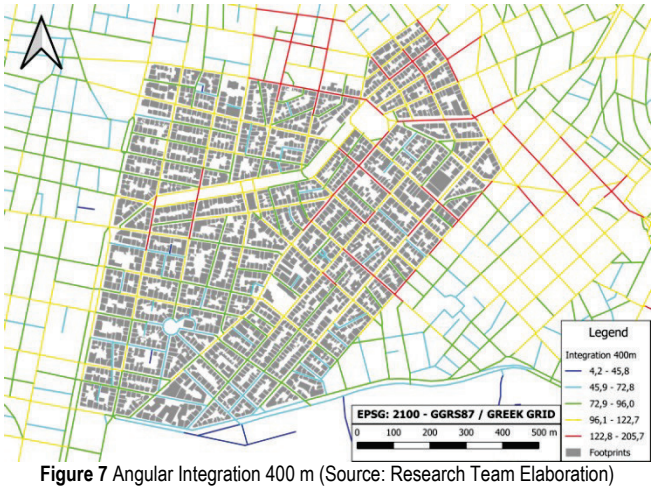

Figure 7 Angular Integration 400 m (Source: Research Team Elaboration)

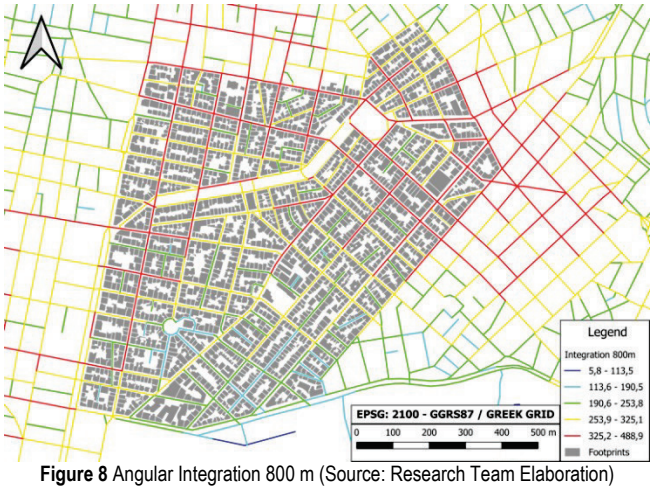

Figure 8 Angular Integration 800 m (Source: Research Team Elaboration)

Based on the angular choice tool (Figs. 4-6), it is concluded that most of the streets located in the study area are local ones; that means that residents usually prefer moving across them only in case the move within Kypseli. In a different case, they usually prefer moving on streets like Pativision Ave., Kastalias Street, Kyprou Street and Kypselis Street. Contrary to that, in case of local scale journeys, people

tend to move across streets that are narrower or even of shorter length.

Although Kanaris's Square consists of a place which is quite livable, as the possibility for someone to move around it is high, in all case scenarios (local and hyperlocal), the same observation is not relevant to the case of Fokionos Negri's pedestrian street. The latter is mainly preferred by people who move in a local scale while people who move on longer distances do not prefer this route.

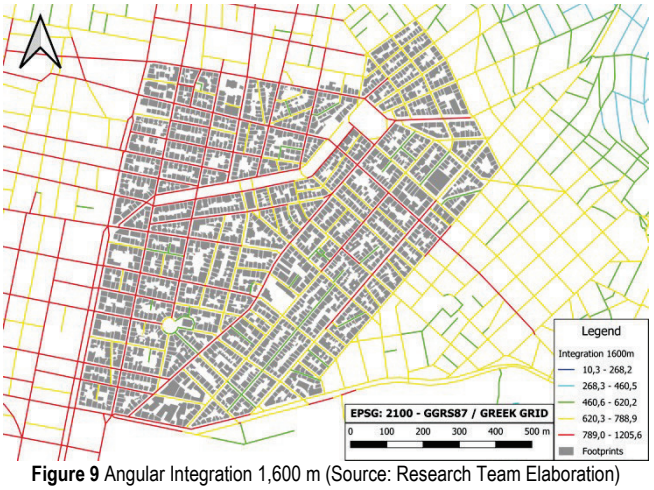

Figure 9 Angular Integration 1,600 m (Source: Research Team Elaboration)

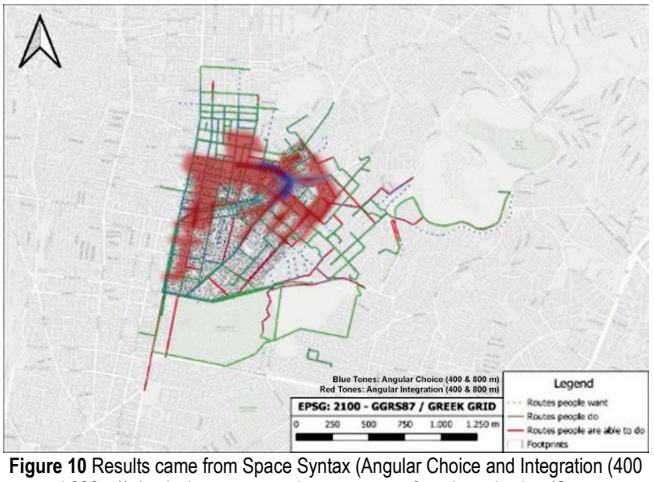

Figure 10 Results came from Space Syntax (Angular Choice and Integration (400 and 800 m)) Analysis contrary to the ones came from interviewing (Source: Research Team Elaboration)

5 DISCUSSION-CONCLUSIONS

This paper focuses on the way people walk within a typical residential area in Greek cities. More specifically, its goal is to identify the way they walk, the routes they would prefer to follow, and their preferable routes. The philosophy besides this differentiation is that people may select a walking route by taking into account criteria that differentiate from the ones that determine the routes they prefer or they could follow. These criteria are not always related to the geometric characteristics of pavements and the urban equipment elements, although they are quite important parameters affecting walkability and perceived walkability. The urban form seems to be another parameter that may define their behaviour.

The research was based on a comparative analysis, in which space syntax analysis and interviewing were the main methods applied. The outcome was, on the one hand, maps analysing the study area in terms of angular choice and integration, and, on the other hand, digitized data about routes people follow, want to follow and can follow. In the latter, it should be underlined that data about geometric characteristics of pavements and urban equipment was also recorded and digitized.

By comparing routes' footprints derived from interviewing with conclusions derived through space syntax analysis, it was found that streets that are well integrated into the wider area are the ones in which most people walk, as they are the easiest, simplest and - usually - the closest way to reach their destination that may be a public transport station. This case is modified in case of short distances where people prefer to "explore" their neighborhood by moving across less integrated streets. However, in the case of Kypseli, most of the interviewees tend to walk in order to move at an external point. This observation proves that although the urban centre in the case of Kypseli is defined in Kanaris's Square, however, in terms of function, the most central location seems to be around Patision Ave., which is mainly used on a daily basis. Taking into account that the streets which are better connected to the neighboring areas are the ones in which pavements are wider - this is the most important parameter when a pedestrian walk - there is no much differentiation among the routes people do with the ones people prefer.

Concerning the routes in which interviewees can walk, most of them indicated streets of the first category.

The in-depth analysis carried out in this study highlights the critical importance of urban space planning to promote walking and sustainable mobility. Space is not just a neutral environment for human activity, but is actively produced, shaped and defined by human actions and the social relations that support them. The findings obtained from the study provide a substantial understanding of the factors that influence commuting in urban areas. Implementation of the recommendations arising from this research can lead to the creation of cities that are more pedestrian-friendly and more ecologically and socially sustainable. At a long-term level, the adoption of the principles proposed can lead to more humane and sophisticated urban areas, promoting health, safety and social inclusion.

At this point, should be mentioned that a statistical analysis may be applied in order for future results to be derived through a quantitative approach. In that way, findings will be derived to be more accurate and give us the chance to generalize them for similar cases across Greece.

6 REFERENCES

[1] Okraszewska, R., Romanowska, A., Wołek, M., Oskarbski, J., Birr, K. & Jamroz, K. (2018). Integration of a multileveltransport system model into sustainable urban mobility planning. *Sustainability, 10*(2), 479. https://doi.org/10.3390/su10020479

[2] Eleftheriou, V., Bakogiannis, E., Vasi, A., Kyriakidis, C. & Chatziioannou, I. (2021). New Challenges for Combined Urban Planning and Traffic Planning in Greek Cities. The Case Study of Karditsa. In *Advances in Mobility-as-a-Service Systems: Proceedings of 5th Conference on Sustainable Urban Mobility, Virtual CSUM2020*, June 17-19, 2020, Greece. Springer International Publishing, 991-1000. https://doi.org/10.1007/978-3-030-61075-3_95

[3] Apostolopoulos, K. & Potsiou, C. (2022). How to improve quality of crowdsourced cadastral surveys. *Land*, *11*(10), 1642. https://doi.org/10.3390/land11101642

[4] Finger, M. & Serafimova, T. (2020). *Towards a common European framework for sustainable urban mobility* indicators.

[5] Mouratidis, K. (2018). Is compact city livable? The impact of compact versus sprawled neighbourhoods on neighbourhood satisfaction. *Urban Studies*, *55*(11), 2408-2430. https://doi.org/10.1177/0042098017712876

[6] van Nes, A. (2021). Spatial configurations and walkability potentials: Measuring urban compactness with space syntax. *Sustainability*, *13*(11), 5785. https://doi.org/10.3390/su13115785

[7] Frackelton, A., Grossman, A., Palinginis, E., Castrillon, F. & Elango, V. (2013). Measuring walkability: Development of an automated sidewalk quality assessment tool. *Suburban Sustainability*. https://doi.org/10.5038/2164-0866.1.1.4

[8] Gehl, J. (2010). *Cities for people*. Island Press.

[9] Shi, Y., Zhang, Y., Wang, T., Li, C. & Yuan, S. (2020). The effects of ambient illumination, color combination, sign height, and observation angle on the legibility of wayfinding signs in metro stations. *Sustainability, 12*(10), 4133. https://doi.org/10.3390/su12104133

[10] Appleyard, D. (1976). *Livable streets: Managing auto traffic in neighborhoods - Final report*. Federal Highway Administration.

[11] Carmona, M., Tiesdell, S., Heath, T. & Oc, T. (2010). *Public* places - *urban spaces: The dimensions of urban design* (2nd ed.). Routledge.

[12] Bakogiannis, E., Kyriakidis, C., Eleftheriou, V. & Giannopoulos, C. (2024). *Anthropos-space-ekistics*. Kallipos. *Open Academic Editions*. https://hdl.handle.net/11419/12356

[13] Paraskevopoulos, Y. & Bakogiannis, E. (2022). Exploring the urban types of built density, network centrality, and functional mixture in the city of Athens.

[14] Stojanovski, T. & Östen, A. (2019). Typo-morphology and environmental perception of urban space.

[15] Wang, X., Tang, P. & Shi, X. (2019). Analysis and conservation methods of traditional architecture and settlement based on knowledge discovery and digital generation: A case study of Gunanjie Street in China. In *24th International Conference on Computer-Aided Architectural Design Research in Asia: Intelligent and informed, CAADRIA 2019*. The Association for Computer-Aided Architectural Design Research in Asia (CAADRIA), 757-766. https://doi.org/10.52842/conf.caadria.2019.1.757

[16] Stojanovski, T. (2018, April). What explains neighborhood type statistically? Mixing typo-morphological and spatial analytic approaches in urban morphology. In *24th ISUF International Conference: Book of Papers*. Editorial Universitat Politècnica de València, 1265-1272. https://doi.org/10.4995/ISUF2017.2017.5151

[17] Bobkova, E., Berghauser Pont, M. & Marcus, L. (2019). *Towards analytical typologies of plot systems.*

[18] Hillier, B. (1999). The hidden geometry of deformed grids: Or, why space syntax works when it looks as though it shouldn't. *Environment and Planning B: Planning and Design, 26*(2), 169-191. https://doi.org/10.1068/b260169

[19] van Nes, A. & Yamu, C. (2017). Space syntax: A method to measure urban space related to social, economic, and cognitive factors. In *The virtual and the real in planning and urban design*. Routledge, 136-150. https://doi.org/10.4324/9781315270241-10

[20] Hillier, B. (2001). The theory of the city as object or how spatial laws mediate the social construction of urban space. In Peponis, J., Wineman, J. & Bafna, S. (Eds.). *Proceedings of the Space Syntax: 3rd International Symposium*. Georgia Tech. https://doi.org/10.1057/palgrave.udi.9000082

[21] Paraskevopoulos, Y. & Photis, Y. (2020). Finding centrality: Developing GIS-based analytical tools for active and human-oriented centres. In *Computational science and its applications – ICCSA 2020*. Springer, 43-54. https://doi.org/10.1007/978-3-030-58820-5_43

[22] Özer, Ö. & Kubat, A. S. (2014). Walkability: Perceived and measured qualities in action. *A|Z ITU Journal of the Faculty of Architecture, 11*(2), 101-117. https://doi.org/10.21601/az.2014.11.2.101

[23] Vaiou, N. & Lafazani, O. (2015). Kypseli and its market: Conflict and coexistence in the neighbourhoods of the centre. In Maloutas, T. & Spyrellis, S. (Eds.), *Social atlas of Athens*. https://doi.org/10.17902/20971.33

[24] Arapoglou, V., Karadimitriou, N., Maloutas, T. & Sayas, J. (2021). Multiple deprivation in Athens: A legacy of persisting and deepening spatial divisions.

[25] Hillier, B., Penn, A., Hanson, J., Grajewski, T. & Xu, J. (1993). Natural movement: Or, configuration and attraction in urban pedestrian movement. *Environment and Planning B: Planning and Design, 20*(0), 29-66. https://doi.org/10.1068/b200029

[26] Vaughan, L. (2007). The spatial syntax of urban segregation. *Progress in Planning*, 67(3), 205-294. https://doi.org/10.1016/j.progress.2007.03.001

[27] Hillier, B. & Vaughan, L. (2007). The city as one thing. Progress *in Planning*, *67*(3), 205-230. https://doi.org/10.1016/j.progress.2007.03.001

[28] Hillier, B. & Iida, S. (2005, September). Network and psychological effects in urban movement. In *International conference on spatial information theory*. Springer Berlin Heidelberg, 475-490. https://doi.org/10.1007/11556114_30

[29] Saelens, B. E. & Handy, S. L. (2008). Built environment correlates of walking: A review. *Medicine and Science in Sports and Exercise, 40*(7), S550-S566. https://doi.org/10.1249/mss.0b013e31817c67a4

[30] Pafka, E. (2017). Integration is not walkability: the limits of axial topological analysis at neighbourhood scale. In Heitor, T., Serra, M., Silva, J. P., Bacharel, M. & Silva, L. C. (2017). *Proceedings of 11th Space Syntax Symposium*. Instituto Superior Technico, Departamento de Engenharia Civil, Arquitetura e Georrecursos, 1-10.

Authors' contacts:

Kyriakidis Charalampos
(Corresponding author)
National Technical University of Athens,
9, Iroon Polytechneiou Street,
15780 Zografos, Athens, Greece
kyriakidisharry@gmail.com

Apostolopoulos Konstantinos
National Technical University of Athens,
9, Iroon Polytechneiou Street,
15780 Zografos, Athens, Greece

Papadima Anna
National Technical University of Athens,
9, Iroon Polytechneiou Street,
15780 Zografos, Athens, Greece

Sideris Athanasios
National Technical University of Athens,
9, Iroon Polytechneiou Street,
15780 Zografos, Athens, Greece

Potsiou Chryssy
National Technical University of Athens,
9, Iroon Polytechneiou Street,
15780 Zografos, Athens, Greece

Bakogiannis Efthimios
National Technical University of Athens,
9, Iroon Polytechneiou Street,
15780 Zografos, Athens, Greece

ISSN 1846-6168 (Print), ISSN 1848-5588 (Online)
https://doi.org/10.31803/tg-20241013235011

Original scientific paper
Received: 2024-10-13, Accepted: 2024-11-11

Optimal Configuration of Spatial Planning for Energy-Efficient Buildings

Figen Balo, Biljana Ivanović, Željko Stević*, Alptekin Ulutas, Dragan Marinković, Hazal Boydak Demir

Abstract: The project phase is where the life-cycle of a building starts. The best decisions are made during the design or pre-project step. In terms of both economic resources and time, changes to specific design decisions made at this step are inexpensive compared to subsequent steps of architectural planning, not to mention the course of the construction's operation itself. The choices made during the design phase determine to a large extent whether the architectural design decisions of a building are achieved, whether the building and site can be used appropriately, and whether the project is economically viable. With BIM, building spatial planning is possible. As a result, architects can evaluate the proposed structure, its impact on the ecology, and the ecology's impact on the structure more comprehensively and at an earlier stage. This research proposes an energy modeling approach for the BIM-based spatial planning phase of a construction. The proposed method will result in an energy model for specific sites and building resolutions when utilized to create a spatial modelling for a construction. The energy model can then be used for new architectural creations. In this study, 36 different alternative scenarios were designed in terms of the rate of construction height to construction spacing, orientation factor, and form factor. With the help of BIM and GBS softwares, the energy consumption values of the alternative scenarios in cooling and heating load conditions were compared, and the alternative scenario with the minimum energy consumption was tried to be determined with spatial planning parameters.

Keywords: BIM; energy efficiency; green building; spatial planning; urbanism

1 INTRODUCTION

In the building and construction sector, sustainable development is a powerful force for financial, environmental, and social progress with less negative results for the ecology. Energy consumption in buildings has been shown to increase rapidly with industrialization and urbanization [1]. Buildings are responsible for 40 percent of total energy usage, 70 percent of electricity load, and 40 percent of CO_2 emissions [2]. It is necessary to build maintainable applications in the construction and building sectors in order to develop energy performance, especially by utilizing spatial management techniques.

The validity of the design is based on the success of its implementation, and both academic and practical circles have placed great emphasis on this issue. Therefore, the objective and scientific assessment of the results of the application of spatial design has long been a topic of debate among designers, managers, and academics. It is quite challenging to determine with accuracy whether spatial design has been successful. It is also theoretically impossible to take one final decision on the relatively static outputs of design in a constant time and space.

Investigators say that the goal of design application assessment is not to debate whether a plan is successful or not, but rather to look at the effectiveness and process of the design application and give feedback based on the data. This feedback is used to make changes to the system of policy, content, operation, and design mechanism [3-5]. Continuous review and reflex on the results of the real application are necessary as a prerequisite for improving the control effectiveness of spatial design [6].

The evaluation of the design application initially depended more on the project evaluation on simulation. Implementation, a seminal work by Pressman and Wildavsky, is important information for early planning, implementation, and evaluation [7]. However, implementation reveals the unique aspects of spatial planning in a physical or geographical form [8]. Therefore, since the mid-2000s, studies on the evaluation of spatial planning implementation have gained more attention, especially at the simulation level [9]. A lot of country rules and regulations do not provide a specification for the spatial planning concept. In norm, spatial design refers to specific methodologies utilized in the industry that impact people's distribution and efficiency in varying sizes of spaces. Spatial planning occurs in a few degrees: regional (region design), urban (city design), international, and national strategies. The most significant aim of strategic spatial design is to connect territorial development's certain aspects through integrating ecological, financial, social, and cultural strategy. In Turkey, the word "spatial design" is often associated with the Turkish term "regional planning" and is used in reference to regional or urban strategy [10].

The degree of functional and a space's physical accessibility from one given reference point is known as its depth. In this respect, special attention is given to structures that serve purposes that require a more in-depth study of the spatial arrangement and have a more complex distribution of social activities. Many authors have studied hygienic buildings in an effort to identify appropriate layouts and measures that integrate theoretical elements with realistic flowcharts and navigational aids [11]. Li et al. determine spatial design as an operation that models the required urban matrix depending on the city's current matrix (by devaluing, continuing, or preserving it) [12]. According to Olugboyega et al., the desire to lead the industry in this area is the primary motivator for adopting Building Information Modelling (BIM), even though there hasn't traditionally been an industrial demand for it [13]. Ribeiro et al. provide environmental, energy, schedule, economic, and geographical analysis using the latest BIM tools to deliver real all-life value to clients. By using BIM, the team can produce new delivery schedules for each scenario that is

implemented, leading to increased efficiency in document production and distribution [14]. According to Sampaio et al., BIM models can provide walk-through representations to help clients make decisions; real-time, online designer input can speed up the design process and improve design quality [15]. BIM models allow the construction process to be visualized and can make the process inherently safer, according to Sampaio et al. [16]. The ability of 4D BIM to present dynamic construction processes on screen facilitates communication between designers and construction planners about the sequence of work, according to Sampaio et al. [17]. According to an evaluation by Green Building Studio simulation, the use of BIM can lead to cost savings and increased efficiency, as it reduced requests for information by 32% [18]. BIM can decrease the time required to prepare a cost estimate at a high ratio, according to research through Nawaz et al. In addition, 4D BIM provides comprehensive scheduling capabilities that can accurately estimate the time required for each construction activity, as well as plan future projects and the resources required for them [19]. To clarify the relationship between space and its content, Qanazi et al. and Srirangam et al. examined the research on mapping the dynamics with Space Syntax [20, 21]. The arrangement of spaces and functions within a particular social activity network is considered form according to The Space's Social Logic. The definition of depth and how it relates to activities are the main points of contention [22].

Rapid construction has emerged due to technological developments in the field of construction and the increase in people's desire for a qualified and comfortable life. In our country, as a result of unplanned urbanization, rapid construction, and ignoring energy-efficient design, the natural environment has been gradually destroyed, and energy resources have come to the point of depletion [18]. For this reason, by adopting the concept of sustainable energy in architecture, it is aimed at creating settlements that reduce the negatory effect of the building on the ecology and use energy resources effectively. The primary aim of the concept of sustainable power is to ensure the natural energy resources' effective utilize without harming the energy demand's natural cycle. A very large portion of energy resources are consumed by residential settlements in our country. For this reason, the energy consumption of residential settlements should be reduced first.

The interest in design aimed at reducing energy consumption has emerged naturally for the solution of environmental consequences. In addition, environmental problems have led to the formation of designs that are energy-efficient. Therefore, in the solution of environmental and energy-related problems, the technical information necessary for determining the design parameters that will reduce energy consumption should be created and presented to the designers. Within the framework of the technical information created, the optimum values of design parameters such as the location of buildings relative to each other, location, direction, and building spacing, which are effective in reducing energy consumption, should be examined.

This study was conducted in Ankara, the capital city of Turkey, where the density of settlements and housing is increasing day by day. While creating the study, BIM systems, which are developing day by day, were used to compare and develop settlement texture design alternatives and to make calculations related to energy efficiency.

In the study, the effectiveness of BIM systems will also be examined by using BIM models in reducing energy expenditures in the settlement texture and building. Within the scope of the study, Autodesk Green Building Studio is utilized for simulation and BIM-based Autodesk Revit 2020 programme is utilized for modelling. Depending on the results of the study, it is expected that residential settlement design proposals aiming to reduce energy consumption for the purpose of the study will be developed through BIM and these design proposals are expected to guide the new settlement textures planned to be designed [23].

2 BUILDING INFORMATION MODELLING

In the construction sector, BIM is a new technique and one of the latest trends. This technique uses three-dimensional modeling to design, communicate information, and analyze a building plan [24]. BIM facilitates the modification and sharing of design data through digitization. Contractors and design consultants can use the BIM simulation to obtain a calculated model of the building plan that closely resembles the actual design for the building area. This improves contact between team members throughout the design lifecycle, manages risk, reduces rework, and allows for more efficiency operation and sustainance of the building plant [25]. Three-dimensional modeling is related to the design database and displays the overall geometric data, spatial relationships, quantities, materials, and dimensions of the design elements [26].

BIM is a strong tool that can be utilized to display the whole life-cycle of a building, from maintenance and operation to construction and design. Through supply a common three-dimensional modelling of the design, it can aid to define potency conflicts among group members prior to operation and allow them to make any changes. It is almost a design stakeholder engagement, involving engineers, architects, owners, contractors, and tool managers, who overall have reach to the shared planning modellings. This ensures that all the stakeholders involved are aware of any changes or updates and makes it easy to make changes to the design. With BIM, even minor changes can be quickly shared and updated with overall planning stakeholders [27].

BIM is the process of managing and generating information about a group of buildings or a building. It involves a considerable amount of data that has an effect on each of the structures (their design, planning, construction, etc.) in the area or environment of the designed construction.

BIM is fast becoming the main strategy for the numerical combination of information and data in the management, implementation, and planning of facilities for building. But, in the present, BIM planning, construction practices, and integrated design have failed and are underestimating the

advantages that BIM supplies to the sector at different indications [28].

Thus, the management and generation of data about the building should start with the management and generation of data about the region in which the building is to be constructed. Recently, the probabilities for the development and application of BIM have been widely analyzed all over the world [29-31]. BIM is researched from different frameworks:

- Data management in the course of building step [32, 33],
- Implementation of online building work researches [34],
- Formation of BIM of present constructions by utilizing laser scanning [35],
- Design effectiveness comparisons of four-dimensional CAD crosscheck to two-dimensional CAD [36],
- Data exchange with respect to International Finance Corporation norms [37], and
- BIM data administration modeling from the form framework [38].

Communication operations and data exchange are such significant prerequisites for the improvement of a project [39]. Some researchers propose the data for BIM and GIS information [40-42]. For this purpose, building components and geographic information system information should be transformed into a semantic virtual information format [43, 44]. Others suggest hybrid modeling for BIM and an increased digital platform [45, 46]. In the actual world, enhanced digital mechanisms can relate an object to a digital model that represents it [47]. Three-dimensional building modeling can also be utilized for analyzing fire extinguishing works [48]. The combination of information from these 2 diverse arenas outputs in an interdependent impact that can encourage the transformation and evolution of industry, institutional collaboration, and processes.

In order to obtain and utilize detailed data about a construction, BIM must be associated with spatial and geographical data, as constructions are inherently linked to their environment; hence, the distances to various engineering substructures influence the utilization of a construction. This is also significant for the maintainable improvement framework. It is significant that overall data about a province is stored together for maintainable improvement. This hybrid data should include data about individual buildings and specific areas in the province [49]. In a country, the implementation of BIM to spatial planning in building planning is extremely dependent on the legislative framework for building. This expresses the specific actions of the law (technical construction rules, laws, regulations, hygiene standards, etc.) that organize the building operation and how they arrange it in a specific region. It is well known that the building industry is organized differently in diverse countries. Therefore, it is important to improve spatial modeling for building design to meet the needs of Turkey.

Two-dimensional floor plans are usually used for planning, discussing, presenting, and evaluating the efficiency of spatial planning projects in the traditional sense. However, each person may interpret the same two-dimensional floor plan in a different way, depending on his or her expectations, thus changing his or her perception of the intended pattern. In other words, the use of two-dimensional floor designs can lead to miscommunication and a waste of valuable time as a result of conflicting participant expectations [50-52]. Building Information Modeling has a parametric feature that allows structural data to be applied to a component and used to determine whether the result complies with applicable codes [53]. BIM helps the designer accurately and quickly understand the information related to the landscape and the drawing when there is an elevation shift [54].

In another way, BIM reduces the time needed to check compliance with regulations while facilitating the design of spatial models of buildings and the rapid presentation of design results [55]. Before using a two-dimensional drawing for space planning, it is usually necessary to confirm the nature and purpose of the space. The use of conventional two-dimensional floor plans also requires a number of procedures;

-Creating several floor projects with diverse positions,
-Simulating the circumstantial relationship among diverse locations utilizing the graph theorem,
- Providing the generation of the detailed technical drawing and the elevation technical drawing after the floor plan, and
- Assessing the relationship between the floor project and the elevation drawing to ensure conformity between the two. BIM speeds up, lowers the cost of, and improves the overall standard of community planning [56, 57].

In daily life, spatial design is thought to be one of the most significant research areas presently in existence, as it has an immediate impact. The modeling operation utilizing the known and current Building Information Modeling processes and tools has existed to develop the energy efficiency of the building body with its spatial planning.

Reducing energy consumption in housing estates, which account for a big proportion of energy usage, will contribute to the national economy and help other ındustries to reduce energy consumption. To this end, it is important that studies to reduce energy consumption are first carried out in settlements that involve more users and are of a larger scale. In order to overcome the problems due to rapid urbanisation, it is important to make optimal energy efficiency decisions at the settlement scale. Energy performance works carried out at the settlement scale will provide a reference for energy performance works to be carried out at the building, element and volume scales, which are smaller units [57-59].

In this context, the use of BIM systems will make it possible to assess the potential for reducing energy consumption in the design phase using BIM systems and to obtain the desired results as a basis for further studies. From the view point of the BIM systems' applicability and the BIM models' production, it will be possible to reduce energy consumption in housing and settlement textures and to widely use energy efficient settlement textures and housing designs. In addition, it will be possible to transfer it to the construction process and application project by using simulation cycles in the design phase of architecture. This will make it possible to create healthy, energy-efficient and comfortable environments [60].

In order to reduce the energy usage of the construction, energy performance targets should be set to include all sectors that consume energy, and priority should be given to the use of space management. The following sections provide information on the proposed changes to the building to achieve this.

Stage 1: The architectural designer specifies a numerical design of the development area from the regional design tool, with its general constraints and requirements, in their Building Information Modelling simulation window. As an element of the Regional Design Tool, this design already takes into consideration the development area's surroundings; health protection areas for agricultural buildings, factories, protection areas for roads, forests, water bodies, buildings, lines, urban development typologies, boundaries and development areas. The area design must also include data on the permitted density of development.

Stage 2: A building's spatial design is interactively carried out. The designer selects where to place the structure within the structure field in the structure zone depend on the structure boundaries or lines.

Stage 3: The designer chooses the building's spatial shape from the spatial shapes' library presented through the simulation, taking into consideration the overall 3D of the structure; width, height, and length.

Stage 4: The designer sets the required characteristics for the exterior separation structures (roof, windows, walls, etc.) from offered a library through the simulation: arrangement and number of windows, degree of acoustic insulation.

Stage 5. Then the modelling is utilized for energy-efficient architectural plan.

The lack of traditional methods and computer-aided design tools in the design phase has led to the prominence of the concept of BIM with the technology's development. In BIM management, all data belonging to the building works in connection with each other and is integrated. BIM software develops simulations by making calculations with various thermodynamic laws, some assumptions, and equations. The inputs of the building energy model are the parameters affecting energy use. These parameters are data such as building geometry, heating, cooling, lighting, ventilation systems, thermophysical properties of building materials, renewable energy systems, control strategies, and efficiency of systems. By combining the inputs of these parameters with local weather data and using physical equations, BIM programs calculate the thermal loads, the response of the systems to these loads, and the resulting energy use. The interaction of heating, cooling, and lighting systems is also taken into account. In addition, measurements such as user comfort and energy costs can be made. These programs can make simulations for a year or less [61]. The inputs required in a BIM-based energy analysis are: land and building location, building orientation, weather data, location and height of the building, type of building use, number of storeys, three dimensional geometry of adjacent buildings, three dimensional model of the building to be analyzed, curtain walls, including walls, floors, windows, roofs, foundations, shading elements, and doors, as well as building elements and detailed specifications [62].

3 RESULTS AND DISCUSSION

In this study, firstly, different settlement texture alternatives were created to reduce the amount of energy consumption in settlement textures. Different settlement texture alternatives were determined for Ankara province based on the frequently used settlement textures. Ankara province is located in the hot-dry climate zone. According to TS-825 Thermal Insulation Rules for Buildings, which are still in force in Turkey, Diyarbakır province is located in the 3rd region as the heating degree day zone [63, 64]. The climate data used in the evaluation were obtained from the weather station closest to the location of the project through the system after determining the location in the Revit program. The Revit program uses a system with a large database of climate data. There is no possibility to enter external climate data into the program yet. The determination of the most appropriate values for energy expenditures in the settlement texture alternatives was made by means of BIM software Autodesk Revit at the building scale and settlement scale. Then, annual energy consumption amounts were calculated for the reference residential structure selected with the developed options. Energy models made in the Autodesk Revit program were analyzed through the Green Building Studio system. Green Building Studio is an Autodesk Revit plugin. The cloud-based tool called Green Building Studio enables it to undertake building performance simulations at the start of the design process in order to maximize energy efficiency and strive toward carbon neutrality. All building components such as roofs, ceilings, windows, doors, and walls are used in Revit to automatically generate an energy analytical modelling. After that, Green Building Studio receives this data for energy simulation. The building, location, and certain detailed modellings and energy can be changed using the energy settings. Designing high-performance buildings in a fraction of the time and expense of traditional approaches is made possible by Green Building Studio [65].

One of the most important parameters in determining the structure of a settlement is the buildings' location in relation to each of the others and the spacing between constructions. As this parameter determines the degree of utilisation and protection of buildings from sunlight, it is important in reducing energy expenditure. In the alternative settlement patterns created, the distance between buildings was determined as the rate of building height to building spacing. Two diverse building height/building spacing ratios, 0.75 and 1.50, were determined during the creation of the settlement patterns. The (building height/building spacing) ratios and road widths in the alternative settlement patterns are shown in Tab. 1.

Table 1 According to (building height/building spacing) ratios and street widths in settlement pattern alternatives

Building Height / Building Spacing	Street Width		
	10 Storeys (30 m)	15 Storeys (45 m)	20 Storeys (60 m)
0.50	60	90	120
0.75	40	60	80
1.50	20	30	40

Another parameter in this evaluation is the building form. In determining the building forms, the common plan types in Ankara province were taken into account. All buildings in the settlement texture are considered to have the same form. The reference buildings to be analysed in the settlement texture consist of modules with a floor area of 169 m^2. 19 m^2 of these modules are allocated to circulation areas and 150 m^2 to residential areas. Form factors were then determined as the ratio of building width to building depth. Two diverse form factor alternatives of 1.00 and 2.00 were created for rectangular and square based plan types. For form factor 1.00, 4 modules were combined to form a square-based plan, while for form factor 2.00, 2 modules were combined (Tab. 2).

Table 2 Identified plan types and dimensions

Form Factor 1.00		Form Factor 2.00	
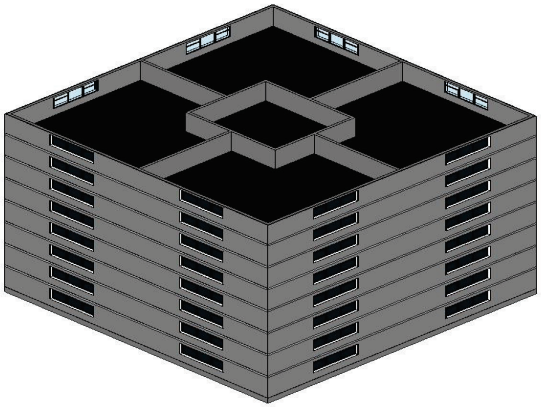		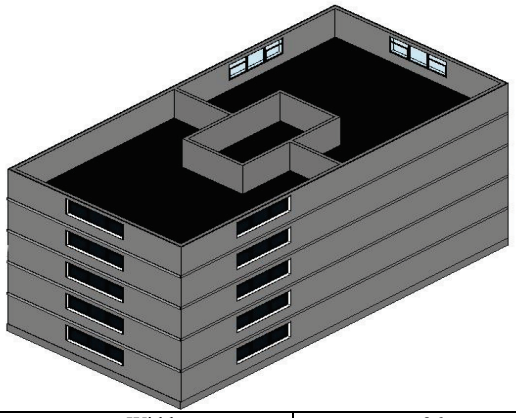	
Width	26 m	Width	26 m
Depth	26 m	Depth	13 m

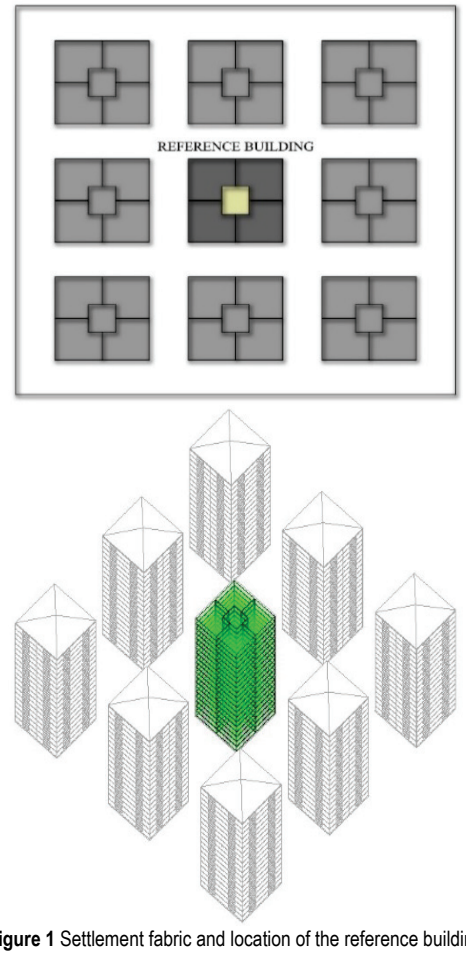

Figure 1 Settlement fabric and location of the reference building

In the settlement pattern alternatives, the all buildings' height is assumed to be 3.00 m. Three different building heights of 10, 15 and 20 storeys were determined. Buildings were created in a split layout. In creating the developed settlement textures, the building layout types commonly used in Ankara province were used as a reference. The settlement textures are composed of 9 equally shaped residential buildings. The building in the centre of the settlement texture was identified as the reference building (Fig. 1).

The orientation of buildings and settlements determines the effect of the external environment on the building. For this reason, orientation is important in assessing the effect of the external environment on reducing energy expenditure. These orientations are northsouth and northeast-southwest. Fig. 2 shows the orientation of the buildings.

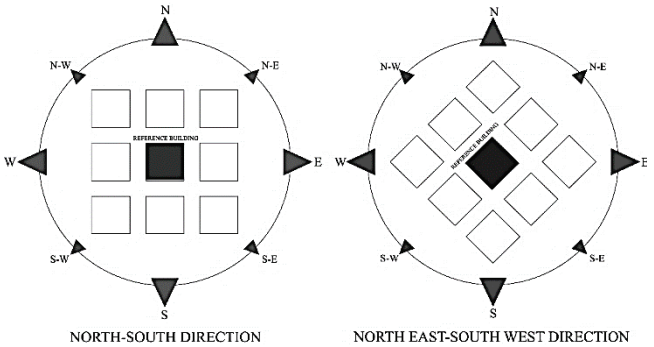

Figure 2 Orientation of buildings in settlement patterns

The thermophysical and optical features of the construction external wall, solar radiation and air temperature are important parameters as they affect the heat gain and heat loss of the construction. The thermophysical and optical

features of the materials used in the outer shell of the buildings in the developed settlement textures were defined taking into account the standard TS 825 - Thermal Insulation Rules in Buildings. The determined layer and thermal values are given in Tab. 3 [17].

The alternatives were coded in order to optimise the parameters determined in the study. The codes are displayed in Tab. 4.

As a result of the research, cooling, total and heating energy consumption were calculated. The energy consumption of 36 different alternatives is shown in the Fig. 3.

Table 3 Determined layer and thermal values

	U Value (W/(m²·K))
Wall	0.4051
Suspended Slab	8.3333
Floor Slab	0.7729
Roof	0.33

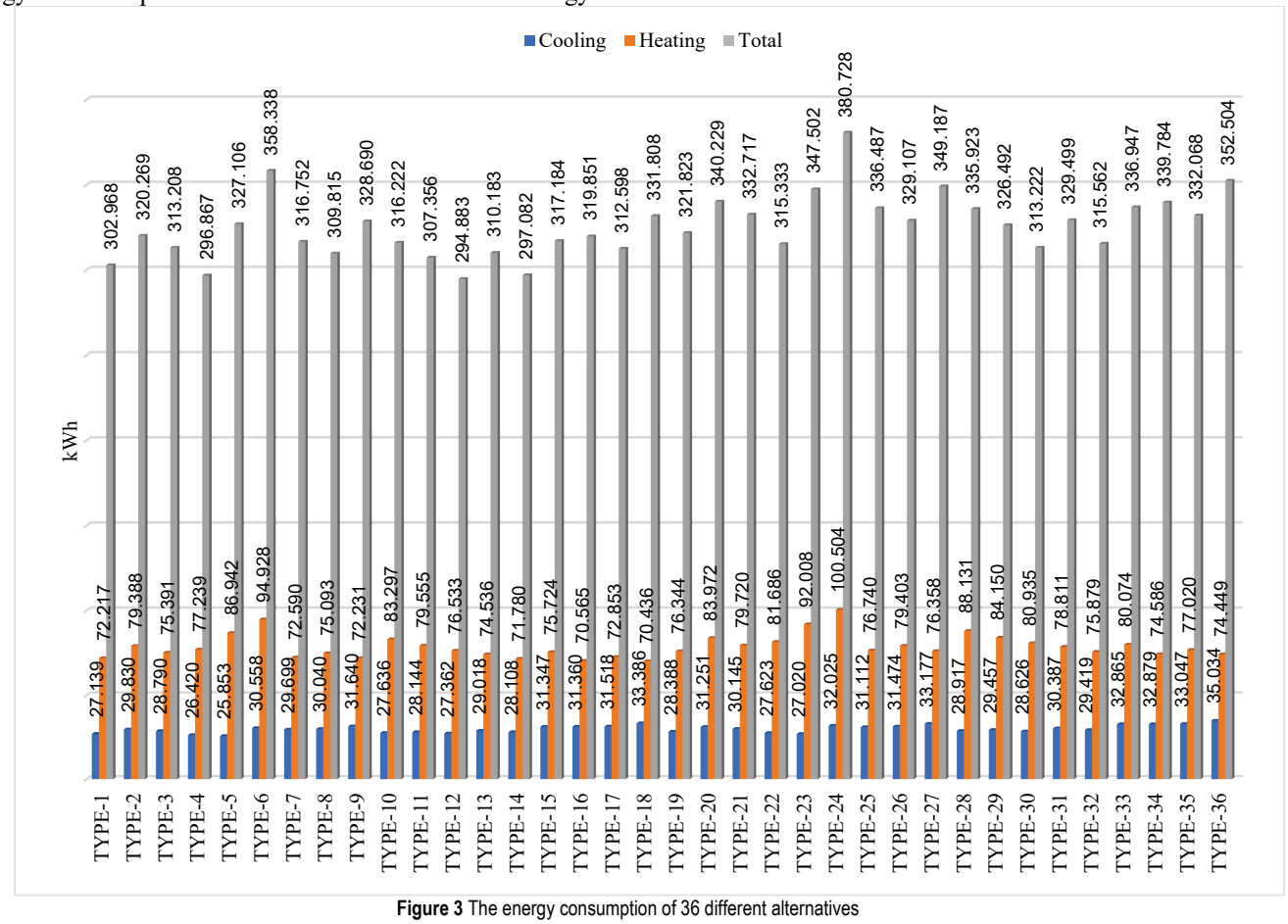

Figure 3 The energy consumption of 36 different alternatives

Table 4 Codes of the alternatives of the settlement structure

Form Factor	Number of Floors	Orientation	Building Height / Building Spacing ratio	Code
1.00	10	N-S	0,50	Type-1
1.00	10	N-S	0,75	Type-2
1.00	10	N-S	1,50	Type-3
1.00	10	NE-SW	0,50	Type-4
1.00	10	NE-SW	0,75	Type-5
1.00	10	NE-SW	1,50	Type-6
1.00	15	N-S	0,50	Type-7
1.00	15	N-S	0,75	Type-8
1.00	15	N-S	1,50	Type-9
1.00	15	NE-SW	0,50	Type-10
1.00	15	NE-SW	0,75	Type-11
1.00	15	NE-SW	1,50	Type-12
1.00	20	N-S	0,50	Type-13
1.00	20	N-S	0,75	Type-14
1.00	20	N-S	1,50	Type-15
1.00	20	NE-SW	0,50	Type-16
1.00	20	NE-SW	0,75	Type-17
1.00	20	NE-SW	1,50	Type-18
2.00	10	N-S	0,50	Type-19
2.00	10	N-S	0,75	Type-20
2.00	10	N-S	1,50	Type-21
2.00	10	NE-SW	0,50	Type-22
2.00	10	NE-SW	0,75	Type-23
2.00	10	NE-SW	1,50	Type-24
2.00	15	N-S	0,50	Type-25
2.00	15	N-S	0,75	Type-26
2.00	15	N-S	1,50	Type-27
2.00	15	NE-SW	0,50	Type-28
2.00	15	NE-SW	0,75	Type-29
2.00	15	NE-SW	1,50	Type-30
2.00	20	N-S	0,50	Type-31
2.00	20	N-S	0,75	Type-32
2.00	20	N-S	1,50	Type-33
2.00	20	NE-SW	0,50	Type-34
2.00	20	NE-SW	0,75	Type-35
2.00	20	NE-SW	1,50	Type-36

When analysing the cooling energy consumption amounts in relation to the building height to building distance ratio, which is the first parameter, it can be seen that the alternatives with a building height to building distance ratio of 0.50 generally have the lowest cooling energy consumption. The alternatives with a building height to building spacing ratio of 0.75 and the alternatives with a building height to building spacing ratio of 1.50 were found to have the lowest cooling energy consumption.

When the cooling energy consumption was analysed in terms of the orientation factor, which is a second parameter, it was found that the north-south orientation generally consumed more energy than the north-east-south-west orientation.

When analysed in terms of the form factor, a third parameter, it was found that alternatives with a form factor of 1.00 used less energy for cooling than alternatives with a form factor of 2.00.

The second step was to analyse the heating energy consumption. In terms of heating energy consumption in the analysed alternatives, it was found that the alternatives with a ratio of building height to building distance of 0.50 generally had the lowest heating energy consumption, followed by alternatives with a ratio of 1.50 and 0.75 respectively.

When analysing the orientation, which is another parameter in terms of heating energy consumption, it is found that north-south orientations generally consume less energy than northeast-southwest orientations.

When analysing the form factor parameter in heating energy consumption, it was found that alternatives with a form factor of 1.00 used less energy than alternatives with a form factor of 2.00.

The final step was to analyse the total energy consumption. When the total energy consumption amounts were first analysed in relation to the building height to building spacing ratio, it was found that the alternatives with a building height to building spacing ratio of 0.50 generally consumed less energy. It was then found that the alternatives with a ratio of 0.75 and 1.50 respectively consumed less energy.

When the orientation parameter was analysed in terms of total energy consumption, it was found that north-south orientations generally consumed less energy than northeast-southwest orientations.

Finally, the form factor parameter was analysed in terms of total energy consumption. In terms of total energy consumption, as with cooling and heating energy, alternatives with a form factor of 1.00 generally consumed less energy than alternatives with a form factor of 2.00.

4 CONCLUSIONS

It makes sense to consider solar gain, ventilation, noise and other factors using BIM. BIM benefits the entire lifecycle of a building project. For example, it enables more productive construction, better design decisions and more efficient maintenance and management of building portfolios. BIM supports architects in all aspects of sustainable design. It harnesses the idea of enhancing reality with greater effectiveness and quality. It enhances artistic vision with cutting-edge technological solutions that influence green planning. The introduction of BIM has ushered in a new age of diverse applications in the field of urban design. While there are many of these applications, the most significant are those related to infrastructure, roads, future planning, land use, engineering management, urban development, spatial analysis, waste management, archaeological area management and other implementations. BIM represents the building as a three-dimensional model and provides a complete library of object-oriented parametric information.

In this research, annual energy consumption amounts were evaluated comparatively. Subsequently, suitable settlement pattern alternatives and optimum values of design parameters were determined. The yearly energy usage amounts of the reference building considered in the settlement pattern designs were compared numerically. The alternatives showing the lowest energy consumption amount among the design parameters were selected as the optimum parameter value for the settlement texture. When comparing the alternatives, it was discovered that those with a building height to building spacing ratio of 0.50 often used less energy. The alternatives with a ratio of 0.75 and 1.50, respectively, were then discovered to use less energy. Similar to the energy utilized for cooling and heating, alternatives with a form factor of 1.00 typically consumed less energy overall than alternatives with a form factor of 2.00.

5 REFERENCES

[1] Chen, S., Zhang, G., Xia, X., Setunge, S. & Shi, L. (2020). A review of internal and external influencing factors on energy efficiency design of buildings. *Energy and Buildings*, *216*, 109944. https://doi.org/10.1016/j.enbuild.2020.109944

[2] Raj, P. V., Teja, P. S., Siddhartha, K. S. & Rama, J. K. (2021). Housing with low-cost materials and techniques for a sustainable construction in India-A review. *Materials Today: Proceedings*, *43*, 1850-1855. https://doi.org/10.1016/j.matpr.2020.10.816

[3] Martins, S. S., Evangelista, A. C. J., Hammad, A. W., Tam, V. W. & Haddad, A. (2022). Evaluation of 4D BIM tools applicability in construction planning efficiency. *International Journal of Construction Management*, *22*(15), 2987-3000. https://doi.org/10.1080/15623599.2020.1837718

[4] Balo, F. & Ulutaş, A. (2023). Energy-performance evaluation with Revit analysis of mathematical-model-based optimal insulation thickness. *Buildings*, *13*(2), 408. https://doi.org/10.3390/buildings13020408

[5] Rusyda Tamma, H., Gabriela Emilly, X., Arianisa Rihana, S. & Anastasia Evangelista, S. (2022). Evaluation toward BIM Learning Process: Case Study on Revit Integration. *Journal of Asian urban environment*, 65-70.

[6] Najafi, P., Mohammadi, M., van Wesemael, P. & Le Blanc, P. M. (2023). A user-centred virtual city information model for inclusive community design: State-of-art. *Cities*, *134*, 104203. https://doi.org/10.1016/j.cities.2023.104203

[7] Alexander, E. R. & Faludi, A. (1989). Planning and plan implementation: Notes on evaluation criteria. *Environment and planning B: Planning and Design*, *16*(2), 127-140. https://doi.org/10.1068/b160127

[8] Talen, E. (1996). Do plans get implemented? A review of evaluation in planning. *Journal of planning literature*, *10*(3), 248-259. https://doi.org/10.1177/088541229601000302

[9] Arimaviciute, M. (2011). The strategic development planning of local governments, following the examples of foreign countries. *Socialiniu Mokslu Studijos*, *3*(1), 59-76.

[10] Iban, M. C. (2020). Lessons from approaches to informal housing and non-compliant development in Turkey: An in-depth policy analysis with a historical framework. *Land Use Policy*, *99*, 105104. https://doi.org/10.1016/j.landusepol.2020.105104

[11] D'Amico, A., Bergonzoni, G., Pini, A. & Currà, E. (2020). BIM for healthy buildings: An integrated approach of architectural design based on IAQ prediction. *Sustainability*, *12*(24), 10417. https://doi.org/10.3390/su122410417

[12] Li, G., Wang, L., Wu, C., Xu, Z., Zhuo, Y. & Shen, X. (2022). Spatial planning implementation effectiveness: review and research prospects. *Land*, *11*(8), 1279. https://doi.org/10.3390/land11081279

[13] Olugboyega, O., Elubode, I. D., Oseghale, G. E. & Aigbavboa, C. (2023). BIM implementation model from the standpoint of concern-based adoption theory. *Frontiers in Engineering and Built Environment, 4*(1), 44-58. https://doi.org/10.1108/FEBE-01-2023-0002

[14] Ribeiro, F. P., Oladimeji, O., de Mendonça, M. B., Boer, D., Maqbool, R., Haddad, A. N. & Najjar, M. K. (2025). BIM-based parametric energy analysis of green building components for the roofs and facades. *Next Sustainability*, *5*, 100078. https://doi.org/10.1016/j.nxsust.2024.100078

[15] Sampaio, A. Z. (2021). Maturity of BIM implementation in the construction industry: Governmental Policies. *Int. J. Eng. Trends Technol*, *69*, 92-100. https://doi.org/10.14445/22315381/IJETT-V69I7P214

[16] Sampaio, A. Z., Gomes, N. & Gomes, A. M. (2023, June). 4D BIM Supporting the Construction Planning Process. In *2023 18th Iberian Conference on Information Systems and Technologies (CISTI)* (pp. 1-6). IEEE. https://doi.org/10.23919/CISTI58278.2023.10211881

[17] Sampaio, A. Z. & Gomes, A. M. (2022). Professional one-day training course in BIM: A practice overview of multi-applicability in Construction. *Journal of Software Engineering and Applications*, *15*(5), 131-149. https://doi.org/10.4236/jsea.2022.155007

[18] Sagbansua, L. & Balo, F. (2017). A novel simulation model for development of renewable materials with waste-natural substance in sustainable buildings. *Journal of Cleaner Production*, *158*, 245-260. https://doi.org/10.1016/j.jclepro.2017.04.107

[19] Nawaz, A., Su, X. & Nasir, I. M. (2021). BIM Adoption and Its Impact on Planning and Scheduling Influencing Mega Plan Projects-(CPEC-) Quantitative Approach. *Complexity*, *2021*(1), 8818296. https://doi.org/10.1155/2021/8818296

[20] Qanazi, S., Hijazi, I. H., Shahrour, I. & Meouche, R. E. (2024). Exploring Urban Service Location Suitability: Mapping Social Behavior Dynamics with Space Syntax Theory. *Land*, *13*(5), 609. https://doi.org/10.3390/land13050609

[21] Srirangam, S., Gunasagaran, S., Mari, T., Ng, V. & Kusumo, C. M. L. (2023). Spatial intelligence: integration of land use to connectivity in the context of eastern urbanism. *Archnet-IJAR: International Journal of Architectural Research*, *17*(1), 184-202. https://doi.org/10.1108/ARCH-12-2021-0355

[22] Jezzini, Y., Assaf, G. & Assaad, R. H. (2023). Models and methods for quantifying the environmental, economic, and social benefits and challenges of green infrastructure: A critical review. *Sustainability*, *15*(9), 7544. https://doi.org/10.3390/su15097544

[23] Pawłowicz, J. A. (2020). Computer-aided design in the construction industry-BIM technology as a modern design tool. *Budownictwo o zoptymalizowanym potencjale energetycznym*, *9*(2), 89-96. https://doi.org/10.17512/bozpe.2020.2.10

[24] Shaban, M. H., & Ali, H. M. Developing A Bim-Based Technique In The Design Phase To Achieve Sustainability In Residential Building Projects.

[25] Aya, A. S., Mohamed, A. F. & Wessam, H. A. (2023). Implementation of Building information model BIM for economic sustainable construction minimizing material waste terms of value engineering. *International conference on construction applications of virtual reality*, pp. 6-9.

[26] Ma, R. (2023). Application of BIM technology in whole life cycle management of assembled buildings. *Applied Mathematics and Nonlinear Sciences*, *9*(1). https://doi.org/10.2478/amns-2024-0679

[27] Xie, P., Zhang, R., Zheng, J. & Li, Z. (2022). Probabilistic analysis of subway station excavation based on BIM-RF integrated technology. *Automation in Construction*, *135*, 104114. https://doi.org/10.1016/j.autcon.2021.104114

[28] Borkowski, A. S. & Wyszomirski, M. (2021). Landscape Information Modelling: an important aspect of BIM modelling, examples of cubature, infrastructure, and planning projects. *Geomatics, Landmanagement and Landscape*, (1). https://doi.org/10.15576/GLL/2021.1.7

[29] Datta, S. D., Tayeh, B. A., Hakeem, I. Y. & Abu Aisheh, Y. I. (2023). Benefits and barriers of implementing building information modeling techniques for sustainable practices in the construction industry—A comprehensive review. *Sustainability*, *15*(16), 12466. https://doi.org/10.3390/su151612466

[30] Al-Dhaimesh, S. H. & Taib, N. (2023). A review: investigation of augmented reality–BIM benefits in design process in AEC industry. *Informatica*, *47*(5). https://doi.org/10.31449/inf.v47i5.4671

[31] Tang, X., Zhang, J. & Liang, R. (2023). The design of heating, ventilation, and air conditioning systems based on building information modeling: A review from the perspective of automatic and intelligent methods. *Journal of Building Engineering*, 108200. https://doi.org/10.1016/j.jobe.2023.108200

[32] Mohammad, W. N. S. W., Nabilah, N. & Azmi, M. (2023). Building information modeling (BIM)-based information management platform in the construction industry. *Int. J. Acad. Res. Bus. Soc. Sci*, *13*, 1957-1967. https://doi.org/10.6007/IJARBSS/v13-i4/16922

[33] Wu Yue, Y. (2023). Research on applications of Building Information Modelling (BIM) in construction project management information systems. *SHS Web of Conferences 169*, 01006. https://doi.org/10.1051/shsconf/202316901006

[34] Sajjad, M., Hu, A., Dorin, R. A. D. U., Waqar, A., Almujibah, H. R. & Mateen, A. (2024). BIM implementation in project management practices for sustainable development: Partial Least square approach. *Ain Shams Engineering Journal*, 103048. https://doi.org/10.1016/j.asej.2024.103048

[35] Sadeghineko, F., Lawani, K. & Tong, M. (2024). Practicalities of Incorporating 3D Laser Scanning with BIM in Live Construction Projects: A Case Study. *Buildings*, *14*(6), 1651. https://doi.org/10.3390/buildings14061651

[36] Liu, Z. (2024). Comparison and analysis of advantages and disadvantages between BIM and CAD in civil drafting software. *Applied and Computational Engineering*, *62*, 192-197. https://doi.org/10.54254/2755-2721/62/20240426

[37] Ding, C. & Kohli, R. (2021). Analysis of a building collaborative platform for Industry 4.0 based on Building

Information Modelling technology. *IET Collaborative Intelligent Manufacturing*, *3*(3), 233-242. https://doi.org/10.1049/cim2.12036

[38] Imoni, S., Tiza, M. T., Ogunleye, E., Jayi, V., Onuzulike, C. & Sesugh, T. (2024). The Impact of Building Information Modelling (BIM) in the Construction Industry. *Journal of Brilliant Engineering*, *1*, 4841.

[39] Lou, J., Lu, W. & Xue, F. (2021). A review of BIM data exchange method in BIM collaboration. In *Proceedings of the 25th International Symposium on Advancement of Construction Management and Real Estate* (pp. 1329-1338). Springer Singapore. https://doi.org/10.1007/978-981-16-3587-8_90

[40] Congiu, E., Quaquero, E. & Rubiu, G. (2024, July). BIM-GIS Integration through Open Tools. In *EC3 Conference*, Vol. 5, pp. 0-0). European Council on Computing in Construction. https://doi.org/10.35490/EC3.2024.308

[41] Wu, Y. (2019). Application Scenarios of GIS+BIM Engineering Construction Platform. Proceedings of the Fifth National BIM Academic Conference. Ed. *China Construction Industry Press*, 187-192.

[42] Zhang, H., Yuan, X., Yang, X., Han, Q. & Wen, Y. (2021, April). The integration and application of BIM and GIS in modeling. In *Journal of Physics: Conference Series, 1903*(1), p. 012074). IOP Publishing. https://doi.org/10.1088/1742-6596/1903/1/012074

[43] Basir, W. N. F. W. A. & Ujang, U. (2021). Building Information Modeling (BIM) and Geographic Information System (GIS) Data Compatibility for Constrcution Project. *Journal of Information System and Technology Management 6*(24), 278-289. https://doi.org/10.35631/JISTM.624026

[44] Vacca, G. & Quaquero, E. (2020). BIM-3D GIS: An integrated system for the knowledge process of the buildings. *Journal of Spatial Science, 65*(2), 193-208. https://doi.org/10.1080/14498596.2019.1601600

[45] Wagner, A., Bonduel, M., Werbrouck, J. & McGlinn, K. (2022). Geometry and geospatial data on the web. In *Buildings and Semantics* (pp. 69-99). CRC Press. https://doi.org/10.1201/9781003204381-5

[46] Xia, H., Liu, Z., Efremochkina, M., Liu, X. & Lin, C. (2022). Study on city digital twin technologies for sustainable smart city design: A review and bibliometric analysis of geographic information system and building information modeling integration. *Sustainable Cities and Society*, *84*, 104009. https://doi.org/10.1016/j.scs.2022.104009

[47] Zhu, J. & Wu, P. (2021). Towards effective BIM/GIS data integration for smart city by integrating computer graphics technique. *Remote Sensing*, *13*(10), 1889. https://doi.org/10.3390/rs13101889

[48] Zhu, J. & Wu, P. (2022). BIM/GIS data integration from the perspective of information flow. *Automation in Construction*, *136*, 104166. https://doi.org/10.1016/j.autcon.2022.104166

[49] Adouane, K., Stouffs, R., Janssen, P. & Domer, B. (2020). A model-based approach to convert a building BIM-IFC data set model into CityGML. *Journal of Spatial Science*, *65*(2), 257-280. https://doi.org/10.1080/14498596.2019.1658650

[50] Zhang, S., Zhongfu, L. I., Tianxin, L. I. & Mengqi, Y. U. A. N. (2021). A holistic literature review of building information modeling for prefabricated construction. *Journal of Civil Engineering and Management*, *27*(7), 485-499. https://doi.org/10.3846/jcem.2021.15600

[51] Hashim Mohammed, B., Sallehuddin, H., Safie, N., Husairi, A., Abu Bakar, N. A., Yahya, F., ... & AbdelGhany Mohamed, S. (2022). Building information modeling and internet of things integration in the construction industry: a scoping study. *Advances in Civil Engineering*, *2022*(1), 7886497. https://doi.org/10.1155/2022/7886497

[52] Junior, C. F. M., Biotto, C. N. & Serra, S. M. B. (2024). The integration of construction planning and budget using Building Information Modelling (BIM): a systematic literature review. *Caderno Pedagógico*, *21*(4), e3611-e3611. https://doi.org/10.54033/cadpedv21n4-039

[53] Girardet, A. & Boton, C. (2021). A parametric BIM approach to foster bridge project design and analysis. *Automation in Construction*, *126*, 103679. https://doi.org/10.1016/j.autcon.2021.103679

[54] Cortés-Pérez, J. P., Cortés-Pérez, A. & Prieto-Muriel, P. (2020). BIM-integrated management of occupational hazards in building construction and maintenance. *Automation in Construction*, *113*, 103115. https://doi.org/10.1016/j.autcon.2020.103115

[55] Han, J. Y., Chen, Y. C. & Li, S. Y. (2022). Utilising high-fidelity 3D building model for analysing the rooftop solar photovoltaic potential in urban areas. *Solar Energy*, *235*, 187-199. https://doi.org/10.1016/j.solener.2022.02.041

[56] Indrajit, A., Van Loenen, B., Ploeger, H. & Van Oosterom, P. (2020). Developing a spatial planning information package in ISO 19152 land administration domain model. *Land use policy*, *98*, 104111. https://doi.org/10.1016/j.landusepol.2019.104111

[57] Peters, R., Dukai, B., Vitalis, S., van Liempt, J. & Stoter, J. (2022). Automated 3D reconstruction of LoD2 and LoD1 models for all 10 million buildings of the Netherlands. *Photogrammetric Engineering & Remote Sensing*, *88*(3), 165-170. https://doi.org/10.14358/PERS.21-00032R2

[58] Palme, M., Privitera, R. & La Rosa, D. (2020). The shading effects of Green Infrastructure in private residential areas: Building Performance Simulation to support urban planning. *Energy and Buildings*, *229*, 110531. https://doi.org/10.1016/j.enbuild.2020.110531

[59] Abd-Elnaby, A. E. H. & Reffat, R. M. (2024). Enhancing BIM-BEM integration: solutions for efficient data exchange and energy performance assessment. *Architectural Engineering and Design Management*, *20*(3), 596-623. https://doi.org/10.1080/17452007.2024.2305734

[60] Abd-Elnaby, H. A., Reffat, R. M. & Morghany, E. (2021, March 13–15). Evaluating the role of building information modeling (BIM) in providing necessary data for the assessment of buildings energy performance. *Al-Azhar Engineering Fifteenth International Conference*, Cairo, Egypt.

[61] Shewale, M., Khartode, B., Shinde, N. & Sawadatkar, S. (2023). Building Information Modeling (BIM) Process and Assessment methods. In *E3S Web of Conferences*, *405*, p. 04011. EDP Sciences. https://doi.org/10.1051/e3sconf/202340504011

[62] Sepasgozar, S. M., Hui, F. K. P., Shirowzhan, S., Foroozanfar, M., Yang, L. & Aye, L. (2020). Lean practices using building information modeling (Bim) and digital twinning for sustainable construction. *Sustainability*, *13*(1), 161. https://doi.org/10.3390/su13010161

[63] Ucar, A. & Balo, F. (2011). Determination of environmental impact and optimum thickness of insulation for building walls. *Environmental Progress & Sustainable Energy*, *30*(1), 113-122. https://doi.org/10.1002/ep.10448

[64] TS 825 (2013). Thermal Insulation Rules Standard for Buildings. Turkish Standards Institute (Binalarda Isı Yalıtım Kuralları Standardı. Türk Standartları Enstitüsü), Ankara, Turkey

[65] https://gbs.autodesk.com/GBS/, accesed on October 29, 2024.

Authors' contacts:

Figen Balo
Department of METE, Engineering Faculty, Firat University,
23119 Elâzığ Merkez/Elazığ, Turkey
fbalo@firat.edu.tr

Biljana Ivanović
Faculty of Civil Engineering, University of Montenegro,
Džordža Vašingtona bb, 81000 Podgorica, Montenegro
biljanai@ucg.ac.me

Željko Stević
(Corresponding author)
Faculty of Transport and Traffic Engineering, University of East Sarajevo,
Vuka Karadžića 30, 71126 Lukavica, East Sarajevo,
Republic of Srpska, Bosnia and Herzegovina
zeljko.stevic@sf.ues.rs.ba
College of Engineering, Korea University,
Building 1 101, 145 Anam-ro, Seongbuk-gu, Seoul, Korea
172317@korea.ac.kr

Alptekin Ulutas
Department of International Trade and Business, Faculty of Economics and Administrative Sciences, Inonu University,
Merkez Kampüsü Malatya Türkiye 44280 Malatya/Malatya, Turkey
alptekin.ulutas@inonu.edu.tr

Dragan Marinković
Department of Structural Analysis, Berlin Institute of Technology,
Strasse des 17, Juni 135, 10623 Berlin, Germany
dragan.marinkovic@tu-berlin.de

Hazal Boydak Demir
Department of Architecture, Dicle University,
Fakulte 8. Sokak 2 21280 Diyarbakır Province/Diyarbakır, Turkey
hazal.boydak@dicle.edu.tr

ISSN 1846-6168 (Print), ISSN 1848-5588 (Online)
https://doi.org/10.31803/tg-20240904220222

Preliminary communication
Received: 2024-09-04, Accepted: 2024-10-25

Selection of an Appropriate Extrinsic Camera Calibration Method for Handheld Mobile Mapping Systems

Luka Zalović*, Siniša Mastelić-Ivić, Ante Rončević

Abstract: Mobile mapping systems integrate multiple sensors to collect large volumes of geospatial data in motion. With the growing demand for mapping enclosed and hard-to-reach areas, there has been significant advancement in handheld mobile mapping systems utilizing SLAM (Simultaneous Localization and Mapping) technology. To ensure their data is efficiently usable, these systems should produce oriented images, which are essential for visualization, point cloud colorization, and monoplotting. Achieving so requires precise extrinsic camera calibration. This research provides a comprehensive overview of existing extrinsic camera calibration methods and evaluates their suitability for application in handheld mobile mapping systems. The goal is to identify a method that meets the accuracy and practical needs of these systems, facilitating more effective data processing and utilization in challenging environments.

Keywords: external camera; extrinsic camera calibration; handheld mobile mapping systems; mobile mapping; SLAM

1 INTRODUCTION

Mobile mapping systems (MMS) are measurement systems that integrate multiple sensors to enable the collection of a large amount of data on the move [1]. Usually, these sensors are IMU (Inertial Measurement Unit), LiDAR (Light Detection and Ranging), GNSS (Global Navigation Satellite System) receiver and one or more cameras for generating high-resolution images. Thanks to the integration of many sensors, as well as precise time synchronization and calibration, it is possible to collect georeferenced 2D imagery and 3D laser scans without the need for the system to be stationary. Such an approach is of utmost importance because it has enabled mobile mapping systems to be mounted on moving platforms such as vehicles or aircraft and used for extremely rapid mapping of cities and infrastructure in a non-invasive manner [2]. Despite the remarkable capabilities of such systems, they also have several significant drawbacks. Firstly, the traditional approach to integration entails the use of high-quality, and consequently expensive, measurement sensors, which often poses a barrier to successful implementation. Furthermore, mobile systems are inflexible regarding mounting methods. Ground-based mobile systems are often unable to be mounted on aircraft, just as aerial mobile systems cannot be mounted on ground-based moving platforms. Finally, both aerial and ground-based mobile systems are quite limited in terms of measuring narrow streets, forested areas, underground structures, and indoor spaces. The reason for this lies in the impossibility or impracticality of direct access to these objects. That is why in recent years, increasing attention has been paid to the development of so called PLS (Personal Laser Scanning) mobile mapping systems [3]. These are systems that, for mobility purposes, do not require standard mobile platforms but are light enough for a person to carry on their back or in their hands.

2 HANDHELD MOBILE MAPPING SYSTEMS

Handheld mobile mapping systems are a type of PLS used by operators who carry them by hand through the area being surveyed. For practical reasons, such systems must be as small, light, and mobile as possible, which require certain compromises in terms of sensor integration. Handheld systems typically integrate only a laser scanner and an inertial measurement unit (IMU). Since sensor quality used in such integrations is not at the level of traditional mobile systems, handheld mobile mapping systems utilize advanced and robust SLAM (Simultaneous Localization and Mapping) algorithms. These algorithms enable precise reconstruction of the scanner trajectory using data from the laser scanner and IMU sensor, regardless of their somewhat lower quality [4]. The addition of SLAM algorithms to mobile mapping systems represents a significant technological advancement in the field of mobile mapping, as it enables the realization of measurement systems that are economically viable, lightweight, highly mobile, and ultimately produce precise and reliable output data [5].

2.1 SLAM Algorithms

Simultaneous Localization and Mapping (SLAM) is a fundamental concept in robotics, wherein a robot incrementally constructs a map of an unknown environment while simultaneously determining its position within that map (Fig. 1). This problem is pivotal for autonomous robot navigation, especially when prior knowledge of the environment is unavailable. SLAM can be framed probabilistically, where the objective is to estimate the joint posterior probability distribution of the robot's pose and the positions of landmarks in the environment, based on the robot's sensor observations and control inputs [6]. The core mathematical formulation of SLAM involves recursive Bayesian estimation. This can be expressed with the motion model:

$$P(\boldsymbol{x}_k \mid \boldsymbol{x}_{k-1}, \boldsymbol{u}_k) \tag{1}$$

which describes the probability P of the robot's current state ($\boldsymbol{x}_k$) given its previous state ($\boldsymbol{x}_{k-1}$) and control input ($\boldsymbol{u}_k$), and the observation model:

$$P(\boldsymbol{z}_k \mid \boldsymbol{x}_k, \boldsymbol{m}) \quad (2)$$

which defines the likelihood of making an observation ($\boldsymbol{z}_k$) given the current state ($\boldsymbol{x}_k$) and map ($\boldsymbol{m}$) [6].

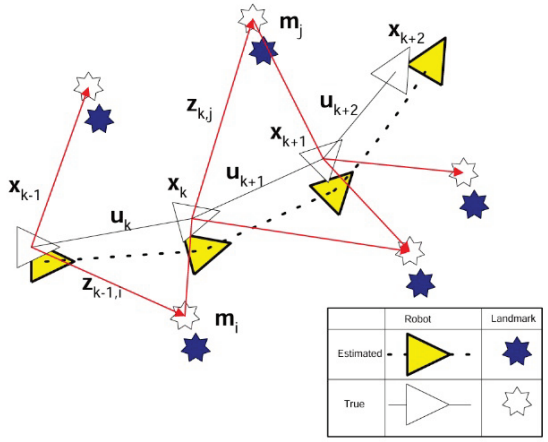

Figure 1 The essential SLAM problem. A simultaneous estimate of both robot and landmark locations is required while true locations are never known or measured directly. Observations are made between true robot and landmark locations.

The recursive nature of this problem allows for continuous updating of the map and pose estimates as new sensor data is acquired. However, the computational complexity of SLAM presents a significant challenge, particularly as the environment becomes more extensive and the number of landmarks increases. In its naive form, the SLAM algorithm scales quadratically with the number of landmarks, leading to prohibitive computational demands that are unsuitable for real-time applications [7]. To address these challenges, various strategies have been developed, such as state augmentation, sparsification, and submapping, which help reduce computational load while maintaining accuracy [8]. Another critical component of SLAM is data association, which involves correctly matching observed landmarks with those already recorded in the map. Errors in data association can lead to catastrophic mapping errors, particularly during loop closure, when the robot revisits previously mapped areas [9]. Loop closure is essential for correcting cumulative errors in the robot's pose estimate but requires accurate data association to avoid significant errors.

Recent advancements in SLAM research have focused on enhancing robustness and accuracy by incorporating richer environmental representations, moving beyond purely geometric models to include appearance-based features, which improve performance in diverse and complex environments. These developments have expanded SLAM's applicability to a wider range of scenarios, including those with dynamic elements and variable lighting conditions. Despite significant progress, challenges remain, particularly in scaling SLAM to large or highly unstructured environments. Ongoing research continues to address these issues, aiming to develop more efficient, scalable, and reliable solutions in the field of SLAM [10].

Today, SLAM is a crucial component of handheld mobile mapping systems, enabling accurate and real-time mapping and localization in diverse environments. SLAM technology has become increasingly vital in fields such as architecture, civil engineering, geodesy, forestry, and speleology, where precise and efficient spatial data collection is crucial.

2.2 Camera Integration

A component that is often missing in handheld mobile mapping systems is the integration of cameras for capturing RGB (Red, Green, Blue) images. Although some applications do not require their use, experience has shown that their availability significantly facilitates and accelerates the utilization of 3D data. Various manufacturers do not integrate cameras into handheld mobile systems because it would increase the mass and decrease mobility, thus reducing the practicality of the system. On the other hand, some opt to integrate small and low-quality imaging sensors, which often result in inadequate photographs. One of the most popular approaches to camera integration in such systems involves using an external camera that can be quickly mounted and removed from the system. All mentioned camera realizations for handheld mobile mapping systems are shown in Fig. 2. Approach with external camera is flexible and gives the user the option to use the camera only when needed. Also, external cameras often have higher-quality optics and image sensors compared to integrated cameras. However, the constant mounting and dismounting of the external camera will lead to changes in positional and angular offsets between the coordinate systems of the camera and the handheld mobile mapping system [11]. Moreover, even the regular usage of system will eventually affect the positional and angular offsets. Such changes can pose a significant problem for determining the exact position and orientation of the images, resulting in difficult manipulation and utilization of the collected data [12]. This issue is generally addressed through extrinsic camera calibration.

a) Integrated camera b) External camera c) No camera

Figure 2 Camera realizations in different handheld mobile mapping systems. Image a) shows system with integrated camera, b) shows system with external camera and c) shows system without camera

3 EXTRINSIC CAMERA CALIBRATION

To efficiently utilize data from handheld mobile mapping systems, it can be argued that 3D laser scan data should be accompanied by oriented imagery. Oriented images are those with known external orientation parameters, specifically 3D coordinates (X, Y, Z) and 3D rotations (angles φ, θ, and ψ) expressed in the mapping coordinate system (m-system) [12]. Such images are an extremely valuable visual tool for identifying and precisely defining the positions of

certain objects, which would be difficult or impractical to detect using only point clouds. Furthermore, oriented images combined with laser scans allow for the definition of 2D image coordinates on the photograph, which, thanks to the known internal and external orientation parameters, can be directly projected onto the laser scans, thereby directly obtaining 3D coordinates in the m-system. This approach is known as monoplotting [13] and is highly useful when working with 3D data since it enables the direct definition of 3D points using images instead of laser scans, contributing to faster and more reliable creation of survey products. Finally, oriented images allow for the colorization, i.e., the assignment of RGB values to the collected 3D points, which is important in many applications for obtaining an accurate impression of the real appearance of the terrain and objects [14].

A crucial prerequisite for obtaining oriented images is the successful extrinsic calibration of the mobile system's sensors. Specifically, in the case of mobile mapping systems with fixed-mounted sensors, calibration involves determining external calibration parameters, i.e., positional and angular offsets between the camera coordinate system (c-system) and the mobile system's navigation unit coordinate system (b-system) [11], as shown in Fig. 3.

Extrinsic camera calibration methods for handheld mobile systems are still insufficiently explored. Most of the methods researched so far are suitable for vehicle-based and aerial mobile mapping systems. However, some of these methods, or their combination, could potentially be used for camera calibration purposes in handheld mobile systems. Camera calibration methods for mobile mapping systems can generally be divided into methods based on measurement targets (target-based), methods based on object characteristics (feature based), methods based on 3D alignment (3D alignment-based), methods based on sensor motion prediction (motion-based), and methods based on dependencies (dependence based).

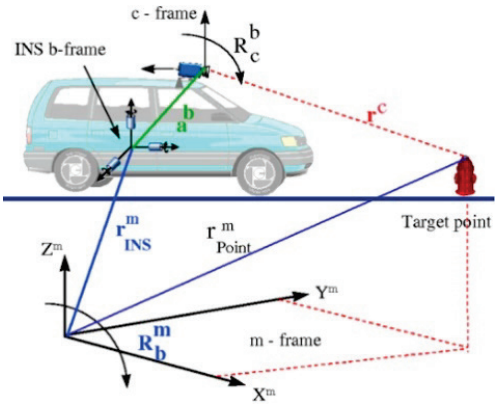

Figure 3 Coordinate systems of the mobile mapping system. External calibration parameters a^b and R_c^b allows for transformation between b-frame and c-frame

3.1 Target-Based Calibration Methods

Target-based methods are certainly the most well-known and thoroughly researched. These methods involve the use of artificial targets of known shape or pattern. The most commonly used targets are two-dimensional black-and-white patterns in the form of crosses, targets, or checkerboards (Fig. 4). Some authors have demonstrated successful implementation of three-dimensional targets such as trihedrals [15] and polygonal plates [16]. Regardless of the specific design of the target, the calibration method relies on finding identical points (in this case, the measurement targets) in the collected images and laser scans. Successfully identifying a sufficient number of identical points in both datasets allows for the mathematical adjustment process and the direct and unambiguous calculation of the external calibration parameters (positional and angular offsets). The use of targets with known shapes and patterns is crucial because images and scans represent two fundamentally different data formats. First and foremost, images are inherently two-dimensional, while laser scans are three-dimensional data. Furthermore, images do not contain information about the scale of the captured object, whereas laser scans do. Finally, the resolution of images is typically higher compared to the resolution of scans [17]. For these reasons, it is very challenging to define a method for the unambiguous and precise selection of identical points on both photographs and scans. Measurement targets with known shapes and patterns significantly simplify, and to a large extent, automate the process of selecting these identical points. The main drawbacks of such methods include the need to select, prepare, and set up the measurement targets, as well as the requirement to use software tools that will automatically (or semi-automatically) detect the targets and find identical points in the photographs and scans. It is important to note that the success of this method depends on the quality and resolution of the sensors used.

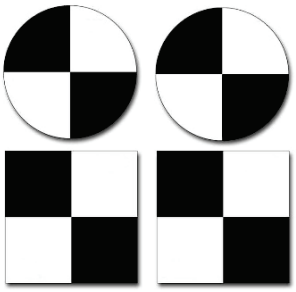

Figure 4 Targets with black-and-white patterns often used for calibration purposes. The difference in measured intensity on black and white segments allows for automatic detection of the target's centre.

3.2 Feature-Based Calibration Methods

Feature-based methods aim to calculate the external calibration parameters by detecting and matching common characteristic points, lines or shapes in 3D scans and images. Unlike target-based methods, the features used in these methods are not artificial targets. The available literature suggests that the most used features are road lines and building planes [18], although some authors have demonstrated successful calibration using car shapes [19], and even the skyline or horizon line [20], as shown in Figure 5. Regardless of the feature type, most of these methods are

based on one or a combination of the following approaches [21]:

- Extracting 3D features from laser scans and photogrammetrically reconstructed 3D models
- Extracting 3D features from laser scans and 2D data from images
- Creating a 2D image from laser scans and extracting the same 2D features from both datasets.

Figure 5 Skyline feature extraction from images and laser scan data. Left photograph is the original image, middle photograph represents threshold image (black pixels represent objects and white the sky) and the right photograph is the laser scan coloured by intensity.

Feature-based methods are well-suited for situations where there is a good distribution and visibility of features used for calibration, such as urban landscapes and built-up areas. On the other hand, these methods often yield poorer results in natural landscapes and areas with significant vegetation. Finally, the accuracy of the calibration itself is highly dependent on the quality of feature extraction in both datasets.

3.3 3D Alignment-Based Calibration Methods

3D alignment-based methods use the so-called "cloud-to-cloud" registration method to align two point clouds in order to determine the external camera calibration parameters [21]. In this process, the first point cloud is obtained from the laser sensor, while the second one needs to be calculated through photogrammetric 3D reconstruction based on the collected images. Point cloud registration involves the application of the well-known ICP (Iterative Closest Point) algorithm (Figure 6), which allows for the precise alignment of the photogrammetric point cloud with the 3D scan of the mobile mapping system, given there is enough overlap between the two datasets [22].

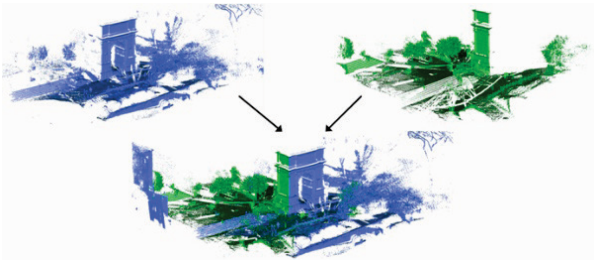

Figure 6 Registration of two point cloud by means of ICP algorithm. To be successful, the algorithm requires an overlap between two datasets.

3D alignment-based methods are accurate and provide reliable data in a wide range of situations; however, they are better suited to aerial mobile systems. This is due to the fact that the reliability of photogrammetric reconstruction heavily depends on the longitudinal and lateral overlaps between images, which are extremely difficult to achieve from the ground but straightforward from the air. Additionally, 3D alignment-based methods require initial rough alignment between the two point clouds and are extremely time-consuming due to the need for dense 3D point cloud reconstruction from the images.

3.4 Motion-Based Calibration Methods

Motion-based methods aim to calculate calibration parameters by utilizing knowledge of the movement of rigidly mounted sensors on a mobile platform [21]. Rigid sensor mounting means that the relative offset between sensors remains constant, regardless of the platform's movement. These methods are closely related to the hand-eye calibration problem (Fig. 7) addressed by the robotic community, where a camera ("eye") is rigidly mounted on a robot gripper ("hand"). The aim of the hand-eye calibration is to estimate the unknown transformation between the camera and the gripper coordinate frames based on the motions undergone by the gripper and camera, with the latter being estimated from captured images [23].

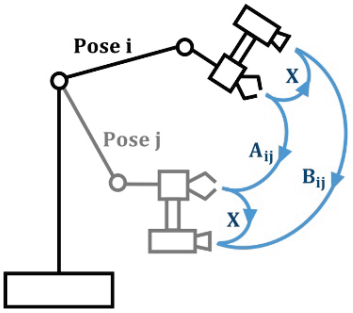

Figure 7 "Hand-eye" calibration problem visualisation. The aim is to find transformation X (camera calibration matrix) by using known transformations A_{ij} between different poses (i, j) and B_{ij} between observed image changes.

In earlier research, the main limitation of these methods was the need to use calibration markers to estimate the camera's motion [24, 25]. Recent studies, however, confirm the feasibility of using visual odometry and Structure from Motion (SfM) algorithms to overcome this limitation [26]. The most common approach in sensor motion prediction-based methods is to estimate the motion of the laser sensor using the ICP (Iterative Closest Point) algorithm, while camera motion prediction is achieved by tracking feature points in the photographs. The advantages of these methods include not requiring overlap between laser and image sensor data and not needing initial values for the calibration parameters. On the other hand, these methods require a significant amount of movement to accurately determine sensor motion, as well as precise temporal synchronization of both sensors.

3.5 Dependence-Based Calibration Methods

Dependence-based methods attempt to estimate the external camera calibration parameters based on the

similarity between the signals of the laser scanner and optical images. Typically, this signal is expressed in a two-dimensional space, making it necessary to generate a 2D image from the laser sensor data by interpolating and projecting the laser data onto the image plane [27]. The fundamental assumption of dependence-based methods is that the two signals, one obtained from the laser sensor and the other from the image sensor, are somehow correlated (Figure 8). An example of such a signal is the reflectivity captured by the laser sensors and the grayscale values derived from RGB images. According to the current research and literature, these methods have been tested on sensors used for traditional terrestrial and aerial mobile systems, as well as on smaller 2D laser profilers and simple image sensors. In both cases, these methods have been proven to be extremely fast, reliable, and capable of automation. Unfortunately, they also have some significant drawbacks. Current studies confirm the need for an exceptionally narrow search space for accurate calibration parameters, which means they are limited to optimizing already precisely determined calibration parameters [28]. Finally, factors such as uneven lighting or shadows can significantly affect the correlation between the signals used, potentially resulting in inaccurate calibration parameters.

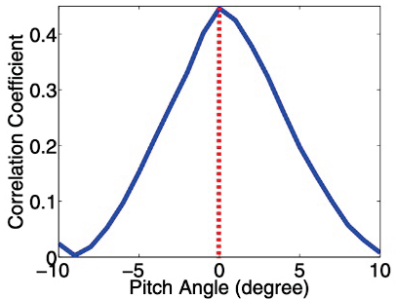

Figure 8 Reflectivity-greyscale Correlation Coefficient rising as it approaches correct calibration parameter (in this case, pitch calibration angle)

4 LIMITATIONS OF EXISTING CALIBRATION METHODS

Despite the advancements and success of the calibration methods discussed above, none of these approaches are fully suited to the specific requirements of handheld mobile mapping systems. The challenges posed by these systems, primarily due to their compact form, lower sensor quality, high degree of movement variability and need for frequent recalibration necessitate a re-evaluation of existing calibration techniques, which are primarily developed for aerial and vehicle-based mobile mapping systems. A brief overview of why each of the described methods faces limitations in the context of handheld mobile mapping systems is given below:

1) Target-based calibration methods require the use of artificial targets that must be carefully selected, prepared, and positioned in the environment. The process is labour-intensive and less practical for handheld systems, where quick deployment and flexibility are critical. Additionally, the lower resolution and quality of sensors in handheld systems can hinder the automatic detection of targets and the accurate identification of identical points across datasets, leading to unreliable calibration.
2) Feature-based calibration methods, while effective in urban environments with clearly defined features, struggle in natural landscapes or areas with sparse or indistinct features. Handheld systems, often used in diverse and uncontrolled environments, may not always have access to the consistent and prominent features required for accurate calibration. Moreover, the dependence on high-quality feature extraction, which can be challenging with the lower-grade sensors typical of handheld devices, further limits the reliability of these methods.
3) 3D alignment-based calibration methods rely heavily on accurate photogrammetric reconstruction and require substantial overlap between images, which is challenging to achieve with handheld systems due to their inherent instability and irregular movement. The need for initial rough alignment and the computationally intensive nature of dense 3D point cloud reconstruction make this approach less feasible for performing camera calibration frequently.
4) While motion-based calibration methods may not require data overlap between the laser and image sensors, they demand precise temporal synchronization and significant sensor movement to determine calibration parameters accurately. Handheld systems, which often experience erratic and inconsistent movement, may not provide the stable conditions needed for these methods to work effectively, rendering them impractical for this application.
5) Dependence-based calibration methods, while fast and potentially automatable, are highly sensitive to variations in lighting and environmental conditions. The correlation between laser and image signals can be disrupted by shadows or uneven lighting, leading to inaccurate calibration. Additionally, the narrow search space required for these methods limits their flexibility, making them less adaptable to the varied and dynamic conditions typical of handheld mobile systems.

All the calibration methods, together with their advantages and disadvantages regarding camera calibration of a handheld mobile mapping system, are summarized in Tab. 1.

Table 1 Existing extrinsic camera calibration methods

	Pros	Cons
Target-based methods	Accurate and computationally fast	Target detection due to sensor quality
Feature-based methods	Effective in urban landscapes and built-up areas	Feature extraction due to sensor quality
3D alignment-based methods	Automatic alignment of point clouds	Image overlap and computational intensity for frequent calibrations
Motion-based methods	No need for data overlap nor initial calibration parameters	Accurate temporal synchronisation and significant amount of motion
Dependence-based methods	Fast, reliable and automated	Narrow search space and influence of shadows on correlation

5 NOVAL CAMERA CALIBRATION APPROACH

Given the limitations of existing calibration methods, it is evident that there is a need for a new method specifically tailored to the unique demands of handheld mobile mapping systems. This new approach should address the challenges posed by lower sensor quality, irregular movement, and diverse operational environments. What is more, it should be straightforward for the end user to implement and conduct frequently, objective, and consider the specific characteristics of handheld mobile systems, which are:

- Unlike aerial or vehicle-based mobile mapping systems, handheld systems can be easily placed over a control point, by utilising so-called "reference plate", as shown in Fig. 9.
- Handheld systems do not require a moving platform or have specific operating limitations, allowing for complete control over the conditions in which the calibration process is carried out.
- Handheld systems often utilise lower resolution external cameras capable of collecting panoramic imagery at a specific time interval. Such images can be efficiently used for photogrammetric purposes by utilising spherical camera model and Structure from Motion algorithms.

Figure 9 Reference plate for handheld mobile mapping systems. The system is placed on a reference point in a way that the cross coincides with the point marker. The positional offset between the centre of the cross and b-system of mobile mapping system needs to be known.

Considering all the characteristics, the new calibration method should be a combination of existing calibration techniques, specifically target-based and motion-based methods. External calibration parameters could be determined through a so-called calibration scan, which would be a short scan (around 1 minute) conducted in a controlled environment suitable for both SLAM and SfM algorithms. Targets with black-and-white patterns should be utilized, as they can be automatically detected in the images. The coordinates of these targets in the mapping system (m-frame) can be extracted by placing the handheld mobile mapping system directly over them using a reference plate. Photogrammetric processing of the collected panoramic images should be performed using optimized SfM algorithms and a spherical camera model, with the target coordinates added as ground control points (GCPs). This process would produce two datasets: images with an initial pose that do not contain positional and angular offsets, and images with an optimized pose that includes these offsets. Finally, the external calibration parameters would be estimated using a least squares adjustment. The described noval approach will be examined in more detail in future research.

6 CONCLUSION

This paper has presented a comprehensive review of extrinsic camera calibration methods, emphasizing their suitability for handheld mobile mapping systems. Handheld systems, while offering unique advantages over aerial and vehicle-based platforms, present distinct challenges, especially when it comes to camera integration and calibration. Due to specific characteristics of handheld mobile mapping systems, such as high versatility and mobility, lower mapping and navigation sensor quality and need for frequent camera calibration, traditional extrinsic camera calibration methods are not suitable for them. The calibration process for handheld systems must therefore be designed to be straightforward and quick, allowing users to perform the calibration independently. It is essential that the process remains objective, minimizing user errors while ensuring accuracy. Finally, the calibration method should take advantage of unique capabilities of handheld systems, such as the possibility do be placed over control point, their independence of vehicle-based moving platform and interval-based panoramic image collection which can be efficiently used for photogrammetric purposes. By focusing on the specific requirements and constraints of handheld systems, a novel calibration method could enhance the accuracy and reliability of these systems, enabling more effective and versatile mapping solutions

7 REFERENCES

[1] Løvås, M. (2017). Increasing the Accuracy of Positioning in Mobile Mapping Systems, a Method Supported by Simultaneous Localization and Mapping. *Master thesis*, NTNU, July 2017.

[2] El-Sheimy, N. (2005). An Overview of Mobile Mapping Systems. *FIG Working Week 2005 and GSDI-8*, Cairo, Egypt April 16-21, 2005.

[3] Lauterbach, H., Borrmann, D., Heß, R., Eck, D., Schilling, K. & Nüchter, A. (2015). Evaluation of a backpack-mounted 3D mobile scanning system. *Remote sensing, 7*(10), 13753-13781. https://doi.org/10.3390/rs71013753

[4] Bosse, M., Zlot, R. & Flick, P. (2012). Zebedee: Design of a Spring-Mounted 3-D Range Sensor with Application to Mobile Mapping. *IEEE Transactions on Robotics, 28*(5). https://doi.org/10.1109/TRO.2012.2200990

[5] Durrant-Whyte, H. & Bailey, T. (2006). *Simultaneous Localisation and Mapping (SLAM): Part I The Essential Algorithms*. Australian Centre for Field Robotics (ACFR) J04, The University of Sydney, Sydney NSW 2006, Australia.

[6] Smith, R. & Cheesman, P. (1987). On the representation of spatial uncertainty. *Int. J. Robotics Research, 5*(4), 56-68. https://doi.org/10.1177/027836498600500404

[7] Dissanayake, G., Newman, P., Durrant-Whyte, H. F., Clark, S. & Csobra, M. (2001). A solution to the simultaneous localisation and mapping (SLAM) problem. *IEEE Trans. Robotics and Automation, 17*(3), 229-241. https://doi.org/10.1109/70.938381

[8] Montemerlo, M., Thrun, S., Koller, D. & Wegbreit, B. (2002). Fast SLAM: A factored solution to the simultaneous localization and mapping problem. *AAAI National Conference on Artificial Intelligence*, 593-598.

[9] Neira, J. & Tardos, J.D. (2001). Data association in stochastic mapping using the joint compatibility test. *IEEE Transactions on Robotics and Automation, 17*(6), 890-897. https://doi.org/10.1109/70.976019

[10] Thrun, S., Liu, Y., Koller, D., Ng, A. & Durrant-Whyte, H. (2004). Simultaneous localisation and mapping with sparse extended information filters. *Int. J. Robotics Research, 23*(78), 693-716. https://doi.org/10.1177/0278364904045479

[11] Gopaul, N.-S., Wang, J. & Hu, B. (2016). Camera auto-calibration in GPS/INS/stereo camera integrated kinematic positioning and navigation system. *The Journal of Global Positioning Systems, 14*(3), 1-15. https://doi.org/10.1186/s41445-016-0003-7

[12] Rau, J.-Y., Habib, A.-F., Kersting, A.-P., Chiang, K.-W., Bang, K.-I., Tseng, Y.-H. & Li, Y.-H. (2011). Direct Sensor Orientation of a Land Based Mobile Mapping System. *Sensors, 11*(7), 7243-7261. https://doi.org/10.3390/s110707243

[13] Santos, R. D., Dal Poz, A. P. & Dalmolin Q. (2010). Indirect orientation of images using control points extracted by the means of monoplotting model. *The Photogrammetric Journal of Finland, 22*(1).

[14] Vechersky, P., Cox, M., Borges, P. & Lowe, T. (2018). Colourising Point Clouds Using Independent Cameras. *IEEE Robotics and Automation Letters, 3*(4). https://doi.org/10.1109/LRA.2018.2854290

[15] Gong, X., Lin, Y. & Liu, J. (2013). 3D LIDAR-Camera Extrinsic Calibration Using an Arbitrary Trihedron. *Sensors, 13*(2), 1902-1918. https://doi.org/10.3390/s130201902

[16] Park, Y., Yun, S., Won, C.-S., Cho, K., Um, K. & Sim, S. (2014). Calibration between Color Camera and 3D LIDAR Instruments with a Polygonal Planar Board. *Sensors, 14*, 5333-5353. https://doi.org/10.3390/s140305333

[17] Mishra, R.-K. & Zhang, Y. (2012). A Review of Optical Imagery and Airborne LiDAR Data Registration Methods. *The Open Remote Sensing Journal, 5*, 54-63. https://doi.org/10.2174/1875413901205010054

[18] Cui, T., Ji, S., Shan, J., Gong, J. & Liu, K. (2017). Line-Based Registration of Panoramic Images and LiDAR Point Clouds for Mobile Mapping. *Sensors, 17*, 70, 1-20. https://doi.org/10.3390/s17010070

[19] Li, J., Yang, B., Chen, C., Huang, R., Dong, Z. & Xiao, W. (2017). Automatic registration of panoramic image sequence and mobile laser scanning data using semantic features. *ISPRS Journal of Photogrammetry and Remote Sensing, 136*, 41-57. https://doi.org/10.1016/j.isprsjprs.2017.12.005

[20] Hofmann, S., Eggert, D. & Brenner, C. (2014). Skyline matching based camera orientation from images and mobile mapping point clouds. *ISPRS Annals of the Photogrammetry, Remote Sensing and Spatial Information Sciences, II-5*, 181-188. https://doi.org/10.5194/isprsannals-II-5-181-2014

[21] Pentek, Q., Kennel, P., Allouis, T., Fiorio, C. & Strauss, O. (2020). A Flexible Targetless LiDAR–GNSS/INS–Camera Calibration Method for UAV Platforms. *ISPRS Journal of Photogrammetry and Remote Sensing, 166*, 294-307. https://doi.org/10.1016/j.isprsjprs.2020.05.014

[22] Abayowa, B.-O., Yilmaz, A. & Hardie, R.-C. (2015): Automatic registration of optical aerial imagery to a LiDAR point cloud for generation of city models. *ISPRS Journal of Photogrammetry and Remote Sensing, 106*, 68-81. https://doi.org/10.1016/j.isprsjprs.2015.05.006

[23] Tsai, R. Y. & Lenz, R. K. (1989). A new technique for fully autonomous and efficient 3D robotics hand/eye calibration. *IEEE Transactions on Robotics and Automation, 5*(3), 345-358. https://doi.org/10.1109/70.34770

[24] Shiu, J.-C. & Ahmad, S. (1989). Calibration of wrist-mounted robotic sensors by solving homogeneous transform equations of the form *AX=XB*. *IEEE Transactions on Robotics and Automation, 5*(1), 16-29. https://doi.org/10.1109/70.88014

[25] Wang, C. C. (1992). Extrinsic calibration of a vision sensor mounted on a robot. *IEEE Transactions on Robotics and Automation, 8*(2), 161-175. https://doi.org/10.1109/70.134271

[26] Schmidt, J., Vogt, F. & Niemann, H. (2005). Calibration–free hand–eye calibration: a structure–from–motion approach. *Joint Pattern Recognition Symposium*, Springer, 67-74. https://doi.org/10.1007/11550518_9

[27] Wang, R., Ferrie, F.-P. & Macfarlane, J. (2012). Automatic Registration of Mobile LiDAR and Spherical Panoramas. *Computer Vision and Pattern Recognition Workshops (CVPRW2012), IEEE Computer Society Conference*. https://doi.org/10.1109/CVPRW.2012.6238912

[28] Pandey, G., McBride, J.-R., Savarese, S. & Eustice, R. M. (2015). Automatic Extrinsic Calibration of Vision and Lidar by Maximizing Mutual Information. *Journal of Field Robotics, 32*(5), 696-722. https://doi.org/10.1002/rob.21542

Authors' contacts:

Luka Zalović, mag. ing. geod. et geoinf.
(Corresponding author)
University of Zagreb, Faculty of Geodesy,
Fra Andrije Kačića Miošića 26, 10000 Zagreb, Croatia
lzalovic@geof.hr

Siniša Mastelić-Ivić, prof. dr. sc.
University of Zagreb, Faculty of Geodesy,
Fra Andrije Kačića Miošića 26, 10000 Zagreb, Croatia
sinisa.mastelic.ivic@geof.unizg.hr

Ante Rončević, prof. dr. sc.
University North, Business Economics,
Jurja Križanića 31b, 42000 Vataždin, Croatia
ante.roncevic@unin.hr

ISSN 1846-6168 (Print), ISSN 1848-5588 (Online)
https://doi.org/10.31803/tg-20240907113323

Preliminary communication
Received: 2024-09-07, Accepted: 2024-10-28

Influence of 3D Barriers on Walkability for the Elderly in a German City

Hartmut Müller*, Konstantin Geist, Klaus Böhm, Markus Schaffert

Abstract: Walking is a sustainable, safe, and active mode of transportation. The benefits that the elderly in particular gain from outdoor walking are manifold, be it free and independent access to stores and services of all kinds or the opportunity to socialize, enjoy parks, et cetera. This article depicts one particular factor that affects outdoor walkability, namely the gradient of walking paths. Steep slopes can be a serious obstacle to walkability, primarily for older people. The evaluation of available geospatial data sources formed the basis for a geospatial analysis of walkability in the larger city of Kaiserslautern, located in southwest Germany. The concept of Walk Score was used to quantify the results obtained. The results demonstrate that the Walk Score can be refined to better address the mobility needs of older adults. The methodology was implemented for the German city of Kaiserslautern by integrating volunteered geographic information with high-quality official datasets.

Keywords: Authoritative Geospatial Data; Geospatial analysis; OpenStreetMap; Volunteered Geographic Information; Walkability

1 INTRODUCTION

When it comes to the ideal of a walkable city, there are many good reasons for it. Walkable neighbourhoods, among other objectives, foster physical mobility and thus promote residents' health [1-4]. Consequently, walkability plays a key role in concepts such as 20-minute neighbourhoods and the 15-minute city (cf. [5, 6]).

Walkability indices provide objective benchmarks as a base for rating neighbourhoods and cities [7-9].

However, most studies have only partially addressed the needs of specific groups, such as the elderly [10-12].

Additionally, factors like city size and structure have rarely been considered in pedestrian mobility studies [13-15].

This article presents a case study on urban walkability with a focus on elderly populations. The approach is based on the generic Walk Score model, which the authors adapt to account for older individuals' needs. The authors consider obstacles such as sloping terrain and stairways, adjusting walking time calculations to reflect these challenges for older people. In addition, the weighting of supply services are tailored to senior citizens' requirements.

The walkability index was implemented for the city of Kaiserslautern, located in the south-west of Germany, as a case study. In the following sections, details of the methodology are given and the results obtained using the adjusted Walk Score in the study area are discussed. Lastly, the conclusions highlight the benefits and limitations of the methodology and suggest areas for future enhancements.

2 METHODOLOGY

The study area was subdivided into a grid of square 100 meter cells. This grid system is used by official statistics in Germany and is also a reference system as defined by the Infrastructure for Spatial Information in Europe INSPIRE [16, 17]. It is therefore possible to link the results of our work with statistical data available in this spatial reference system. Walkability can then easily be further detailed by age or other socio-demographic variables of the population.

Walking time depends on the inclination of the walking paths. After Weidmann [18], the average horizontal gait speed of a pedestrian can be set at 1.34 m/s (metres per second). A gradient of 5% slows the speed uphill to 1.29 m/s and slightly accelerates the speed downhill to 1.38 m/s. The corresponding figures for a 10% gradient are 1.19 m/s uphill and 1.40 m/s downhill. For a 15% gradient, Weidmann estimates 1.07 m/s uphill and 1.40 m/s downhill. All these figures refer to the average population and are not specifically tailored to older people. Artmann et al. [19] set the walking speed of seniors on a horizontal surface at 1 m/s. Assuming the same influence on gait speed on inclined walking paths on a percentage base, the figures reported by Weidmann can be reduced by a factor of 1/1.34. The resulting gait speeds for senior citizens are then: at 5% incline uphill 0.96 m/s, downhill 1.03 m/s, at 10% incline uphill 0.89 m/s, downhill 1.04 m/s and at 15% incline uphill 0.80 m/s, downhill 1.04 m/s. Similarly, the speed value for climbing stairs was set at 0.65 m/s, using the same factor derived from Artmann. Gradients of more than 15% are considered to be obstacles that cannot be overcome.

The authors have calculated Walk Score, WS, values, see [20], for the 100 × 100 meter grid of the study area. Following [21], a predefined walking time limit of 20 minutes is applied. Using a standard network routing algorithm, the number of facilities accessible on foot within this time frame is determined. Unlike the original WS, this approach accounts for path inclines, addressing the specific mobility challenges faced by elderly individuals. The maximum WS value of 100 represents the scenario where all facility types (as outlined in Tab. 1) are reachable within a 5-minute walk. The WS value decreases as the walking time increases or fewer facilities can be accessed within 20 minutes. A WS value of 0 indicates that no facility is accessible within a 20-minute walk. Walking time is a linear function of walking speed, which, in turn, depends on the route's incline. The methodology of this Walk Score approach, more specifically tailored to the needs of the elderly, is detailed further in [22].

Most existing walkability models that factor in terrain utilize freely available, low-resolution data such as the SRTM DEM. However, the relatively low 1-arc-second resolution and limited height accuracy of such data make them insufficient for this application. In the model, inclines

are calculated using a high-resolution Digital Terrain Model (DTM), in Germany known as DGM, provided by official German mapping agencies [23]. The highest level DGM 1 model describes the terrain surface with a 1-meter grid of ground points and height accuracy of 0.15 meters. This high-quality data, both in terms of spatial resolution and elevation accuracy, is crucial for calculating meaningful gradients over short distances.

3 STUDY AREA AND DATA SOURCES

The main objective for selecting the study area was its suitability to demonstrate the importance of 3D barriers to walkability, particularly for older people. The data sources used include both official and unofficial databases.

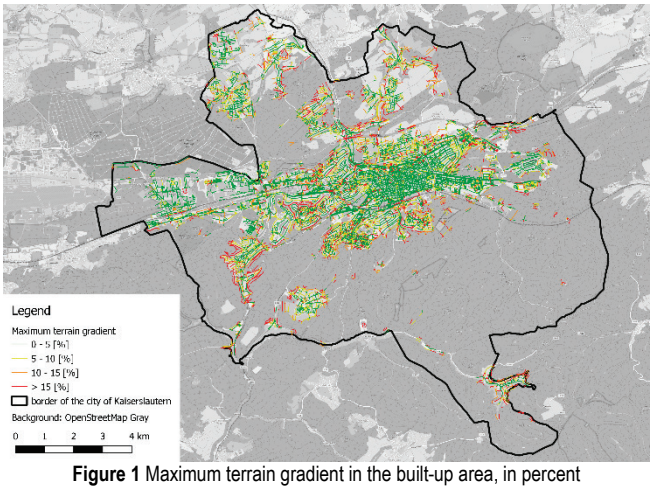

Figure 1 Maximum terrain gradient in the built-up area, in percent

3.1 Study Area

Kaiserslautern, with a population of 100,000, is one of the larger cities in Germany. The city's varying elevation significantly influences citizens' mobility. While the central areas are mostly flat, the peripheral regions are characterized by sloping terrain (see Fig. 1). Kaiserslautern shows the typical pattern of German cities, a spatially coherent city centre and disjoint neighbourhoods that have been created by the absorption of surrounding villages. In Kaiserslautern, the pattern of flat areas in the centre and sloping terrain on the periphery is repeated in the separate settlements, though on a smaller scale.

3.2 Data Sources

To calculate the Walk Score, it's necessary to create a network of walkable paths and roads. Despite its unofficial status and well documented regional variations, the quality of OpenStreetMap (OSM) road data in Central Europe is deemed sufficient for our analysis, as referenced in [24, 25]. Therefore, OSM data is used to construct the network model, encompassing all walkable pathways within the study area.

The network routing algorithm starts from each of the centre points of the 100 × 100 m grid and calculates the number of supply facilities reachable within the predefined walking time. The endpoints for the routing are based on OSM features, as detailed in Tab. 1. The network routing algorithm then outputs an individual WS value for each grid cell (see Figs. 2 and 3).

Table 1 Supply facility categories

Entertainment Recovery Sports	*Food*	*Healthcare*	*Public Transport*	*Service*	*Social*
Bar/Pub	Bakery	Pharmacy	Train station	Bank/ATM	Seniors' community centre
Library/Bookstore	Kiosk	Doctors/Hospital	Bus stop	Hair-dresser	
Church	Supermarket	Nursing home		Post	
Cinema	Butcher			Cleaning	
Museum/Theatre/Gallery	Other food			Cobbler/Lock-smith	
Restaurant/Café				Tailor Optician	
Swimming pool/Bathing place				Hearing aids	
Sports centre				Other facilities	

Categories are OSM key values
https://wiki.openstreetmap.org/wiki/Map_features, accessed 15 Aug 2024

4 RESULTS AND DISCUSSION

In the following section, the results obtained for the walkability of the inhabited areas in the study area using the original Walk Score classification framework (see Tab. 2) are presented.

Generally speaking, the walkability of Kaiserslautern neighbourhoods is not very high (see Tab. 3). Most grid cells are categorized as 'Car dependant', regardless of whether one takes sloping terrain into account or not. The number of grid cells classified as 'Walker's Paradise' remains unchanged when slopes are included in the calculations. The areas ranked as 'Very Walkable' and 'Somewhat walkable' decrease by –12.2 and –12.8 percent, respectively. The lowest classes of walkability 'Car dependent' show an increase in area size of +1.1 and +10.0 percent.

Table 2 Walk Score classification framework

Walk Score WS value	
90 - 100	*Walker's Paradise* Daily errands do not require a car
70 - 89	*Very Walkable* Most errands can be accomplished on foot
50 - 69	*Somewhat walkable* Some errands can be accomplished on foot
25 - 49	*Car Dependent* Most errands require a car
0 - 24	*Car Dependent* Almost all errands require a car

Source: https://www.redfin.com/how-walk-score-works, accessed 15 Aug 2024

Tab. 3 provides a statistical overview of walkability in the study area, with Fig. 2 visualising the results in their spatial context.

Table 3 Impact of pathway sloping on the Walk Score

Walk Score		*Number of grid cells*		*Difference 2D – 3D in percent*
		2D	*3D*	
90 - 100	Walker's Paradise	117	117	0
70 - 89	Very Walkable	286	251	–12.2
50 - 69	Somewhat walkable	765	667	–12.8
25 - 49	Car Dependent	1088	1100	+1.1
0 - 24	Car Dependent	1208	1329	+10.0

Unsurprisingly, Kaiserslautern's city centre achieves the highest WS values. The so-called Walker's Paradise encompasses an almost circular area with a diameter of more than one kilometre (each spot represents a 100 × 100 m grid cell), followed by a very walkable area in the city centre. The scores decrease as one moves further into the suburban settlements, ending in areas almost entirely dependent on motorized transport in some peripheral settlements. Some red spots are even visible in areas with high WS values. Data errors in the walking path network may be one reason for this, but other reasons cannot yet be ruled out. This issue must be investigated further on a case-by-case basis.

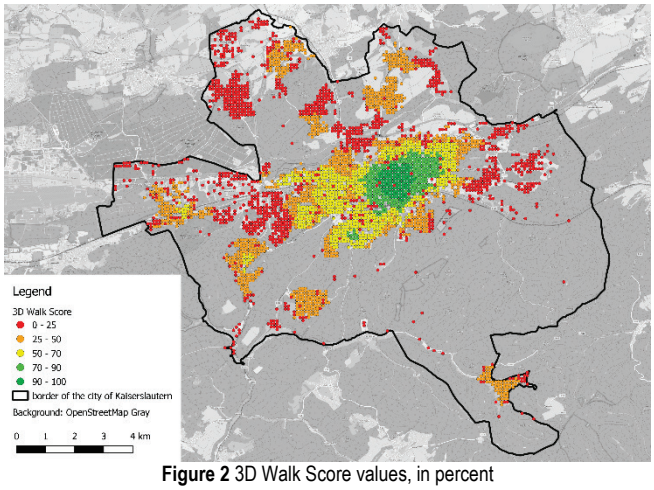

Figure 2 3D Walk Score values, in percent

The city extends in an east-west direction along a river valley; the inner city is flat, with sloping areas on both sides of the valley. The impact of slopes on the Walk Score shown in Fig. 3 reflects this situation. There is no apparent influence in the inner city, while in some areas the influence of slopes reaches values of up to 20 percent. The periphery, which tends to be less well-served anyway, is adversely affected by steeper walking routes. In some districts north of the city centre, WS values of less than 50 percent suffer an additional reduction of more than 10 percent and thus show even more clearly the disadvantageous situation, especially for older people.

Fig. 4 exemplifies the detailed insights that can be drawn from a high-resolution spatial analysis. The neighbourhood Hohenecken is one of Kaiserslautern's settlements detached from the contiguous inner city (see Fig. 2). Accessibility to services on foot is quite limited, but still available, with some errands being able to be done on foot, but most, if not almost all errands having to rely on other modes of transport.

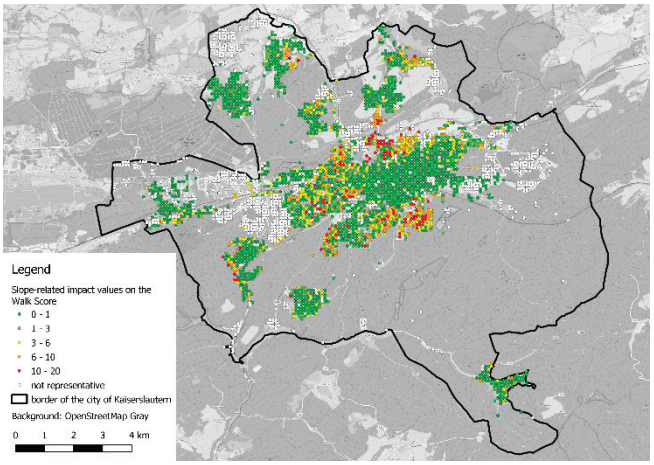

Figure 3 Slope-related impact on Walk Score values, in percent

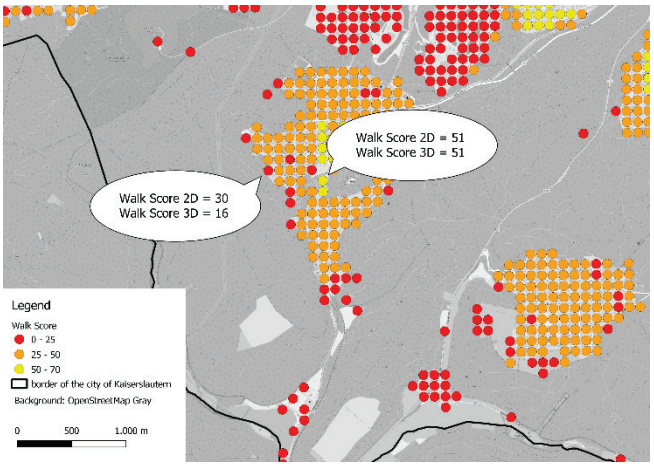

Figure 4 Walk Score in Kaiserslautern South Western neighbourhood Hohenecken

The marked cell in the centre of the village has a WS value of 51, the second marked cell on the western periphery only achieves a WS value of 30 without considering slopes, 16 with slopes included. The sharp decrease between the two cells is due to two reasons. The first is the location, the second is the slope. The location, about 500 metres west of the main service road, is for the major part the cause of the decrease, from WS value 51 down to WS value 30. But steep slopes in this area (see Fig. 1) account for another decrease, further reducing the WS value from 30 down to 16. The average effects of slopes listed in Tab. 3 provide an overall picture. However, when looking at the local situation, a different picture may emerge, namely a considerably higher impact not only of the location, but also of the slopes.

5 CONCLUSIONS AND FURTHER WORK

The results presented demonstrate that the slope of walking paths can have a significant impact on the accessibility of facilities such as shops and services on foot. This is a particular problem of senior citizens, who may be

limited their ability to use different modes of transport and are therefore more dependent on reaching services by foot. The topographical conditions of the built-up areas of cities and municipalities are decisive factors that determine accessibility on foot. For the study area of the city of Kaiserslautern, the impact of terrain gradients amounts to more than 11 points out of a maximum of 100 points for the Walk Score value, which is an established indicator of walkability of areas. The peripheral areas of the city are particularly affected, which amplifies the negative impact of a typically low-density of services in these areas. The significant differences between 2D and 3D accessibility suggest that urban planning would benefit from a 3D perspective that more adequately considers the needs of all, but in particular the elderly. With the increasing use of the Walk Score WS in spatial planning, this becomes particularly relevant.

Whether there are differences between 2D and 3D analyses or how substantial these are must be examined individually for each real case scenario. In particular, the quality of available data on terrain slope and distribution of services must be examined in detail. While data on accessible roads and paths is generally available with sufficient accuracy, this cannot be assumed for the other required data. This issue must therefore be addressed separately in each case, as the quality of the initial data always has a decisive influence on the validity of the results obtained.

Further work is needed to investigate other factors that affect accessibility for older people in particular, such as the surface of the path, barriers that prevent use by people who rely on walking aids, the safety of crosswalks and more. In addition, the integration of barriers outside and inside buildings within walkabiltiy estimates should be considered in future. From the perspective of the individual senior citizen, it is probably of secondary importance whether the stairs that prevent access to the supermarket are located inside or outside a building. From a technical point of view, this requires improved interaction between building information models (BIM) and geospatial information models (GIM), which could enable integral accessibility analyses in the future.

Acknowledgement

This article was authored within the project "RAFVINIERT - Raumintelligenz für die integrierte Versorgung von Senioren in ländlichen Quartieren / Spatial intelligence for the integrated care of senior citizens in rural neighbourhoods", funded by Carl Zeiss Foundation.

6 REFERENCES

[1] Smith, K. R., Brown, B. B., Yamada, I., Kowaleski-Jones, L., Zick, C. D. & Fan, J. X. (2008). Walkability and body mass index: Density, design, and new diversity measures. *Am. J. Prev. Med., 35*, 237-244. https://doi.org/10.1016/j.amepre.2008.05.028

[2] Alves, F., Cruz, S., Ribeiro, A., Silva, A. B., Martins, J. & Cunha, I. (2020). Walkability Index for Elderly Health: A Proposal. *Sustainability*, *12*, 7360. https://doi.org/10.3390/su12187360

[3] Shielvds, R., Gomes da Silva, E. J., Lima e Lima, T. & Osorio, N. (2021). Walkability: A review of trends. *J. Urban. Int. Res. Placemak. Urban Sustain.*, *16*, 1-23. https://doi.org/10.1080/17549175.2021.1936601

[4] Yang, S., Chen, X., Wang, L., Wu, T., Fei, T., Xiao, Q. & Jia, P. (2021). Walkability indices and childhood obesity: A review of epidemiologic evidence. *Obes. Rev.*, *22*, e13096. https://doi.org/10.1111/obr.13096

[5] Dunning, R., Calafiore, A. & Nurse, A. (2021). 20-minute neighbourhood or 15-minute city? *Town Ctry. Plan*.

[6] Caselli, B., Carra, M., Rossetti, S. & Zazzi, M. (2022). Exploring the 15-minute neighbourhoods. An evaluation based on the walkability performance to public facilities. *Transp. Res. Procedia*, *60*, 346-353. https://doi.org/10.1016/j.trpro.2021.12.045

[7] Maghelal, P. K. & Capp, C. J. (2011). Walkability: A Review of Existing Pedestrian Indices. *J. Urban Reg. Inf. Syst. Assoc.*, *23*, 5-19.

[8] Wang, H. & Yang, Y. (2019). Neighbourhood walkability: A review and bibliometric analysis. *Cities*, *93*, 43-61. https://doi.org/10.1016/j.cities.2019.04.015

[9] Lam, T. M., Wang, Z., Vaartjes, I., Karssenberg, D., Ettema, D., Helbich, M., Timmermans, E. J., Frank, L. D., Braver, N. R. D., Wagtendonk, A. J. et al. (2022). Development of an objectively measured walkability index for the Netherlands. *Int. J. Behav. Nutr. Phys. Act.*, *19*, 1-16. https://doi.org/10.1186/s12966-022-01270-8

[10] Bayar, R. & Yılmaz, M. (2022). Measuring age-friendliness based on the walkability indices of older people to urban facilities. *Urban Design Int.*, *28*, 35-51. https://doi.org/10.1057/s41289-022-00194-w

[11] Horak, J., Kukuliac, P., Maresova, P., Orlikova, L. & Kolodziej, O. (2022). Spatial Pattern of the Walkability Index, Walk Score and Walk Score Modification for Elderly. *ISPRS Int. J. Geo-Inf.*, *11*, 279. https://doi.org/10.3390/ijgi11050279

[12] Distefano, N., Pulvirenti, G. & Leonardi, S. (2021). Neighbourhood walkability: Elderly's priorities. *Res. Transp. Bus. Manag.*, *40*, 100547. https://doi.org/10.1016/j.rtbm.2020.100547

[13] Ujang, N., Salim, A. & Maulan, S. (2012). The Influence of Context and Urban Structure on the Walkability of Bukit Bintang Commercial District, Kuala Lumpur. *ALAM CIPTA Int. J. Sustain. Trop. Des. Res. Pract.*, *5*, 15-26.

[14] Bereitschaft, B. (2022). Older adult population and neighborhood walkability by metropolitan area size and degree of urban sprawl. *Pap. Appl. Geogr.*, *8*, 249-267. https://doi.org/10.1080/23754931.2021.1978526

[15] Schmitz, J., Fina, S. & Gerten, C. (2023). How Walkable are German Cities? New Results from the Field of Walkability Research. Raumforschung Und Raumordnung | *Spatial Research and Planning, 81*(4), 327-341. https://doi.org/10.14512/rur.1664

[16] Kirchner, T., Pflanz, F., Techen, A. & Wagenknecht, L. (2014): Kleinräumige Gliederung, Georeferenzierung und Rasterdarstellung im Zensus. *Zeitschrift für amtliche Statistik Berlin-Brandenburg*, 3/2014, 28-32. (in German)

[17] https://knowledge-base.inspire.ec.europa.eu/publications/inspire-data-specification-geographical-grid-systems-technical-guidelines_en

[18] Weidmann, U. (1993). Transporttechnik der Fußgänger: Transporttechnische Eigenschaften des Fußgängerverkehrs, Literaturauswertung. *IVT Schr.*, *90.* 6585. (in German)

[19] Artmann, M., Mueller, C., Goetzlich, L. & Hof, A. (2019). Supply and demand concerning urban green spaces for recreation by elderlies living in care facilities: The role of

accessibility in an explorative case study in Austria. *Front. Environ. Sci.*, *7*, 136. https://doi.org/10.3389/fenvs.2019.00136
[20] Hall, C. M. & Ram, Y. (2018). Walk score® and its potential contribution to the study of active transport and walkability: A critical and systematic review. *Transp. Res. Part D Transp. Environ.*, *61*, 310-324. https://doi.org/10.1016/j.trd.2017.12.018
[21] Burgdorf, M., Krischausky, G., & Müller-Keißler, R. (2021). *Indikatoren zur Nahversorgung: Erreichbarkeit von Gütern und Dienstleistungen des erweiterten täglichen Bedarfs*; Bundesinstitut für Bau-, Stadt-und Raumforschung: Bonn, Germany, 2021. (in German)
[22] Schaffert, M., Geist, K., Albrecht, J., Enners, D. & Müller, H. (2023). Walk Score from 2D to 3D—Walkability for the Elderly in Two Medium-Sized Cities in Germany. *ISPRS International Journal of Geo-Information, 12*(4), 157. https://doi.org/10.3390/ijgi12040157
[23] AdV. (2021). Produkt- und Qualitätsstandard für Digitale Geländemodelle, Version 3.2. (in German)
[24] Mobasheri, A., Bakillah, M., Rousell, A., Hahmann, S. & Zipf, A. (2015). On the completeness of sidewalk information in OpenStreetMap, a case study of Germany. In *The 18th AGILE International Conference on Geographic Information Science*, Lisbon, Portugal (Vol. 2).
[25] Brückner, J., Schott, M., Zipf, A. & Lautenbach, S. (2021): Assessing shop completeness in OpenStreetMap for two federal states in Germany. *Agil. GIScience Ser. 2*, 20. https://doi.org/10.5194/agile-giss-2-20-2021

Authors' contacts:

Hartmut Müller, Prof. Dr.-Ing.
(Corresponding author)
Hochschule Mainz, University of Applied Sciences
Lucy-Hillebrand-Str. 2, D-55128 Mainz, Germany
+49 6131 628 1438, hartmut.mueller@hs-mainz.de

Konstantin Geist, M.Sc.
Hochschule Mainz, University of Applied Sciences
Lucy-Hillebrand-Str. 2, D-55128 Mainz, Germany
+49 6131 628 1495, konstantin.geist@hs-mainz.de

Klaus Böhm, Prof. Dr.-Ing.
Hochschule Mainz, University of Applied Sciences
Lucy-Hillebrand-Str. 2, D-55128 Mainz, Germany
+49 6131 628 1431, klaus.boehm@hs-mainz.de

Markus Schaffert, Prof. Dr.-Ing.
Hochschule Mainz, University of Applied Sciences
Lucy-Hillebrand-Str. 2, D-55128 Mainz, Germany
+49 6131 628 1443, markus.schaffert@hs-mainz.de

ISSN 1846-6168 (Print), ISSN 1848-5588 (Online)
https://doi.org/10.31803/tg-20240909111151

Preliminary communication
Received: 2024-09-09, Accepted: 2024-11-04

BIM-GIS Integration for Interactive, Open and Low-Cost 3D Land Use Registration and Urban Neighbourhood Management

Dimitra Andritsou*, Chryssy Potsiou

Abstract: This paper is part of an on-going research study on developing a low-cost and approachable methodology for f-f-p, transparent and future inclusive 3D land use management for an urban neighbourhood by constructing a homogenous, open, cloud-based and free-to-use virtual BIM-GIS geospatial infrastructure. The proposed platform is structured for registering, classifying and visualizing volumetric land use prisms, distributing conceptual and geometric information, conducting statistical analyses and data exchange aiming for optimal decision making, urban neighbourhood management and land use tracking. The proposal aspires to aid the successful and timely achievement of the UN Sustainable Agenda 2030, in particular SDGs 1,9 and 11. The methodology includes: 1) the creation of approximate BIMs by utilizing open and available data and platforms, 2) modelling of land uses as 3D volumetric prisms, 3) registering semantic and geometrical land use information and 4) crafting statistical graphs, emphasising on data compilation and BIM-GIS standards implementation.

Keywords: BIM; Crowd-Enabling Urban Neighbourhood Management; Data Integration; Fit-For-Purpose; GIS; Open 3D Land Use Registry

1 INTRODUCTION

1.1 Objective of the Research

The complexity of modern urban environments is characterized by overlapping facilities, vertical extensions of property rights, superimposed legal spaces or operational systems, conflicting benefits and the constant need for utilizing land. Consequently, proper and constant land management, land use tracking, 3D cadastral registration policies, crowd-enabling incentives and digitization of neighbourhoods are needed for optimal, inclusive, fair, transparent and modernized urban governance and planning. The SDGs of the United Nations (UN) Agenda can pave the way for the implementation of all the above, tailored to each country's distinct needs and problems, creating a homogenous conceptual background between different countries and administrative systems with fit-for-purpose solutions.

3D representation and distribution of key urban instances such as land uses and property boundaries can reform the 2D static establishment of contemporary cadastral and land administration systems. 3D visualization of land use spaces can contribute to interactive, dynamic, personalized and fit-for-purpose (f-f-p) urban management procedures with many outlets to future smart applications, real-time facility management, digitization of old neighborhoods, parking spaces planning, sustainability, optimal urban segmentation, etc.

3D land use registration and management applications are favored to start at a neighborhood-scale extent as neighbourhoods represent a small-scaled indicative simulation of the entirety of an urban environment, serving as a possible stepping-ground for crowdsourcing, tracking and registration applications.

An open, low-cost and interactive 3D land use registry could contribute in the optimal deployment, usage and distribution of parcels and urban space while it could aid the establishment of permanent crowdsourcing urban incentives, inclusive policies and transparent urban management procedures. One important factor is the protection of personal and sensitive data. Various 2D data portals around the globe follow data protection rules and the same has to be applied to 3D portals. Open and available data dictate transparency, citizen-engagement and incentives leaving no one behind but not at the expense of privacy and safety standards.

Building Information Modelling (BIM) and Geographic Information Systems (GIS) technologies and standards are leading the trends of 3D representation, data compilation, urban management, chartography, urban planning, decision-making and digitization while they contribute in the merge of static 2D geospatial instances with dynamic 3D models. BIM serves as a proper host for volumetric land use modelling, registration, classification and representation while GIS possess an array of tools, platforms and programs for disposing, querying and analyzing both semantic and geometric information.

Proper, accurate and thorough synthesizing of the above-mentioned standards is a major research theme across the global academic and technical community as the BIM extraction format, the Industry Foundation Class (IFC), is not fully compatible with GIS-based interfaces. IFC also tends to not transfer important textural information across platforms while BIM data are more frequently adjustable to GIS-based programs through rigorous and demanding programming transformations i.e. JSON format.

The paper proposes the construction of a low-cost, cloud-based, open and interactive platform called "LAURET" for the compilation of approximate BIMs, GIS tools, 3D spatial and semantic data, embedded sites, pop-up windows and statistical graphs for creating a seamless, quick and accessible 3D land use registry of an urban neighbourhood for future crowd-enabling applications. The interface proposes the simultaneous visualization of 3D BIMs, categorization of volumetric land uses both semantically and visually, a 2D land use registry and graphical analyses. The

proposed "LAURET" platform contains all the needed tools and official pages for registering 3D urban neighbourhood land use prisms while it utilizes open and available data aspiring to aid 3D land use registration purposes, reform 2D procedures, back up digitization incentives and push forward future crowdsourced policies for inclusive urban neighbourhood management.

The contribution highlights the importance of BIM-GIS integration in aiding optimal neighbourhood decision-making and digitization procedures while establishing modernized urban functionality, social equality and fostering the cooperation between experts and citizens regarding urban planning and tracking. The proposed platform can support crowdsourced urban neighbourhood management, proposes a f-f-p and approachable solution for the creation of approximate yet detailed BIMs, emphasizes the importance of data reproducibility and interoperability while being in terms with SDG 9 (Industry, Innovation and Infrastructure), 10 (Reduced Inequalities) and 11 (Sustainable Cities and Communities).

1.2 State of the Art

One of the most important factors of the contribution is researching, implementing and highlighting the merge of BIM data with GIS standards for the betterment of urban planning and land use registering. BIM is translated as IFC format containing the various modelled structural and architectural elements as classes and subclasses. IFC is a highly interoperable dataset that can boost interconnectivity and multisectoral workflows.

The research field has developed various methodologies based on the interconnection of BIM and GIS technologies by utilizing the IFC schema for cadastral, urban planning and city functionality tracking purposes. BIM and GIS integration is a recently advancing trend with many researches focusing mostly on interoperability and merging methods rather than consequent analyses [1]. The combination of BIM and GIS can be helpful for public administration and 3D cadastral issues [1]. BIM and GIS synthesization is a possible supportive factor for sustainable urban management as it fosters capabilities regarding data interoperability, exchange, analyses and technologies [2].

BIM hosts vast information regarding a built construction throughout its lifecycle [3] while GIS technologies are characterized by multiple analytical and visualization tools that enable geospatial decision-making [4]. IFC is one of the two most prominent data formats that is used for BIM-GIS compilation [5] with City-GML taking the other spot. In the last decade, BIM-GIS merge has been utilized for urban energy management [6] and ecological assessments [7] while applications on emergency and unexpected factor handling have also been developed [8].

Theoretically, BIM-GIS compilation has been split into two categories, one being the geometric and the other the semantic, leading to continuous research that revolves around FM (Facility Management) and AEC (Architecture, Engineering and Construction) sectors. [9]. For instance, the ArcGIS Pro platform has been used to host 3D BIMs of complex buildings, 3D volumetric rights and a semantic cadastral database following the LADM (Land Administration Domain Model) standard [10]. Other paradigms entail the development of a crowdsourced application by utilizing GIS toolboxes for a cost-effective, quick and approachable 3D cadastral registration [11] while a BIM and 3D GIS-empowered cadastral system has been created for the 3D visualization of cadastral entities [12]. Through BIM-GIS compilation it has been researched that spatial planning can take place before the construction, enabling the possibility to solve upcoming problems ahead of time [13]. Regarding the construction domain, supply chains and material sequences can be visualized by using complex BIM-GIS systems [14].

Further applications regarding optimal and sustainable building energy management and tracking have been developed under the prism of BIM-GIS implementation such as energy mapping which makes possible the visualization and monitoring of spatial motifs of energy consumption across a multi-storey building [15]. Sustainable management, especially in real-time, consists a key-factor for Smart City establishment. Consequently, research regarding the merge of IoT (Internet of Things) devices, GIS meteorological and weather systems with BIM models has been carried out [16].

Regarding urban management and optimization, GIS has been incorporated with BIM datasets to digitally present flood-jeopardized urban areas [17] while applications about tunnel creation have also been made [18]. GIS-BIM systems can support the constant flow and interconnection of indoor building data with urban facility information resulting in possible future Smart City solutions [19]. BIM-GIS complied systems, enriched with GPS technologies, can host various important urban data such as construction costs or rentable areas which play a lead role to urban are development [20].

3D Cadastral applications around the theme of GIS-BIM integration have focused on creating a homogenous 3D cadastral data model which follows both GIS standards and BIM storage capabilities [21]. A BIM-GIS integrated platform enriched with 3D BIM data and cadastral information has also been developed [22]. In 3D cadastral applications that regard BIM and GIS, georeference plays a major role as it hosts all the important geospatial and coordinate data for the correct and proper location of the properties under study. Research showcasing the automated georeference by utilizing building footprints by merging GIS with BIM has been developed [23].

A highly integrated model that entails information about varying building and construction phases alongside data regarding economic, environmental and operational factors has been proposed in [24]. In China, a case study concerning the application of BIM-GIS compiled methods for underground piping management has been developed and tested [25].

BIM terminology and technologies have also been researched considering green and sustainable purposes such as the evaluation of the sustainability score in existing buildings as well as green retrofitting [26]. The need for maintaining and tracking green building components throughout the construction phases is also another sector that

calls for BIM implementation [27]. Certification procedures for safeguarding green building complexes can have also been extensively studied in literature [28].

BIM has furtherly been implemented in preventive, risk-management and security applications which is a key-instrument for future Smart City and interconnected building complexes. A BIM Risk Identification Expert System has been developed, for instance, regarding tunnel construction procedures compiling BIM models [29]. Many times, mistakes and mis happenings during construction competition lead to revealing foundings. A framework concerning empirical safety risk data and BIM datasets has been proposed in [30]. Automation safety excavation modelling has also been presented by merging BIM, safety regulations, visual programming and automatic rule checking [31]. A more universal research regarding validating the performance of BIM-based applications has been shaped [32].

Scheduling toolsets have been mingled with BIM technologies both for railroad tracking [33] and bridge construction procedures [34]. Clash detection and mistake finding utilizing BIM has been developed regarding large construction projects, equipment bump and machinery failures due to inadequate time schedule structuring or deficient site management [35].

An open, communicative and online virtual hub has been developed which stores the approximate crowdsourced BIMs of an entire neighbourhood enriched with street furniture, environmental elements and various mechanical, electrical and pluming (MEP) devices [36]. The developed cloud-based and all-in-one platform of this proposal, LAURET, has been based on previous conducted research which covers the low-cost, fast and engaging 3D registration of property units by utilizing embedded sites and official open portals [37].

2 METHODOLOGY

2.1 Overview of the Methodology

The presented methodology is based on creating the approximate yet highly detailed BIM of an urban neighbourhood while modelling land use boundaries as 3D volumetric prisms for their collective distribution in a holistic and multifaceted interactive platform named LAURET. LAURET stands for "land use registry" and it is a cloud-based 3D land use and urban neighbourhood analysis as well as visualization platform. The methodology, in general, depends on the availability of floor and architectural plans as well as the open distribution of 2D data and portals.

The technical part is relying on the utilization of low-cost techniques, open platforms and available data such as the National Cadastral Portal or Google Earth Pro. The delineation of the 3D volumetric land use prisms is mainly based on floor and topographical plans. The methodology is largely leaning on the previously developed contributions of the authors [36] and [37] that thoroughly cover the creation of f-f-p and low-cost BIMs and the modelling of land use prisms.

Fig. 1 showcases the proposed methodology for the compilation of the LAURET platform. According to the graph:

- Firstly, the BIMs of the urban neighbourhood under study are going to be modelled, following the f-f-p and low-cost methods proposed in [36] and [37].
- The spatial extent of the land use prisms is going to be modelled by delineating the 2D plans and categorized.
- Statistical and analytical graphs as well as a semantic registry in the form of a queried table are going to be constructed.
- All the elements are going to be compilated in the online ArcGIS Experience interface for the final synthesization of LAURET.

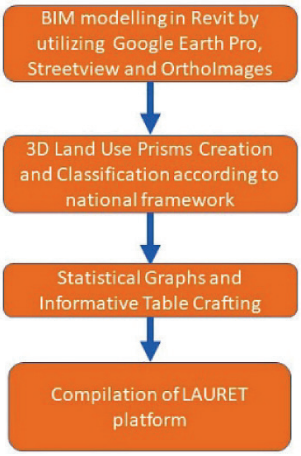

Figure 1 The followed methodology for the creation of LAURET platform

The entire methodology is a paradigm for modelling, registering, visualising, categorising, analysing, quiring and openly distributing 3D land use data in Greece under the prism of a homogenous, available, communicative and cloud-based interface.

2.2 Compilation of the BIM of the Urban Neighbourhood

As it is stated, the current contribution follows precisely the previously developed methodologies that are analyzed in [36] and [37] for the creation of the BIMs which cover thoroughly:

- The construction of BIMs of existing buildings in an urban neighbourhood by utilizing 2D data such as Orthophotos from the Official Cadastral Portal for the delineation of boundaries.
- Obtaining textural information for the coating and materials of the buildings from Streetview.
- Approximate elevation data and measurements deriving from Google Earth Pro.
- Collection of appropriate 2D and 3D information for constructing the outer shell and the surrounding area of each building in Autodesk Revit.
- Insertion of BIMs in the online, open and communicative platform of Autodesk Tandem for their semantic and visual classification and management.

Figure 2 Compilation of 3D BIM of the neighbourhood

Fig. 2 presents the approximate, f-f-p, low-cost and detailed BIMs of the urban neighbourhood under study that consist of a reliable and satisfactory 3D geospatial infrastructure. The BIMs in Fig. 3 consist of thorough rendition of the real structure and geometric configuration of the buildings while entailing information about the surrounding area and urban elements.

Figure 3 Cross sections of the 3D model of the neighbourhood

The BIMs serve as the modelling and presentation basis for the creation of the land use prisms and the platform.

2.3 Creation and Classification of 3D Land Use Prisms

Important information about each land use prism is obtained through the platform of StreetView. The spatial extent of each land use is approximately modelled and visualized following the boundaries of the 2D architectural and topographical plans. The geometric information and the structural layout of the plans serves as the guideline for the creation of the 3D land use volumes. Height information for each volume is either deriving from the height diagrams or vertical measurements conducted in Google Earth Pro. The digitization of the volumetric prisms is based on the Greek legislation while it follows the external wall boundaries and inwards.

The online platform of Tandem is utilized for the presentation, management and categorization of the 3D land use volumes according to their different class as shown in Fig. 4. Tandem enables the insertion, selection, management, editing, configuration, colorization, classification, display and storing of the volumetric prisms.

The classification of the volumetric land use prisms is in full accordance with the Greek legal framework, presenting the following categories which entail different types:

- Residential: which entails housing, lofts and detached houses
- Repository which includes storages and stockrooms.
- Retail-Store which covers shops and stores i.e. pet shops, bakeries, mechanical or computer parts, comic stores, DVD rental stores, etc.
- Services which entail offices and associations i.e. technical, engineer and doctors' office, technical companies, neighborhood associations, etc.

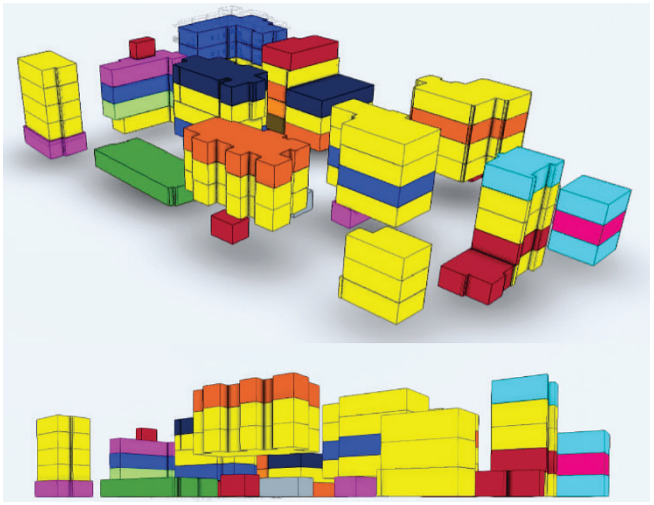

Figure 4 The different categories of land use prisms

The various 3D land use prisms can be both visually and semantically classified according to different filters such as "type" as shown in Fig. 5 (i.e. pet shop, technical office, doctors' office, bakery, neighborhood association, loft, detached house, etc.) and "category" as analyzed previously (i.e. Residential, Storage Room, Retail – Store and Service), while important information such as area (in m^2), perimeter (m) and volume (m^3) is stored.

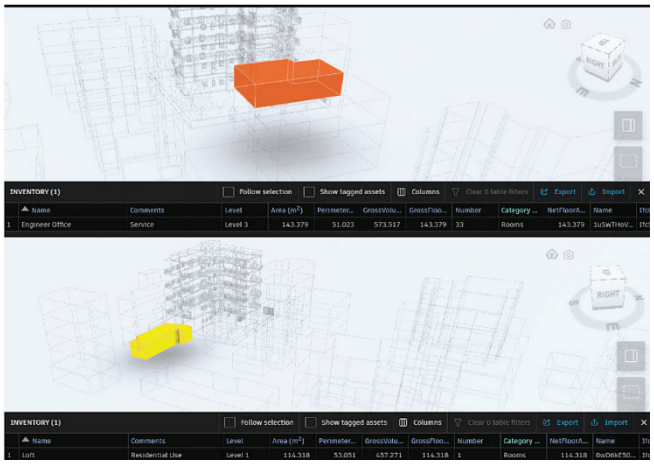

Figure 5 Classification according the "Type", an engineer office (above) and a loft (below)

Fig. 6 presents classification according to the categories of the land uses that are present in the neighborhood.

By selecting one land use prism, an interactive table is presented with all the needed information about it as shown in Fig. 7.

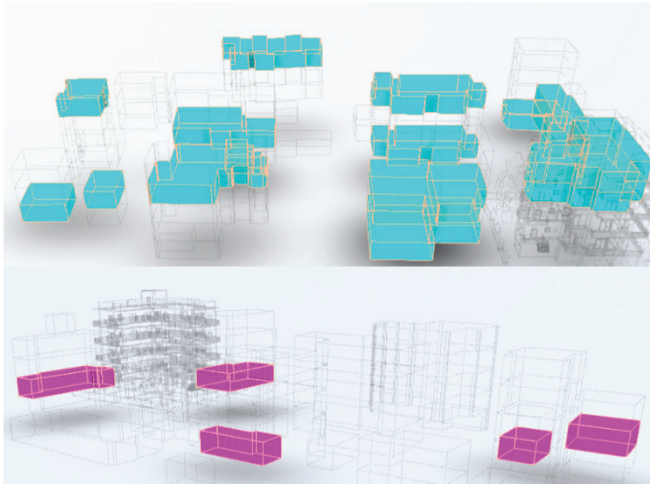

Figure 6 Classification according the "Category", services (above) and retail (below)

Figure 7 Selection of a prism and the distribution of information

Land use prisms that belong to the same category are depicted with similar colorations. By example, Tab. 1 presents the different colour schemes for each land use category making them easy to stand out, differentiate and spot.

Table 1 Colours for each Category

Category	Colour
Residential	yellow
Repository	burgundy
Retail	magenta
Services	azure

3 TECHNICAL APPLICATION - THE LAURET PLATFORM

The platform of LAURET is created by utilizing the ArcGIS Experience interface of ArcGIS Online by ESRI. ArcGIS Online grants access to its products through any type of license either institutional, public or paid. ArcGIS Online is an easily accessible, cloud-based and communicative community which offers a plethora of toolsets for digitizing, mapping, storing, visualising and exchanging both spatial and semantic data.

ArcGIS Experience entails a wide range of widgets for creating personalized, modular, online and interactive interfaces and platforms that can be publicly distributed for wider usage. It offers a plethora of toolsets for merging datasets from different sources and combining various information. An extensive presentation of the operations and functualities of the various widgets of ArcGIS Experience is presented in the previously conducted research that can be found in [37].

ArcGIS Experience is also chosen as it is a GIS-generated environment that it can host alternative, seamless and multiple BIM-GIS compilation options. BIM data and more specifically IFC files are interconnected easily within the GIS environment as online links or embedded shortcuts. So basically, the IFC files are easily converted into uniform research locators (urls) which later are incorporated in the interface of the constructed platform.

LAURET is an open, low-cost and communicate platform for uploading, managing and analysing BIM-generated 3D land use data in a GIS environment. It is built aspiring to be able to host future crowdsourced and cooperative procedures for the registration of volumetric land use prisms for optimal urban neighbourhood management and land distribution.

Consequently, LAURET entails all the needed tools for tracking, modelling, categorizing, managing, storing, visualising and analysing volumetric land use prisms under one low-cost and cloud-operated interface with future crowd-enabling expansions.

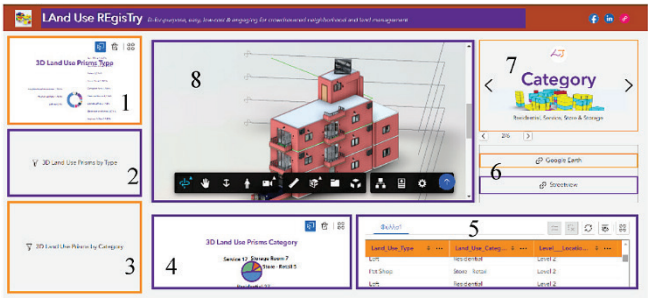

Figure 8 The platform of LAURET with enumeration of the widgets

LAURET consists of many interactive widgets, as shown in Fig. 8 with them being:

1) Statistical pie chart showcasing the percentage of each "type" of volumetric land use prism i.e. pet store, office, storage, loft, etc.
2) A redirection button which seamlessly opens up another window in the user's browser, enabling the visualisation and management of the 3D land use prisms according to the "type" classification.
3) A redirection button that immediately and easily grants access to the visual and semantic classification of the land use prisms according to their "category" i.e. residential, retail, service, repository.
4) An interactive pie chart that presents the numeric allocation of each land use "category".
5) The 2D semantic registry of the volumetric land use prisms that entails informative and geometric information.
6) Two embedded links that seamlessly transcend the user to the official portals of either Google Earth Pro or Streetview.
7) An interactive frame with alternating photocards of the 3D land use prisms and their according visual classifications.
8) The embedded official portal of "Online BIMViewer" as an interactive window in which the BIMs can be

uploaded, viewed, edited and managed straight through the LAURET platform.

In [37], a thorough explanation of the operation of embedded pages, pop-windows, interconnected official portals and graphs is given. As mentioned above, the BIMs can be seamlessly incorporated in the GIS environment of the LAURET platform. In Fig. 9 the inside modelling of a BIM is presented in detail while it is completely incorporated in the platform.

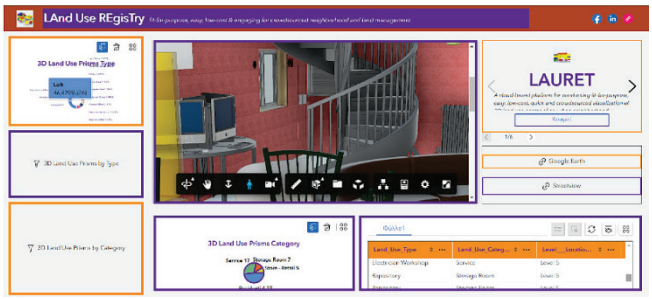

Figure 9 The interchangeable and interactive interface of the platform

Fig. 10 presents the pie graph of the percentage that each "type" of land use covers in the neighbourhood under study.

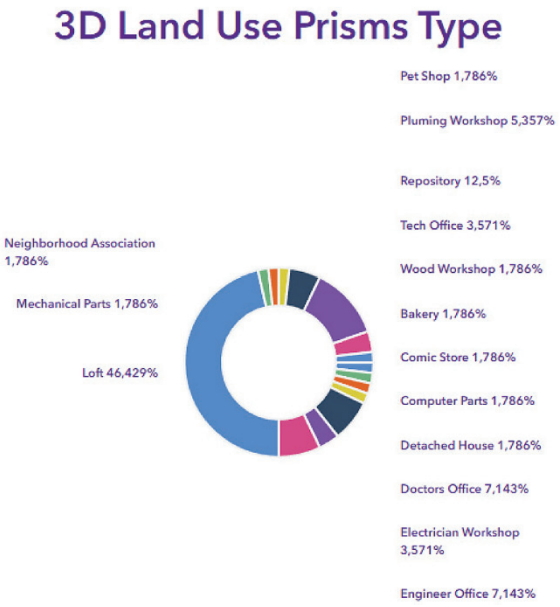

Figure 10 Land Use percentage pie graph

Fig. 11 displays the pie graph of the numeric distribution that each "category" of land use has in the neighbourhood under study.

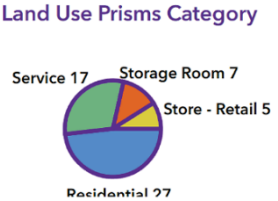

Figure 11 Land Use percentage pie graph

Fig. 12 showcases the embedded semantic and geometric land use registry in the form of a table.

Fig. 13 presents the entirety of the platform from a closer view.

Land_Use_Type	Land_Use_Categ...	Level__Locatio...	Area__m2_	Perimeter
Loft	Residential	Level 1	72	40
Repository	Storage Room	Level 1	26	20
Mechanical Parts	Store - Retail	Level 1	67	38

Figure 12 Land use prism 2D registry in the platform

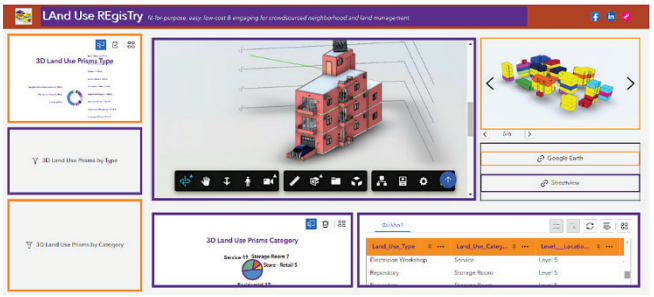

Figure 13 The entirety of the platform

4 CONCLUSIONS

One homogenous interface is created by utilizing the ESRI tool of ArcGIS Online, the ArcGIS Experience. With ArcGIS Experience a personalized, modular, openly accessed and low-cost platform for future crowdsourced 3D land use registration procedures is created. This interface presents all the needed tools for conducting 3D crowdsourced urban land management processes, in a singular, engaging and interactive platform.

The platform is seamlessly linked to:

- 3D BIM Online Viewer.
- Tandem interface where all the 3D land use prisms are categorized and stored.
- Google Earth Pro.
- Streetview.

Statistical diagrams and graphs such as pie graphs can also be provided by the platform, presenting analyses and further information on the 3D land use prisms. A thorough land use registry is also presented as a table storing vital information for each 3D land use prism.

The described methodology is satisfactory for the purposes of creating a fast, low-cost and approximate yet detailed geospatial infrastructure of an urban neighbourhood. It is also adequate for conducting 3D urban land management procedures utilizing available 2D data as the architectural, floor and topographic plans can be either provided by the stakeholders or by accessing the electronic building identity (especially for new constructions).

The proposed platform can easily host 3D crowdsourced land use registration procedures as it is easy to use, enables cooperation and it is available online without a charge. Gamification elements, rewards and motivations can also be inserted in the future, for boosting further the dedication of users. In many countries, crowdsourced cadastral procedures

are prominent thus making it easier to be applicable and adapted. The compilation of the approximate BIMs of existing building with BIMs of newly made constructions is going to result in a 3D homogenous geospatial basemap for viewing simultaneously both the 3D models and the 2D semantic information.

The methodology also showcases seamless, easy and fast BIM-GIS compilation options as the IFC datasets are either uploaded as online URL extensions directly to LAURET platform of interconnected with the GIS environment through redirection buttons. The proposal presents a programming-free and conversion-deprived BIM-GIS combination method for the simultaneous distribution of both 3D BIM data and GIS widgets.

5 REFERENCES

[1] Song, Y., Wang, X., Tan, Y., Wu, P., Sutrisna, M., Cheng, J. C. P. & Hampson, K. (2017). Trends and Opportunities of BIM-GIS Integration in the Architecture, Engineering and Construction Industry: A Review from a Spatio-Temporal Statistical Perspective. *ISPRS Int. J. Geo-Inf., 6*, 397. https://doi.org/10.3390/ijgi6120397

[2] Fosu, R., Suprabhas, K., Rathore, Z. & Cory, C. (2015). Integration of Building Information Modeling (BIM) and Geographic Information Systems (GIS)—A literature review and future needs. *Proceedings of the 32nd CIB W78 Conference, Eindhoven*. Retrieved from http://sites.umuc.edu/library/libhow/apa_examples.cfm

[3] Volk, R., Stengel, J. & Schultmann, F. (2014). Building Information Modeling (BIM) for existing buildings—Literature review and future needs. Autom. *Constr., 38*, 109-127. https://doi.org/10.1016/j.autcon.2013.10.023

[4] Berry, J. (1996). GIS evolution and future trends. *In Beyond Mapping III, Compilation of Beyond Mapping Columns Appearing in GeoWorld Magazine.* Retrieved from http://www.innovativegis.com/basis/mapanalysis/Topic27/Topic27.pdf

[5] Gröger, G. & Plümer, L. (2012). CityGML—Interoperable semantic 3D city models. *ISPRS J. Photogramm. Remote Sens., 71*, 12-33. https://doi.org/10.1016/j.isprsjprs.2012.04.004

[6] Romero, A., Izkara, J. L., Mediavilla, A., Prieto, I. & Perez, J. (2016). Multiscale building modelling and energy simulation support tools. *In Ework and Ebusiness in Architecture, Engineering and Construction.* Retrieved from https://www.researchgate.net/publication/322077461_Multiscale_building_modelling_and_energy_simulation_support_tool

[7] Miller, J. & Smith, T. (Eds.). (1996). *Cape Cod stories: Tales from Cape Cod, Nantucket, and Martha's Vineyard*. San Francisco, CA: Chronicle Books.

[8] Teo, T. A. & Cho, K. H. (2016). BIM-oriented indoor network model for indoor and outdoor combined route planning. *Adv. Eng. Inform., 30*, 268-282. https://doi.org/10.1016/j.aei.2016.04.007

[9] Zhu, J., Wright, G., Wang, J. & Wang, X. A. (2018). Critical Review of the Integration of Geographic Information System and Building Information Modelling at the Data Level. *ISPRS Int. J. Geo-Inf., 7*, 66. https://doi.org/10.3390/ijgi7020066

[10] Andritsou, D., Gkeli, M., Soile, S. & Potsiou, C. (2022): A BIM/IFC – LADM Solution Aligned to the Greek Legislation. *The International 621 Archives of the Photogrammetry, Remote Sensing and Spatial Information Sciences, XXIV ISPRS Congress, vol. XLIII-B4-2022*.

[11] Gkeli, M., Potsiou, C. & Ioannidis, C. (2021). BIM data as Input to 3D Crowdsourced Cadastral Surveying—Potential and Perspectives. *Proceedings of the FIG e-Working Week 2021*. https://doi.org/10.1016/j.landusepol.2019.104419

[12] Hajji, R., Yaagoubi, R., Meliana, I., Laafou, I. & Gholabzouri, A. E. (2021). Development of an Integrated BIM – 3D GIS Approach for 3D Cadastre in Morocco. *ISPRS Int. J. Geo-Inf., 10*, 351. https://doi.org/10.3390/ijgi10050351

[13] Bansal, V. K. (2011). Use of GIS and topology in the identification and resolution of space conflicts. *Journal of Computing in Civil Engineering 25*(2), 159-171. https://doi.org/10.1061/(asce)cp.1943-5487.0000075

[14] Wang, T.-K., Zhang, Q., Chong, H.-Y. & Wang, X. (2017). Integrated supplier selection framework in a resilient construction supply chain: An approach via analytic hierarchy process (AHP) and grey relational analysis (GRA). *Sustainability, 9*(2). https://doi.org/10.3390/su9020289

[15] Salimzadeh, N., Sharif, S. A. & Hammad, A. (2016). Visualizing and analyzing urban energy consumption: A critical review and case study. In: Perdomo-Rivera, J. L., Gonzalez-Quevedo, A., Lopez DelPuerto, C., Maldonado-Fortunet, F. & Molina-Bas O. I. (Eds.), *Construction Research Congress*. https://doi.org/10.1061/9780784479827.133

[16] Ronzino, A., Osello, A., Patti, E., Bottaccioli, L., Danna, C., Lingua, A., Acquaviva, A., Macii, E., Grosso, M., Messina, G. & Rascona, G. (2015). The energy efficiency management at urban scale by means of integrated modelling. In: Howlett, R. J. (Ed.), *The 7th International Conference on Sustainability and Energy in Buildings*. https://doi.org/10.1016/j.egypro.2015.12.180

[17] Amirebrahimi, S., Rajabifard, A., Mendis, P. & Tuan, N. (2016). A BIM-GIS integration method in support of the assessment and 3D visualisation of flood damage to a building. *Journal of Spatial Science, 61*(2), 317-350. https://doi.org/10.1080/14498596.2016.1189365

[18] Zhou, W., Qin, H., Qiu, J., Fan, H., Lai, J., Wang, K. & Wang, L. (2017). Building information modelling review with potential applications in tunnel engineering of China. *Royal Society Open Science, 4*(8). https://doi.org/10.1098/rsos.170174

[19] Teo, T.-A. & Cho, K.-H. (2016). BIM-oriented indoor network model for indoor and outdoor combined route planning. *Advanced Engineering Informatics, 30*(3), 268-282. https://doi.org/10.1016/j.aei.2016.04.007

[20] Forsythe. P. J. (2014). In pursuit of value on large public projects using "spatially related value-metrics" and "virtually integrated precinct information modeling". In: Radujkovic, M., Vukomanovic, M. & Wagner, R. (Eds.), *The 27th World Congress of the International Project Management Association*. https://doi.org/10.1016/j.sbspro.2014.03.016

[21] Aien, A., Kalantari, M., Rajabifard, A., Williamson, I. & Bennett, R. (2013). Utilising data modelling to understand the structure of 3D cadastres. *J. Spat. Sci., 58*, 215-234. https://doi.org/10.1080/14498596.2013.801330

[22] Andrianesi, D. E. & Dimopoulou, E. (2020). An integrated BIM-GIS platform for representing and visualizing 3D cadastral data. https://doi.org/10.5194/isprs-annals-VI-4-W1-2020-3-2020

[23] Diakite, A. A. & Zlatanova, S. (2020) Automatic geo-referencing of BIM in GIS environments using building footprints. *Comput. Environ. Urban Syst., 80*, 101453. https://doi.org/10.1016/j.compenvurbsys.2019.101453

[24] D'Amico, F., Calvi, A., Schiattarella, E., Prete, M. D. & Veraldi, V. (2020). BIM and GIS Data Integration: A Novel Approach of Technical/Environmental Decision-Making Process in Transport Infrastructure Design. https://doi.org/10.1016/j.trpro.2020.02.090

[25] Tang, L., Chen, C., Li, H. & Mak, D., Y., Y. (2022). Developing a BIM GIS–Integrated Method for Urban Underground Piping Management in China: A Case Study. https://doi.org/10.1061/(ASCE)CO.1943-7862.0002323

[26] Lim, Y.-W., Chong, H.-Y., Ling, P. C. H. & Tan, C. S. (2021). Greening Existing Buildings through Building Information Modelling: A Review of the Recent Development. *Build. Environ., 200*, 107924. https://doi.org/10.1016/j.buildenv.2021.107924

[27] Ismail, Z.-A. (2021). Maintenance Management Practices for Green Building Projects: Towards Hybrid BIM System. Smart Sustain. *Built. Environ., 10*, 616-630. 2046-6099. https://doi.org/10.1108/SASBE-03-2019-0029

[28] Olanrewaju, O. I., Enegbuma, W. I., Donn, M. & Chileshe, N. (2022). Building Information Modelling and Green Building Certification Systems: A Systematic Literature Review and Gap Spotting. *Sustain. Cities Soc., 81*, 103865. https://doi.org/10.1016/j.scs.2022.103865

[29] Zhang, L., Wu, X., Ding, L., Skibniewski, M. J. & Lu, Y. (2016). BIM-based risk identification system in tunnel construction. *J. Civ. Eng. Manag., 22*, 529-539. https://doi.org/10.3846/13923730.2015.1023348

[30] Hallowell, M. R., Hardison, D. & Desvignes, M. (2016). Information technology and safety: Integrating empirical safety risk data with building information modeling, sensing, and visualization technologies. *Constr. Innov., 16*, 323-347, 1471-4175. https://doi.org/10.1108/CI-09-2015-0047

[31] Khan, N., Ali, A. K., Skibniewski, M. J., Lee, D. J. & Park, C. (2019). Excavation safety modeling approach using BIM and VPL. *Adv. Civ. Eng., 15*, 1515808. https://doi.org/10.1155/2019/1515808

[32] Sadeghi, H., Mohandes, S. R., Hamid, A. R. A., Preece, C., Hedayati, A. & Singh, B. (2016). Reviewing the usefulness of BIM adoption in improving safety environment of construction projects. *J. Teknol., 78*, 175186. https://doi.org/10.11113/jt.v78.5866

[33] Moon, H., Kim, H., Kim, C. & Kang, L. (2014). Development of a schedule-workspace interference management system simultaneously considering the overlap level of parallel schedules and workspaces. *Autom. Constr., 39*, 93-105. https://doi.org/10.1016/j.autcon.2013.06.001

[34] Moon, H., Dawood, N. & Kang, L. (2014). Development of workspace conflict visualization system using 4D object of work schedule. *Adv. Eng. Inf., 28*, 50-65. https://doi.org/10.1016/j.aei.2013.12.001

[35] Yi, S. L., Zhang, X. & Calvo, M. H. (2015). Construction safety management of building project based on BIM. *J. Mech. Eng. Res. Dev., 38*, 97-104.

[36] Andritsou, D., Soile, S. & Potsiou, C. (2023). Merging BIM, Land Use and 2D Cadastral Maps into a Digital Twin Fit – For – 687 Purpose Geospatial Infrastructure. *Recent Advances in 3D Geoinformation Science*. https://doi.org/10.1007/978-3-031-43699-4

[37] Andritsou, D. & Potsiou, C. (2024). CadaSPACE: A Cloud Based Platform for a low - cost 3D visualization of property rights available in a 2D cadastral registry. An example for urban multi – storey buildings. *ISPRS Annals X-4-W5-2024*. https://doi.org/10.5194/isprs-annals-X-4-W5-2024-25-2024

Authors' contacts:

Dimitra Andritsou, PhD Candidate
(Corresponding author)
National Technical University of Athens (NTUA),
School of Rural and Surveying Engineering,
Zografou Campus, 9, Iroon Polytechniou str.,
15772 Zografou, Greece
+30 6947190805, andimitra@hotmail.gr

Chryssy Potsiou, Professor Doctor
National Technical University of Athens (NTUA),
School of Rural and Surveying Engineering,
Zografou Campus, 9, Iroon Polytechniou str.,
15772 Zografou, Greece
chryssy.potsiou@gmail.com

ISSN 1846-6168 (Print), ISSN 1848-5588 (Online)
https://doi.org/10.31803/tg-20240910124250

Preliminary communication
Received: 2024-09-10, Accepted: 2024-10-28

Challenges and Opportunities for BIM-GIS Integration – BIRGIT Case Study

Sanja Šamanović*, Olga Bjelotomić Oršulić, Vlado Cetl, Danko Markovinović, Anders Östman

Abstract: The integration of Building Information Modelling (BIM) and Geographic Information Systems (GIS) is becoming increasingly important in the construction industry and urban planning, helping to create smart cities and digital twins. The research, which involved expert interviews, and an online survey conducted among specialists from partner countries, shows that there is a significant skills gap, as many professionals lack expertise in combining BIM and GIS. It also indicates that while the integration of these technologies is advancing, it is still in the early stages. To tackle this issue, the BIRGIT project—featuring partners from Sweden, Italy, Spain, Belgium, and Croatia—aims to develop new educational programs that meet market demands. Ongoing initiatives like BIRGIT are vital for bridging the skills gap and ensuring that professionals are well-equipped to effectively implement these technologies, ultimately improving project management and decision-making in the industry.

Keywords: BIRGIT; Building Information Modelling (BIM); Geographic Information Systems (GIS); industry demand; integration; technical skills; training needs

1 INTRODUCTION AND LITERATURE REVIEW

As for the construction and urban planning industries today, specialists are commonly trained in BIM or GIS. BIM, being at the centre, is concerned with the creation, administration, and analysis of virtual models of buildings, while GIS is focused on the spatial data analysis and managing information concerning geographic locations.

Even though the two systems are crucial for effective infrastructure planning and management, there exists a huge gap among professionals. A great number of engineers and architects hold a solid understanding of the BIM methodologies, but they hardly have similar abilities in GIS. On the other hand, specialists of GIS, like geoinformatics specialists and urban planners, mostly stick to spatial data analysis but rarely know much about BIM tools and methodologies.

This knowledge compartmentalization might hinder the proper conversion of BIM to GIS and vice versa. Professionals focusing solely on one of the two technologies often experience limited communication and collaboration with their colleagues in other disciplines, which can be detrimental to the entire project and may lead to data integration issues.

The lack of specialists who possess skills in both areas further hampers the effectiveness of a functional team. In this regard, educational solutions that promote the training of specialists and develop human capital with expertise in BIM and GIS can help bridge this gap. Enabling professionals to acquire competencies in both domains facilitates the integration process, which can improve the efficiency and sustainability of construction projects

BIRGIT is a research project that is geared toward the integration of BIM and GIS for more efficient community planning and the optimization of construction projects [1]. This integration has its drawbacks, such as the lack of skills and the knowledge gaps of the professionals. However, to overcome these problems, the BIRGIT project will provide some interdisciplinary educational materials to give the professionals the competencies that they need to have a successful BIM-GIS integration.

Information, features and capabilities from BIM and GIS are combined to enhance built environment management and analysis. By integrating BIM data with GIS operations, GIS enables the viewing and analysis of BIM data within a geographic context. BIM-GIS integration is becoming more widely used globally, helping to build infrastructure and smart city projects that align with the objectives 2030 Agenda for Sustainable Development (SDG) [2]. The integration uses detailed geometric and attribute data from BIM and the spatial analysis capabilities of GIS to create a more comprehensive picture of the construction site and its environment. A recent study proposed a semi-automated process for a hybrid BIM-GIS model, which enhances information management from both infrastructure and environmental perspectives, thereby enabling informed decision-making throughout the lifecycle of the infrastructure [3].

The joint use of these complementary technologies facilitates the solving real-world problems, particularly in the development of smart cities and digital twins [4, 5]. Another important area of application is in the construction and urban planning sector.

Diverse national strategies for combining BIM and GIS technology result in differences in the application of BIM and its effects. Strategies include industry-driven projects, in which the industry itself drives BIM adoption but the government plays a less significant role, and government-driven programs with required BIM policies [6]. On the other hand, some countries have opted for the opposite approach, where integration is initiated by the state administration [7].

The foundation for integrated digital approaches in major infrastructure projects has been established in the UK, a pioneer in requiring the usage of BIM [8, 9]. Although there is no federal law requiring the use of BIM in the USA, several state governments have implemented BIM to be used in public projects, and large-scale infrastructure projects are increasingly integrating BIM with GIS.

Recent studies have also addressed the interoperability between BIM and GIS in the research on cultural heritage preservation, emphasizing the need for converting objects from BIM models into a standardized GML format. This approach facilitates the linking of BIM and GIS with databases, enabling efficient data management and comprehensive risk analysis within the fields of urban planning and cultural heritage preservation [10].

Encouraging the use of BIM has been a constant endeavour of the European Union thanks to several guidelines and initiatives. For the first time in a legal context, BIM was introduced to the Member States by means of European Directive No. 24 published in 2014 and served as a baseline for further, more progressive development of this strategy across the continent [11]. The directive addressed how the construction industry could benefit from the adoption of information technology in improving efficiencies, sustainability and lowering costs. Nevertheless, in several countries, there is a lack of satisfaction among the stakeholders as to the outcomes which BIM can achieve, as well as an imbalance in its theoretical and practical application [12]. This is mainly due to a lack of standards, and inadequate training on best practices that would help embrace BIM in daily routines and the reluctance of the different stakeholders involved in the management system to adopt these integrated models [13].

Asian nations like Singapore and South Korea are investigating the integration of GIS into urban planning and smart city development, and they have established strict regulations and guidelines for the use of BIM in public projects [14]. The adoption is growing but more scattered in other areas. Hong Kong, for example, has issued guidelines for the integration of BIM and GIS to facilitate urban planning and smart city applications [15].

The incorporation of BIM and GIS technologies in infrastructure management is becoming increasingly important, especially regarding to underground infrastructure, which often remains invisible during design and construction. The traditional reliance on 2D drawings does not provide sufficient information for construction managers to make effective decisions throughout the lifecycle of the project. Therefore, “an integrated framework is needed that is based on advanced technologies such as BIM and GIS, where all geometric and semantic information can be stored, managed, accessed, retrieved, and updated in a standardized manner at different project stages” [16].

Effective communication, data sharing, and coordination between architects, engineers, and other stakeholders involved in the design, construction, and operation of built environments are facilitated by BIM-GIS integration. The integration together with quantitative analysis, technology application, and urban management, greatly contributes to the development of smart sustainable cities [17]. Integration makes it possible to improve urban sustainability, rationalize resource management in construction projects, and enhance governance in smart cities.

New methods for urban planning, design, and asset management are needed in both the public and private sectors. Planning maintenance, asset tracking, and facility management are all made more effective by this connectivity. To leverage these benefits, it is crucial to have well-educated professionals who are adept in BIM-GIS integration. Therefore, developing high-quality courses and educational materials is essential to ensure that individuals have the skills and knowledge required to implement and manage these technologies successfully.

In construction management, BIM-GIS integration is a rapidly emerging technology that has advanced significantly in the last ten years [17]. However, organizational, cultural, technological, commercial, and practical limitations have frequently been surpassed by the conceptual comprehension of these promising notions [18]. BIM and GIS systems can communicate more easily thanks to common data interchange standards as Industry Foundation Classes (IFC) for BIM and Geography Markup Language (GML) for GIS. This promotes interoperability between the two technologies. However, compatibility issues and integration challenges across various systems and technologies continue to be major obstacles [19]. By expanding the application of BIM technology beyond individual buildings to larger city scales, current research, best practices, and technological improvements are opening the door for more thorough and effective industrial processes [4].

Data interoperability must be fully resolved before integration of BIM and GIS at the application level can be achieved. This is because integration involves multiple levels, including the application level and a more detailed data level, which comprises sublevels such as the geometry level and semantic level (Fig. 1) [20].

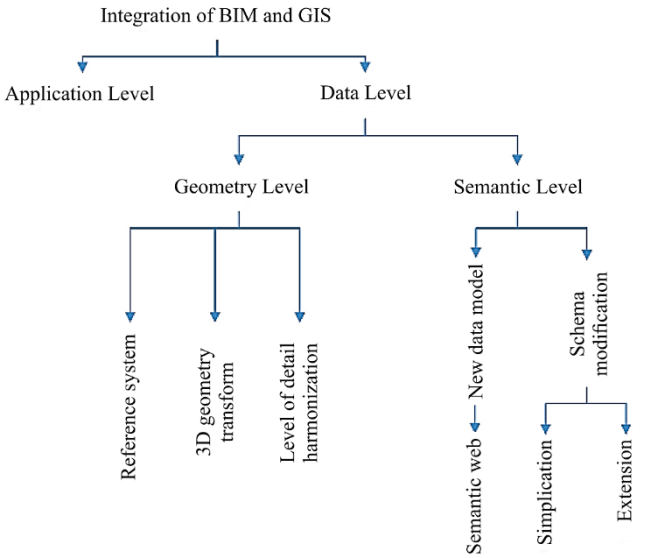

Figure 1 Levels of integration of BIM and GIS

The complexity of integration is also linked to technical aspects; for example, certain functionalities, such as the scheduling tool, are not readily or fully adopted. Although this tool enables the planning of activities, it does not adequately address project complexity or the recurrence of activities [21]. Moreover, research into the integration of BIM and GIS has been insufficient. This gap exists at both the macro level—covering processes, project management,

and commercial and organizational dynamics—and at the micro level, which includes technical integration [5]. This indicates the need for more comprehensive research and development efforts to address both the macro and micro-level challenges to fully realize the potential of BIM and GIS integration in the AEC industry.

To address these challenges, the BIRGIT project has been initiated. BIRGIT is a three-year project funded by the Erasmus+ Programme, which runs from February 2022 to January 2025. Its mission is to bridge the gap between the growing demand for and the current supply of skills in BIM-GIS integration. To achieve this, BIRGIT focused on enhancing vocational education and training by creating new curricula and educational resources that provide people the know-how needed to integrate BIM and GIS effectively. The project's participants include the scientific community, BIM and GIS providers, public sector organizations, academic and research centres, EU networks of VET organizations, managers of technical education and training, trainers, trainees, and VET providers. The partnership includes seven organizations: University North (Croatia), Forma Azione s.r.l. (Italy), GISIG (Geographic Information Systems International Group) (Italy), Ocellus Information Systems AB and Novogit AB (Sweden), and EfVET (European Forum of Technical and Vocational Education and Training) (Belgium) [22].

The growing need for experts and education in the fields of architecture, engineering, and construction (AEC) has led to the creation of initiatives such as the BIRGIT project, which aims to close the skills gap in these rapidly evolving fields. The path towards successful BIM and GIS integration includes the technical complexities of aligning data from diverse sources, the lack of standardized practices across the industry, and the educational gap among professionals who are expected to navigate both BIM and GIS environments.

By integration real data with 3D city models, the integration of IoT, BIM, and GIS would significantly enhance the effectiveness and quality of urban administration [23]. Professionals in both fields must be well educated to integrate data. According to surveys conducted in Sweden, Italy, Spain, and Croatia, indicate a shortage of trained personnel and vocational programs that address the skills required for integrating BIM and GIS. GIS and BIM courses are typically offered within existing curricula; however, they are not integrated [20]. The labour market is necessary more and more BIM and GIS integration skills, which emphasizes the need for ongoing skill development and adaptability. Addressing these gaps through targeted educational programs and ongoing professional training is essential for meeting the growing demand and ensuring the successful application of integrated technologies across all areas of application.

2 METHODOLOGY

This chapter describes the methodology used for our survey of industry professionals, focusing on assessing knowledge and skill gaps in the BIM-GIS sector. The flowchart (Fig. 2) illustrates the methodology we defined and used for assessing knowledge and skill gaps in the BIM-GIS sector. The process begins with the Planning and Design phase, where we have defined survey objectives and created questions which could capture key skill areas. Following this, in the Data Collection and Distribution phase, an online survey targeting the BIM-GIS community was distributed to selected industry experts, and responses are monitored and collected for analysis. Next, the Data Processing and Analysis phase involves cleaning and analysing the responses to get to the important information which is then uncovered into current knowledge levels and required competencies. Based on these insights, the Insights and Recommendations phase focuses on summarizing the findings and proposing actionable steps to address identified gaps. At the end of the flowchart, there is the Development of E-Learning Materials phase which transforms the recommendations into structured e-learning modules designed to bridge the identified skill gaps. The materials are then deployed and refined based on feedback, ensuring continuous improvement in the sector's skill development.

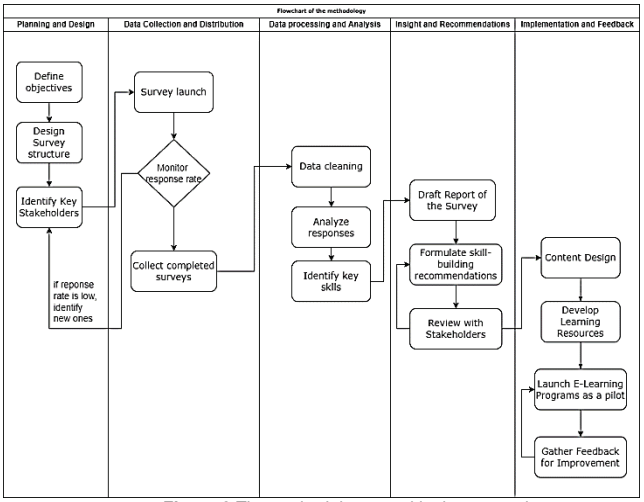

Figure 2 The methodology used in the research

Beside launched online survey, and for the better understanding of the evolving needs and challenges of BIM-GIS integration, we also conducted further interviews with professionals in the BIM and/or GIS domain. Nine interviews were done, with two coming from Italy, one each from Spain, Sweden, and Croatia. The interview's focus was on the knowledge and abilities that are required for BIM and GIS integration. Despite having access to a list of suggested questions, the interviewers were allowed to assign more weight to some points based on the interviewee's profile and context, as well as the unique characteristics of the nation in which the interview is being conducted. The interviews are impartial considering the respondents' professional backgrounds (established experts in the BIM and GIS fields), but they also consider their individual opinions on the subjects and fields in which they use BIM-GIS integration. The online survey was created with the intention of gathering more precise and in-depth data regarding training needs, as well as to enhance the information already gathered with the

involvement of other specialists. 53 responses were gathered during the online survey, which was created using EUSurvey, the official survey management tool of the European Commission.

Most of the companies that took part in the survey are involved in the AEC industry (27), education and training (16), and software development/distribution (11). The questionnaire's questions are mostly divided into:

The questions asked in the questionnaire are classified into:

- General organisation information
- Demand for BIM-GIS integration skills in the industry
- Views on BIM-GIS integration process.

Within the methodology, a systematic approach was applied to assess current skill levels and identify gaps. By categorizing questions into general organizational information, the industry's need for BIM-GIS integration skills, and perspectives on integration, specific training needs and areas for development can be pinpointed, as shown in the next section.

3 RESULTS AND DISCUSSION

The largest response to the survey (47.17%) was from organizations of small and medium enterprises (SME). Also, a significant number of respondents come from the domain of education and research (18.87%) and administration and public bodies (15.09%). These results reflect the traditional usage of BIM primarily in the private sector, where it facilitates efficient project management and design processes, while GIS is more frequently utilized by public administration and government agencies for effective spatial planning and resource management.

As the professional profiles of the participants are equally divided between BIM and GIS (only 3.77% of the participants deal with both fields), analysis with professional profile and sector in which the organization operates was made. Participants identifying as BIM professionals predominantly work in the Architecture, Engineering, and Construction (AEC) sector, whereas GIS experts are spread across various sectors, varying by country. This research coincides with the previous ones, in which it was stated that many respondents use BIM in educational facility projects, and it was found that respondents with professional backgrounds in BIM are primarily engaged in the Architecture, Engineering and Construction (AEC) sector, which aligns with the predominant application of BIM in this sector [24].

3.1 Current Status of Integration

One of the most important questions that fully supports the necessity of tackling the problem of BIM and GIS integration is the question of the current status/maturity of the adoption of BIM-GIS integration (Fig. 3). A large percent of respondents think that the integration of BIM and GIS has not yet been fully implemented or it is at a certain stage of development (86.80%). Surveys reveal that respondents from Sweden and Spain tend to view the adoption status as "emerging/early adoption". In contrast, about one-third of respondents from Croatia consider the integration to be at the "growth" stage, which represents a more advanced phase. This view is even more prevalent among respondents from Italy. Although a smaller part of respondents (16.66%) believes that integration has not been adopted, the ratio of Emerging/early adoption and "In grow" phase is 50% - 50%. This implies that Italy may be a country where integration practices are further along in development, possibly resulting in greater efficiency and better collaboration among different sectors.

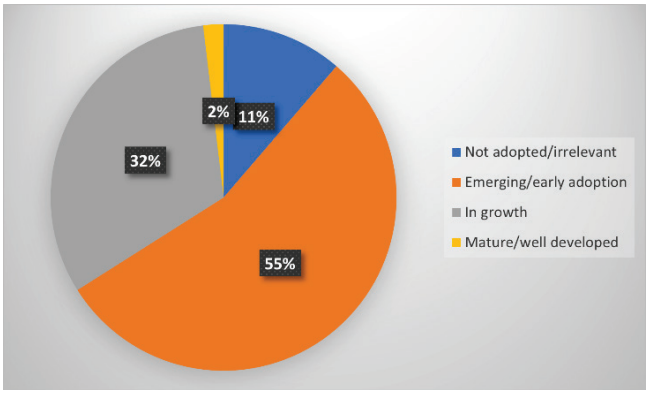

Figure 3 The level of adoption of BIM/GIS integration

Even though a lot of technical challenges in integrating BIM and GIS have been tackled to some extent, there aren't many theoretical studies that look at how to effectively combine the strengths of both for deeper quantitative analysis. This indicates that while BIM-GIS integration has made significant progress, it has not yet reached full implementation, reinforcing the notion that its adoption is still evolving [25].

BIM/GIS integration is imperative in several areas in the construction industry as it provides effective data handling and representation through different phases of the project life cycle. There are different modes of this integration like migrating from BIM to GIS or from GIS to BIM or from both to another system [26, 27]. BIM and GIS are useful management information systems, providing managers with essential data, procedures, and total facility performance management software systems and decision supervision, providing data and metadata analysis for performance management and supporting analytical applications for internal and external building infrastructure management workflows [28].

The interviewee was able to choose several options to define the primary areas where BIM-GIS integration technologies are currently applied or hold potential for future application. Most respondents think that BIM/GIS integration technologies are mainly used in Land use and Urban planning (64.15%), Architecture (62.26%), Roads and highways (58.49%) and Smart Cities (52.83%). Use in Railways, Bridges, Utilities underground networks, Facility management also have a significant percentage (over 40%). When analysed by country, out of 14 respondents in Croatia, 12 of them decided on architecture. On the contrary, in Italy,

most respondents think that the application of BIM and GIS integration makes the most significant contribution in Land use and Urban planning and especially in the domain Utilities underground network which is not at all significant for Spanish respondents. They are most interested in the field of Land and urban planning, and Swedes in field Roads and motorways.

Given the opinions that the integration of BIM and GIS is in the early stages of development/early adoption or has not even started at all, the respondents' views on the current necessary skills for implementation are logical (Fig. 4). The general feedback is that the skills of current employees in the Geospatial and AEC industries only partially meet job requirements, which means they'll need more training and the acquisition of additional skills. 15.09% of respondents believe that current employees do not have the necessary skills to implement BIM/GIS integration, while as many as 56.6% of respondents believe that current employees need further training. What is also significant regarding this question is the significant percentage (22.64%) of respondents who did not know how to answer this question. The reason probably lies in the fact that many employers have not even begun to seriously consider integration.

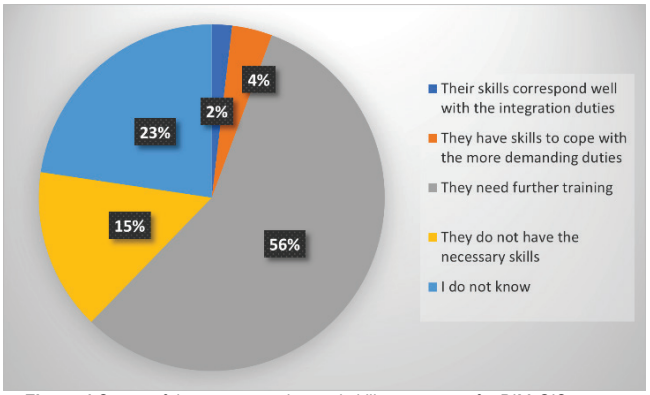

Figure 4 Status of the competencies and skills necessary for BIM-GIS among current employees in the Geospatial and AEC industries

Such high percentages in certain areas define the starting point for competence research and identify the most common fields in which a suitable candidate for a BIM-GIS integration role should possess training (Fig. 5). Distinct hiring preferences favour candidates from the fields of Engineering (69.81%), Architecture (52.83%), and Geoinformatics. (56.6%). Participants also found relevant Computer sciences (45.28%), Data science and statistics (39.62%), Cartography (35.85%) and Geodesy (24.53%). Observing respondents from the two researched sectors separately, those with BIM-related backgrounds believe that having a foundation in Architecture and Engineering is ideal. On the other hand, GIS respondents stress the importance of training in Geoinformatics and point out that education in fields like Geodesy, Geography, and Cartography is relevant for BIM-GIS integration.

The BIRGIT survey focuses significantly on identifying and evaluating the specific competencies and skills necessary for BIM-GIS integration. Respondents were asked to assess their expertise in various competencies and skills as 'basic', 'intermediate', or 'expert'. Analysis of the required general competencies suggests that a strong foundation in both disciplines, particularly the fundamental principles, is essential for effective BIM-GIS integration work [16].

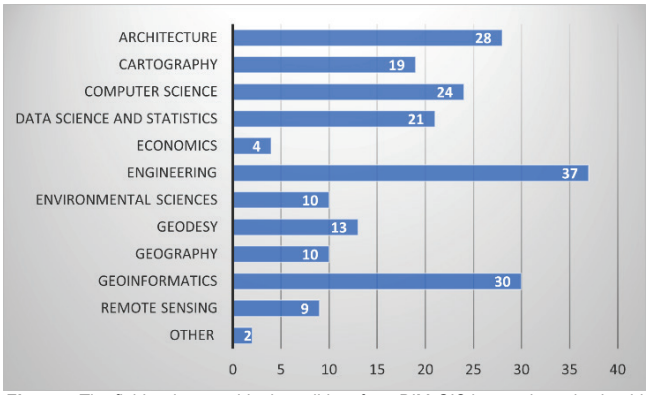

Figure 5 The fields where an ideal candidate for a BIM-GIS integration role should be trained

3.2 Technical Skills

In the research, 22 software were offered, 9 from the GIS and 13 from the BIM domain. Additionally, the survey revealed that respondents tend to believe that having a solid understanding of both software tools is necessary. The survey indicates that knowledge of GIS software is regarded as necessary at an intermediate level. Additionally, research shows that both BIM and GIS professionals agree on the necessity of achieving an intermediate proficiency in tools from either domain to effectively tackle integration tasks. (Fig. 6).

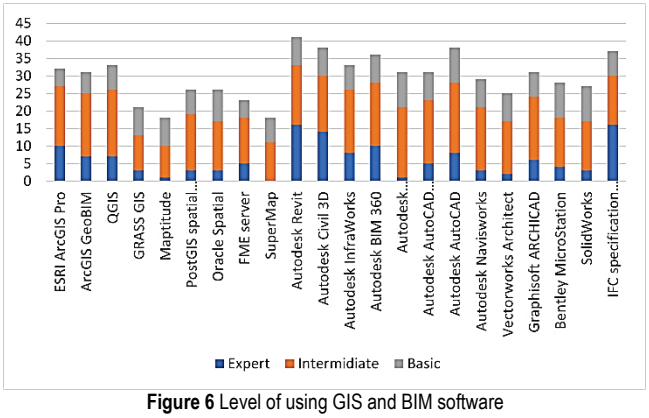

Figure 6 Level of using GIS and BIM software

When analysing the total number of answers regarding the necessary knowledge of software, it is interesting that many respondents did not give their opinion about individual GIS and BIM software. This result indicates a notable gap in familiarity with these tools and suggests that certain software is used less or not at all.

Commercial ESRI's software and open-source software QGIS are regarded as the most significant. In terms of BIM software, Autodesk Revit stands out as the most recognized, which aligns with the findings from the interviews. Advanced proficiency in Autodesk Revit is viewed as the

most valuable skill. Autodesk software is heavily involved in commenting for a variety of uses. Emphasis should be placed on the fact that respondents, particularly BIM experts, place a high value on mastery of the IFC specification [5]. There is little to no focus on the other software items that are unrelated to Autodesk or ESRI. However, there are several obstacles in the way of a smooth BIM-GIS integration, such as standardization requirements and technical complexity [29]. To maximize the benefits of BIM-GIS integration and improve resource management and urban sustainability, it is imperative that these issues be resolved.

Regarding the category of BIM skills (Fig. 7), respondents in almost all categories opted for an intermediate or expert level of knowledge. 52.83% of the respondents believe that for the integration of BIM and GIS, competence related to BIM fundamentals is needed at the expert level, and 26.42% at the intermediate level. Significant emphasis is placed on tasks related to 3D modelling and the utilization of model-oriented software, with a summary indicating that this is important for both intermediate and expert levels (79.25%). Knowledge of data specifications and other standards (such as IFC) is also considered important (67,92%).

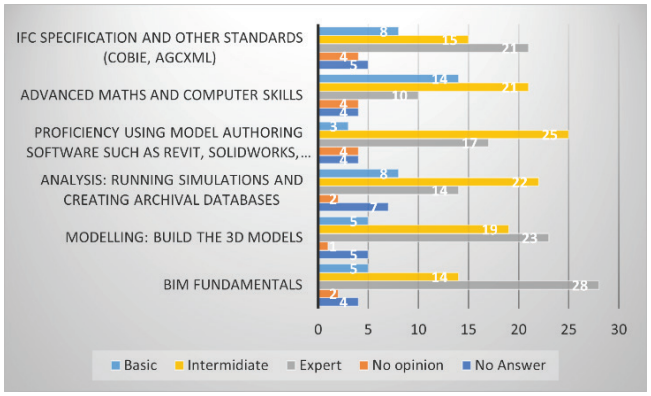

Figure 7 BIM skills set for a BIM/GIS integration job

Regarding GIS data skills (Fig. 8) 52.83% of the respondents believe that for the integration of BIM and GIS, competence related to GIS fundamentals is needed at the expert level, and 16.98% at the intermediate level. Skills in 3D GIS and data models can also be emphasized (summary for intermediate and expert levels: 69.82%), along with tasks related to georeferencing, map projections, and data resampling (71.7%).

These findings indicate that advanced skills in handling BIM and GIS data are essential, with the required skill level generally falling between intermediate and expert. Both BIM and GIS professionals acknowledge the necessity of intermediate skill levels, with many emphasizing the importance of advanced capabilities across nearly all areas. This indicates the increasing complexity of tasks related to BIM and GIS integration, which requires a high level of expertise. As a result, it's clear that BIM-GIS integration requires a variety of skills, with an advanced level of knowledge being important.

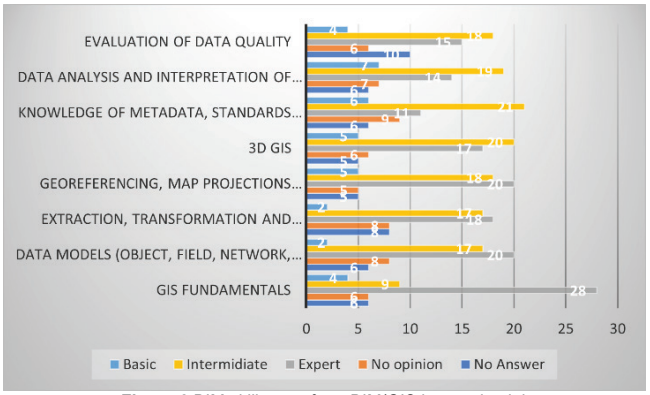

Figure 8 BIM skills set for a BIM/GIS integration job

From an organizational and institutional perspective, there is significant emphasis on the importance of adopting GIS and BIM standards. It is recognized that without appropriate standards, successful integration may be hindered or even impossible. Even 56.6% of the respondents believe that it should be at the expert level and 18,87% on the intermediate level. This specific skill stands out as a major finding from the survey, highlighting the necessity of advanced knowledge in using and implementing standards, which play a crucial role in ensuring interoperability between systems. This skill not only enhances individual expertise but also encourages teamwork across various platforms, helping to create smoother and more connected workflows.

3.3 Education and Perspective

The last part of the survey focused on exploring trends and key aspects of education and training that need to be addressed for strengthening BIM-GIS integration in the future. Fig. 9 shows that respondents emphasize the significance of ongoing training investments for employees (39.62% of them considered this assumption as very important). Additionally, significant importance is given to practical experience through real-world business scenarios (case-based learning), with 28.3% of respondents highlighting this aspect.

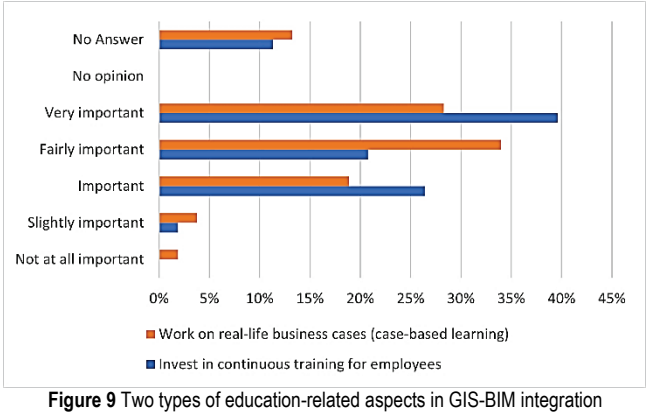

Figure 9 Two types of education-related aspects in GIS-BIM integration

As per the suggestions made by the participants, enhancing the integration of BIM and GIS might be accomplished through staff training and support and by incorporating new technologies and procedures into

educational establishments. The need to create national standards and provide training that is accessible to all members is emphasized, with a focus on training for the most popular BIM and GIS applications. Furthermore, they advocate for GIS and BIM to be required subjects in civil engineering and architectural curriculum.

In addition, In the future, GIS-BIM integration will be more seamlessly integrated into larger information management systems, reducing the significance of discipline boundaries. Although there will be a rise in the use of integrated GIS-BIM, its ideal application may be limited by skill gaps, and its expansion into domains such as Life Cycle Assessment (LCA) and Environmental Impact Assessment (EIA) may be gradual. With prominent examples from nations like the USA, Singapore, and Germany, the integrated market is predicted to expand; nevertheless, it might take some time for Croatia and the EU to see comparable developments. It is expected that surveyors would produce extensive GIS databases that give builders and architects comprehensible, georeferenced project data.

4 CONCLUSION

The objective of the research describe in this paper was to investigate BIM-GIS integration by covering different aspects, namely:

1) Current status of integration
2) Technical skills needed for the integration
3) Education and Perspective

The method used was a combination of interviews and surveys in BIRGIT project partner countries.

While the studies mentioned in the introduction focused on the theoretical foundations and potential applications of BIM-GIS integration, our research shifts attention to the urgent need for improving education and skill development, particularly highlighting differences in professional competencies. Emphasizing regional variations in BIM and GIS integration techniques not only reflects the complexity of adoption but also underscores the importance of tailored educational programs, like those initiated by the BIRGIT project.

The results achieved through the interviews and surveys can be summarized as follows:

1) BIM-GIS integration is still in its infancy; 86.8% of respondents think it isn't being used correctly at the moment, and 47.17% stress the need for further training. Only 16.66% of respondents consider the integration complete, while 50% see it as either "early adoption" or "in progress."
2) Effective integration requires advanced BIM and GIS skills—52.83% of respondents noted the necessity for expert-level BIM skills, and 71.7% highlighted the importance of GIS expertise.
3) Addressing these needs through standardized methods and enhanced educational programs is crucial. Initiatives such as the BIRGIT project, which focuses on improving education and training, play a vital role in overcoming these challenges.

The findings presented in this paper should be combined with other studies to enhance synergy and a holistic view of the BIM-GIS integration. There are still issues that need to be tackled in future research.

The benefits of combining BIM with GIS include better resource management, increased sustainability in urban areas, and more effective planning and construction procedures. However, there remain challenges, including data compatibility and interoperability, scale and level-of-detail disparities lack of common understanding on type-appropriate variable formats issues regarding the volume problems with storing that much information having technical double-use criteria or software dependencies regulatory/standardization efforts. Addressing these challenges is crucial for reaping the rewards of BIM-GIS integration and take advantage of what it has to offer.

The integration of BIM-GIS is anticipated to be even better for project visualization, sustainability and cost savings. Its role in enabling smarter and more efficient urban and infrastructure planning will become increasingly important. The integration will benefit from advancements in AI and data analytics, providing deeper insights and predictive capabilities for urban planning. Digital twins and smart cities will benefit from real-time monitoring and simulation, while cloud computing and IoT will offer scalable and accessible storage solutions. Augmented Reality (AR) and Virtual Reality (VR) will facilitate immersive interactions with integrated BIM-GIS data, improving collaboration and project understanding. Additionally, stronger regulatory support will drive sustainable development by supporting environmental impact assessments and mitigations in public infrastructure projects.

The BIRGIT training materials for the integration of BIM in GIS is under development and testing at this time which will be further disseminated by conducting several multiplier events throughout partner countries stakeholders. These outputs are due to be made available, openly accessible and free of charge at the conclusion of the project — across all output formats — with a view to helping address current circumstances where actual expertise in this area remains rare or embryonic.

Further refining skills and adapting, will undoubtedly protect processes for urban planning and building whilst allowing for better resource management to improve the manner that cities are sustainably handled. In the end, BIM integrates with GIS to deliver modern urbanization through efficient expert collaboration and enhancing infrastructure administration across all segments.

Acknowledgements

This article was made with the support of scientific project "High-precision georadar mapping", project number UNIN-TEH-24-1-17 funded by the University North, Varazdin, Croatia.

5 REFERENCES

[1] https://birgitproject.eu/

[2] Liu, Z., Liu, Y. & Osmani, M. (2024). Integration of Smart Cities and Building Information Modeling (BIM) for a Sustainability Oriented Business Model to Address Sustainable Development Goals. *Buildings, 14*, 1458. https://doi.org/10.3390/buildings14051458

[3] Cepa, J. J., Pavon, R. M., Alberti, M. G. & Carames, P. (2023). Towards BIM-GIS integration for road Intelligent management system. *Journal of Civil Engineering and Management, 29*(7), 621-638. https://doi.org/10.3846/jcem.2023.19514

[4] Basir, W. N. F. W. A., Ujang, U. & Majid, Z. (2021). Building Information Modeling (BIM) and Geographic Information System (GIS) data compatibility for construction project. *Journal of Information System and Technology Management, 6*, 278-289. https://doi.org/10.35631/JISTM.624026

[5] Wang, H., Pan, Y. & Luo, X. (2019). Integration of BIM and GIS in sustainable built environment: A review and bibliometric analysis. *Automation in Construction, 103*, 41-52. https://doi.org/10.1016/j.autcon.2019.03.005

[6] Yang, J.-B. & Chou, H.-Y. (2018). Mixed approach to government BIM implementation policy: An empirical study of Taiwan. *Journal of Building Engineering, 20*, 337-343. https://doi.org/10.1016/j.jobe.2018.08.007

[7] Galić, M., Venkrbec, V., Chmelik, F., Feine, I., Pučko, Z. & Klanšek, U. (2017). Review of BIM's Implementation in some EU AEC Industries. *13th International Conference Organization, Technology and Management in Construction Conference Proceedings*. Zagreb: Hrvatska Udruga za Organizaciju Građenja, 462-476.

[8] Burgess, G., Jones, M. & Muir, K. (2018). BIM in the UK house building industry: opportunities and barriers to adoption. Cambridge University, Cambridge, March 1-8.

[9] Atkinson, L., Amoako-Attah, J. & B-Jahromi, A. (2014). Government's Influence on the Implementation of BIM. *Computing in Civil and Building Engineering*, 520-527. https://doi.org/10.1061/9780784413616.065

[10] Colucci, E., De Ruvo, V., Lingua, A., Matrone, F. & Rizzo, G. (2020). HBIM-GIS Integration: From IFC to CityGML Standard for Damaged Cultural Heritage in a Multiscale 3D GIS. *Applied sciences, 10*(4), 1356. https://doi.org/10.3390/app10041356

[11] Fiamma, P. & Biagi, S. (2023). Critical Approaches on the Changes Taking Place after 24/2014/EU in BIM Adoption Process. *Buildings, 13*, 850. https://doi.org/10.3390/buildings13040850

[12] Kolarić, S., Pavlović, D. & Vukomanović, M. (2015). Developing a methodology for preparation and execution phase of construction project. *Organization, Technology & Management in Construction: An International Journal, 7*(1), 1197-1208. https://doi.org/10.5592/otmcj.2015.1.4

[13] Matos, R., Rodrigues, H., Costa, A. & Rodrigues, F. (2022). Building condition indicators analysis for BIM-FM integration. *Archives of Computational Methods in Engineering, 29*(6), 3919-3942. https://doi.org/10.1007/s11831-022-09719-6

[14] Shafiullah, M., Rahman, S., Imteyaz, B., Aroua, M. K., Hossain, M. I. & Rahman, S. M. (2023). Review of Smart City Energy Modeling in Southeast Asia. *Smart Cities, 6*, 72-99. https://doi.org/10.3390/smartcities6010005

[15] The Government of the Hong Kong Special Administrative Region. Smart City Blueprint. Retrieved from: https://www.smartcity.gov.hk/blueprint/HongKongSmartCity Blueprint_e-flipbook_EN/mobile/index.html#p=2

[16] Sharafat, A., Khan, M. S., Latif, K., Tanoli, W. A., Park, W. & Seo, J. (2021). BIM-GIS-Based Integrated Framework for Underground Utility Management System for Earthwork Operations. *Applied Sciences, 11*, 5721. https://doi.org/10.3390/app11125721

[17] Song, Y., Wang, X., Tan, Y., Wu, P., Sutrisna, M., Cheng, J. C. P. & Hampson, K. (2017). Trends and Opportunities of BIM-GIS Integration in the Architecture, Engineering and Construction Industry: A Review from a Spatio-Temporal Statistical Perspective. *ISPRS Int. J. Geo-Inf., 6*, 397. https://doi.org/10.3390/ijgi6120397

[18] Sacks, R., Eastman, C., Lee, G. & Teicholz, P. (2018). B*IM handbook: A guide to building information modeling for owners, designers, engineers, contractors, and facility managers*. John Wiley & Sons. https://doi.org/10.1002/9781119287568

[19] Shirowzhan, S., Sepasgozar, S. M. E., Edwards, D. J., Li, H. & Wang, C. (2020). BIM compatibility and its differentiation with interoperability challenges as an innovation factor. *Automation in Construction, 112*, 103086. https://doi.org/10.1016/j.autcon.2020.103086

[20] Zhu, J., Wright, G., Wang, J. & Wang, X. (2018). Critical Review of the Integration of Geographic Information System and Building Information Modelling at the Data Level. *ISPRS Int. J. Geo-Inf., 7*, 66. https://doi.org/10.3390/ijgi7020066

[21] Pedó, B., Tezel, A., Goethals, D., Koskela, L. J., Leaver, M., Victory, A., Vrabie, E. & Bocian, E. (2023). BIM and GIS integration: lessons learned from multiple case studies. *EC3 Conference 2023*, 4, 0. European Council on Computing in Construction. https://doi.org/10.35490/EC3.2023.248

[22] PR1 – Industry requirements on BIM-GIS training programs and courses. Birgit project. Retrieved from: https://birgitproject.eu/wp-content/uploads/2023/02/PR1_ Report-1.pdf

[23] Roumyeh, M. & Badenko, V. (2022). Integration between BIM and GIS for decision-making. *BIM Modeling for Construction and Architecture*, Saint Petersburg, Russia. https://doi.org/10.23968/BIMAC.2022.003

[24] Moreno, C., Olbina, S. & Issa, R. R. (2019). BIM Use by Architecture, Engineering, and Construction (AEC) Industry in Educational Facility Projects. *Advances in Civil Engineering*, 1-19. https://doi.org/10.1155/2019/1392684

[25] Song, Y., Wang, X., Tan, Y., Wu, P., Sutrisna, M., Cheng, J. C. P. & Hampson, K. (2017). Trends and Opportunities of BIM-GIS Integration in the Architecture, Engineering and Construction Industry: A Review from a Spatio-Temporal Statistical Perspective. *ISPRS International Journal of Geo-Information, 6*, 397. https://doi.org/10.3390/ijgi6120397

[26] Elsheikh, A., Alzamili, H., Al-Zayadi, S. & Shadhan, A. (2021). Integration of GIS and BIM in Urban Planning - A Review. *IOP Conference Series: Materials Science and Engineering*, 1090, 012128. https://doi.org/10.1088/1757-899X/1090/1/012128

[27] Wan Abdul Basir, W. N. F., Ujang, U., Majid, Z., Azri, S. & Choon, T. (2020). The integration of BIM and GIS in construction project – a data consistency review. *ISPRS - International Archives of the Photogrammetry, Remote Sensing and Spatial Information Sciences*, XLIV-4/W3-2020, 107-116. https://doi.org/10.5194/isprs-archives-XLIV-4-W3-2020-107-2020

[28] Ismaeil, E. M. H. (2024). Asset Information Model Management-Based GIS/BIM Integration in Facility Management Contract. *Sustainability, 16*, 2495. https://doi.org/10.3390/su16062495

[29] Garramone, M., Moretti, N., Scaioni, M., Ellul, C., Re Cecconi, F. & Dejaco, M. C. (2020). BIM and GIS integration for infrastructure asset management: a bibliometric analysis. *ISPRS Annals of the Photogrammetry, Remote Sensing and Spatial Information Sciences, 6*(4/W1), 77-84. https://doi.org/10.5194/isprs-annals-VI-4-W1-2020-77-2020

Authors' contacts:

Sanja Šamanović, PhD, Assistant Professor
(Corresponding author)
Department of Geodesy and Geomatics, University North,
42 000 Varaždin, 104. brigade 3, Croatia
+38598757989 / sanja.samanovic@unin.hr

Olga Bjelotomić Oršulić, PhD, Assistant Professor
Department of Geodesy and Geomatics, University North,
42 000 Varaždin, 104. brigade 3, Croatia
+385977740321 / olga.bjelotomic.orsulic@unin.hr

Vlado Cetl, PhD, Full Professor
Department of Geodesy and Geomatics, University North,
42 000 Varaždin, 104. brigade 3, Croatia
+385915021888 / vlado.cetl@unin.hr

Danko Markovinović, PhD, Associate Professor
Department of Geodesy and Geomatics, University North
42 000 Varaždin, 104. brigade 3, Croatia
+385916655777 / danko.markovinovic@unin.hr

Anders Östman, PhD, Professor emeritus
Novogit AB,
Glansbaggestigen 12, SE-611 63 Nyköping, Sweden
+46706491975 / anders.ostman@novogit.se

ISSN 1846-6168 (Print), ISSN 1848-5588 (Online)
https://doi.org/10.31803/tg-20241008141610

Preliminary communication
Received: 2024-10-08, Accepted: 2024-11-04

Analyzing Depth Uncertainty of Near-Shore Bathymetric Survey Conducted by Single-Beam Echo Sounder

Nedim Tuno*, Nedim Kulo, Dean Perić, Muamer Đidelija, Adis Hamzić, Jusuf Topoljak, Admir Mulahusić, Dušan Kogoj

Abstract: Single-beam echo sounders have gained popularity for various applications due to their compact dimensions, ease of use, and cost-effectiveness. The question that often arises among the users is whether these devices can fulfill the necessary accuracy requirements. This paper concentrates on assessing the accuracy that can be achieved using a single-beam echo sounder. An accuracy assessment was performed by comparing the depths derived from the 3D model created from the single-beam echo sounder data to those obtained through more accurate and independent method (tacheometric surveying) in the test area. Accurate depth determination was achieved through trigonometric leveling, employing a specific methodology that allows for precise depth measurements up to 4.5 meters. The assessment results were compared to the vertical accuracy requirements for surveying and mapping in shallow waters, recommended by the International Hydrographic Organization. The results indicate that, with a 95% probability, the depths determined by the single-beam echo sounder meet the total vertical uncertainty (TVU) requirements specified by the S-44 standard for Order 1a survey.

Keywords: accuracy; depth measurements; IHO S-44; single-beam echo sounder; total station

1 INTRODUCTION

In a narrow sense, hydrography involves surveying and exploring the sea to produce nautical charts to ensure safe navigation [1, 2]. The basic tasks of hydrography are positioning on the water, determining the coastline, measuring depths (bathymetry), and creating navigational information systems [3].

Modern bathymetry (Greek bathus: depth) is the science of determining depths, i. e. determining the physical characteristics of the seabed based on the analysis of data from recorded profiles [4]. Seabed research and presentation of its characteristics, in a manner similar to topographic maps of land areas, is the subject of bathymetry. There are different methods and techniques of bathymetric surveys, that depend on the complexity of the project tasks [5].

The collection of depth data aims to show the topography of the sea, river, or lake bed, including all features, whether natural or man-made [6]. The term depth measurement refers to the determination of the vertical distance from the current water surface to the bottom.

From the point of view of hydrographic measurements, the two factors that define the position of a point (on Earth) are [7]:

- The horizontal position of the point, which can be represented as latitude and longitude, or by the Cartesian coordinates (in a geodetic network), or by angle and distance from a known control point.
- The depth of a point below the surface of the water, corrected for the vertical distance between the point of measurement and the water level and for the height of the tide above the datum or reference level to which the depths refer.

The rapid technological progress, that took off in the 20th century, also left its mark on instruments for determining depths. Technological developments resulted in the emergence of acoustic sensors such as side-scan sonars and single-beam echo sounders. This was a prelude to modern instruments that are now used in hydrography, such as interferometric sonar, wide-angle multibeam echo sounder, bathymetric lidar, and various types of integrated systems that combine multiple measurement sensors [2]. Ultrasonic depth sounders (or echo sounders) are instruments that measure the depth of the seabed using sound waves. Considering the number of sound beams that they transmit simultaneously, they can be classified as single-beam or multi-beam echo sounders [8, 9]. Echo sounders are the most commonly used in the process of bathymetric measurement because they have the best ratio of price and quality of collected data [10]. Acoustic methods cover all depth ranges and meet the International Hydrographic Organization (IHO) S-44 standard for hydrographic measurements [11]. Single-beam echo sunders are an appealing solution for many users, since they cost significantly less than multi-beams, and they can be mounted on smaller vessels. The data collected by such instruments has been successfully used in studies by numerous authors, among which are [12-19], etc. Other examples of such studies include the creation of detailed digital models of the seabed [20], the determination of morphometric changes in the river bed [21], the creation of digital bathymetric models of the lakebed [22], etc. Based on 15 years of data collection with a single-beam echo sounder, [23] created a map of the seabed showing sediment accumulations at certain locations along the western coast of the Adriatic Sea.

This study examines the vertical accuracy of hydrographic data collected using a single-beam echo sounder. The location on the Adriatic Sea, in the area of the Stobreč marina in Croatia, was examined. To make an accuracy analysis, data collected by an independent, more accurate method was used. Therefore, in the area of the Stobreč marina, a reference set of measurements for analysis was collected employing the tachymetric surveying (polar method), where the electronic tachymeter Leica Geosystems TS06 was used. The results of the analysis of the accuracy of

depth determination utilizing a single-beam echo sounder, regarding the depths determined by another more accurate method, indicate that the used methodology for data collection and processing gives satisfactory results

2 TEST SITE

The research site was located on the eastern side of Stobreč (Republic of Croatia, 7 km east of Split), and covered the area around the outer breakwater of the marina (Fig. 1). The measurement was commissioned by the Port Authority of Split-Dalmatia County, to create project documentation for the reconstruction of the sports and nautical port of Stobreč. According to the project assignment, the measurement had to include the mentioned breakwater and the surrounding areas. Therefore, the boundaries of the survey area were set at approx. 50 m from the planned reconstruction site. The map had to be made at a scale of 1:500, and contain the data necessary for the reconstruction project (measurements of depths, land, and overlay with cadastral map).

Figure 1 Site location in Stobreč, Republic of Croatia

3 SINGLE-BEAM ECHO SOUNDER

The single-beam echo sounder (SBES) is composed of a transducer that sends only one beam of ultrasound pulses vertically toward the seabed at a time. The depth is determined based on the time it takes for the sound wave to travel from the transmitter to the bottom and back. The time delay is calculated based on the speed of sound in the water, which depends on salinity, temperature, and pressure [24]. This principle is also used in GPR (Ground Penetrating Radar) and TPS (Total Positioning) instruments. Although ways of better physical modeling and understanding of oceanic processes are being researched [25], turbulence in ocean water is unpredictable and affects measurements [26]. Echo sounders usually work with two frequencies in the range between 12 and 710 kHz. One of them has a shorter wavelength. A shorter wavelength enables more accurate measurements, while a lower frequency allows deeper penetration of the sound pulse. Instruments are generally suitable for smaller vessels as they are portable, energy efficient, and very easy to use and maintain [27]. The transducer can be mounted on the hull of the vessel [24] or a rod (pole) [28]. Alternatively, the transducer can be towed behind the vessel [28]. Single-beam echo sounders are suitable for generating seabed profiles and are most often used for measuring depths directly below the vessel, i.e. for recording smaller parts of narrow sinkholes to determine their depth [24].

The beam width of a SBES is up to 30°. Until the mid-1980s, narrow beam echo sounders with a beam width of $\beta = 2 \cdot \theta \leq 5°$, were also used. Operations using narrow beam echo sounders require mechanical or electronic stabilization of the transmitter to reduce the rock and pitch effects of the vessel. Narrow beam echo sounders are used for:

- Measuring depths directly under the vessel, thus avoiding wide beam errors caused by a sloping seabed. These measurements are used either for the safety of navigation or for mapping the seabed.
- Improving data quality in resolution and accuracy.

To create a narrow beam, larger transmitters are needed than for a wide beam. Narrow beam echo sounders do not provide information about the topography located to the side of the vessel, but only the topography directly below the vessel. Taking this into account, they are usually used in integration with wide beam systems, as an additional data source [2]. The quality of the data collected by a SBES depends on the characteristics of the sensor, the water depth, and the adopted measurement plan [24, 10, 29].

The echo sounder used to collect the primary data set in this study is a MIDAS Surveyor, manufactured by Valeport. It is a single-beam, two-frequency echo sounder (33 kHz, resolution 0.01 m and 210 kHz, resolution 0.04 m), which can be installed on a small vessel for surveying in shallow or medium-deep waters. It has a built-in internal rechargeable battery (up to 24 hours of operation) with the option of an external power supply. MIDAS Surveyor is also equipped with an internal GNSS receiver for positioning (accuracy of 2 m with SBAS correction, WGS84, or local coordinate system), with a possibility for connecting an external RTK GNSS receiver. Additionally, the device can connect with an external sound velocity profiler, a salinity meter, and a motion sensor. Collected data is stored in the internal flash memory [30].

During the process of measurement, the internal GNSS receiver was not used. Instead, the GNSS receiver S8 Plus, manufactured by Stonex, was used. It was connected to the echo sounder via the connection for the external RTK GNSS receiver. The employed receiver was used in the RTK (Real Time Kinematic) mode of operation, for which the manufacturer states horizontal precision of 8 mm; 1 ppm RMS (Root Mean Square), and vertical precision of 15 mm; 1 ppm RMS [31].

The software package Hypack was used for the data collection, i.e. combining the data collected by the echo sounder and the GNSS receiver. It is a hydrographic application that was developed as a measurement and navigation system for vessels at sea. Hypack integrates the operation of the echo sounder and GNSS receiver, while the observed data is automatically displayed on the laptop screen, or stored in LOG files. The application allows pre-defined measurement lines to be imported. The application also has a geodetic module, in which the parameters describing the selected map projection are set.

4 MATERIALS AND METHODS

Depth measurement in practice consists of several steps, among which are the creation of a measurement plan, the calibration of the depth-measuring instrument, the measurement itself, the processing of the collected data, and the creation of the final product. An important element for bathymetric data collection is a measurement plan (Fig. 2). This plan enables monitoring the course of the measurement, as well as the organization of the measurement from start to finish. The measurement plan determines the way of working and the instrumentation that will be used, and thus the expected accuracy that will be achieved. The measurement plan for the Stobreč marina was created concerning the commissioned requests (lines spacing and orientation parallel and perpendicular to shore), in such a way that the measurement lines were placed in a grid covering the area of interest. Such arrangement of measurement lines ensured adequate data density, good distribution, and measurement control.

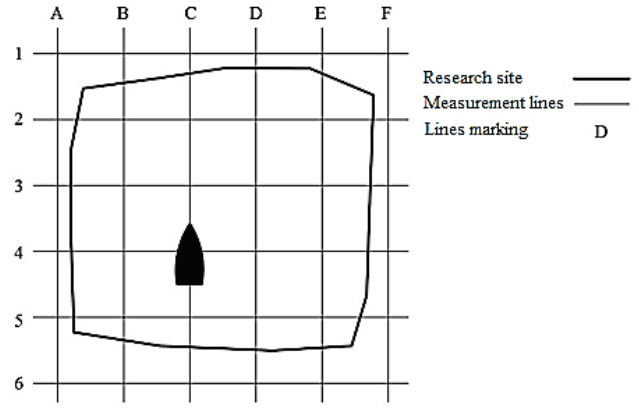

Figure 2 Sketch of the measurement lines placement

Echo sounder calibration is also an important step since different water environments affect the readings produced by the echo sounder differently. During the calibration, the readings are recorded. Based on these readings, in the data processing phase, the measurements are corrected to obtain the final product (e.g. a bathymetric map). While calibrating the echo sounder, care was taken to make the calibration at a place with a flat seabed, near the measurement site. The calibration procedure is as follows: first, an iron plate is lowered directly under the echo sounder to a shallow depth (in this case depth was 12.7 cm). The additional constant of the echo sounder was adjusted until the correct reading of 12.7 cm is obtained. After that, the iron plate was lowered to the average depth expected for the measurement and the sound speed was adjusted until an accurate reading is obtained. The procedure was repeated by returning to the initial shallower calibration depth (change in the reading is possible due to a change in the speed of sound). The additional constant of the echo sounder was set again, and with that new value, echo sounder was descended to the deeper depth, where the speed of sound was adjusted according to the value of the measured depth. Iteratively, by alternately setting the addition constant shallowly below the echo sounder transmitter and the multiplication constant deeper, the procedure was repeated until the observed values were satisfactory for both depths at the same parameters of the echo sounder constants. The vessel was acquired in the area of Stobreč, and the equipment was installed on it. Marine conditions allowed smooth navigation without requiring special adaptation; i.e., the measurements were conducted in a calm wave environment, with no wind or sea currents. The only obstacles were vessels tied up along the coast, and they were relocated upon request.

4.1 Measurement (Data Collection)

Measurements, i.e. data collection, were performed using a combination of the GNSS positioning method and dual-frequency bathymetry. As mentioned earlier, GNSS measurements were conducted using a Stonex S8 plus receiver (RTK DGP). The measurements of both systems are combined in such a way that a position obtained by the satellite positioning method was assigned to each recorded point, whose depth was measured. The GNSS antenna is placed on the mount that is attached to the side of the vessel. The transducer of the echo sounder is placed on the same mount. Since there was an offset between the phase center of the GNSS antenna and the echo sounder transducer, its value was determined on the site when the antenna and transducer were placed on the mount. All recorded measurements were corrected for the value of the mentioned offset.

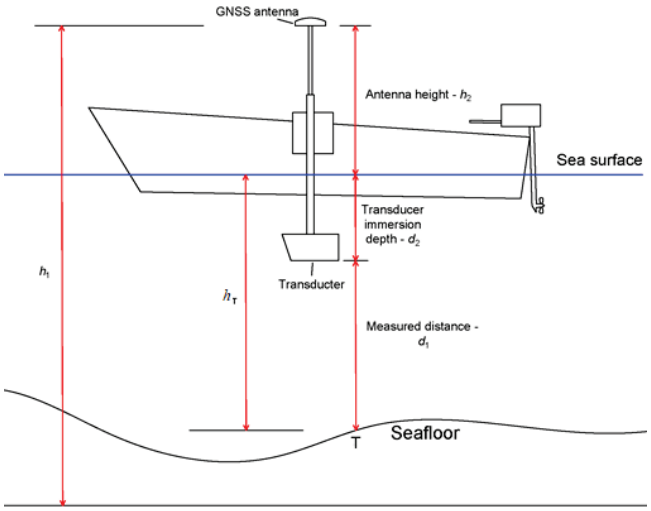

Figure 3 Schematic representation of the method of determining the depth of the recorded point

The area (about 1,5 ha) where the data was collected is on the eastern side of Stobreč, around the breakwater of the marina itself. The measurement process was conducted in such a way that the vessel, on which the GNSS system/echo sounder was installed, sailed along the measurement lines, and at predetermined time intervals (1 second) the horizontal position and depth of the submerged transducer were recorded. After that, the depth obtained by the echo sounder was assigned to each recorded point. Both devices (GNSS

receiver and echo sounder) were connected to a portable computer, which synchronizes the data collected by both instruments with a control software.

The depth of the point was obtained by the following formula (Fig. 3):

$$h_T = h_1 - h_2 - (d_1 + d_2), \quad (1)$$

where: h_1 – ellipsoidal height of the phase center of the GNSS antenna, h_2 – height of the antenna above the water surface, d_1 – depth measured by echo sounder, d_2 – transducer immersion depth.

4.2 Processing of Collected Data (Creation of a 3D Model of the Seabed)

The results of the data collection were the coordinates, i.e. the positions (E, N, h) of each recorded point. First, it was necessary to filter the data to eliminate outliers that would affect the interpolation process and creation of a 3D model of the surveyed seabed. The filtering process was performed visually, where data that deviated grossly from other surrounding values was removed. After filtering, the data was interpolated to obtain a denser, more regular mesh. Subsequently, a 3D model of the recorded seabed was created using Golden Software Surfer 11, with Kriging employed as the interpolation method. As stated by [32], Kriging is a geostatistical interpolation method, which retains the trends expressed in the input values, since it takes them as fixed during the interpolation process. The Kriging method is classified as the best linear unbiased estimator. The processing results are most often displayed in the form of contour lines (isobates) (Fig. 4) and 3D surface models (Fig. 5).

4.3 Accuracy Assessment

To ensure the quality of marine observations, it is necessary to independently validate the data [33]. The focus of the study was to analyze the accuracy of depths determined from data collected by a single-beam echo sounder. To achieve this, depths derived from a 3D model created using data from a single-beam echo sounder were compared with depths determined by another independent and more accurate method. That second (or reference) set of measurements was collected using the tachymetric (polar) method of surveying. The tacheometry is used to determine the relative polar coordinates of detailed points with respect to the instrument station, where the instrument is oriented in a known bearing toward another known point. Based on the collected measurement data (distances, horizontal and vertical angles), the coordinates of detailed points were calculated. Those coordinates are in the same coordinate system in which the control points are defined. The advantage of the polar method is the high accuracy in determining the 3D position of detailed points [34]. Robotic total stations can be used in hydrographic surveying to track and position reflectors mounted on vessels equipped with sonar and other depth-measuring instruments [35].

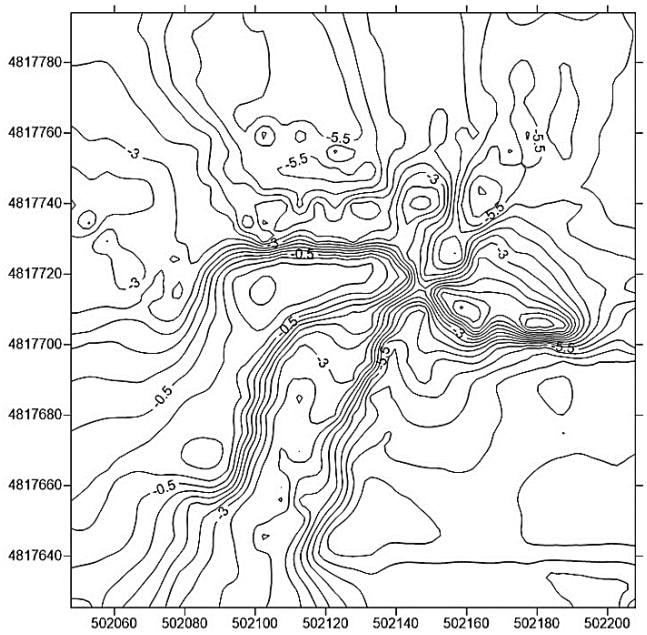

Figure 4 Representation of the seabed with contour lines (cutout)

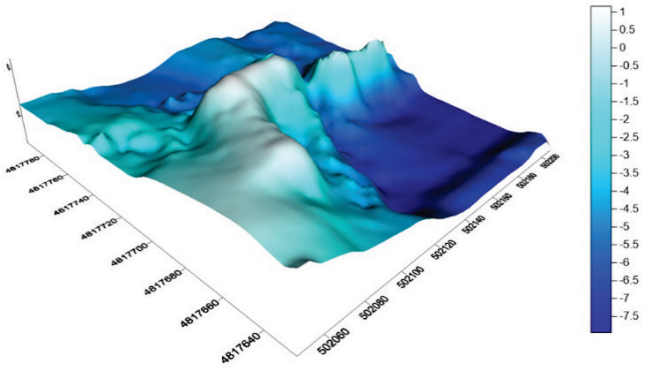

Figure 5 Representation of the seabed with a 3D surface model (cutout)

In this study, polar measurements were carried out using the Leica Geosystems TS06 total station (Fig. 6). The instrument precision according to ISO17123-3 and ISO17123-4 standards is 1 mgon for angle measurement and 1.5 mm; 2 ppm for distance measurement [36]. A custom fishing pole, chosen for its length (more than 4 m), strength, and build quality, was employed for marking the positions of detailed points at greater depths. A retro-reflective sheet was placed on the top of the pole to manually aim the instrument towards the target and for distance measurements. At the end of the pole that enters the water, a plate-shaped iron head was placed. This allowed the pole to take a vertical position, and at the same time prevented it from sinking into the seabed. The reflector mounted on a standard range pole was used in the shallower parts of the test area, and in that case the pole was held by a surveyor standing on the seafloor. In both cases (fishing pole and range pole), the surveyor holding the rod had to take special care in plumbing it, by carefully watching the circular bubble attached to the pole.

Figure 6 .Control measurements from the inside of the breakwater

The result of this type of point positioning is a set of coordinates representing position (E and N) and depth (hP). Based on collected data, coordinates for 50 detailed points were determined in the area of interest in the Stobreč marina. The calculated depths for those 50 detailed points vary from –0.7 to –4.3 m, indicating that a certain part of the test site, that exceeds this depth, was not included in the accuracy evaluation.

The vertical accuracy of detail point determination can be expressed as:

$$s_{\mathrm{h}} = \sqrt{s_{\mathrm{hA}}^2 + s_{\mathrm{s}}^2 \cdot \cos^2 z + s^2 \cdot \left(\frac{s_z^2}{\rho}\right) \cdot \sin^2 z + s_{\mathrm{i}}^2}, \qquad (2)$$

where: s_{hA} – standard deviation of the height of the stand point, z – measured zenith angle, s – measured slope distance, s_{i} – standard deviation of instrument height, s_{s} – standard deviation of slope distance, s_z – standard deviation of zenith angle, ρ - angular conversion coefficient (200 gon/π).

Due to excellent coordination between the surveyor operating the total station and the surveyor holding the rod, aiming errors can be neglected. Taking all factors into account, it can be concluded that the theoretical accuracy of determining the depths of detailed points in the Stobreč marina area is about 3 mm, if the uncertainty of holding the pole in a vertical position is 1° or better. That accuracy significantly exceeds the accuracy of depths determined using an echo sounder and RTK receiver.

The accuracy was evaluated based on the differences between the depths of points measured by tachymetry and corresponding points obtained from a 3D model (hD). The depth differences were compared with the accuracy standards defined in publication S-44 of the International Hydrographic Organization, which defines the required accuracy of hydrographic surveys. It should be noted that the 6th edition of S-44 introduced the quality matrix to provide a tool for broader classification of surveys.

The maximum allowable vertical measurement uncertainty is defined as [11]:

$$TVU_{\max}(d) = \pm\sqrt{a^2 + (b \cdot d)^2}, \qquad (3)$$

where: a – the portion of the uncertainty that does not vary with the depth, b – a coefficient which represents that portion of the uncertainty that varies with the depth, d – the depth.

The parameters a and b to compute the maximum allowable TVU are taken from publication S-44, and in this study, they had values corresponding to the survey Order 1a, i.e. a = 0.5 m and b = 0.013. Since the test area involved shallow depths (they ranged from –0.69 to –7.27 m), it can be determined that $TVU_{\max}(d)$ is 0.50 m.

5 RESULTS AND DISCUSSION

As previously stated, the depths of 50 points obtained by the polar method were compared with the corresponding depths from the 3D model of the seabed, and the differences were calculated: $\Delta h_{\mathrm{PD}} = h_{\mathrm{P}} - h_{\mathrm{D}}$. Statistics of differences in depths are given in Tab. 1.

Table 1 Statistics of differences in depths determined by the polar method and single-beam echo sounder

Indicator		Δh_{PD}
Minimum, m		–0.53
Mean, m		–0.07
Maximum, m		0.22
Range, m		0.75
RMSE, m		0.17
Difference values, %	|0-5 cm|	26.0
	|5-10 cm|	24.0
	|10-15 cm|	14.0
	|15-20 cm|	18.0
	|20-25 cm|	8.0
	> |25 cm|	10.0

In the assessment of the quality of the depths resulting from the application of a single-beam echo sounder, the root mean squared error (*RMSE*) was used as the basic indicator of accuracy:

$$RMSE_{\mathrm{h}} = \sqrt{\frac{1}{n-1}\sum_{i=1}^{n} d\Delta h_{\mathrm{PD}i}^2} = 0.17 \text{ m}. \qquad (4)$$

By analyzing all the points, it was found that the mean difference between the depths determined by the polar method and the 3D model is –7 cm. The maximum negative depth difference is –53 cm, and the maximum positive difference is 22 cm. Even 82% of the differences Δh_{PD} had an absolute value less than 20 cm, and only one difference exceeds the $TVU_{\max}(d)$ value, by only 3 cm.

According to the S-44 standard, the total vertical uncertainty, calculated with a probability of 95%, is determined as $1.96 \cdot RMSE_{\mathrm{h}}$ = 0.33 m. If that value is compared with the maximum allowed vertical uncertainty $TVU_{\max}(d)$, it can be concluded that the 3D model of depths created by data collected with the MIDAS Surveyor echo sounder exceeds the vertical accuracy requirements prescribed by the S-44 standard, for the Order 1a.

The results show that 92% of the points meet the TVU requirements prescribed for the class of special order of accuracy, where the parameters a = 0.25 m and b = 0.0075 are used to calculate $TVU_{\max}(d)$.

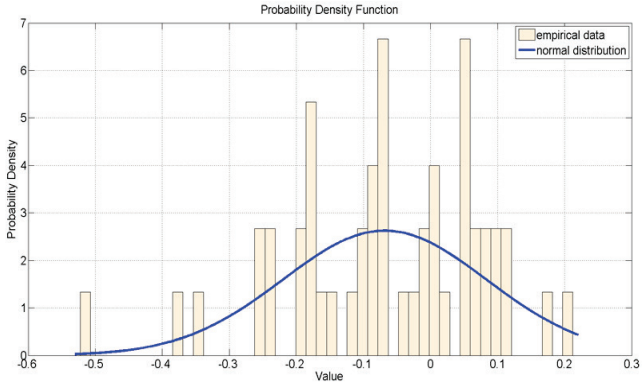

Figure 7 Histogram and difference distribution curve Δh_{PD}

Based on the available data, a histogram of the differences between the theoretical heights of the detailed points and their values obtained from the 3D model was made, as well as the corresponding curve of the standard normal distribution, which best matches the empirical data (Fig. 7). Fig. 7 clearly shows that there is no shift in the arithmetic mean $\overline{dh}$ that would be caused by the presence of significant systematic errors.

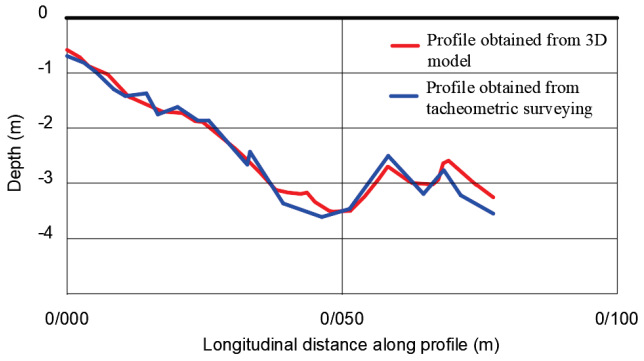

Figure 8 Comparison of two seabed profiles

In addition to a numerical evaluation of the results, visual controls were also performed. They confirmed the previous statements. To conduct a visual control, a longitudinal profile corresponding to the order of recorded points by the total station on the western side of the marina was analyzed. By comparing the profile obtained from measurements by the polar method and the corresponding profile extracted from the 3D model of the seabed, it can be concluded that the basic shape is the same, but that there are expected deviations. These deviations are not uniform, i.e. the deviations range from approx. –35 cm to +20 cm, which is visible in Fig. 8. It is evident that the 3D model produced a smoothed surface, and differences increase with the roughness of the seafloor.

6 CONCLUSION

Determining the depths is the basis for the creation of bathymetric maps, which are later used for various purposes. As different methods provide depths of different accuracy, in today's hectic pace the aim is to collect a sufficient amount of data with appropriate accuracy, in the shortest time possible. Therefore, doubts and questions often arise as to which devices can perform this task with the required accuracy. Single-beam echo sounders, compared to multi-beam ones, are cheaper, easier to operate, and have a solid data acquisition speed. However, that speed is not at the level of multi-beam echo sounders, which on the other hand, cost significantly more and in practice provide more accurate data.

This study aims to investigate the feasibility of using a relatively low-cost echo sounder for collecting accurate water depth data, which is essential for obtaining reliable bottom contour information. The research revealed that a single-beam echo sounder can indeed provide data of satisfactory vertical accuracy (referring to the S-44 rulebook of the International Hydrographic Organization for seabed surveying and mapping, TVU for Order 1a survey). The example of the Stobreč marina demonstrated that 98% of points derived from the 3D model, created from measurements collected with a single-beam echo sounder, met the prescribed vertical accuracy. The study demonstrates that there are no significant systematic errors in the depths measured with sonar. The method of control measurements with a total station gave high-quality results, but to achieve this, it was necessary to fulfill certain prerequisites. The tachymetric measurement was performed in extremely good weather conditions, to reduce the movement of the vessel at sea and thus reduce the error of non-verticality of the pole during observations. Also, good weather allowed taking observations at regular intervals at different depths. In this study, a conventional manually operated total station was used, necessitating precise coordination among the instrument operator, boat driver, and the surveyor holding the pole. It was crucial to quickly make observations, when the pole was in the vertical position. However, if this method is applied in unfavorable marine environmental conditions, with a stronger influence of waves, wind, and sea currents, it would be challenging to maintain the verticality of the pole at all points. The collection of reference data would certainly be much easier with the use of a robotic total station with the ability to automatically find, track, and aim the target. In that case, it would be necessary to mount a 360° reflector on the pole. Finally, by integrating the IMU-based tilt compensation sensor with the surveying pole, measurements can be taken with a pole tilted at any angle.

From an economic perspective, it can be concluded that measurements with a single-beam echo sounder have the full potential to be used for planning and monitoring water construction projects, as well as creating bathymetric maps and charts essential for navigation safety. Of course, S-44 defines more criteria and all of them have to be met. In this manner, it can be concluded that a single-beam echo sounder can be used for the safety of navigation purposes, but only for survey orders 1B and 2 when used as a standalone technique and for much deeper areas where underkeel clearance is not an issue. The accuracy of the bathymetric survey can be increased using a large number of survey lines as well as using the conventional base-rover RTK solution (correction services provided by the active GNSS network CROPOS were used in this study). Furthermore, better results could be achieved by integrating INS sensors within the depth measuring system to determine and reduce the heave, pitch, and roll effects in hydrographic surveying.

Acknowledgement

The authors would like to thank the Ministry of Science, Higher Education, and Youth of Sarajevo Canton (Bosnia and Herzegovina) for their support.

Funding Declaration

All authors certify that they have no affiliations with or involvement in any organization or entity with any financial interest or non-financial interest in the subject matter or materials discussed in this manuscript.

This research received no specific grant from any funding agency in the public, commercial, or not-for-profit sectors.

7 REFERENCES

[1] Kolenc, R. (2005). Hidrografske meritve. *Geodetski vestnik, 49*(1), 18-28. (in Slovenian)

[2] Pribičević, B. (2005). *Pomorska geodezija*. Zagreb: Geodetski fakultet Sveučilišta u Zagrebu. (in Croatian)

[3] de Jong, C., Lachapelle, G., Skone, S. & Elema, I. (2002). *Hydrography*. DUP Blueprint Delfth.

[4] Sandwell, D. T., Smith, W. H., Gille, S., Jayne, S., Soofi, K. & Coakley, B. (2001). *Bathymetry from Space: White paper in support of a high-resolution, ocean altimeter mission*. San Diego: Scripps Institution of Oceanography, accessed 10 January 2023.

[5] Šiljeg, A., Jurišić, M. & Marić, I. (2016). Batimetrijska izmjera jezera Skradinskog buka. *Geodetski list, 70*(3), 231-252. (in Croatian)

[6] Jovanović, B. (1978). Izučavanje metode mjerenja dubina mora, unapređenje obrade dubina i definiranje obalne linije sa hidrografskog, geodetskog i pomorskog gledišta. *Diploma thesis*. Zagreb: Geodetski fakultet Sveučilišta u Zagrebu. (in Croatian)

[7] Đapo, A. & Medved, I. (2003). Trodimenzionalni geodetski model jezera šljunčare Novo Čiče. *Ekscentar, 5*, 13-17. (in Croatian)

[8] Fridl, J., Kolega, N. & Žerjal, A. (2008). Pomen digitalnega batimetričnega modela za trajnostni razvoj morja. *Geodetski vestnik, 52*(4), 854-866. (in Croatian)

[9] Pandian, P., Ruscoe, J., Shields, M., Side, J., Harris, R., Kerr, S. & Bullen, C. (2009). Seabed habitat mapping techniques: an overview of the performance of various systems. *Mediterranean Marine Science, 10*(2), 29-44. https://doi.org/10.12681/mms.107

[10] Šiljeg, A. (2013). Digitalni model reljefa u analizi geomorfometrijskih parametara - primjer PP Vransko jezero. *Diploma thesis*. Zagreb: Prirodoslovno-matematički fakultet, Geografski odsjek. (in Croatian)

[11] International Hydrographic Organization. (2020). *IHO Standards for Hydrographic Surveys* S-44.

[12] Schimel, A. C. G., Healy, T. R., Johnson, D. & Immenga, D., 2010: Quantitative experimental comparison of single-beam, sidescan and multibeam benthic habitat maps. *ICES Journal of Marine Science, 67*(8), 1766-1779. https://doi.org/10.1093/icesjms/fsq102

[13] Savini, A. & Corselli, C. (2010). High-resolution bathymetry and acoustic geophysical data from Santa Maria di Leuca Cold Water Coral province (Northern Ionian Sea - Apulian continental slope). *Deep Sea Research Part II: Topical Studies in Oceanography, 57*(5-6), 326-344. https://doi.org/10.1016/j.dsr2.2009.08.014

[14] Graham, A. G. C., Nitsche, F. O. & Larter, R. D. (2011). An improved bathymetry compilation for the Bellingshausen Sea, Antarctica, to inform ice-sheet and ocean models. *The Cryosphere, 5*, 95-106. https://doi.org/10.5194/tc-5-95-2011

[15] Falcão, A. P., Matias, M., Pestana, R., Gonçalves, A. B. & Heleno, S. (2016). Methodology to combine topography and bathymetry data sets for hydrodynamic simulations: Case of Tagus River. *Journal of Surveying Engineering, 142*(4), 05016005. https://doi.org/10.1061/(ASCE)SU.1943-5428.0000192

[16] Dorokhov, D., Dudkov, I. & Sivkov, V. (2019). Single beam echo-sounding dataset and digital elevation model of the southeastern part of the Baltic Sea. *Data in Brief, 25*, 104123. https://doi.org/10.1016/j.dib.2019.104123

[17] Bio, A., Gonçalves, J. A., Magalhães, A., Pinheiro, J. & Bastos, L. (2022). Combining Low-Cost Sonar and High-Precision Global Navigation Satellite System for Shallow Water Bathymetry. *Estuaries and Coasts, 45*, 1000-1011. https://doi.org/10.1007/s12237-020-00703-6

[18] Muchowski, J., Umlauf, L., Arneborg, L., Holtermann, P., Weidner, E., Humborg, C. & Stranne, C. (2022). Potential and Limitations of a Commercial Broadband Echo Sounder for Remote Observations of Turbulent Mixing. *Journal of Atmospheric and Oceanic Technology, 39*(12), 1985-2003. https://doi.org/10.1175/JTECH-D-21-0169.1

[19] Brenner, S., Thomson, J., Rainville, L., Torres, D., Doble, M., Wilkinson, J. & Lee, C. (2023). Acoustic Sensing of Ocean Mixed Layer Depth and Temperature from Uplooking ADCPs. *Journal of Atmospheric and Oceanic Technology, 40*(1), 53-64. https://doi.org/10.1175/JTECH-D-22-0055.1

[20] Passaro, S., de Alteriis, G. & Sacchi, M. (2015). Bathymetry of Ischia Island and its offshore (Italy). *Journal of Maps, 12*(1), 152-159. https://doi.org/10.1080/17445647.2014.998302

[21] Arseni, M., Rosu, A., Iticescu, C., Georgescu, L. P., Timofti, M., Pintilie, V., Calmuc, M. & Roman, O. (2018). A review of bathymetric measurements from August 2018 campaign on the lower course of the Danube. *Annals of "Dunarea de Jos" University of Galati - Fascicle II, 41*(2), 212-219. https://doi.org/10.35219/ann-ugal-math-phys-mec.2018.2.14

[22] Moknatian, M., Piasecki, M., Moshary, F. & Gonzalez, J. (2019). Development of digital bathymetry maps for Lakes Azuei and Enriquillo using sonar and remote sensing techniques. *Transactions in GIS, 23*(4), 841-859. https://doi.org/10.1111/tgis.12532

[23] Trincardi, F., Campiani, E., Correggiari, A., Foglini, F., Maselli, V. & Remia, A. (2014). Bathymetry of the Adriatic Sea: The legacy of the last eustatic cycle and the impact of modern sediment dispersal. *Journal of Maps, 10*(1), 151-158. https://doi.org/10.1080/17445647.2013.864844

[24] Kearns, A. & Breman, J. (2010). Bathymetry - The art and science of seafloor modeling for modern applications. *Ocean Globe, J. Berman, Ed., ESRI Press Redlands*, 1-36.

[25] Hodges, B. A., Grare, L., Greenwood, B., Matsoyoshi, K., Pizzo, N., Statom, N. M., Farrar, J. T. & Lenain, L. (2023). Evaluation of Ocean Currents Observed from Autonomous Surface Vehicles. *Journal of Atmospheric and Oceanic Technology, 40*(10), 1121-1136. https://doi.org/10.1175/JTECH-D-23-0066.1

[26] Zeiden, K., Thomson, J. & Girton, J. (2023). Estimating Profiles of Dissipation Rate in the Upper Ocean Using Acoustic Doppler Measurements Made from Surface-Following Platforms. *Journal of Atmospheric and Ocean Technology, 40*(12), 1571-1589. https://doi.org/10.1175/JTECH-D-23-0027.1

[27] Fridl, J., Kolega, N. & Žerjal, A., 2009: Primjena mjerenja morskoga dna preciznim dubinomjerima. *Kartografija i geoinformacije, 8*(11), 15-25. (in Croatian)
[28] Letessier, T. B., Hosegood, P. J., Nimmo-Smith, A., Fernandes, M. C., Proud, R., Turner, J., Carr, P., Schaellert, R., Froman, N., Belamy, Z., Addison, S. & Brierley, A. S. (2016). Chagos Archipelago Pelagic Expedition, February 5–24, 2016. *Scientific Report to The Bertarelli Foundation and the Foreign and Commonwealth Office*, accessed 28 January 2023.
[29] Šiljeg, A., Cavrić, B., Marić, I. & Barada, M. (2019). GIS modeling of bathymetric data in the construction of port terminals – An example of Vlaška channel in the Port of Ploče, Croatia. *International Journal for Engineering Modelling, 32*(1), 17-37. https://doi.org/10.31534/engmod.2019.1.ri.01m
[30] Valeport. (2020). *MIDAS Surveyor - Echo Sounder Data Sheet*, accessed 12 January 2023.
[31] Stonex. (2020). *S8 Plus Data Sheet – Stonex*, accessed 11 January 2023.
[32] Medved, I., Pribičević, B., Medak, D. & Kuzmanić, I. (2010). Usporedba metoda interpolacije batimetrijskih mjerenja za praćenje promjena volumena jezera. *Geodetski list, 64*(2), 71-86. (in Croatian)
[33] Hay, A., Watson, C., Legresy, B., King, M. & Beardsley, J. (2023). In Situ Validation of Altimetry and CFOSAT SWIM Measurements in a High Wave Environment. *Journal of Atmospheric and Oceanic Technology, 40*(10), 1137-1152. https://doi.org/10.1175/JTECH-D-23-0031.1
[34] Baykal, O., Tari, E., Coşkun, M. & Erden, T. (2005). Accuracy of Point Layout with Polar Coordinates. *Journal of Surveying Engineering, 131*(3), 87-93. https://doi.org/10.1061/(ASCE)0733-9453(2005)131:3(87)
[35] Tuno, N., Mulahusić, A., Savšek, S. & Kogoj, D. (2019). Pet generacij integriranih elektronskih tahimetrov. *Geodetski vestnik, 63*(1), 41.56. (in Slovenian). https://doi.org/10.15292/geodetski-vestnik.2019.01.41-56
[36] Tuno, N., Mulahusić, A., Marjetič, A. & Kogoj, D. (2010). Pregled razvoja elektronskih tahimetrov Leica geosystems. *Geodetski vestnik, 54*(4), 643-660. (in Slovenian). https://doi.org/10.15292/geodetski-vestnik.2010.04.643-660

Authors' contacts:

Nedim Tuno, Associate Professor dr.
(Corresponding author)
Department of Geodesy and Geoinformatics,
Faculty of Civil Engineering, University of Sarajevo,
Patriotske lige 30, 71000 Sarajevo,
Bosnia and Herzegovina
E-mail: nedim_tuno@gf.unsa.ba

Nedim Kulo, MA geod. et geoinf., Senior teaching assistant and PhD student
Department of Geodesy and Geoinformatics,
Faculty of Civil Engineering, University of Sarajevo,
Patriotske lige 30, 71000 Sarajevo,
Bosnia and Herzegovina
E-mail: nedim.kulo@gf.unsa.ba

Dean Perić, MA geod. et geoinf., Surveyor
Van Oord, Rotterdam, South Holland,
Netherlands
E-mail: dean.peric@hotmail.com

Muamer Đidelija, MA geod. et geoinf., Senior teaching assistant and PhD student
Department of Geodesy and Geoinformatics,
Faculty of Civil Engineering, University of Sarajevo,
Patriotske lige 30, 71000 Sarajevo,
Bosnia and Herzegovina
E-mail: muamer_djidelija@hotmail.com

Adis Hamzić, Assistant Professor dr.
Department of Geodesy and Geoinformatics,
Faculty of Civil Engineering, University of Sarajevo,
Patriotske lige 30, 71000 Sarajevo,
Bosnia and Herzegovina
E-mail: hamzicadis87@gmail.com

Jusuf Topoljak, Associate Professor dr.
Department of Geodesy and Geoinformatics,
Faculty of Civil Engineering, University of Sarajevo,
Patriotske lige 30, 71000 Sarajevo,
Bosnia and Herzegovina
E-mail: jusuf.topoljak@gf.unsa.ba

Admir Mulahusić, Full Professor dr.
Department of Geodesy and Geoinformatics,
Faculty of Civil Engineering, University of Sarajevo,
Patriotske lige 30, 71000 Sarajevo,
Bosnia and Herzegovina
E-mail: admir_mulahusic@gf.unsa.ba

Dušan Kogoj, Associate Professor dr.
Department of Geodetic Engineering,
Faculty of Civil and Geodetic Engineering,
University of Ljubljana,
Jamova cesta 2, 1000 Ljubljana, Slovenia
E-mail: dusan.kogoj@fgg.uni-lj.si

ISSN 1846-6168 (Print), ISSN 1848-5588 (Online)
https://doi.org/10.31803/tg-20230508125238

Preliminary communication
Received: 2023-05-08, Accepted: 2024-10-25

Reliability Index for Steel Structure's Technical State and Residual Life Assessment

Sergiy Kolesnichenko*, Inna Chernykh, Valentyna Halushko, Polianskyi Kostiantyn

Abstract: The article is dedicated to problem of technical state assessment of real steel truss under operation for residual life prediction after technical investigation. The reliability index is calculated based on design, real and prospective loads. Method of statistical data analysis adopted for stress-strain determination also for all kinds of applied loads. The residual life with the reliability index determined as a transition from satisfactory to emergency technical state. The method provides the possibility for estimation of future safety steel structures operation with technical investigation results only that exclude any subjective opinion.

Keywords: reliability index; residual life; steel truss; technical state

1 INTRODUCTION

During designing of structures, the steel structures include, must be provided the safety operating control during all service life. The safety is guaranteed by the conditions that the limit states will not be reached – the loads on structure and appropriate stresses in elements must have sufficient level of reliability. This main demand contains all designing standards [1, 2].

The safety operation indicators which determined on the results of technical investigations are both: the technical state and residual life - the guaranteed post-investigated operational life. So, the main task of technical investigation is the appointment of these indicators. During the structure's life, the existing degradation processes (corrosion, fatigue and materials conditions) together with loads changing (often increased during operation) may lead to decreasing of reliability. The values of these indicators, determined by the comparison of designing and real technical parameters for structure, could be defined only based on the results of technical investigation.

As a basis for reliability determination, all statistical information that describing structure's life during service, must be considered. But the lack of this information is a reason of restriction for wide application of reliability methods. The way to get statistical information is to carry out the regular technical investigation of existing structures. In this case may be solved a few tasks:

- to establish really structural and cross-sectional dimensions;
- to analyze all possible deterioration processes for elements (corrosion, fatigue);
- to fix changing of loads and for materials;
- to estimate a technical state for each separate structure and building in general;
- to assess a residual life for structures.

If the first three tasks may be solved sufficiently easy, the definition of technical state and residual life mostly assess subjectively and depends on expert experience. Usually during estimation any statistical data do not consider.

In this paper we tried to show the way for the investigators how to prepare the objective assessment of technical state for structure and how to calculate the residual life for it with the strong procedure of reliability calculation if some results of technical investigation exist.

2 LITERATURE REVIEW, RELATED WORKS AND INVESTIGATION CONCEPTS

In modern standards [1, 3, 4] the safety of building structures is proposed to calculate with the common reliability parameter called as "reliability index" β which reflects the possibility of structure's failure depends on actions, cross-section and resistance of materials probabilistic nature [5, 6]. This parameter was proposed by Cornell C. A. [7, 8].

The designing of new structures, also as estimation of safety for operating structures, should be executed depends on consequence class – CC. There are three CC exists [1]: CC1 (low consequence), CC2 (medium consequence) and CC3 (high consequence).

The different values of β proposed for every CC [4, 8, 9, 10], but all these values based on the same approaches and principles: it depends either possibility of human life losses, economic losses, social and environmental consequences and all of these related to the number of structure operated years which corresponds to possibility of structure failure.

In general, the β defined as:

$$\beta = \frac{\overline{S}}{\sigma(S)} = \frac{\overline{R} - \overline{F}}{\sqrt{\sigma^2(R) + \sigma^2(R)}}, \tag{1}$$

$$\overline{S} = \overline{R} - \overline{F}, \tag{2}$$

$$\sigma(S) = \sqrt{\sigma^2(R) + \sigma^2(R)}. \tag{3}$$

In the Eqs. (1)-(3): $\overline{R}$ – mean value of resistance or bearing capacity of the element (structure) – generalized durability of element (structure); $\overline{F}$ - mean value of action effect on element (structure); $\overline{S}$ – reserve of strength for all laws of distribution of R and F; $\sigma^2(R)$ and $\sigma^2(F)$ – resistance capacity and action effect respectively.

Reliability index also can be determined as:

$$\beta = \frac{1}{V(S)}, \tag{4}$$

where $V(S)$ – variation coefficient of random strength reserve variable.

Also, in some scientific research [10, 12, 13, 14], the values of reliability index β proposed for different technical conditions of building structures. There are three levels of it: new, repair and unfit to use. Also proposed so-called "reliability classes – RC" or consequences of failure: insignificant, normal and large. In fact, these conditions, classes or consequences of failure may be accepted as technical states when exists necessity of technical conditions definition for operated structures during investigation procedure.

After the technical state determination, the task of residual life calculation for the structure also is very significant. We suggest that the residual life is an estimation of the remaining useful service of an element or structure (building) considering of its present condition and future functioning (the element or structure will next require reconstruction, rehabilitation, restoration, renewal or replacement) [15, 16]. With accordance of this suggestion, it is possible to connect the technical states and residual life, when the residual life is a time that defines as a transition from one technical state to another, for example from state that need of repair to the emergency state.

After calculation of β for more stressed structure's elements, the general β for all structure should be determined where the types of elements connection (series, parallel or mutual) examined. Now do not exist of correct rules for it, some examination formulae proposed in [6, 17]. For normal statically determined structures recommended [5, 18] to calculate it as for serial elements connection.

3 DETERMINATION OF STRUCTURE'S TECHNICAL STATE BASED ON TECHNICAL INVESTIGATION

Two main tasks must be solved for the building structures under operation when the reliability index β is applied:

- the β must be accepted with such its values, that building structure could not be possible for future operation if these values are lower than determine for every consequence class CC;
- the β levels must be determined for possible fulfillment of repairing works – reconstruction or repairing works.

The Tab. 1 contains the maximum values of reliability index β for different technical states - new structures, structures which need to be repaired and for structures in emergency state. The values, given in the Tab. 1 taken as more appropriate for industrial steel structure from the [9] based on recommendations [3, 19].

Table 1 Maximum values of β depends of CC and types of structure's technical states

Consequence class - CC	β (new structures)	β (needs to repair state)	β (emergency state)
CC1	3,3	2,8	1,8
CC2	3,8	3,3	2,3
CC3	4,3	3,8	2,8

There was a task to determine the technical state for steel roof trusses which are situated in industrial machine making building. The state must be determined based on technical complex investigation with theoretical value of β.

The framework of the industrial building consists with steel columns and trusses with the span of 18 meters and 6 meters of columns bay spacing. Consequence class of the building – CC2.

General view of industrial building and trusses with defects and damages are shown on the Fig. 1.

There was analysis of actions with normative values of loads on 1966 year of construction have done. The structures were investigated in 1988, 2011 and 2021 years. On the moment of last investigation, the building was under operation 55 years with the designing life of $T_0 = 60$ years.

1) Based on the results of technical investigation fulfilled in 2021 year, there were the measuring drawings have prepared with all necessary cross-sectional values with real parameters (influence of corrosion, differences with standard values). The design drawings were absent.
2) Non-destructive method was used for determination of real steel resistance R_y (MPa) with future calculation of variation coefficient VR_y.
3) The calculation of structure on following actions (loadings) have done - see Tab. 2 (column - number of loadings):

- Project (q_1), ideal parameters: dead loads + roof load + snow – parameters taken on building standards on the year of designing.
- Investigation 1 (q_2): dead loads + roof load + snow – parameters taken on building standards on the year of investigation in 22 years. Corrosion deterioration is absent.
- Investigation 2 (q_3): dead loads + roof load + snow – parameters taken on building standards on the year of investigation in 45 years. Corrosion deterioration of upper chord elements close to 15%.
- Investigation 3 (q_4) – the real actions 4 after 55 years of operation, with defects and damages – corrosion damages: dead load + roof load + snow load (values in the current building standards). Corrosion damages for upper chord elements – 30%, bearing elements – 15%, other elements – up to 5%.
- Predictive (q_5), the corrosion process continuation in time up to 45%: dead loads + roof load + snow load (values in the current building standards), operating period – 60 years.

4) For probabilistic calculation additionally have defined (Tab. 3):

- the geometrical dimensions of areas, including corrosion damages for mean, minimum and maximum values: $\overline{A}$, $A_{\min}$, $A_{\max}$;
- designing loads of all standards demands on the day of design - N_d;
- designing loads of modern standards on the day of technical investigation - $\overline{N}$;
- loads of modern standards on the day of technical investigation but only with characteristic (normative)

values, where all reliability coefficients with designing values are equal of $1 - N_n$;

- there were nine values of stresses have been calculated for each loading with combination of N and A: $s_1 = f(N_d; A_{min})$; $s_2 = f(N_d; \overline{A})$; $s_3 = f(N_d; A_{max})$; $s_4 = f(\overline{N}; A_{min})$; $s_5 = f(\overline{N}; \overline{A})$; $s_6 = f(\overline{N}; A_{max})$; $s_7 = f(N_n; A_{min})$; $s_8 = f(N_n; \overline{A})$; $s_9 = f(N_n; A_{max})$. During calculation the real geometrical characteristics for area A were taken, were calculated the mean values of actions $s_{mv} = \overline{F}$ and variation coefficients $V \cdot \overline{F}$.

5) The mean value for steel resistance have accepted as: $R_y = \overline{R}$ (MPa) and variation coefficient $V \cdot R_y = V \cdot \overline{R}$.

6) For each truss elements were calculated the values of $\xi = \overline{R}/\overline{F}$ and β. For each β value was defined values of P_f and P_s.

General view of industrial building

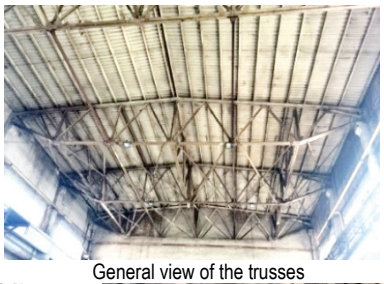

General view of the trusses

Curvature of the truss's elements

Roof flowing with intensive corrosion damages of trusses elements

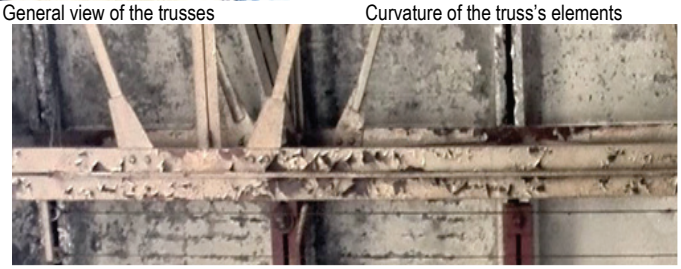

25-30% corrosion of trusses elements cross-section

Figure 1 General view of industrial building and trusses with defects and damages

Table 2 Calculation of stresses in the truss elements

Element	Number of loadings	Internal forces, N, (kN)	Length, l, (mm)	Cross-section profile	Area, A (см^2)	Stresses, σ (MPa)	Yield strength f_y, (MPa)
Upper chord element	q_1 (project)	–288.7	1510	2L90×8	27,92	123,1	205
	q_2 (22 years)	–322		2L90×8	27,92	137,3	215
	q_3 (45 years)	–340		2L90×8 (–15%)	23,7	165,0	
	q_4 (55 years)	–345.4		2L90×8 (–30%)	19,54	200,8	
	q_5 (60 years)	–349.9		2L90×8 (–45%)	13,4	**274,8**	
Lower chord element	q_1	294.5	3000	2L75x6	17,56	167,7	205
	q_2	328.4			17,56	187,0	223
	q_3	346.8			17,56	197,5	
	q_4	352.3		2L75×6 (–5%)	16,68	211,2	
	q_5	356.9		2L75×6 (–10%)	15,8	**225,8**	
Bearing element	q_1	–212.6	2690	2L90×8	27,92	124,9	205
	q_2	–237.5			27,92	139,4	215
	q_3	–250.7			27,92	147,2	
	q_4	–254.7		2L90×8 (–15%)	23,7	161,6	
	q_5	–258		2L90×8 (–25%)	20,94	178,56	
Inclined element (+)	q_1	148.8	2690	2L60×6	13,82	107,7	205
	q_2	165.4			13,82	119,7	209
	q_3	175.2			13,82	126,8	
	q_4	177.9		2L60×6 (–5%)	13,1	135,8	
	q_5	180.2		2L60×6 (–10%)	12,44	144,9	
Inclined element (–)	q_1	–105.7	2950	2L75×6	17,56	146,8	205
	q_2	–117.9			17,56	163,8	223
	q_3	–124.5			17,56	172,9	
	q_4	–126.5		2L75×6 (–5%)	16,68	177,2	
	q_5	–128.1		2L75×6 (–10%)	15,8	176,3	
vertical element (–)	q_1	–31.7	2700	2L60×6	13,82	69,5	205
	q_2	–36.4			13,82	79,8	209
	q_3	–37.4			13,82	82	
	q_4	–38		2L60×6 (–5%)	13,13	83,9	
	q_5	–38.6		2L60×6 (–10%)	12,44	79,36	

Table 3 Results for reliability index calculations for truss elements

Element	Number of loadings	Mean $s_{mv} = \overline{F}$ (MPa)	Dispersion	Deviation	$V\overline{F}$	$\overline{R}$	$V\overline{R}$	$\xi = \overline{R}/\overline{F}$	β	P_f	Ps
Upper chord (–)	q_1 (project)	118,20	43,60	6,60	0,06	205	0,024	1,73	10,54	≈0	≈1
	q_2 (22 years)	127,12	52,50	7,25	0,057	215	0,024	1,69	9,88	≈0	≈1
	q_3 (45 years)	137,54	236,39	15,37	0,11	215	0,024	1,56	4,78	≈0	≈1
	q_4 (55 years)	151,59	964,31	31,05	0,20	215	0,024	1,42	2,01	0,0222	0,9778
	q_5 (60 years)	172,19	3169,37	56,30	0,327	215	0,024	1,25	0,76	0,2265	0,7735
Lower chord (+)	q_1	162,91	67,26	8,20	0,050	205	0,025	1,26	4,35	≈0	≈1
	q_2	175,22	92,24	9,60	0,0548	223	0,025	1,27	4,30	≈0	≈1
	q_3	182,15	176,63	13,29	0,073	223	0,025	1,22	2,83	0,0023	0,9977
	q_4	186,52	241,04	15,53	0,083	223	0,025	1,20	2,21	0,0135	0,9865
	q_5	193,02	381,57	19,53	0,101	223	0,025	1,16	1,48	0,0706	0,9294
Bearing element (–)	q_1	119,96	63,98	8,00	0,066	205	0,024	1,71	9,06	≈0	≈1
	q_2	129,12	69,49	8,34	0,064	215	0,024	1,67	8,76	≈0	≈1
	q_3	133,98	111,26	10,55	0,078	215	0,024	1,60	6,90	≈0	≈1
	q_4	132,83	241,32	15,53	0,116	215	0,024	1,62	5,02	≈0	≈1
	q_5	137,41	563,86	23,75	0,172	215	0,024	1,56	3,19	≈0	≈1
Inclined element (+)	q_1	105,23	19,43	4,41	0,042	205	0,025	1,95	14,76	≈0	≈1
	q_2	112,96	32,52	5,70	0,050	209	0,021	1,85	13,35	≈0	≈1
	q_3	117,52	71,94	8,48	0,072	209	0,021	1,78	9,58	≈0	≈1
	q_4	120,57	100,82	10,04	0,083	209	0,021	1,73	8,07	≈0	≈1
	q_5	124,63	160,57	12,67	0,102	209	0,021	1,68	6,29	≈0	≈1
Inclined element (–)	q_1	143,02	43,58	6,60	0,046	205	0,025	1,43	7,42	≈0	≈1
	q_2	153,86	66,90	8,18	0,053	223	0,025	1,45	6,98	≈0	≈1
	q_3	159,73	135,02	11,62	0,072	223	0,025	1,40	4,91	≈0	≈1
	q_4	156,93	170,80	13,07	0,083	223	0,025	1,42	4,65	≈0	≈1
	q_5	151,07	235,67	15,35	0,102	223	0,025	1,48	4,40	≈0	≈1
vertical element (–)	q_1	68,13	6,61	2,57	0,037	205	0,025	3,01	23,87	≈0	≈1
	q_2	74,79	21,31	4,62	0,062	209	0,021	2,79	21,07	≈0	≈1
	q_3	76,21	30,89	5,56	0,073	209	0,021	2,74	18,75	≈0	≈1
	q_4	74,75	39,71	6,30	0,084	209	0,021	2,80	17,48	≈0	≈1
	q_5	68,38	51,16	7,15	0,104	209	0,021	3,06	16,76	≈0	≈1

7) Because of truss designed as statically determined structure, the serial type of its members connections have accepted. The calculation of general β for every loading defined with formulae [5, 18] for $P_s(q)$ as:

$$P_s(q) = \prod_{i=1}^{n} \left[1 - P_{fi}(q)\right]. \quad (5)$$

where $P_{fi}(q)$ – failure probability for i element (Tab. 4).

The β for probabilistic calculation provides the results that are not the same as for discrete ones, determined for structure as static determine system - see Table 2 and Table 3. As an example, based on discrete structure calculation, the result of fourth loading with maximum stress values σ = 211,2 MPa, do not exceed the real steel yield strength f_y = 223 MPa, but reliability index here is β = 1,805, what is lower, than proposed level for emergency technical state 3, which is 2.8 (Tab. 1 and Tab. 4). Also, already for loading 3, the reliability index β = 2,83, that responds of "needs to repair state" $\beta \in$[2,3 - 3,8] and coincide with the results of investigation - the corrosion damages are bigger than 15%, but comparing with static discrete results calculation, this technical state may be defined almost as for a new structure, which needs not the repairing works.

These results came to illusion for the building's proprietor who ordered the technical investigation that renovation works for the building are not necessary for this time and residual life should not be determined for this case.

Table 4 Results of calculation for truss as a system

Year, loadings	Operation time	P_s	β
1966 – q_1	0	≈1	4,3
1988 – q_2	22	≈1	4,3
2011 – q_3	45	0,9977	2,83
2021 – q_4	55	0,9646	1,805
2026 – q_5	60	0,72	0,585

4 DETERMINATION OF RESIDUAL LIFE

Based on reliability index determination, the definition of residual life for analyzed structure (CC2) may be proposed with the following recommendations.

1) The analysis of function β calculated on the results of technical investigations (Fig. 2) shows that residual life could not exceed 4 years maximum and must be appointed even after third investigation (45 years of operation) for prevention of transition to the emergency state (3 state). It had not done because of results of static calculations answered for demands of safe operation. So, any repairing works were not fulfilled.
2) After 55 years of operation some repairing works were completed and a new value of β = 3.8 have done. Here, we consider that steel structures may be partially renewed [20] and a new value of β may be defined. This value is equal as for a new structure for CC2. To set a

value β = 4.3 is not correct, because of only the most damaged elements of the truss were reinforced and some old elements have insignificant degradation corrosion process.

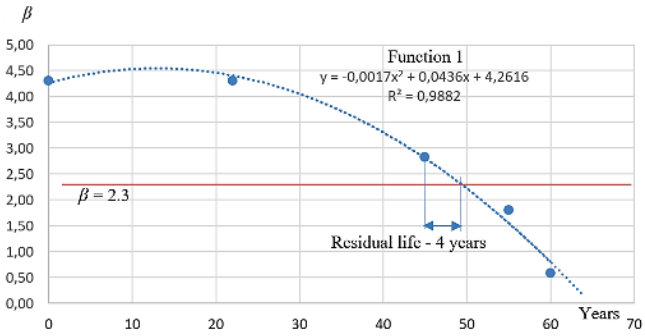

Figure 2 The values of β calculated on the results of technical investigations

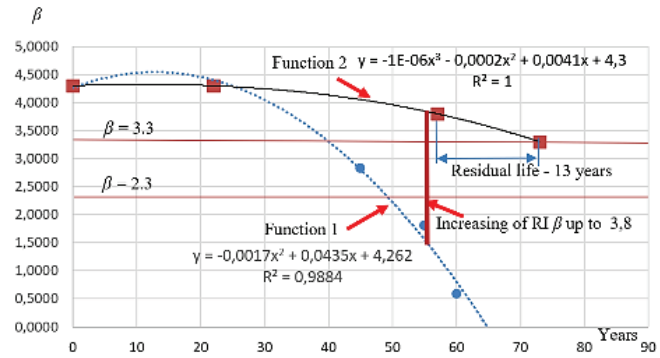

Figure 3 The calculation results for RI β and residual life for roof trusses of the industrial building

3) A new function for β has defined – the function 2, see Fig. 3. As the points of definition for the function were: point 1 – as for a new structure (0 years of operation) and point 2 – the results of β calculation after first investigation (22 years of operation). There were the values that are bigger than current β value after repairing works. The last point for function is the point with the current values of β = 3.8 (55 years of operation).
4) Then, the residual life may be defined in 13 years – the time for future compulsory technical investigation, when the technical state will come from the state as for a new structure to the state which needs the repair with β = 3.3. After that the technical investigation should be completed, the corresponding value of β will determine as new point for the function 2. This function will be corrected for the future calculation of residual life.

5 CONCLUSIONS

Based on demands of modern standards and scientific research, with the example of calculation of real steel structure, proposed the following:

1) Algorithm of reliability index β assessment taking in consideration of technical investigation results during a long term of structure's operation.
2) The assessment provided the possibility for technical state of structure determination in probabilistic kind.
3) The determination of residual life as transition from one to another technical state with fixed values of reliability index β could be possible for analyzed structure.

Also, this method may be applicated for other types of steel structures, especially for those, which are under potential corrosion influences and dynamic loadings – bridges, crane beams, bunkers, reservoirs, pipelines. All these structures potentially dangerous on corrosion and fatigue, needs to be regular technical investigated with prediction of real residual life and terms of repairing works.

6 REFERENCES

[1] Eurocode 0: ENV 1990:2002+A1. *Basic of structural design*. CEN, Brussels, 2002. 116.
[2] Eurocode 3: ENV 1993-1-1, Part 1.1. *Design of steel structures*. CEN, Brussels, 2005.
[3] ISO 13822:2010. *Bases for design of structures – Assessment of existing structures*. ISO 2010. 44.
[4] ISO 2394:2015. *International standard. General principles on reliability for structures*. ISO 2015. 112.
[5] Rosowsky, D. V. (1999). Structural Reliability. *Structural engineering handbook*. Ed. Chen Wai-Fah. Boca Raton: CRC Press LLC.
[6] Yumei, K. & Xue, D. (2019,). Failure mode and reliability analysis of frame structure. *13th International conference on applications of statistics and probability in civil engineering, ICASP13*. May 26-30, Seoul, South Korea, 1-8.
[7] Cornell C. A. (1969). A Probability based structural code. *ACI-Journal, 66*(12), 974-985.
[8] Cornell C. A. (1969). Stochastic process models in structural engineering. Dept. of Civil Engineering. Stanford University. *Technical Report No. 34*, 14-18.
[9] Steenbergen, R. D. J. M., Rózsás, Á. & Vrouwenvelder, A. C. W. M. (2018). Target reliability of new and existing structures - A general framework for code making. *HERON, 63*(3), 219-242.
[10] Diamantidis, D. & Sykora, M. (2019, October 17). Reliability differentiation and uniform risk in standards: a critical review and a practical appraisal. *Scientific symposium future trends in civil engineering*. Zagreb, Croatia, 241-260. https://doi.org/10.5592/CO/FTCE.2019.11
[11] Rackwitz, R. (2000). Optimization – the basis of code-making and reliability verification. *Structural Safety, 22*, 27-60.
[12] Steenbergen, R. D. J. M. & Vrouwenvelder, A. C. W. M. (2010). Safety philosophy for existing structures and partial factors for traffic loads on bridges. *HERON, 55*(2), 123-140.
[13] Van Coilea, R., Hopkinc, D., Bisbyb, L. & Caspeelea, R. (2017). The meaning of eta: background and applicability of the target reliability index for normal conditions to structural fire engineering. *Procedia Engineering, 210*, 528-536.
[14] Diamantidis, D., Holicky, M. & Sykora, M. (2016). Risk and reliability acceptance criteria for civil engineering structures. *Conference Structural Reliability and Modelling in Mechanics*. Ostrava, Czech Republic.
[15] Hovde, P. J. & Moser, K. (2004). Performance Based Methods for Service Life Prediction. CIBPublication, 294, Rotterdam: International Council for Building Research, *Studies and Documentation*, pp. 107, (ISBN 90-6363-040-9).

[16] Omoare, A., Arum, C. & Olanitori, L. (2022). Models for the Prediction of Service Life of Buildings - A Review. *LAUTECH Journal of Civil and Environmental Studies, 9*(1), 48. https://doi.org/10.36108/laujoces/2202.90.0160
[17] Beck, A. T. (2020). Optimal design of redundant structural systems: fundamentals. *Engineering Structures, 219*, 110542. https://doi.org/10.1016/j.engstruct.2020.110542
[18] Hawraa Qasim Jebur & Salah Rohaima Al-Zaidee. (2019). Non-deterministic approach for reliability evaluation of steel portal frame. *Civil Engineering Journal, 5*(8), 1684-1697. https://doi.org/10.28991/cej-2019-03091363
[19] Holicky, M., Diamantidis, D. & Sykora, M. (2015). Determination of target safety for structures. *12th International conference on application of statistics and probability in civil engineering, ICASP12*. Vancouver, Canada. 1-9.
[20] Kolesnichenko, S., Selyutin, Y., Chernykh, I. & Mnatsakanian, K. (2017). General principles of steel structures risk operation estimation and assessment of their residual life (in Ukrainian). *ScienceRise, 11*(40), 37-42. https://doi.org/10.15587/2313-8416.2017.116444

Authors' contacts:

Sergiy Kolesnichenko, DSc, PhD, Assoc. Prof
(Corresponding author)
Donbas National Academy of Civil Engineering and Architecture,
Faculty of Civil Engineering,
Heroiv Nebesnoi Sotni str., 14, Kramatorsk, Donetsk reg., Ukraine 84333
ksv@donnaba.edu.ua

Inna Chernykh, PhD, Assoc. Prof
Donbas National Academy of Civil Engineering and Architecture,
Faculty of Civil Engineering,
Heroiv Nebesnoi Sotni str., 14, Kramatorsk, Donetsk reg., Ukraine 84333
I.Y.Chernykh@donnaba.edu.ua

Valentyna Halushko, DSc, PhD, Assoc. Prof
Donbas National Academy of Civil Engineering and Architecture,
Faculty of Civil Engineering,
Heroiv Nebesnoi Sotni str., 14, Kramatorsk, Donetsk reg., Ukraine 84333
v.o.halushko@donnaba.edu.ua

Polianskyi Kostiantyn, PhD, Assoc. Prof
Donbas National Academy of Civil Engineering and Architecture,
Faculty of Civil Engineering,
Heroiv Nebesnoi Sotni str., 14, Kramatorsk, Donetsk reg., Ukraine 84333
k.v.polyansky@donnaba.edu.ua

ISSN 1846-6168 (Print), ISSN 1848-5588 (Online)
https://doi.org/10.31803/tg-20230811143809

Preliminarily communication
Received: 2023-08-11, Accepted: 2024-02-07

Plume Rise from a Stack Based on the Volkov Formula

P. Jafari Shalkouhi, F. Atabi, F. Moattar*, H. Yousefi

Abstract: Plume rise from most sources is an important factor in determining ground-level concentration of air pollutants. Various attempts have been done to compute plume rise from stationary sources. Volkov (1979) proposed a formula for calculation of plume dimensions (height and length) from a stack, while most of the well-known plume rise equations can only compute plume rise or plume height. Both plume height and plume length should be determined in some cases, for example in study of stack and cooling tower plume mergence, plume behavior (lofting, fanning, coning, looping, trapping and fumigation) etc. Because there are little studies in the world regarding the accuracy of the Volkov equation, the aim of the present work is to investigate the validity of the Volkov formula based on 5 statistical tests including the relative error, mean square error, root mean square error, coefficient of determination and Nash-Sutcliffe coefficient. The results revealed that (1) the Volkov equation better predicts plume rise at the distance of 60 m than 30 m from a typical stack, (2) considering the value of 0.5 instead of 0.4 or 0.65 for *n* in the Volkov formula will lead to more accurate results and (3) plume dispersion pattern was categorized as lofting. Overall, the Volkov equation can be an acceptable method to study of plume rise; nevertheless more studies must be conducted in the future with regard to the accuracy of the Volkov formula.

Keywords: plume rise; stack; Volkov equation

1 INTRODUCTION

Air pollution is defined as the presence of contaminants or pollutant substances in the air that interfere with human health or welfare, or produce other adverse environmental effects. For example, fossil fuels have an impact on human health and emit harmful emissions to the environment when burned. Air pollutants reach receptors through being transported and perhaps transformed in the atmosphere. The location of receptors with regard to sources and atmospheric effects influences pollutant concentrations, and the sensitivity of receptors to these concentrations determines the influences. The location, height, and duration of release, as well as the amount of pollutant released, are also of significance [1, 2].

In order to accurately compute air pollutant concentrations and plume trajectory in the atmosphere, it is necessary to consider the effects of interactions between plume and the surrounding environment [3].

Plume rise or plume height from most sources is an important factor in determining ground-level concentration of air pollutants since it increases effective stack height by a factor of 2-10 times the actual release height. Effective stack height is defined as the physical stack height plus plume rise. Because ground-level concentration is roughly proportional to the inverse square of the effective stack height, it is clear that plume rise can reduce ground-level concentration by a factor of as much as 100 [4, 5]. Ground-level concentration of air pollutants can be calculated via the following formula [6]:

$$C_x = \frac{Q}{\pi \sigma_y \sigma_z u} \mathrm{e}^{-\frac{1}{2}\left[\frac{H}{\sigma_z}\right]} \mathrm{e}^{-\frac{1}{2}\left[\frac{y}{\sigma_y}\right]^2} \quad (1)$$

where C_x is the ground level concentration of air pollutants at some distance x downwind (gr/m^3), Q is the average emission rate of air pollutants (gr/sec), u is the mean wind speed at the stack top (m/sec), H is the effective stack height (m), σ_y is the standard deviation of wind direction in the horizontal (m), σ_z is the standard deviation of wind direction in the vertical (m), y is the off-centerline distance (m) and e is the natural log (2.71828). Plume rise depends on the number of factors such as: gas flow rate, temperature of the effluent at the top of the stack, the stack exit diameter, wind speed at the top of the stack, air temperature at the top of the stack, wind speed gradient with height and atmospheric stability [7]. Guevara et al. [8] reported that in order to maximize the precision of plume rise computations, the use of stack parameters based on real-world data is mandatory. Various attempts have been made to predict plume rise from stationary sources. Two types of equations have been resulted: theoretical and empirical. Theoretical models/equations are generally derived from the laws of momentum and buoyancy. They are often adjusted for empirical data. Empirical models are developed from large amounts of observed data including tracer studies, wind tunnel experiments and photographic evidence [9]. Most of the proposed plume rise equations are empirical in nature, as the theory has not been developed sufficiently. The plume rise theory can be expressed as follows [10]:

$$\Delta h = K \frac{Q^{\alpha}}{\overline{u}^{\beta}} \quad (2)$$

Where Δh is the plume rise (m), α, β and K (dimensional) are constant, Q is the heat emission rate from the stack, $\overline{u}$ is the mean wind speed at the stack height. In the CCRL (Canadian Combustion Research Laboratory) formula $\alpha = 1/4$, $\beta = 1$, $K = 66.4$ and Q and $\overline{u}$ are expressed in kcal/s and m/s respectively. A series of observations at the Tilbury power plant indicate that $\alpha = 1/4$, $\beta = 1$, $K = 450$ - 500 and Q and $\overline{u}$ are expressed in MW and m/s respectively. It is also observed that K is a function of the height of emission source.

Briggs recognised the need to express plume height as a function of plume length as a way to address the issue of unobservable maximum plume height [11]. Essa et al. [12] observed maximum value of ground level concentration in unstable stability when plume height was a function of plume length. Knudson's results [13] revealed that smoke plumes emitted from stacks frequently merge with vapor plumes released from cooling towers in a power plant in USA, where the height and length differences between stacks and cooling towers were about 100 m and 1000 m respectively. Shalkouhi et al. [14] reported that most of the studies with regard to vapor and smoke plume mergence are dated back to the 70s and 80s. Recently, Shalkouhi et al. [15] found that mergence of smoke and vapor plume occurs in a power plant in Hungary. It should be pointed out that mergence of vapour and smoke plume can lead to formation of sulfuric acid which can corrode metals and building materials [13, 16].

Volkov [17] proposed a formula for calculation of plume dimensions (height and length) from a stack, while most of the well-known plume rise equations (e.g. Holland, Rauch, Stone and Clarke etc.) can only compute plume rise or plume height. Because there are little studies in the world with regard to the validity of the Volkov formula, the aim of the present work is to investigate the accuracy of the Volkov equation.

2 METHOD

Volkov [17] proposed the following equation for calculation of plume rise from a stack:

$$z = Kx^n \tag{3}$$

where

$$K = \sqrt{0.42\frac{w_0 D_0}{u} + 0.3\frac{g w_0 D_0^2}{u^3 \varepsilon}\frac{\Delta T}{T_g}} \tag{4}$$

$$\varepsilon = \frac{\sqrt{u'^2}}{u} \tag{5}$$

$$x = \frac{K^2 + 2h\varepsilon + K\sqrt{K^2 + 4h\varepsilon}}{2\varepsilon^2} \tag{6}$$

In Eqs. (3)-(6) z is the plume rise (m), w_0 is the exit gas velocity (m/s), D_0 is the inside stack top diameter (m), u is the mean wind speed at the stack top (m/s), g is the gravitational acceleration (9.8 m/s^2), ΔT is the difference between exit gas temperature and ambient temperature (K), T_g is the exit gas temperature (K), x is the plume length (m), u' is the wind speed fluctuation at the stack top (m/s), h is the stack height (m) and n for $x/D_0 \leq 120$ is 0.5 (averaged over 0.4-0.65) and for $x/D_0 > 120$ is 0.35. Meanwhile, the variable ε in Eq. (5) is called the atmospheric turbulence.

Fig. 1 shows schematic diagram of study methodology. Accordingly, for prediction of plume rise based on the Volkov formula mean data presented in Tab.1 were used. Moreover, as stated sooner, n for $x/D_0 \leq 120$ is 0.5 (averaged over 0.4-0.65), hence the Volkov plume rise was computed for n = 0.4, n = 0.5 and n = 0.65. Finally, for data analysis 5 statistical tests including the relative error [19], mean square error (*MSE*), root mean square error (*RMSE*) ($\sqrt{MSE}$) [20], coefficient of determination (R^2) [21] and Nash-Sutcliffe coefficient [22] were taken into consideration.

Table 1 Stack and meteorological parameters*

Wind speed (m/s)	Ambient temperature (K)	Stack exit gas velocity (m/s)	Stack exit gas temperature (K)	Plume rise at 30 m from stack (m)	Plume rise at 60 m from stack (m)
3.94	304.0	8.03	320.0	3.7	3.9
1.00	297.9	12.25	314.7	9.3	11.7
1.61	297.6	12.53	311.9	4.7	6.3
1.39	298.2	6.49	326.9	9.9	13.1
1.25	298.2	4.83	320.8	3.2	5.2
4.47	297.5	4.73	330.2	1.3	1.4
0.98	301.8	9.63	320.0	8.3	10.2
1.12	301.6	9.65	321.0	10.7	16.9
1.12	301.4	6.71	326.0	3.6	5.3
3.40	304.7	12.68	319.7	6.5	5.7
2.21	303.4	8.15	330.0	4.7	6.6
2.26	302.8	8.27	327.0	4.8	7.1
1.98	303.5	13.18	326.0	4.1	2.6
6.50	299.7	10.33	323.0	3.8	6.4
5.50	292.0	12.94	313.0	2.6	3.8
7.02	291.5	10.54	314.7	4.2	7.9
6.17	291.4	7.70	319.7	6.7	9.0
7.30	291.5	7.70	319.7	1.6	2.2
6.17	291.5	4.87	327.4	3.6	6.8
6.35	292.9	13.00	308.0	1.2	1.7
5.94	292.8	10.78	310.0	2.0	2.3
5.50	292.6	7.98	317.0	2.0	3.1
3.67	280.1	13.00	297.4	2.2	2.1
3.95	281.0	12.94	295.2	3.6	4.9
4.47	281.4	12.97	295.8	3.9	5.8
3.42	282.1	13.03	299.1	3.2	4.4
2.83	282.7	13.07	300.8	4.2	4.0
2.07	283.2	13.08	301.3	5.9	6.6
5.59	291.4	12.94	309.0	4.6	6.7
5.36	291.8	12.83	308.0	6.1	7.7
5.36	291.9	12.83	308.0	5.4	7.9
Min=0.98 Max=7.30 Mean= 3.87 Median= 3.94 Coefficient of Variation= 53.11% Confidence Interval= 3.87±0.72 Normal Distribution : shifted right Skewness= 0.013(right-skewed)	Min=280.1 Max=304.7 Mean= 294.0 Median= 292.8 Coefficient of Variation= 2.57% Confidence Interval= 294±2.66 Normal Distribution : shifted right Skewness= -0.41(left-skewed)	Min=4.73 Max=13.18 Mean= 10.31 Median= 10.78 Coefficient of Variation= 28.15% Confidence Interval=10. 31±1.02 Normal Distribution : shifted right Skewness= -0.61(left-skewed)	Min=295.2 Max=330.2 Mean= 314.9 Median= 317 Coefficient of Variation= 3.34% Confidence Interval=31 4.9±3.71 Normal Distribution : shifted right Skewness= -0.42(left-skewed)	Min=1.2 Max=10.7 Mean= 4.6 Median= 4.1 Coefficient of Variation= 53.31% Confidence Interval= 4.6±0.86 Normal Distribution : shifted right Skewness= 0.99(right-skewed)	Min=1.4 Max=16.9 Mean= 6.1 Median= 5.8 Coefficient of Variation= 56.94% Confidence Interval= 6.1±1.22 Normal Distribution : shifted right Skewness= 1.19(right-skewed)

*Stack height and inside diameter are 111 feet and 17.5 inches respectively. Meanwhile, all the data except the calculated values (mean, median, coefficient of variation, confidence interval, normal distribution and skewness) are transcribed from the Moses and Strom's paper [18].

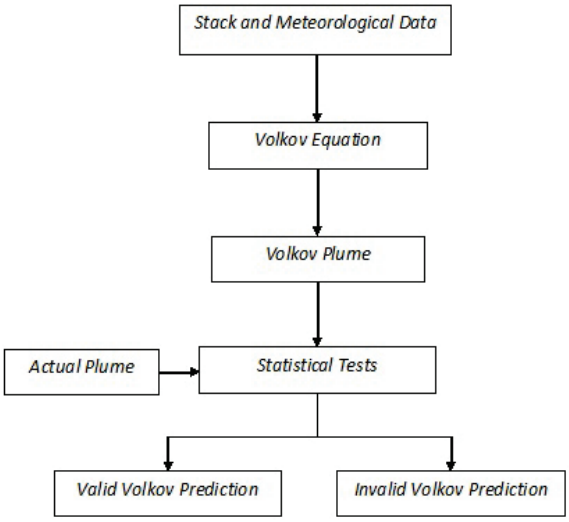

Figure 1 Flow chart of study methodology

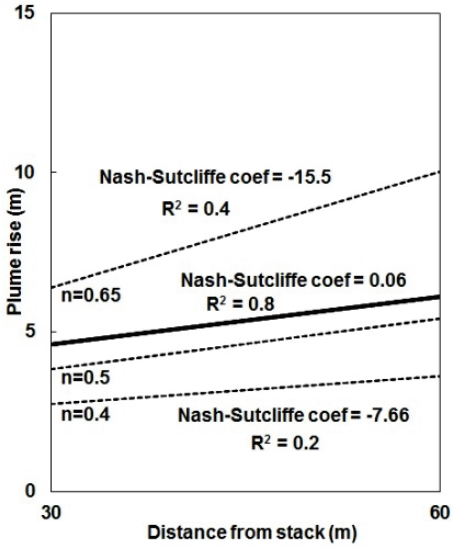

Figure 2 Comparison between the Volkov plumes (dashed lines) and actual plume (solid line)

3 RESULTS AND DISCUSSION

The results of predicted plume rise based on the Volkov formula are given in Tab. 2 and Fig. 2. As can be seen in Tab. 2, the relative error of the Volkov formula for 30 m ranges from 16.7 % to 40.7 % and for 60 m from 11.1 % to 64.3 %. Also, the mean square error of the Volkov formula for 30 m ranges from 0.59 to 3.5 and for 60 m from 0.46 to 15.37. Fig. 2 shows that the Nash-Sutcliffe coefficient between the Volkov and actual plume for $n = 0.4$, $n = 0.5$ and $n = 0.65$ are –7.66, 0.06 and –15.5 respectively. Moreover, the coefficient of determination between the Volkov and actual plume for $n = 0.4$, $n = 0.5$ and $n = 0.65$ are 0.2, 0.8 and 0.4 respectively.

Therefore, based on the findings of the present study it can be stated that the best prediction result is for $n = 0.5$; this suggests that Volkov correctly considered the mean of 0.4-0.65 for n in Eq. (3). Moreover, despite the Volkov prediction is not accurate, it can be statistically considered reasonable. In contrast, Carson and Moses [23] investigated the accuracy of 11 plume rise formulas including Holland, Stümke, CONCAWE, CONCAWE Simplified, Lucas-Moore-Spurr, Rauch, Stone and Clarke, Carson and Moses, Moses and Carson, Briggs Transitional and Csanady.

Table 2 Comparison between the Volkov and actual plumes

Distance from stack (m)	Actual plume [18] (m)	Volkov plume	Relative error	Mean square error	Root mean square error
30	4.6	2.73 m for $n = 0.4$	40.7 % for $n = 0.4$	3.5	1.87
		3.83 m for $n = 0.5$	16.7 % for $n = 0.5$	0.59	0.77
		6.39 m for $n = 0.65$	38.9 % for $n = 0.65$	3.2	1.79
60	6.1	3.60 m for $n = 0.4$	41.0 % for $n = 0.4$	6.25	2.5
		5.42 m for $n = 0.5$	11.1 % for $n = 0.5$	0.46	0.68
		10.02 m for $n = 0.65$	64.3 % for $n = 0.65$	15.37	3.92

Their results revealed that none of the equations predicts plume rise significantly better than the others. Moses and Strom [18] evaluated the accuracy of 6 plume rise equations such as Holland, Davidson/Bryant, Sutton, Scorer, Bosanquet et al. and Bosanquet. They found that about 75% of the measured plume rises fall within the range of the calculated values. Macey [24] performed a study to investigate the validity of the Bosanequet plume rise formula using the Tennessee Valley Authority data. He reported that the mentioned formula can be a reliable method to predict plume rise provided that a minor change is made in the model. Guldberg [25] evaluated the accuracy of 3 plume rise formulas including Briggs, Carpenter et al. and Montgomery et al. and concluded that at low wind speed the Briggs equation best predicts plume rise and at higher wind speed the Montgomery et al.'s formula performs best. Okamoto et al. [26] investigated the ability of 26 plume rise equations and found that most of the formulas overestimate plume rise at low wind speed. Saxena [27] predicted plume rise from a boiler stack based on the Briggs and Holland formulas. She found that the Briggs and Holland equations tend to overestimate and underestimate plume rise respectively. Findings of Li et al. [28] showed that the Briggs formula underestimates plume rise. Shalkouhi [29] proposed a formula for calculation of plume rise. His equation overestimates plume rise by a factor of approximately two. Alessandrini et al. [30] and Kozarev and Ilieva [31] proposed methods for prediction of plume rise. Their results showed satisfactory agreements with experimental data. Results of Leroy et al. [32] revealed that the Holland formulation for plume rise calculation, combined with the Briggs model, allows a better agreement between the predicted and observed ATC (Atmospheric Transfer Coefficient) than combined with the Doury model. It must be pointed out that study of plume rise is not only limited to stack and/or chimney. For example, Pandey et al. [33] proposed an acceptable formulation of aircraft emissions. Also, Bogdanyuk et al. [34] performed a satisfactory simulation of

supersonic gas-particle flows expanding from a nozzle into rarefied atmosphere. In the area of aerospace engineering, various instruments are used, during the operation of which jet flows develop. These include, in particular, devices that produce control forces necessary for the orientation of spacecraft.

Dispersion of pollutants can be described qualitatively simply by looking at the plume and categorizing it as looping, coning, fanning, lofting, fumigating and trapping. However, it is often necessary to estimate plume dispersion features quantitatively, such as by using the Briggs (1973) formula [35]. As can be seen in Fig. 2, the Volkov and actual plume shapes are analogue to lofting plumes, and this corresponds to the findings obtained by Shobakh and Widodo [36] and Achtemeier et al. [37]. Lofting plume is the most favorable plume type because it does not result in any significant ground-level concentration of air pollutants [6, 38]. Fig. 3 shows a 3D form of lofting plume in Rijeka oil refinery in Croatia. It was planned to modernize the mentioned refinery during the period of 2013-2023 [39]. Most plumes emitted from modern plants are virtually invisible [40]. Stacks with invisible plumes may still be in full operation, hence airspace in the vicinity should be treated with caution [41]. The results of the present paper revealed that the Volkov and actual plumes are more near to each other in 60 m than in 30 m, and this implies that the variable "distance from stack" had a significant influence on the Volkov plume. Hence to investigate the accuracy of the Volkov equation in the future, it is recommended to consider multiple distances from stack.

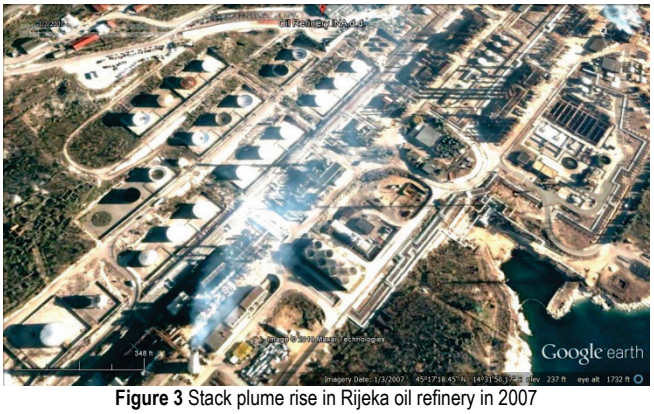

Figure 3 Stack plume rise in Rijeka oil refinery in 2007

For discussion goals, stacks are divided into two categories: small (<100 feet) and tall (≥100 feet) [42]. Therefore, as can be seen in Tab.1, the stack considered in the present paper is categorized as tall. In contrast, Flori and Milostean [43] and Bhargava [44] considered tall stacks for study of smoke plumes. Taller stacks disperse pollutants better than shorter ones because the plume has to travel through a greater depth of atmosphere before it reaches ground level [45]. In the present study despite a large data set with regard to each of the variables "wind speed, ambient temperature, stack exit gas velocity and actual plume" was considered, it was unfortunately not possible to consider multiple stack heights and diameters.

This study used 5 statistical tests to investigate the validity of the Volkov equation; while few studies (e.g. Moses and Strom [18] and recently Wheida et al. [46]) used several statistical methods to examine the accuracy of plume rise formulas. Apart from statistical analysis, one can consider the EVA (Earn Value Analysis) method to performance evaluation of any plume rise equation. The mentioned method can be used in various areas of science. For example, Ugural and Burgan [47] recently used the EVA technique in civil engineering.

4 CONCLUSIONS

The validity of the Volkov equation was investigated based on 5 statistical tests including the relative error, mean square error, root mean square error, coefficient of determination and Nash-Sutcliffe coefficient. The results revealed that 1) the Volkov formula better predicts plume rise at the distance of 60 m than 30 m from the 111 feet stack, 2) considering the value of 0.5 instead of 0.4 or 0.65 for n in the Volkov formula will lead to more accurate results and 3) the Volkov and actual plume dispersion patterns were analogue to each other. Overall, the Volkov formula can be an acceptable method to study of plume rise; nevertheless more studies must be conducted in the future with regard to the accuracy of the Volkov equation.

5 REFERENCES

[1] Vallero, D. (2008). *Fundamentals of air pollution*. Oxford: Elsevier. https://doi.org/10.1016/B978-012373615-4/50031-5

[2] Obrecht, M., Rosi, B. & Potrč, T. (2017). Review of low emission zones in Europe: Case of London and German cities. *Tehnički glasnik, 11*(1-2), 55-62. Retrieved from https://hrcak.srce.hr/183746

[3] Affad, E., Saadeddine, S., Assou, M. & Sbaibi, A. (2006). Effect of the relative humidity on an industrial plume behavior. *Global NEST Journal*, 8, 297-305. https://doi.org/10.30955/gnj.000294

[4] Hanna, S. R., Briggs, G. A. & Hosker, R. P. (1982). *Handbook on atmospheric diffusion*. Technical Information Center, U.S. Department of Energy. https://doi.org/10.2172/5591108

[5] Office of the Federal Register. (2018). *Title 40: Protection of environment-parts 266 to 299*.

[6] Mitchell, R. & Sweeney, F. (2018). *Air pollution*. London: E.D-Tech Press.

[7] Ganesan, K., Theodore, L. & Dupont, R. R. (1996). *Air toxic: Problems and solutions*. Amsterdam: OPA (Overseas Publishers Association).

[8] Guevara, M., Albert, S., Arévalo, G., Martínez, G. & Baldasano, J.M. (2014). Implementation of plume rise and its impacts on emissions and air quality modelling. *Atmospheric Environment*, 99, 618-629. https://doi.org/10.1016/j.atmosenv.2014.10.029

[9] Liu, H. F. D. & Liptak, B. G. (1999). *Air pollution*. Boca Raton: CRC Press.

[10] Rao, M. N. & Rao, H. V. N. (1989). *Air pollution*. New Delhi: Tata McGraw-Hill Publishing Company Limited.

[11] Tory, K. (2018). *Models of buoyant plume rise*. Melbourne: Bushfire and Natural Hazards CRC.

[12] Essa, K. S. M., Mubarak, F. & Elsaid, S. E. M. (2006). Effect of the plume rise and wind speed on extreme value of air

pollutant concentration. *Meteorology and Atmospheric Physics*, 93, 247-253. https://doi.org/10.1007/s00703-005-0168-1

[13] Knudson, D. A. (1979). *Cooling tower and steam plant plume mergence at the Watts Bar site*. TVA/AQB-I79/13, Tennessee Valley Authority, Air quality Branch.

[14] Shalkouhi, P. J., Atabi, F., Moattar, F. & Yousefi, H. (2017). Smoke and vapor plume mergence. *Croatian Meteorological Journal*, 52, 51-57.

[15] Shalkouhi, P. J., Atabi, F., Moattar, F. & Yousefi, H. (2020). On the reliability of CALPUFF and AUSTAL 2000 modeling systems regarding smoke and vapor plume mergence. *IDŐJÁRÁS*, 124, 299-309. https://doi.org/10.28974/idojaras.2020.2.8

[16] Shafi, S. M. (2005). *Environmental pollution*. New Delhi: Atlantic.

[17] Volkov, E. P. (1979). Plume rise above a stack. *Journal of Engineering Physics and Thermophysics*, 36, 466-471. Translated from Rusian. https://doi.org/10.1007/BF00866974

[18] Moses, H. & Strom, G. H. (1961). A comparison of observed plume rises with values obtained from well-known formulas. *Journal of the Air Pollution Control Association*, 11, 455-466. https://doi.org/10.1080/00022470.1961.10468024

[19] Jaiswal, A. K. & Khandelwal, A. (2009). *Computer based numerical & statistical techniques*. New Delhi: New Age International Publishers.

[20] Witten, I. H. & Frank, E. (2005). *Data mining: Practical machine learning tools and techniques*. Oxford: Elsevier.

[21] Burt, J. E., Barber, G. M. & Rigby, D. L. (2009). *Elementary statistics for geographers*. London: Guilford Press.

[22] Surhone, L. M., Tennoe, M. T. & Henssonow, S. F. (2011).*Nash-Sutcliffe model efficiency coefficient*. Beau Bassin: Betascript Publishing.

[23] Carson, J. E. & Moses, H. (1969). The validity of several plume rise formulas. *Journal of the Air Pollution Control Association*, 19, 862-866. https://doi.org/10.1080/00022470.1969.10469350

[24] Macey, H. H. (1970). Bosanquet's plume rise formula and the T.V.A. data. *Atmospheric Environment*, 4, 577-583. https://doi.org/10.1016/0004-6981(70)90024-7

[25] Guldberg, P. H. (1975). A comparison study of plume rise formulas applied to tall stack data. *Journal of Applied Meteorology*, 14, 1402-1405. https://doi.org/10.1175/1520-0450(1975)014%3C1402:ACSOPR%3E2.0.CO;2

[26] Okamoto, S., Okanishi, S., Hiroh, A. & Shiozawa, K. (1977). Comparison and evaluation of plume rise formulas. *Journal of the Japan Society of Air Pollution*, 12, 456-465.

[27] Saxena, N. (2005). Comparision of short term concentration of sulfur dioxide (SO_2), and suspended particulate matter (SPM) PM pollution from a point source using different plume rise formulae. *Journal of Industrial Pollution Control*, 21, Issue 1.

[28] Li, Y., Tong, D., Ma, S., Freitas, S. R., Ahmadov, R., Sofiev, M., Zhang, X., Kondragunta, S., Kahn, R., Tang, Y., Baker, B., Campbell, P., Saylor, R., Grell, G. & Li, F. (2023). Impacts of estimated plume rise on $PM_{2.5}$ exceedance prediction during extreme wildfire events: A comparison of three schemes (Briggs, Freitas, and Sofiev). *Atmospheric Chemistry and Physics*, 23, 3083-3101. https://doi.org/10.5194/acp-23-3083-2023

[29] Shalkouhi, P. J. (2023). Prediction of stack plume rise. *Ecological Engineering and Environment Protection*, No. 2, 29-33. https://doi.org/10.32006/eeep.2023.2.2933

[30] Alessandrini, S., Ferrero, E. & Anfossi, D. (2013). A new Lagrangian method for modelling the buoyant plume rise. *Atmospheric Environment*, 77, 239-249. https://doi.org/10.1016/j.atmosenv.2013.04.070

[31] Kozarev, N. & Ilieva, N. (2011). Plume rise in particular meteorological conditions. *Journal of the University of Chemical Technology and Metallurgy*, 46, 305-308.

[32] Leroy, C., Derkx, F., Connan, O., Roupsard, P., Maro, D., Hébert, D. & Rozet, M. (2011). A study of the atmospheric dispersion of an elevated release with plume rise in rural environment: Comparison between field SF_6 measurements and computations of Gaussian models (Briggs, Doury and ADMS 4.1). *WIT Transactions on Ecology and the Environment*, 147, 399-410. https://doi.org/10.2495/AIR110371

[33] Pandey, G., Venkatram, A. & Arunachalam, S. (2023). Accounting for plume rise of aircraft emissions in AERMOD. *Atmospheric Environment*, 314, 120106. https://doi.org/10.1016/j.atmosenv.2023.120106

[34] Bogdanyuk, D., Emelyanov, V., Pustovalov, A. & Volkov, K. (2023). Simulation of supersonic gas-particle flows expanding from the nozzle into rarefied atmosphere. *Acta Astronautica*, 204, 794-806. https://doi.org/10.1016/j.actaastro.2022.09.043

[35] Rohli, R. V. & Li, C. (2011). *Atmospheric dispersion in the coastal zone. In: Meteorology for coastal scientists*. Switzerland: Springer.

[36] Shobakh, M. N. & Widodo, A. S. (2022). Prediksi pola sebaran plume rise pada variasi kecepatan emisi gas buang chimney dengan simulasi komputer. *Jurnal Rekayasa Mesin*, 13, 939-945. (in Indonesian) https://doi.org/10.21776/jrm.v13i3.1515

[37] Achtemeier, G. L., Goodrick, S. A., Liu, Y., Menendez, F. G., Hu, Y. & Odman, M. T. (2011). Modeling smoke plume-rise and dispersion from southern United States prescribed burns with Daysmoke. *Atmosphere*, 2, 358-388. https://doi.org/10.3390/atmos2030358

[38] Rao, C. S. (2006). *Environmental pollution control engineering*. New Delhi: New Age International Publishers.

[39] Billege, I., Ahmetoviæ, D., Medarac, I. & Hill, Z. (2012). Natural gas consumption in Croatian refineries 2013-2023. *NAFTA*, 63, 373-376.

[40] Stessel, R. I. (1996). *Recycling and resource recovery engineering: Principles of waste processing*. Berlin: Springer. https://doi.org/10.1007/978-3-642-80219-5

[41] Elite Aviation Solutions. (2013). *Aeronautical information manual study guide for the private pilot: An extensive easy to use study guide to help private pilots fully understand the aeronautical information manual (AIM)*. United States of America.

[42] Vatavuk, W. M. (2019). *Estimating costs of air pollution contro*l. Boca Raton: CRC Press.

[43] Flori, M. & Milostean, D. (2020). Mathematical analysis of air pollution from stacks using Briggs method. *Annals of Faculty Engineering Hunedoara-International Journal of Engineering*, 18, 145-148.

[44] Bhargava, A. (2016). Effect of stack exit velocity and gas temperature on plume rise using different equations. *International Journal of Scientific Development and Research*, 1, 1-5.

[45] Spellman, F. R. (2009). *The science of air: Controls and applications*. Boca Raton: CRC Press.

[46] Wheida A. A., Essa, K. S, Saied, S. L. & El-Nazer, M. (2023). Studying the effect of different shapes of plume rise on Gaussian plume models and it's maximum on unstable conditions. *Open Journal of Analytical and Bioanalytical Chemistry*, 7, 011-015. https://doi.org/10.17352/ojabc.000029

[47] Ugural, M. N. & Burgan, H. I. (2021). Project performance evaluation using EVA technique: Kotay bridge construction project on Kayto River in Afghanistan. *Tehnički vjesnik, 28*(1), 340-345. https://doi.org/10.17559/TV-20200114133619

Authors' contacts:

P. Jafari Shalkouhi, PhD Candidate
Department of Environmental Engineering,
Faculty of Agriculture, Water, Food and Parabens,
Science and Research Branch, Islamic Azad University,
Daneshgah Blvd, Simon Bulivar Blvd, Tehran, Iran

F. Atabi, Associate Professor
Department of Environmental Engineering,
Faculty of Agriculture, Water, Food and Parabens,
Science and Research Branch, Islamic Azad University,
Daneshgah Blvd, Simon Bulivar Blvd, Tehran, Iran

F. Moattar, Professor
(Corresponding author)
Department of Environmental Engineering,
Faculty of Agriculture, Water, Food and Parabens,
Science and Research Branch, Islamic Azad University,
Daneshgah Blvd, Simon Bulivar Blvd, Tehran, Iran
E-mail: pedram121212@yahoo.com

H. Yousefi, Assistant Professor
Department of Renewable Energies and Environmental Engineering,
Faculty of New Sciences and Technologies, University of Tehran,
North Kargar Street, Tehran, Iran

ISSN 1846-6168 (Print), ISSN 1848-5588 (Online)
https://doi.org/10.31803/tg-20240925140236

Professional paper
Received: 2024-09-25, Accepted: 2024-11-19

Harnessing Remote Sensing Technologies for Successful Large-Scale Projects

Josip Lisjak*, Matej Petrinović, Stjepan Keleminec

Abstract: The integration of remote sensing technologies, such as Mobile Mapping Systems (MMS), Ground Penetrating Radar (GPR), airborne LiDAR, high-speed terrestrial laser scanner and airborne multispectral cameras, is transforming the execution and management of large-scale infrastructure projects. These tools enable efficient and accurate data collection without requiring operators to be physically present in the observed area, enhancing the ability to map, analyze, and model both surface and subsurface features. This paper explores the synergy of these technologies, focusing on their application in critical sectors such as climate change mitigation, smart cities, and digital twins. It examines the benefits of technology integration, the challenges of data interpretation, and the opportunities for improving project efficiency and sustainability. Through a detailed analysis of each remote sensing technology, this paper highlights their potential to redefine large-scale project execution, driving innovation in infrastructure development and to bring business benefits to organisation which implements it.

Keywords: 3D spatial data; business breakthrough; ground penetrating radar; mobile mapping system; remote sensing technologies

1 INTRODUCTION

The remote sensing technologies has revolutionized the execution and management of large-scale infrastructure projects, integrating innovative tools such as Mobile Mapping Systems (MMS), Ground Penetrating Radar (GPR), airborne LiDAR and airborne multispectral camera, terrestrial laser scanner, airborne echosounder, and high-performance computing capabilities.

Regarding the technology background, the Mobile Mapping Systems are the combination of various navigation and remote sensing technologies on a common moving platform. What makes them a remote sensing technology is the fact that the operator does not need to be physically in the observed area of detail in order to collect the spatial data on details, while the system works from a distance. The same applies to Ground Penetrating Radar. The relevant literature defines them as remote sensing technologies [1]. Also, there is an entire Special Issue of Open Access Journal by MDPI - Remote Sensing which is devoted to the latest developments in GPR systems and applications, called Recent Progress in Ground Penetrating Radar Remote Sensing [2].

When it comes to MMS, to date there were several papers which addressed the MMS capabilities and possible applications. The obvious application is mainly in road measurements and there are many research papers regarding this application [3, 4, 5]. Also, some of the research addresses other applications like geotechnical and landslide monitoring with MMS [6]. Thus, the recent research work has brought an overview of applications where MMS can be used. These include wide range of applications like road asset management and condition assessment, BIM, emergency and disaster response, vegetation mapping and detection or digital heritage conservation. On the other hand, given the complex terrain environment, a single MMS or even a few MMSs could hardly be sufficient at all levels of mobile mapping applications [7].

The Ground Penetrating Radar technology has been gradually adopted in civil engineering since mid-1990s, but after 2000, technological advancements and tremendous improvements of digital computation power have led to the blossoming of GPR applications on infrastructure [8]. The applications range from engineering geophysics, buildings inspection, to infrastructure applications like road, pavement and bridge observations, tunnel liners. The GPR usage in road layers thickness analysis is shown in [9, 10, 11], but also there are papers showing GPR application in detection of anomalies such as cracks [12, 13]. Also, the GPR is used to position and map underground utilities of different kinds like pipes or cables [14, 15].

Despite of all those previous research papers, use of GPR is still in an ad-hoc based but not regular-based, while the technology is still evolving with much future potential [8]. Furthermore, the survey results of the GPR mapping undoubtedly yield much larger errors than the above-ground surveying technologies. Therefore the GPR is proposed to be complemented with other remote-sensing technologies in this paper.

The MMS and GPR technologies present a comprehensive solution for mapping and analyzing spatial features crucial for climate change mitigation, development of smart cities, and creation of digital twins, embodying a new wave of green technology. Their application extends beyond the surface to provide detailed 3D data of underground structures, thereby enhancing project efficiency and environmental sustainability. Both have some shortcomings, thus other sensors are introduced to provide competent overall spatial data collection.

With respect to that, the inclusion of remote sensing in large-scale projects poses unique challenges, including the integration of diverse technologies and the interpretation of complex data sets. This paper aims to explore the synergy of remote sensing technologies and their potential in application on large-scale infrastructure projects. By examining the advantages of technology integration, applications in critical sectors, and solutions to implementation hurdles, the discussion extends to the role of these technologies in addressing climate change, advancing smart cities, and promoting the concept of digital twins. This overview not only sets the stage for a detailed analysis of each technology's contribution but also underscores the potential of remote sensing to redefine project execution and outcomes in the face of evolving global demands.

2 THE PROPOSED TECHNOLOGIES COMBINATION IN REMOTE SENSING

The proposed technologies for enhancing large-scale projects through remote sensing are both diverse and integrated, aimed at providing comprehensive coverage and detailed data acquisition. This tested combination includes advanced systems like the Mobile Mapping System (MMS) Leica Pegasus TRK700 EVO, Ground Penetrating Radar (GPR) Leica Stream Up, and innovative tools such as underwater robots and airborne geomagnets, but also airborne echosounders. Additionally, the integration of multi-spectral cameras, such as the VUX160 LiDAR combined with a PhaseOne camera, and air-pollution measurement devices like Sniffer4D, further broadens the scope of environmental monitoring and mapping accuracy.

The synergy of these technologies not only supports traditional applications such as transportation planning and construction but also extends to innovative uses like real-estate mass valuation, emergency response planning and ad-hoc interventions, and the development of digital twins. This technological combination is a game changer in managing and executing large-scale projects efficiently, particularly those requiring rapid data collection over extensive areas.

The combination of these technologies is not only pivotal in general mapping but also in specific applications which are stressed out in the paper, such as cadastral measurements and real estate valuation. For instance, in a multi-year cadastral measurements program [16] covering 600,000 hectares, the integration of these technologies can facilitate the efficient mapping and valuation of vast land areas, optimizing both time and resources. Furthermore, the use of Multiple Regression analysis (MRA) in real estate valuation considers a variety of internal and external variables, from physical characteristics of the property to environmental factors, which all can be captured and quantified through these advanced remote sensing technologies. The use of MRA for mass real estate valuation is defined in the Regulation on mass real estate valuation [17], where the variables for the evaluation are also defined (e. g. location, area, usage, position in the building, existence of an elevator, etc.). Although, relevant experts states that there are rather more complex variables in place which impacts the value of real estate, like field of view [18], which can be seen in Fig. 1.

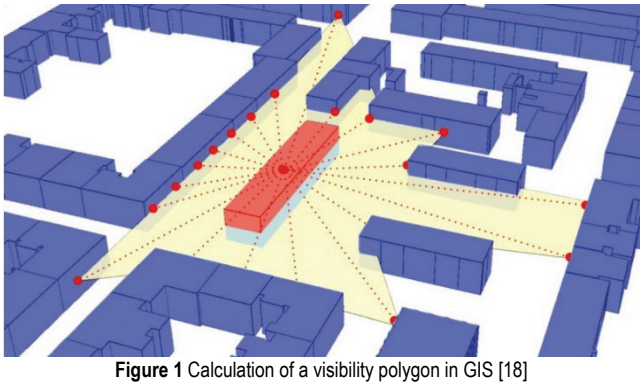

Figure 1 Calculation of a visibility polygon in GIS [18]

This can be analyzed with advanced GIS systems for which the highly defined, accurate and reliable spatial data should be collected. The government intended to implement the real-estate tax, but with delay, with the main reason of not having the appropriate datasets for the real-estate valuation. The proposed technology combination in this paper can be an efficient game changer to collect this kind of data on real-estate. Furthermore, the introduction of regulations such as ePhysicalPlans, which require thematic basemaps, showcases the growing reliance on advanced remote sensing technologies for compliance and advanced planning. These technologies facilitate the creation of detailed, multi-spectral maps essential for physical planning as well as many other thematic basemaps which are up to date. Only in 2024, there are already more than 250 municipalities which have applied for financing of the physical plan creation or amendments in new ePhysicalPlan form [19]. This creates a vast economic potential and demand for all kinds of spatial data or thematic basemaps.

3 TECHNICAL INFORMATION AND EXAMPLE USAGE IN A LARGE-SCALE PROJECT

For the first technical demonstration it is aimed to show how these devices can be used in multi-year cadastral measurements and real estate valuation - speeding up the existing workflow significantly. The aim of this project is to scan all buildings fast and efficiently utilizing more scanning angles. From the software side the following is needed: speed up the vectorization workflow while retaining precision.

Figure 2 Example of a building facade captured from the street inside of Pegasus Office

First up - aerial scanning LiDAR solution is utilized. While not much different from any other solution on the market the VUX 160 offers one main benefit - nadir-forward-backward facets in the scanning mechanism are used to get as much coverage on the facades as possible. The system offers selectable pulse repetition rate which allows for greater accuracy of the laser beam [20].

Paired with an external inertial measurement unit AP+50 system can be mounted on a smaller aircraft or an unmanned aerial vehicle. Limitation of this technique is not being able to pick up finer details in the more complex buildings and their eaves.

Advantage of this scanner is in option for defining own customisable set of parameters for each flight mission in RiParameter. Since the aim is to capture as much detail in -

10 and +10 degrees from nadir, the scan rate is maximised to 400 lines per second - achieving a point every 4 centimetres and a new line every 2 centimetres. This can be further improved by lowering the flight speed.

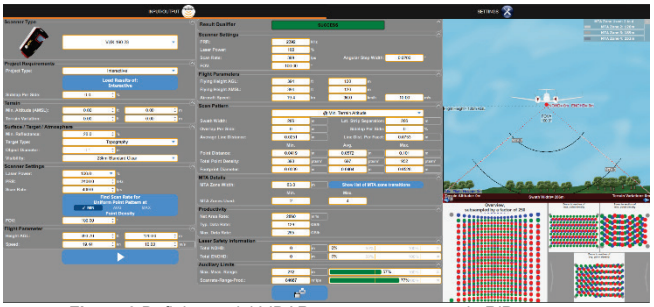

Figure 3 Defining aerial LIDAR scanner parameter in RiParameter

Another tool is the mobile mapping system - TRK 700 Evo. Utilizing a phase-shift LiDAR allows for greater precision at the cost of range which is opposite from time of flight LiDAR systems [21]. Majority of urban areas can be accessed from the roadways. Mobile system needs to be initialized beforehand because the inertial unit needs to be adapted and trained for the upcoming data collection. Having two Z&F 9020 laser profilers allows for 2 million points per second which allows greater driving speeds thus enhancing the operation. Limitation of this approach is the laser obstruction along the driving lane.

These two systems collect about 80% of needed data - there are still some gaps which cannot be measured beneath eaves and more complex buildings.

Last tool used is the VZ-600i. Its main advantage is the integrated GNSS antenna, IMU sensor and a fast pulse repetition rate (2200 kHz) resulting in the scan times of 30 seconds, delivering on-site registered point clouds. The field workflow is straightforward which means that the remaining gaps can be measured wherever there is an RTK connection available. Only one scan position outside the building is needed, then the remaining positions indoors can be scanned and everything is within the specified accuracy. This system would actually be the best for completing the project but its drawback is the speed of acquisition.

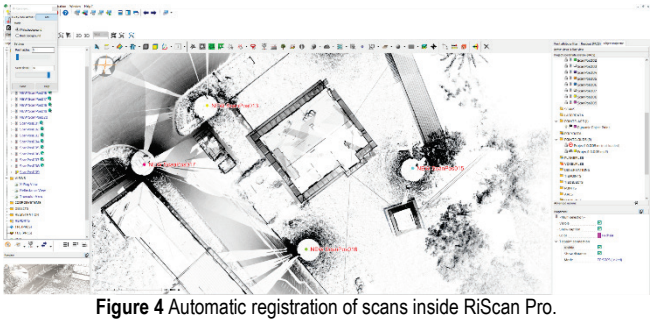

Figure 4 Automatic registration of scans inside RiScan Pro.

As the data is acquired in the field - each scan position on the scanner saves its RTK position, IMU heading, roll and pitch value. Having this additional data enables the onboard computer to calculate the scanner's position and orientation "on-the-fly" without the operator needing to roughly fit the scans in post-processing. This results in very quick turnover time with no user input required. Inside the software it is also possible to remove the noise generated by moving objects.

Moving to the software and modelling side - all data sources need to be registered and data quality needs to be confirmed against checkpoints. Although the data lies well within the specification stated by the State Geodetic Administration [22] there are still vertical discrepancies which can be resolved by utilizing plane patching and multi-station adjustment inside the RiScan Pro software.

After all three data sources are optimized the next step is vectorization. This research tries to resolve the problem with two various methods: semi-automatic vectorization using TerraScan and manual extraction using Microstation Connect with Topodot. Each method has its own pros and cons. The semi-automatic method gives the outlines for the whole area way faster than manual extraction but at the cost of having polyline artifacts and miscellaneous errors. Using manual extraction the user is slower but has utmost control along the whole process, utilizing various quality assurance and checks along the way.

Another example usage in a large scale project would be ground penetrating radar for archeological purposes.

As GPR is a non-invasive/non-destructive method of collecting subsurface data [23], its use over a possible archeological area is described. The instrument used is IDS Stream Up - having 2 crossed antennas at 200 mHz and 600 mHz and the scan width of 1.6 meters while being mounted on a vehicle, area can be scanned significantly faster than other solutions.

Figure 5 The IDS Stream Up device mounted on a vehicle

Using proprietary software IQ Maps tomography data is analyzed to extract existing pipelines and point out areas of archeological interest before the site is demolished.

One example usage of this device is the archeological need for detecting possible historical remains and to detect unregistered utilities. To ensure the best possible coverage, the site is scanned after closing all of the traffic on the site. Through using RTK antenna, total station or even mobile mapping system (tested TRK700 EVO) the data is generated and filtered in IQMaps software. Afterwards the B-scans of the GPR data were generated and from there it was possible to assess existing underground utilities and possible areas of archeological value. Data can be exported as linestrings, points or hatches straight to any CAD program.

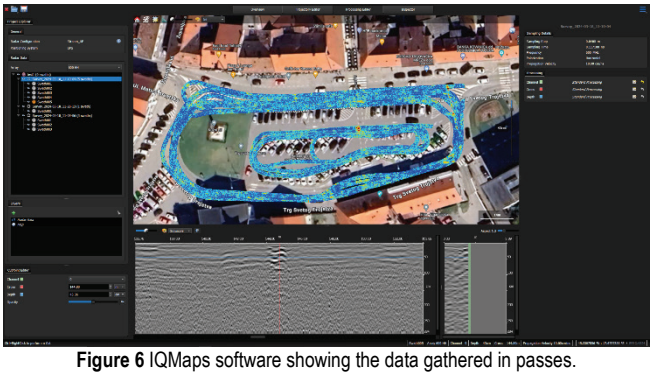

Figure 6 IQMaps software showing the data gathered in passes.

The same procedure can be applied to observation of any road, underground utilities, bridges, tunnels, or any large-scale infrastructure object. With respect to stated issus regarding GPR in the Introduction, by combining with the MMS it is rather more efficient to map the underground structures, and by introducing other data collection methods it is possible to perform the accuracy assessment and data quality control, but with almost on-the-fly performance and delivery of the results.

4 DISCUSSION AND PROPOSAL FOR APPLICATIONS BEYOND TRADITIONAL BOUNDARIES

Latest amendments of Law on Forests are now more data-driven, thanks to remote sensing technologies. Also, the new ISPU (Information System of Spatial Planning) [24] assists in creating a comprehensive Green Infrastructure Register, crucial for sustainable development. The data of greenery should yet be collected, which is a huge task for geodetic operatives. Recently, many local self-government (LGU) units in Croatia are procuring the services of making Strategies of Green Urban Renewal, and are bringing them into force [25-27]. The Guidelines for making the Strategies for Green Urban Renewal [28], define that within the scope of delivery of every strategy, the team behind the strategy should prepare the dataset for the Green Infrastructure Register. The Ministry of Spatial Planning, Construction and State Property created the Green Register infrastructure, a new module of the ISPU system, which enables input, maintenance and analysis of data on green infrastructure for urban areas in the Republic of Croatia and entry of spatial data from the above-mentioned strategic documents. The entry of data into the Register is overseen in accordance with the Typology of Green Infrastructure, which are defined as open spaces, green and blue areas, which make up the green infrastructure in construction areas. Green urban renewal strategies need to be created in accordance with the mentioned Typology green infrastructure. But as most questionable instruction from the Guidelines stands the one that the strategy of green urban renewal must include cartographic representation in open GIS format (GDB or shp) and must contain:

- the scope for which the Strategy is being prepared
- the area which includes planned green urban renewal projects
- and the mapping of existing green infrastructure in accordance with the Typology of Green Infrastructure.

Therefore, it is instructed that, on the level of making strategic document, the green infrastructure in urban areas should be mapped and delivered in a specific GIS format. When considering the economic engagement and the amount of procurement contract for the strategies, which is mostly on the level of making a strategic document which does not predict the terrain spatial data collection, this presents a gap in the initiative, while most of the green infrastructure mapping are missing in the strategies. Therefore, it is a leverage to have the ability to rapidly collect the spatial data in urban areas based on which one can map the initial state of green infrastructure within the scope of strategic document making. Also, from the perspective of economic feasibility, the solution is in MMS in combination with other technologies presented in this paper.

eBuildingInspection is announced, while the combination of remote sensing technologies streamline building inspections and enhance the efficiency of the supervision process by providing detailed subsurface data, crucial for safety and compliance. Through periodic monitoring with remote sensing, primarily with combination of MMS+GPR can aid in identifying changes in transport infrastructure and detecting non-evidenced landslides, crucial for maintaining safety and continuity.

Furthermore, reality capture technologies used to create Digital Twins enable precise modelling of physical assets, which can be crucial in emergency response scenarios. Although, previous and recent research in this area stresses the issue of integration of massive data from remote sensing into the digital twins; they conclude that future work should consider the development of methodologies and protocols to integrate the massive data streams coming from heterogeneous sensors and complex systems [29]. These heterogeneous sensors are for sure in modern time exactly the ones used here.

The potential applications of remote sensing technologies are extensive and largely underexplored. Their advantages become particularly evident when integrated with various professions and scientific fields. Some additional prospective applications of these technologies include forest biomass estimation, landslide detection, real estate valuation, tree root detection, mass grave identification, automated road asset extraction, and the creation of pollution maps.

Furthermore, there are several existing ideas that, despite their potential, have not been widely implemented in practice. For example, the swift scanning of crash accident sites could minimize road closures time periods. Previous research related to road accident site investigation [30] include the application of UAV drones for data collection on site of the accident. Their conclusion is that they bring progress in terms of the time needed to record the scene of the accident, but problems related to the presence of illumination poles, overhead electricity and telecommunication lines, as well as road-side trees, may present challenges for accident investigators, especially in urban areas. Furthermore, that research found that higher altitudes of UAV result in lower image resolution, potentially diminishing the overall accuracy of the data. On the other hand, combination of technologies like in this paper which includes MMS and high speed terrestrial laser scanner would

potentially eliminate identified problems in applying consumer level UAV in order to increase the speed of scene investigation, and to prevent long road traffic closures. In addition, the technology like applied here is more likely to be faster than the time measured in previous research related to this issue.

Similarly, roads could be monitored to detect potholes, swelling, and rotting, thereby enabling the early identification and remediation of potential defects.

5 ADVANTAGES WHICH MAKE THESE TECHNOLOGIES COMBINATION A REAL GAME CHANGER

Mobile Mapping Systems (MMS) and Ground Penetrating Radar (GPR) work in tandem to provide detailed surface and subsurface data. This is crucial for projects requiring detailed geological assessments or for locating underground utilities without excavation.

Underwater robots and airborne geomagnetics play a pivotal role in exploring and monitoring aquatic and remote terrains, which are often inaccessible to traditional survey methods.

Multi-spectral cameras and airborne echo sounders facilitate the analysis of environmental conditions by capturing data across different wavelengths, thus providing insights into vegetation health, water quality, and other critical environmental indicators.

The integration of advanced remote sensing technologies significantly enhances the efficiency and environmental sustainability of large-scale projects. These technologies facilitate rapid and accurate data collection, which minimizes the environmental impact typically associated with extensive physical surveys. For example, the use of mobile mapping systems and multi-spectral cameras allows for precise data acquisition without the need for disruptive land-based activities, thereby preserving natural habitats and reducing carbon footprints.

They are cost efficient, because implementing these technologies can lead to substantial cost savings by reducing the need for physical inspections and the associated labor and travel expenses. There is a potential for developing a new method for continuous geodetic monitoring of transport infrastructure development and maintenance, which can now be dynamic due to an affordable data collection.

In a project-oriented economy, this technology combination is making a real contribution in time efficiency as well. Projects in regions with harsh climates or limited survey windows benefit immensely from these technologies. For instance, in projects with stringent administrative deadlines, the integration of geodetic equipment with this technology accelerates data collection, ensuring projects stay on schedule.

The ability to gather precise data in challenging outside conditions without physical intrusion makes remote sensing technologies particularly valuable. This is evident in tasks like air-pollution detection and the exploration of underground structures, where traditional methods might falter.

6 CONCLUSION

Implementing remote sensing technologies in large-scale projects involves complex challenges that require strategic solutions. One of the primary hurdles is the integration of various sensors and systems. These technologies, although powerful individually, must be synchronized to work seamlessly together which is believed to be the greatest challenge for successful utilization. This synchronization ensures that the data collected is coherent and can be processed efficiently. The proposed technology combination can provide the solution which fills the gaps identified in the Introduction. The confirmation of this is in the fact that with shown set of instruments, the operator is able to collect the spatial data above ground, underground, concrete data and abstract data (air-pollution detection with Sniffer4D), accessible areas as well as inaccessible areas, and with desirable accuracy to meet the strict requirements of engineering applications as well (now with subcentimeter accuracy for large area and rapid data collection). This could be called a total spatial data collection, such as desired in Digital Twins applications.

Advanced remote sensing technologies are becoming indispensable in the realm of large-scale infrastructure projects. Their application significantly enhances the efficiency and accuracy of projects such as road constructions, tunnels, and extensive cross-regional infrastructure developments. The future announced initiatives at the state level for the establishment of various spatial databases, harmonization of spatial planning documents and their digitization, as well as tackling the integrity of cadastral and land registry records for the entire territory of the Republic of Croatia through large projects financed by the EU, not only that they promise business opportunities for the application of this combination of technologies, but also set the basis and necessity for the application of advanced technologies and new processes in geodetic tasks so that all national plans and priorities in this area can be realized on time.

The future work should address the analysis and development of a specific workflow for combination of the mentioned technologies, considering the development of Unified Modelling Activity Diagram (UML), or a process diagram to achieve a standard operating procedures for different case scenarios of data collection. This can include scenarios for different phases of infrastructure development, i.e. design phase, construction phase, and maintenance phase, but also for different infrastructure facilities and objects.

7 REFERENCES

[1] El-Sheimy, N. (2005). An overview of mobile mapping systems. Proceedings of the FIG Working Week (pp. 16-21).

[2] https://www.mdpi.com/journal/remotesensing/special_issues/GPR_RS, accessed 9.6.2024.

[3] Kim, G.-H., Sohn, H.-G. & Song, Y.-S. (2006). Road Infrastructure Data Acquisition Using a Vehicle-Based Mobile Mapping System. *Computer-Aided Civil and Infrastructure Engineering, 21*(5), 346-356. https://doi.org/10.1111/j.1467-8667.2006.00441.x

[4] Ishikawa K., Amano Y., Hashizume T. & Takiguchi J. (2007). A study of precise road feature localization using mobile

mapping system. *IEEE/ASME International conference on advanced intelligent mechatronics*, Zurich, Switzerland, 1-6. https://doi.org/10.1109/AIM.2007.4412541
[5] Sairam, N., Nagarajan, S. & Ornitz, S. (2016). Development of Mobile Mapping System for 3D Road Asset Inventory. *Sensors, 16*, 367. https://doi.org/10.3390/s16030367
[6] Di Stefano, F., Cabrelles, M., García-Asenjo, L., Lerma, J. L., Malinverni, E. S., Baselga, S., Garrigues, P. & Pierdicca, R. (2020). Evaluation of Long-Range Mobile Mapping System (MMS) and Close-Range Photogrammetry for Deformation Monitoring. A Case Study of Cortes de Pallás in Valencia (Spain). *Appl. Sci., 10*, 6831. https://doi.org/10.3390/app10196831
[7] Elhashash, M., Albanwan, H. & Qin, R. (2022). A Review of Mobile Mapping Systems: From Sensors to Applications. *Sensors, 22*, 262. https://doi.org/10.3390/s22114262
[8] Wai-Lok Lai, W., Dérobert, X., & Annan, P. (2018). A review of Ground Penetrating Radar application in civil engineering: A 30-year journey from Locating and Testing to Imaging and Diagnosis. *NDT & E International, 96*, 58-78. https://doi.org/10.1016/j.ndteint.2017.04.002
[9] Fauchard, C., Derobert, X., Cariou, J. & Cote, P. (2003). GPR performances for thickness calibration on road test sites. *NDT & E International, 36*, 67-75. https://doi.org/10.1016/S0963-8695(02)00090-7
[10] Varela-González, M., Solla, M., Martínez-Sánchez, J. & Arias, P. (2014). A semi-automatic processing and visualisation tool for ground-penetrating radar pavement thickness data. *Autom Constr, 45*, 42-29. https://doi.org/10.1016/j.autcon.2014.05.004
[11] Zhao, S. & Al-Qadi, I. L. (2016). Development of an analytic approach utilizing the extended common midpoint method to estimate asphalt pavement thickness with 3-D ground-penetrating radar. *NDT & E International, 78*, 29-36. https://doi.org/10.1016/j.ndteint.2015.11.005
[12] Diamanti, N. & Redman, D. (2012). Field observations and numerical models of GPR response from vertical pavement cracks. *J Appl Geophys, 81*, 106-116. https://doi.org/10.1016/j.jappgeo.2011.09.006
[13] Solla, M., Lagüela, S., González-Jorge, H. & Arias, P. (2014). Approach to identify cracking in asphalt pavement using GPR and infrared thermographic methods: preliminary findings. *NDT & E International, 62*, 55-65. https://doi.org/10.1016/j.ndteint.2013.11.006
[14] Birken, R. & Oristaglio, M. (2014). Mapping subsurface utilities with mobile electromagnetic geophysical sensor arrays. *Sens Technol Civil Infrastruct: Appl Struct Health Monit*, 347. https://doi.org/10.1533/9781782422433.2.347
[15] Plati, C. & Dérobert, X. (2015). Inspection procedures for effective GPR sensing and mapping of underground utilities and voids, with a focus to urban areas. *Civil engineering applications of ground penetrating radar*. Springer, 125-145. https://doi.org/10.1007/978-3-319-04813-0_5
[16] Official Gazette: Multi-year cadastral measurements program of construction areas for period 2021.-2030. (OG 109/21)
[17] Official Gazette: Regulation on mass real estate valuation (OG 28/19)
[18] Tomić, H. (2010). Geospatial Data Analysis in Purpose of Real Estate Valuation in Urban Areas. *Doctoral Thesis*, Faculty of Geodesy, University in Zagreb.
[19] https://fondovieu.gov.hr/pozivi/93, accessed 25.6.2024.
[20] Csanyi, N. & Toth, C. K. (2006). LiDAR data accuracy: The impact of pulse repetition rate. *Proceedings of MAPPS/ASPRS 2006 Fall Conference*.
[21] San José Alonso, J. I., Martínez Rubio, J., Fernández Martín, J. J. & García Fernández, J. (2012). Comparing time-of-flight and phase-shift. The survey of the Royal Pantheon in the Basilica of San Isidoro (León). *The International Archives of the Photogrammetry, Remote Sensing and Spatial Information Sciences, 38*, 377-385. https://doi.org/10.5194/isprsarchives-XXXVIII-5-W16-377-2011
[22] Official Gazette: Rulebook on Cadastral Survey (OG 59/20)
[23] Jol, H. M. (2009). Ground Penetrating Radar Theory and Applications. Elsevier B. V. All https://doi.org/10.1016/B978-0-444-53348-7.X0001-4
[24] https://ispu.mgipu.hr/, accessed 25.6.2024.
[25] http://top-green.com.hr/doc/strategija_zou_opcine_topusko.pdf, accessed 14.11.2024.
[26] https://www.samobor.hr/dokumenti/download/6545, accessed 14.11.2024.
[27] https://www.novalja.hr/db/db_dir/news/extra_dir/201120238416/strategija_zuo_grad_novalja.pdf/, accessed 14.11.2024.
[28] https://mpgi.gov.hr/UserDocsImages/dokumenti/NPOO/ZUO_NPOO/Smjernice_Strategija_ZUO_2.0.pdf, accessed 14.11.2024.
[29] Zio, E. & Miqueles, L. (2024). Digital twins in safety analysis, risk assessment and emergency management. *Reliability Engineering & System Safety, 246*. https://doi.org/10.1016/j.ress.2024.110040
[30] Vida, G., Melegh, G., Süveges, Á., Wenszky, N. & Török, Á. (2023). Analysis of UAV Flight Patterns for Road Accident Site Investigation. *Vehicles, 5*, 1707-1726. https://doi.org/10.3390/vehicles5040093

Authors' contacts:

Josip Lisjak, PhD
(Corresponding author)
TEMPO savjetovanje d.o.o.,
Hrvatskih branitelja 14, HR-34000 Požega, Croatia
E-mail: josip.lisjak@temposavjetovanje.hr

Matej Petrinović, MSc
Geometricus d.o.o.,
Ferovac 32, HR-34340 Kutjevo, Croatia
E-mail: matej.petrinovic@geometricus.hr

Stjepan Keleminec, MSc
Geometricus d.o.o.,
Ferovac 32, HR-34340 Kutjevo, Croatia
E-mail: stjepan.keleminec@geometricus.hr

ISSN 1846-6168 (Print), ISSN 1848-5588 (Online)
https://doi.org/10.31803/tg-20241004154503

Professional paper
Received: 2024-10-04, Accepted: 2024-10-21

A Model-Driven Architecture Solution for Multi-Platform Mobile App Development

Ayoub Korchi*, Mohamed Karim Khachouch, Younes Lakhrisi

Abstract: This paper presents a comprehensive Model Driven Architecture (MDA) approach for multi-platform mobile app development. We introduce a UML-based metamodel that encapsulates essential mobile app elements, including views, controls, resources, and events. Our approach leverages the Acceleo code generation tool to transform Platform Independent Models (PIMs) adhering to this metamodel into platform-specific source code. We demonstrate the effectiveness of our method through a case study, generating Android user interface code from a sample PIM. The results show that our approach can significantly streamline the development process for multi-platform mobile apps, reducing the need for platform-specific coding. This work contributes to the field of model-driven mobile development by providing a flexible and extensible framework for automatic code generation across multiple mobile platforms.

Keywords: Cross-platform; MDA; Mobile-development

1 INTRODUCTION

Smartphones have evolved over the years to become essential companions, incorporating a wide range of applications that simplify our daily lives. Since their emergence in the early 2000s [1], smartphone sales have seen exponential growth. In 2007, the year the iPhone was launched, around 122 million smartphones were sold worldwide [2, 3]. By 2023, this number had surged to over 1.3 billion units [4], highlighting the ubiquity of smartphones and the significance of mobile applications in our routines.

However, the proliferation of smartphones comes with the challenge of mobile platform diversity, which has led to the rise of cross-platform development. Each mobile operating system has its own specific programming languages and development tools, making native app development for each platform complex and costly [5]. This technical diversity requires developers to manage multiple development environments and maintain separate codebases, increasing the risk of inconsistencies and bugs.

To address this diversity, cross-platform development has emerged as a solution, allowing developers to create an application once and deploy it on multiple platforms like Android and iOS [6]. Cross-platform development can be implemented through various approaches such as compilation, interpretation, component-based methods, cloud solutions, or hybrid approaches. Among these, Model-Driven Architecture (MDA) is particularly noteworthy for its ability to abstract platform complexity, providing a more adaptable solution for developers.

Model-Driven Architecture (MDA), developed by the Object Management Group (OMG), is a software development approach based on the principle of separating application functionality from platform-specific implementation details. MDA focuses on creating Platform Independent Models (PIMs) that capture application functionality, which can then be automatically transformed into Platform-Specific Models (PSMs) and executable code. This method enables consistent and efficient code generation across various platforms, reducing development time and enhancing maintainability [7].

In our approach to mobile application development, we leverage MDA to automate source code generation, transforming PIMs into PSMs specific to each target platform. This automation reduces the development effort required for each platform, while ensuring code consistency and allowing flexibility for platform-specific adaptations.

The main objectives of this research are to explore the potential of MDA for streamlining mobile app development and to provide a framework that enhances efficiency and maintainability. The primary contributions of this work include a comprehensive UML-based metamodel for mobile applications, the implementation of an Acceleo-based code generation framework, and a demonstration of our solution through a case study, which illustrates the automatic generation of an Android user interface from a sample PIM model.

This article is structured as follows: Section 2 presents a literature review of existing cross-platform solutions and the background of MDA. Section 3 outlines the research methodology, including a description of the MDA approach, the proposed metamodel, and the Acceleo tool. Section 4 provides a case study demonstrating our solution, and Section 5 concludes with perspectives for future work.

2 LITERATURE REVIEW

To systematically review existing literature on model-driven mobile application development, we utilized the Kitchenham method [8, 9], a structured approach in software engineering for collecting, analyzing, and synthesizing data. This method involves three main phases: planning, execution, and reporting (Fig. 1). During the planning phase, we established research questions, search protocols, and criteria for study inclusion and exclusion. The execution phase entailed a comprehensive search across various databases, selecting relevant studies, assessing quality, and extracting key data. Finally, in the reporting phase, we synthesized findings to present a thorough overview, highlighting gaps and establishing a foundation for our research.

Our study centers on the Model-Driven Architecture (MDA) approach to mobile source code generation, which has become a crucial area due to the increasing demand for robust, maintainable, and scalable mobile applications. The MDA methodology supports mobile development by enabling developers to create high-level models that can be

automatically transformed into platform-specific code. This capability facilitates consistency between specifications and implementation, minimizes human error, and accelerates development. However, MDA presents challenges such as complex transformations, platform diversity, and integration with existing development tools. Our research questions, therefore, seek to identify the main models, methodologies, tools, benefits, limitations, and empirical results related to MDA in mobile application development.

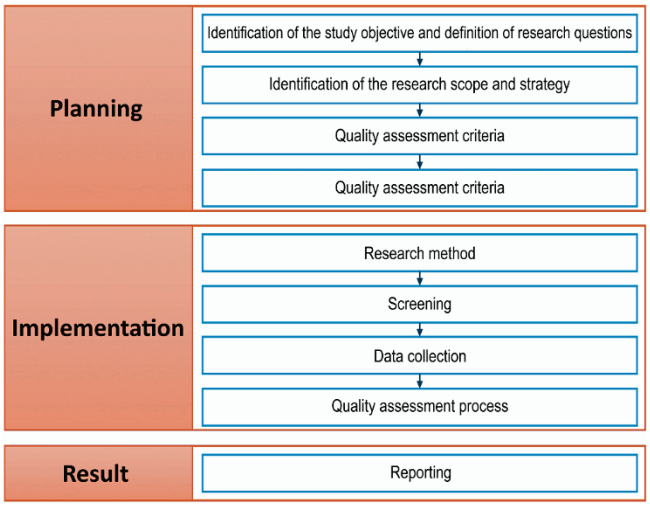

Figure 1 Kitchenham's SLR process

2.1 Research Questions

- What are the main models and methodologies used for generating mobile source code with MDA?
- What tools and development environments support this code generation?
- What are the advantages and limitations of using MDA for mobile code generation?
- What empirical studies and practical results have been documented on the effectiveness of this approach?
- What best practices and challenges have been encountered in implementing MDA for mobile applications?

2.2 Research Objectives

- Provide a comprehensive overview of the models and methodologies for mobile code generation using MDA.
- Identify available tools and development environments.
- Analyze the benefits, limitations, and challenges of this approach.
- Synthesize existing empirical results on the effectiveness of MDA.

2.3 Inclusion Criteria

- Articles published between 2000 and 2023.
- Studies focused on mobile code generation using MDA.
- Peer-reviewed journal and conference publications.
- Articles written in English.

2.4 Exclusion Criteria

- Non-peer-reviewed studies (e.g., white papers, blogs).
- Publications irrelevant to mobile code generation or not using MDA.
- Incomplete articles or those lacking concrete experimental data.

2.5 Data Sources

- Academic databases: IEEE Xplore, ACM Digital Library, SpringerLink, ScienceDirect, Google Scholar.
- Conference proceedings and journals focused on software engineering, modeling, and mobile development.

2.6 Search Strategy

- Formulating search queries with keywords like "Model-Driven Architecture", "MDA", "code generation", "mobile applications", "model-to-code", "source code generation".
- Applying time (2000-2023) and language (English) filters to refine results.
- Conducting manual searches in selected study bibliographies to identify additional relevant articles (snowball approach).

2.7 Metamodeling Approaches in MDA for Mobile Applications

Various studies emphasize the role of metamodels in the MDA framework. Metamodels provide the structure for Platform Independent Models (PIMs) and support the transformation into Platform Specific Models (PSMs). For example, [10] proposed a metamodel to design Android GUIs through UML object diagrams. Similarly, [11] utilized domain-specific languages (DSLs) to define the PIM, facilitating transformations to PSMs for Android. These approaches establish consistency in PIM-to-PSM transformations but often introduce additional complexity in terms of learning requirements and modeling expertise.

More recent works, such as [12], have extended this research by systematically reviewing MDA-based mobile development frameworks. Their study identifies recurring metamodeling approaches and highlights the need for adaptable frameworks capable of handling rapidly evolving mobile technologies. Our work contributes by offering a more streamlined metamodeling process, emphasizing ease of use and maintainability.

2.8 Code Generation Techniques

Code generation is a core aspect of MDA and is facilitated through various transformation languages and tools. Earlier works, such as [13], implemented transformations using QVT for M2M and Acceleo for M2T, generating Android-specific code. The Acceleo tool, in particular, supports the model-to-text (M2T) transformation essential for generating XML layouts and Java code. However, defining and maintaining transformation rules

often require specialized skills, as noted by [14].

Newer methodologies incorporate tools like Xtend, as used by authors in [15], who demonstrated an Android development approach based on MDA with flexible and efficient M2T transformations. These approaches, however, remain limited in platform coverage and frequently require substantial manual intervention. Our work seeks to minimize these issues by using Acceleo templates that streamline transformation steps and reduce the need for extensive tool proficiency.

2.9 Platform Coverage and Portability

Cross-platform support remains a significant motivation behind MDA approaches. Authors in [16] explored platform variability in MDA through role-based app development for both Android and iOS, highlighting the need for adaptable frameworks. However, these solutions tend to concentrate on UI elements, often neglecting aspects such as sensor integration, event handling, and complex data management, which limits their applicability for complete mobile applications. Our approach addresses these gaps by proposing a metamodel capable of supporting various platform-specific features while ensuring consistency across platforms.

2.10 Synthesis of Gaps in Existing Research

While existing studies have advanced MDA-based mobile application development, several gaps persist:

- **Complexity in Transformation:** Current solutions require specialized knowledge of transformation languages and tools (e.g., QVT, ATL), making them challenging to adopt for general developers. Our solution addresses this by simplifying the transformation process with predefined Acceleo templates.
- **Platform-Specific Limitations:** Many MDA approaches primarily focus on Android and lack support for other mobile platforms. Our work expands on these limitations by proposing a metamodel that allows for easy extension to other platforms.
- **Partial Coverage of Application Components:** Previous studies primarily address UI elements, leaving out critical functionalities like sensor integration, event handling, and advanced resource management. Our approach integrates these aspects into the metamodel to enable a more holistic mobile development process.

By addressing these gaps, our solution aims to provide a more accessible, efficient, and robust framework for MDA-based mobile development, enabling a streamlined transition from high-level models to platform-specific implementations.

3 RESEARCH METHODOLOGY

Our solution is founded on the MDA methodology, so the initial subsection will offer a comprehensive review of this approach, highlighting its strengths and weaknesses. We will then present the source metamodel we have developed, which plays a pivotal role in our work. This metamodel is essential to ensuring consistency when creating the platform-independent model. Lastly, we will display the Acceleo tool, which enabled us to directly generate native code from the platform-independent model.

3.1 MDA Approach

Model-Driven Architecture (MDA) is a software development approach that emphasizes the creation of abstract models and their transformation into executable code. This approach is based on the principle of separation of concerns, where high-level aspects of the application are modeled independently of the underlying technology. There are three levels of models: Conceptual Independent Model (CIM), Platform-Independent Model (PIM), and Platform-Specific Model (PSM), which ultimately leads to the generation of source code [17] [18] [19].

The Computation-Independent Model (CIM) is the first crucial step in the Model-Driven Architecture (MDA) software development process. By capturing business requirements in an abstract and general way, the CIM provides a solid foundation for the further development of the application while ensuring its independence from technical implementation details [20].

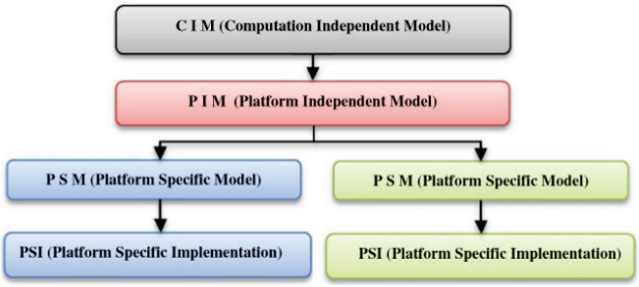

Figure 2 Model levels in the MDA approach

The Platform-Independent Model (PIM) represents an important intermediate stage in the Model-Driven Architecture (MDA) software development process. By offering a detailed yet generic representation of the application's functionality, the PIM allows the transition from the abstract business needs defined in the CIM to more concrete software specifications, while still preserving independence from specific implementation technologies [21].

The Platform-Specific Model (PSM) is a critical stage in the Model-Driven Architecture (MDA) software development process. By adapting the PIM models to meet the specific requirements of the target platform, the PSM enables the automatic generation of optimized, executable code tailored to the deployment platform.

Code generation within the Model-Driven Architecture (MDA) enables the efficient conversion of the Platform-Specific Model (PSM) into executable source code for the target platform. This automated process ensures consistency, quality, and efficiency in the generated code, while also facilitating the maintenance and evolution of the software application.

Model transformation is a key step in the Model-Driven Architecture (MDA) software development process. By converting models from one level of abstraction to another, this transformation helps create more detailed or platform-specific representations of the software application, ensuring consistency and quality in the results [22].

The MDA approach relies on the creation of platform-independent models (PIM) as a starting point, allowing the separation of design from technical implementation details. The PIMs are then transformed into platform-specific models (PSM), which allows the same model to be adapted to different technologies. This transformation can lead to automatic code generation, accelerating the development process and facilitating portability across various technical environments [23, 24].

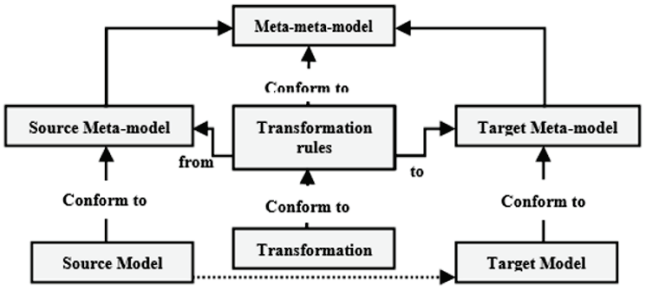

Figure 3 MDA Transformation process

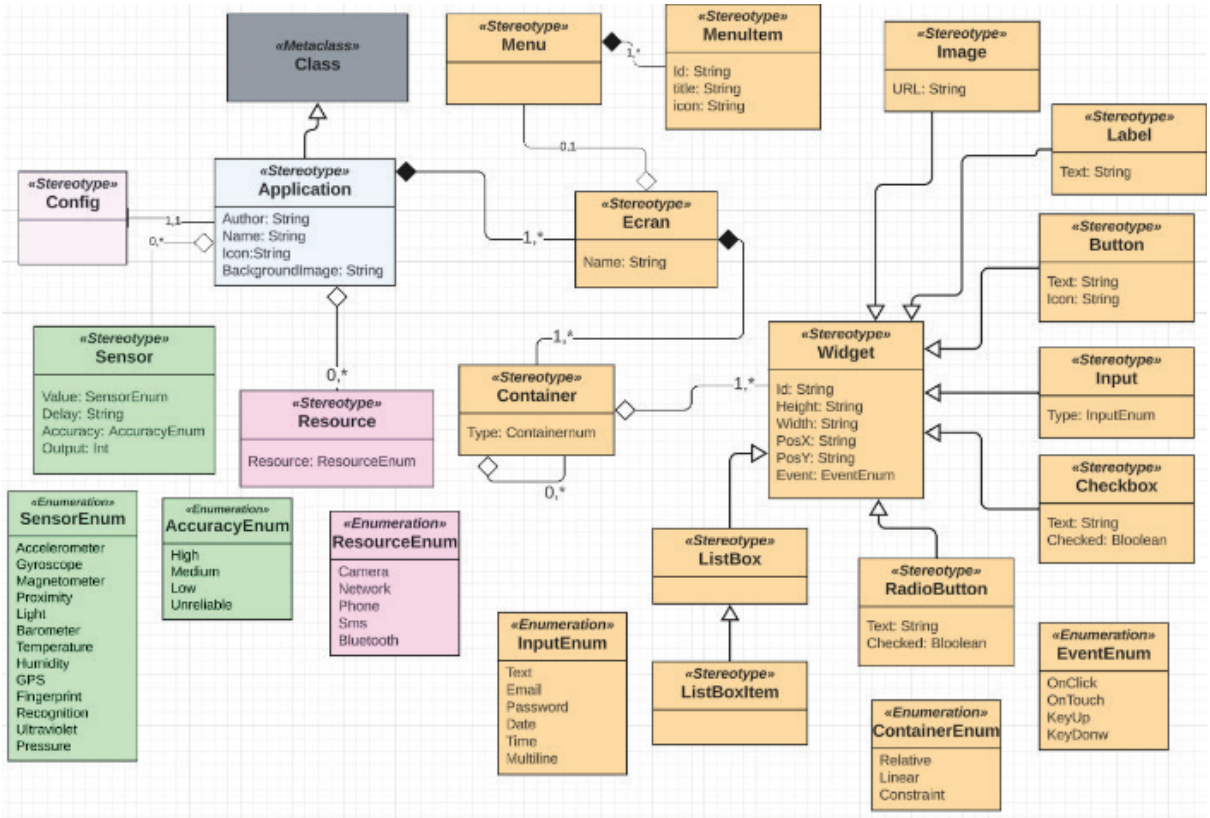

Figure 4 Proposed source metamodel

3.2 Source Meta-model

This metamodel, implemented as a UML profile, captures the essential elements required for mobile application development. UML (Unified Modeling Language) is widely recognized and supported across various development tools, making it an ideal choice for modeling complex systems in a standardized manner.

At the core of the UML profile, the Application entity is defined with attributes such as author, name, and background image, which represent general information about the mobile application. The Screens (or pages) within the application contain Containers (Layouts) and Widgets, which are crucial for creating a flexible user interface. The Widgets are interactive elements such as buttons, labels, checkboxes, input fields, and lists (ListBox), each with specific attributes like ID, size, position, and associated events (e.g., onClick or onTouch). These elements correspond to essential UI components in Android, such as Button, TextView, EditText, and Spinner.

Justification of Key Metamodel Elements:

- Menus and MenuItems: Menus structure the application's navigation, enhancing user experience by allowing easy access to various functionalities. These elements correspond to Android's Menu and MenuItem components.
- Input Types and Layouts: Enumerations like InputEnum define input types (e.g., text, email, password) and ContainerEnum for layout types (e.g., relative, linear, constraint). This is critical for adapting UI elements to specific Android layouts, ensuring a flexible and adaptable design.
- Resources and Sensors: To support modern mobile app functionality, the metamodel incorporates resources such

as email, messaging, and camera, as well as Embedded Sensors like GPS, accelerometers, and proximity sensors. These elements facilitate interaction with the physical environment, enabling the development of applications that are context-aware and responsive to real-world changes.

The Tab. 1 summarizes key elements of the metamodel and their Android equivalents, providing an overview of how each component maps to the Android platform.

Table 1 Mapping between PIM and Android Code

Metamodel Element	Description	Android Equivalent
Application	General app information	N/A
Screen	UI Screen or Page	Activity/Fragment
Container	Layout for UI Elements	LinearLayout, RelativeLayout, ConstraintLayout
Widget - Button	Interactive button	Button
Widget - Label	Display text	TextView
Widget - Input	User input field	EditText
ListBox	Dropdown list	Spinner
Menu/MenuItem	Navigation structure	Menu, MenuItem
Sensor	Device sensor integration	SensorManager
Resource	Device functionality (e.g., camera)	Camera, TelephonyManager

3.3 PIM to PSM Transformation Process

The transformation from Platform Independent Model (PIM) to Platform Specific Model (PSM) is a critical step in the MDA approach. This process involves mapping abstract, platform-agnostic elements from the PIM to platform-specific components defined in the PSM, tailored to Android in our case.

- Modeling the Application in PIM: We start by defining the UI elements and application structure in the PIM, conforming to the source metamodel. Elements such as Screens, Containers, and Widgets are instantiated with specific attributes and relationships, creating a high-level representation of the application's structure.
- Transformation Rules with Acceleo: Using Acceleo, we define transformation rules that map each PIM element to its Android equivalent. For example:

Container elements in the PIM map to Android Layouts such as LinearLayout or ConstraintLayout.

Button widgets transform to Android's Button components with attributes like text, onClick, and layout properties.

Input Fields are translated to EditText with appropriate input types (e.g., text, password) from the InputEnum.

Acceleo templates define these rules, ensuring that attributes like ID, size, and event handling are faithfully converted to platform-specific implementations.

Generation of Platform-Specific Code: The PSM is processed by Acceleo's M2T (model-to-text) transformation capabilities, generating the final Android XML layout files and Java classes. The transformation ensures fidelity to the Android platform while maintaining alignment with the original model design. Generated files, such as AndroidManifest.xml and the XML layout files, are structured according to Android's requirements, providing a ready-to-use code base for the application.

Fig. 5 is a flowchart illustrating the steps from metamodel creation to code generation.

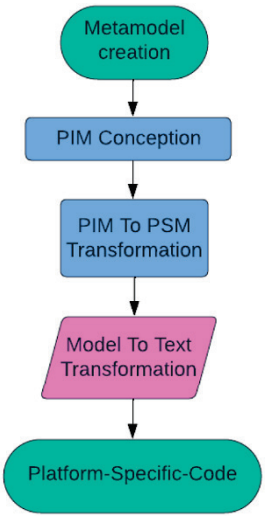

Figure 5 steps of platform-specific-code generation

3.4 Acceleo Tool

Acceleo is an open-source code generation tool within the Eclipse ecosystem, primarily used in the Model-Driven Architecture (MDA) approach to generate source code from models. It is based on the MOF Model to Text Transformation (MTL) standard from the Object Management Group (OMG), making it compatible with other UML-based modeling tools.

Key Features of Acceleo:

- Code Generation Language: Acceleo uses its own transformation language, inspired by the Object Constraint Language (OCL), allowing complex logic and expressions to define rules for generating code from models.
- Eclipse Integration: Acceleo is integrated with the Eclipse environment, making it easy to use with other modeling tools like the Eclipse Modeling Framework (EMF) and Papyrus for UML.
- Support for Multiple Languages: While often used for Java code generation, Acceleo can generate code in other languages such as C++, Python, or PHP, depending on project needs.
- EMF Model Support: Acceleo works with EMF models, making it ideal for code generation in the MDA context.

Acceleo generates source code from PSMs (Platform-Specific Models) based on predefined rules, enabling quick implementation of software systems from models. It allows customization of the generated code through its transformation language, letting developers create templates and rules for flexible code generation. Acceleo can also be integrated into automated development processes, such as continuous integration pipelines, to automatically generate code from updated models.

Advantages of Acceleo for MDA:

- Reduced Development Time: By generating code from models, Acceleo shortens the time from design to implementation.
- Flexibility and Customization: Its transformation language enables highly customizable code generation, adaptable to various platforms and technologies.
- Eclipse Ecosystem Integration: Being part of Eclipse, Acceleo works seamlessly with other modeling tools, supporting consistent MDA workflows.
- Support for Multiple Programming Languages: Acceleo's ability to generate code in different languages makes it versatile for various project types.

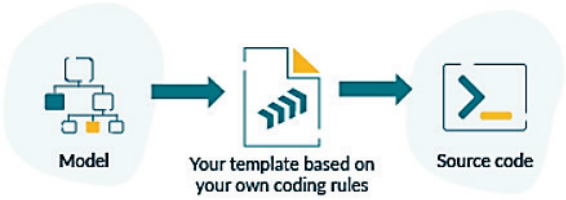

Figure 6 Acceleo process

Using Acceleo, our solution consists of three steps. Firstly, we develop a platform-independent-model conform to our source meta-model. This Platform-independent-model models the UI component of an application. Then, we create an Acceleo template, which defines how the target code should be generated from the input platform-independent-model. Finally, Acceleo processes the platform-independent-model with the template created, generating the platform-specific code. The following figure shows the Acceleo process according to Eclipse Foundation, 2021.

3.5 Results and Discussion

In this section, we will present a step-by-step demonstration of our solution using a case study. For this case study, we have selected an Android application that allows adding a new book to the library database. This application will consist of two graphical interfaces: the first will be dedicated to authentication, and the second will serve for adding a new book to the database. The latter will include a title, a label and a text field for the book's name, a label and a text field for the author's name, a label and a text field for the publisher's name, and a label and a number field for the number of copies. It will also contain two buttons to either submit or cancel the form. Based on this test case description, the platform-independent models must conform to the previously presented metamodel. Then, each element will be transformed into its equivalent in the Android-specific models using the ATL language, and finally, source code will be generated using Acceleo templates.

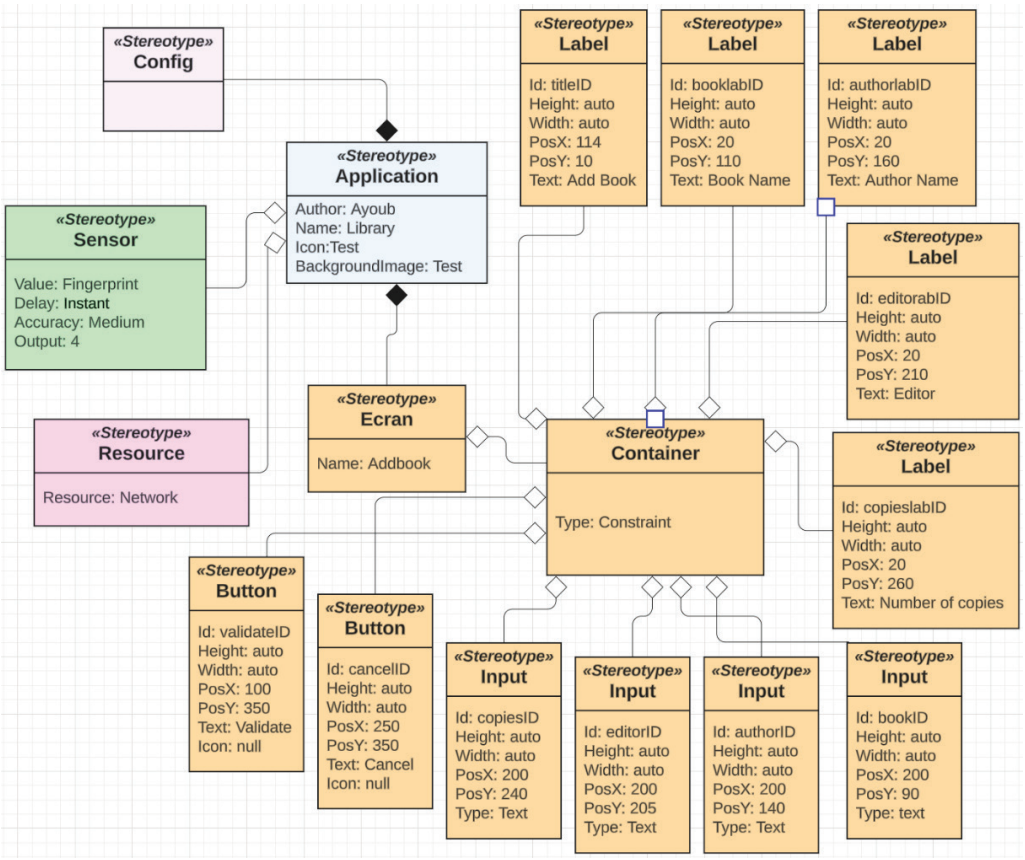

Figure 7 PIM of Add book interface

The platform-independent model of this interface will consist of a title, a label and a text field for the book's name, a label and a text field for the author's name, a label and a text field for the publisher's name, as well as a label and a number

field for the number of copies. It also includes two buttons to either submit or cancel the form. The following figure represents the platform-independent model incorporating the aforementioned user interface elements to create this Android interface for adding a new book. This platform-independent model conforms to the previously presented metamodel.

The following model represents the PSM (Platform-Specific Model) of the Add book interface for the Android platform, which was generated from the PIM (Platform Independent Model) shown above through a transformation performed using the ATL (Atlas Transformation Language). Here is a detailed description of the elements that make up this model.

Using an Acceleo template, we generate the AndroidManifest file, which is the configuration file of the Android application. We also generate the view XML file by transforming each component of this platform-independent-model to each equivalent in the android user interface.

The code is written in Acceleo Query Language, which allows navigating and querying input model within templates defined by Acceleo (Eclipse Foundation, 2021). As we mentioned above, Acceleo is a powerful tool for generating code from models, streamlining development processes, and ensuring consistency across projects, based on templates. The template takes the platform-independent-model as input. It transforms each element and its attributes to their android equivalent component. For example, this template transforms the label element to the TextView component, it transforms the width attribute in the PIM to the layout width in the Android code. It also affects the values of each element' attribute to its Android equivalent.

The following Fig. 9 shows a part of the template code.

Once the template is executed, two files are generated, the AndroidManifest and the XML view files, following the transformation rules defined in the Acceleo template as it shown in the figures above. This file represents a model-to-text transformation between Configuration class modeled in the platform-independent-model and the AndroidManifest.xml file with its contents as it shown in the Fig. 11.

The template also generates the XML file of Android UI. The following Fig. 10 shows an extract of the XML view file containing android component generated from the platform-independent-model presented above such as: the constraint layout which corresponds to the container in the PIM, the EditText which corresponds to the text Input in the PIM, etc.

In order to visualize our solution result, we create an application on Android Studio. We drug & drop these two files: android manifest and xml view file in their corresponding folders, before running the application to visualize the result. The following Fig. 12 shows the result interface containing elements modeled in the platform-independent-model and transformed to android code using the Acceleo template.

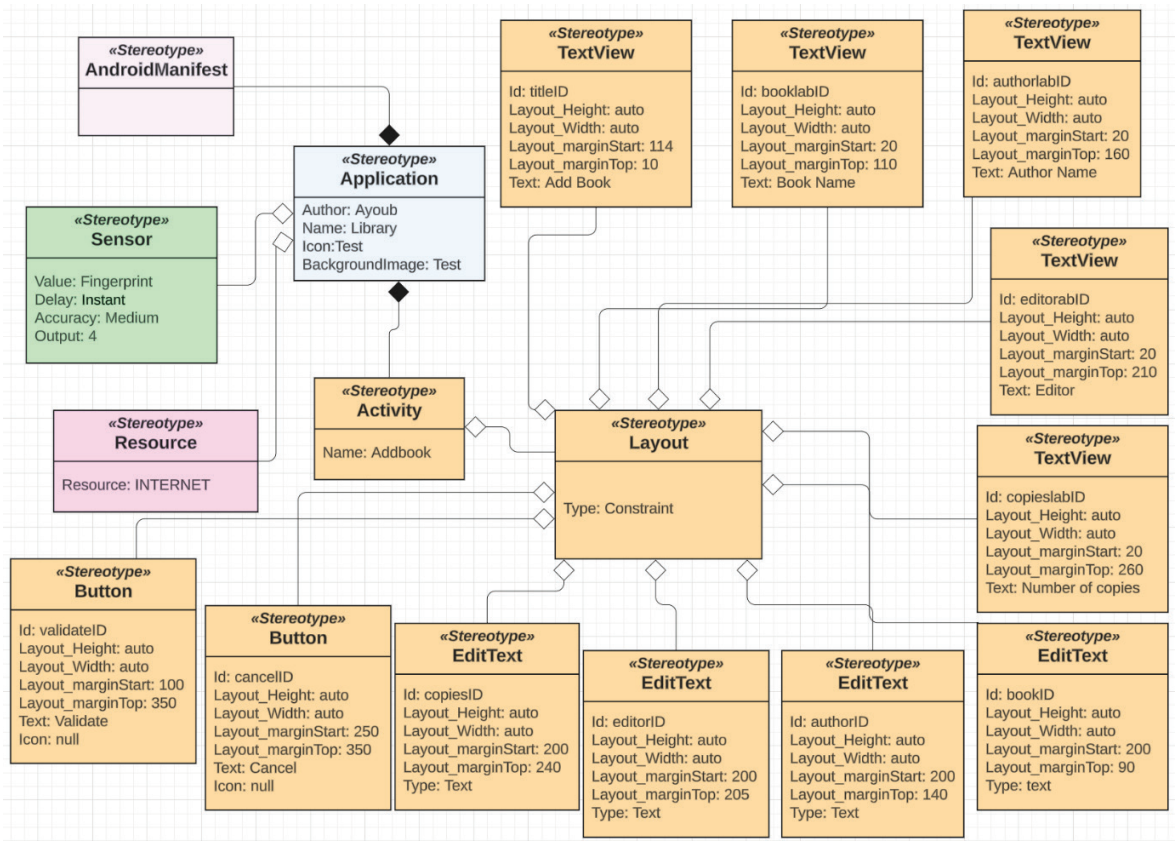

Figure 8 PSM generated from the PIM

generate.mtl × AndroidManifest.xml activity_main.xml class diagram

```
[/if]
[if (anEClass.name.equalsIgnoreCase('Label'))]
    [file ('activity_main.xml', true, 'UTF-8')]
<TextView
    android:id="@+id/[anEClass.eAllAttributes->at(1).defaultValue.toString()/]"
    android:layout_width="[anEClass.eAllAttributes->at(2).defaultValue.toString()/]"
    android:layout_height="[anEClass.eAllAttributes->at(3).defaultValue.toString()/]"
    android:text="[anEClass.eAllAttributes->at(4).defaultValue.toString()/]"
    android:layout_marginStart="[anEClass.eAllAttributes->at(5).defaultValue.toString()/]dp"
    android:layout_marginTop="[anEClass.eAllAttributes->at(6).defaultValue.toString()/]dp" />
    [/file]
[/if]
[if (anEClass.name.equalsIgnoreCase('Input'))]
    [file ('activity_main.xml', true, 'UTF-8')]
<EditText
    android:id="@+id/[anEClass.eAllAttributes->at(1).defaultValue.toString()/]"
    android:layout_width="[anEClass.eAllAttributes->at(2).defaultValue.toString()/]"
    android:layout_height="[anEClass.eAllAttributes->at(3).defaultValue.toString()/]"
    android:layout_marginStart="[anEClass.eAllAttributes->at(6).defaultValue.toString()/]dp"
    android:layout_marginTop="[anEClass.eAllAttributes->at(7).defaultValue.toString()/]dp"
    android:inputType="[anEClass.eAllAttributes->at(5).defaultValue.toString()/]"
    android:text="[anEClass.eAllAttributes->at(4).defaultValue.toString()/]" />
    [/file]
[/if]
[if (anEClass.name.equalsIgnoreCase('ListBox'))]
    [file ('activity_main.xml', true, 'UTF-8')]
<Spinner
    android:id="@+id/[anEClass.eAllAttributes->at(1).defaultValue.toString()/]"
    android:layout_width="[anEClass.eAllAttributes->at(2).defaultValue.toString()/]"
    android:layout_height="[anEClass.eAllAttributes->at(3).defaultValue.toString()/]"
    android:layout_marginStart="[anEClass.eAllAttributes->at(4).defaultValue.toString()/]dp"
    android:layout_marginTop="[anEClass.eAllAttributes->at(5).defaultValue.toString()/]dp" />
    [/file]
[/if]
[if (anEClass.name.equalsIgnoreCase('Button'))]
    [file ('activity_main.xml', true, 'UTF-8')]
<Button
    android:id="@+id/[anEClass.eAllAttributes->at(1).defaultValue.toString()/]"
    android:layout_width="[anEClass.eAllAttributes->at(2).defaultValue.toString()/]"
```

Figure 9 Template code

activity_main.xml × generate.mtl AndroidManifest.xml class diagram

```
<?xml version="1.0" encoding="utf-8"?>
<androidx.coordinatorlayout.widget.CoordinatorLayout xmlns:android="http://schemas.android.com/apk/res/android"
    xmlns:app="http://schemas.android.com/apk/res-auto"
    xmlns:tools="http://schemas.android.com/tools"
    android:layout_width="match_parent"
    android:layout_height="match_parent"
    android:fitsSystemWindows="true"
    tools:context=".MainActivity">

<androidx.constraintlayout.widget.ConstraintLayout
        android:layout_width="match_parent"
        android:layout_height="match_parent">

<TextView
    android:id="@+id/titleid"
    android:layout_width="wrap_content"
    android:layout_height="wrap_content"
    android:text="Add Book"
    android:layout_marginStart="114dp"
    android:layout_marginTop="10dp"
    app:layout_constraintStart_toStartOf="parent"
    app:layout_constraintTop_toTopOf="parent" />

<EditText
    android:id="@+id/booknamevalue"
    android:layout_width="wrap_content"
    android:layout_height="wrap_content"
    android:layout_marginStart="200dp"
    android:layout_marginTop="90dp"
    android:inputType="text"
    android:text="Book name"
    app:layout_constraintStart_toStartOf="parent"
    app:layout_constraintTop_toTopOf="parent" />

<TextView
    android:id="@+id/bookname"
    android:layout_width="wrap_content"
    android:layout_height="wrap_content"
    android:text="Book name"
```

Figure 10 Generated UI code

AndroidManifest.xml × activity_main.xml class diagram

```
<?xml version="1.0" encoding="utf-8"?>
<manifest xmlns:android="http://schemas.android.com/apk/res/android"
        xmlns:tools="http://schemas.android.com/tools">
    <application
        android:allowBackup="true"
        android:dataExtractionRules="@xml/data_extraction_rules"
        android:fullBackupContent="@xml/backup_rules"
        android:icon="@mipmap/ic_launcher"
        android:label="@string/"
        android:roundIcon="@mipmap/ic_launcher_round"
        android:supportsRtl="true"
        android:theme="@style/Theme.Test"
        tools:targetApi="31">
        <activity
            android:name=".MainActivity"
            android:exported="false"
            android:label="@string/title_activity_main"
            android:theme="@style/Theme.Test" />
         </application>

</manifest>

```

Figure 11 Generated Manifest

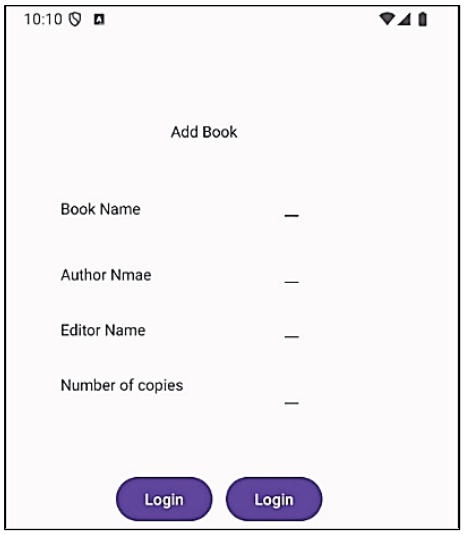

Figure 12 Android interface

This case study uses a PIM composed of multiples mobile components such as, View, Configuration, Container, Label, button, ListBox, input text and input number. This PIM respects our proposed source metamodel. Using Acceleo tool, we generate an AndroidManifest file, which is the configuration file of android applications and constitutes a model-to-text transformation between configuration class and the generated manifest file. We also generate an Android view code by transforming each component in the PIM to its equivalent android component. The layout tag refers to container class, TextView tags refer to Label classes, EditText tags refer to input classes, Spinner tag refers to ListBox class, and Button tags refers to Button classes. Until now, our solution allows to generate UI interface and not a mobile application that can be executed in different platforms, which needs some manual adaptations to create a mobile application and drug & drop the result code in the appropriate folder of the mobile application. In our future works, we will expand our source meta-model to respect mobile app creation with different folders.

3.6 Analysis of Generated Code

After executing the Acceleo template on the Platform-Independent Model (PIM), the generated code includes the AndroidManifest and XML layout files. Below is an in-depth analysis of the code:

- AndroidManifest.xml: This file specifies essential application metadata, permissions, and components, including Activities. The generated AndroidManifest aligns well with Android standards, specifying the main activity for launching the application and permissions for network access if specified in the PIM. The automatic generation of this file ensures consistency, as updates to the PIM automatically reflect changes here. However, additional permissions and services, such as location services or background processing, may require manual inclusion as these aspects are not fully automated in the current version of our model.
- XML Layout Files: The XML layout accurately represents the user interface described in the PIM. Each component is mapped to its Android equivalent:

Container to Layout Mapping: Containers defined in the PIM translate directly to layout components such as ConstraintLayout or LinearLayout in Android.

Widget to View Mapping: Each Widget (e.g., Labels, Buttons) is generated as its corresponding Android component (e.g., TextView, Button, EditText). Attributes like text, layout_width, layout_height, and event listeners such as onClick are defined according to the template's transformation rules.

The quality of the generated code is high, with a clear, organized structure that adheres to Android's recommended layout hierarchy. However, the generated code currently only supports basic UI components and lacks some advanced features like nested views or custom styles. Developers may need to make manual adjustments for more complex layouts or additional styling.

3.7 Comparison with Traditional Development Methods

Table 2 MDA vs Tradition development methods

Aspect	Traditional Development	Model-Driven Approach
Development Time	Requires manual coding of UI components, configuration, and repetitive tasks for layout and manifest files.	Significantly reduced due to automated generation from PIM, especially for simple UIs.
Consistency	High risk of inconsistencies due to manual updates across multiple files.	Maintained across the application since modifications are made directly in the PIM.
Adaptability	Changes in design require updates in multiple places (XML, Java/Kotlin files).	Adaptations are easier as updates to the PIM are automatically reflected in generated files.
Learning Curve	Requires knowledge of Android development tools and languages like Java/Kotlin.	Lower learning curve with Acceleo, especially for developers familiar with UML and MDA concepts.
Scalability	Manual coding becomes more time-consuming and error-prone as application complexity increases.	Model-driven approach may face challenges with complex applications due to limitations in model representation.

The model-driven approach generally accelerates the development process for basic UIs, saving time on manual coding and minimizing human error. However, for complex

applications with custom animations, extensive styling, or device-specific features, the model-driven approach may require substantial template customization or manual adjustments post-generation.

3.8 Challenges and Limitations with Complex Applications

While this approach is effective for simple to moderately complex applications, applying it to more sophisticated mobile applications present several challenges:

- Advanced UI Components: For complex user interfaces involving custom views, animations, and dynamic content, the current model may lack sufficient granularity. Extending the metamodel to support these components could make the process cumbersome and reduce template reusability.
- Integration with Native Android Features: Certain Android-specific features, such as fragments, services, and broadcast receivers, are not fully automated in the current version of the metamodel. Customizing the metamodel and transformation templates to support these features would increase the initial setup time and require in-depth knowledge of both Android and Acceleo's transformation language.
- Performance Optimization: Generated code may not always be optimized for performance, especially in terms of layout complexity and memory usage. In traditional development, developers can manually refine layout hierarchies to reduce memory footprint, which might not be as straightforward in a generated environment.
- Maintenance Over Time: As Android evolves, the model-driven approach needs frequent updates to the metamodel and transformation templates to stay compatible with the latest APIs and best practices. This adds a layer of ongoing maintenance that must be managed alongside the application development lifecycle.

4 CONCLUSION AND PERSPECTIVES

In this paper, we introduced an approach based on Model-Driven Architecture (MDA) to automatically generate native source code for mobile applications, beginning with a Platform Independent Model (PIM). We developed a UML metamodel that encapsulates key mobile application elements, ensuring that PIMs remain consistent and reusable across projects. By utilizing Acceleo, a model-to-text transformation tool, we were able to generate Android user interface code directly from the PIM. Through a case study, we demonstrated how this approach can streamline mobile development, reducing both the cost and time required compared to traditional platform-specific coding.

Our case study focused on an Android interface for adding a new book to a library database, where a PIM adhering to the metamodel was used as input for an Acceleo template to generate corresponding Android source code. By bypassing the typical intermediate transformation to a Platform-Specific Model (PSM), our approach simplifies the development process, reducing both effort and potential for error.

Broader Impact on Mobile Development Practices. This approach has the potential to significantly impact mobile development practices, especially in environments that require multi-platform support and rapid development cycles. By abstracting the application design process from platform-specific details, developers can focus more on the core functionality and user experience, rather than on managing multiple codebases. This abstraction can streamline the onboarding process for developers and enhance collaboration within teams, as the PIM provides a unified framework that aligns with widely understood UML standards.

Moreover, as mobile applications continue to evolve to incorporate more complex features—such as advanced sensors, machine learning integrations, and real-time data processing—automating code generation can help developers manage the increasing complexity. The MDA approach allows for rapid prototyping and iteration, as modifications to the PIM can be propagated through to the generated code, ensuring alignment between high-level design and implementation. This capability could lead to faster time-to-market for mobile applications, as well as improved code quality through standardized model-driven practices.

Planned Extensions to the Metamodel and Code Generation Capabilities. To further enhance the versatility and effectiveness of our MDA approach, we plan to extend the current metamodel to include additional features:

- Device-Specific API Access: To maximize cross-platform functionality, we aim to provide built-in support for accessing device-specific APIs, including camera functionality, storage access, and network communication. By defining these features within the metamodel, the PIM can be transformed to include calls to platform-native APIs, such as Android's Camera or iOS's CoreLocation. This will facilitate seamless cross-platform code generation, enhancing the usability of generated applications across different devices.
- Business Logic and Data Management: Currently, the focus is on generating user interface components. Future iterations will include business logic elements and data management structures within the metamodel. For instance, we will enable the generation of basic CRUD operations and database interactions, which will support applications with more complex data needs. Our goal is to eventually provide end-to-end code generation, covering not only UI but also the underlying logic and data layers, supporting platforms such as iOS and Windows.
- Multi-Platform Support: In addition to Android, we plan to extend support to other platforms like iOS and Windows. By generalizing the transformation rules and utilizing platform-specific templates, the PIM can be translated into PSMs that are compatible with multiple operating systems. This extension will allow developers to leverage a single metamodel to generate fully functional applications across a variety of platforms with minimal manual adjustments.

These planned enhancements aim to expand the scope and applicability of the MDA approach, enabling developers to create richer, more sophisticated mobile applications with reduced manual effort. By continuing to refine and extend the metamodel, our approach will support a broader range of mobile development needs, making model-driven development a practical and efficient choice for modern application creation.

5 REFERENCES

[1] Castelain, Q. (2015). Elaboration d'un outil d'analyse d'alignement IT-Business adapté aux spécificités des PMEs. (in France)

[2] Štimac, H., Vajda, T. & Franjkovic, J. (2019). Lifecycle of Smartphones: Brand Representation and Their Marketing Strategy.

[3] Market Share: Smartphones, Worldwide, 4Q07 and 2007. https://www.gartner.com/en/documents/619509 Accessed: July 19, 2024.

[4] Smartphone sales worldwide 2007-2023 | Statista. https://www.statista.com/statistics/263437/global-smartphone-sales-to-end-users-since-2007/ Accessed: July 19, 2024.

[5] Hui, N. M., Chieng, L. B., Ting, W. Y., Mohamed, H. H. & Hj Mohd Arshad, M. R. (2013). Cross-platform mobile applications for android and iOS. *The 6th Joint IFIP Wireless and Mobile Networking Conference (WMNC2013)*, 1-4. https://doi.org/10.1109/WMNC.2013.6548969

[6] Dickson, P. E. (2012). Cabana: a cross-platform mobile development system. *Proceedings of the 43rd ACM technical symposium on Computer Science Education, in SIGCSE'12*. New York, NY, USA: Association for Computing Machinery, 529-534. https://doi.org/10.1145/2157136.2157290

[7] Truyen, F. (2006). *The fast guide to model driven architecture the basics of model driven architecture*. Cephas Consulting Corp.

[8] Prabowo, Y. D., Kristijantoro, A. I., Warnars, H. & Budiharto, W. (2021). Systematic literature review on abstractive text summarization using Kitchenham method. *ICIC Express Letters, Part B: Applications, 12*(11), 1075-1080.

[9] Luque, S., Maréchal, D. & de Thomas Sanz, C. (2014). Modélisation des compartiments phyto-écologiques des milieux ouverts d'altitude par la théorie des graphes et les modèles de distribution d'espèces. (in France)

[10] Sabraoui, A., El Koutbi, M. & Khriss, I. (2012). GUI code generation for android applications using a MDA approach. *IEEE International Conference on Complex Systems (ICCS2012)*, 1-6. https://doi.org/10.1109/ICoCS.2012.6458567

[11] Lachgar, M. & Abdali, A. (2014). Generating Android graphical user interfaces using an MDA approach. *Third IEEE International Colloquium in Information Science and Technology (CIST2014)*, 80-85. https://doi.org/10.1109/CIST.2014.7016598

[12] Tufail, H., Azam, F., Anwar, M. W. & Qasim, I. (2018). Model-driven development of mobile applications: A systematic literature review. *The 9th IEEE Annual Information Technology, Electronics and Mobile Communication Conference (IEMCON2018)*, 1165-1171. https://doi.org/10.1109/IEMCON.2018.8614821

[13] Benouda, H., Azizi, M., Esbai, R. & Moussaoui, M. (2016). MDA approach to automate code generation for mobile applications. *Mobile and Wireless Technologies 2016*, Springer, 241-250. https://doi.org/10.1007/978-981-10-1409-3_27

[14] Benouda, H., Azizi, M., Moussaoui, M. & Esbai, R. (2017). Automatic code generation within MDA approach for cross-platform mobiles apps. *First IEEE International Conference on Embedded & Distributed Systems (EDiS2017)*, 1-5. https://doi.org/10.1109/EDIS.2017.8284045

[15] Parada. A. G. & De Brisolara, L. B. (2012). A model driven approach for android applications development. *IEEE Brazilian Symposium on Computing System Engineering 2012*, 192-197. https://doi.org/10.1109/SBESC.2012.44

[16] Vaupel, S., Taentzer, G., Gerlach, R. & Guckert, M. (2018). Model-driven development of mobile applications for Android and iOS supporting role-based app variability. *Software & Systems Modeling, 17*, 35-63. https://doi.org/10.1007/s10270-016-0559-4

[17] Korchi, A., Khachouch, M. K. & Lakhrissi, Y. (2024). A Model-Driven Architecture Solution for Multi-Platform Mobile App Development. *Journal of System and Management Sciences, 14*(5), 1-13. https://doi.org/10.33168/JSMS.2024.0501

[18] Bali, S. et al. (2023). A framework to assess the smartphone buying behaviour using DEMATEL method in the Indian context. *Ain Shams Engineering Journal*. https://doi.org/10.1016/j.asej.2023.102129

[19] Lachgar, M. & Abdali, A. (2014). Modélisation et Génération des Interfaces Graphiques Android et JSF 2.2 selon une approche MDA. (in France)

[20] Korchi, A., Khachouch, M. K., Lakhrissi, Y., Marzouki, N. E., Moumen, A. & Mohajir, M. E. (2024). Classification of existing mobile cross-platform approaches and proposal of decision support criteria. *International Journal of Information and Communication Technology, 24*(1), 86-111. https://doi.org/10.1504/IJICT.2024.135305

[21] El-Kassas, Wafaa S. et al. (2017). Taxonomy of Cross-Platform Mobile Applications Development Approaches. *Ain Shams Engineering Journal, 8*(2), 163-190. https://doi.org/10.1016/j.asej.2015.08.004

[22] Korchi, A., Khachouch, M. K., Lakhrissi, Y. & Moumen, A. (2020). Classification of existing mobile cross-platform approaches. *International Conference on Electrical, Communication, and Computer Engineering (ICECCE2020)*, Istanbul, Turkey, 2020, 1-5. https://doi.org/10.1109/ICECCE49384.2020.9179222

[23] Khachouch, M. K., Korchi, A., Lakhrissi, Y. & Moumen, A. (2020). Framework Choice Criteria for Mobile Application Development. *International Conference on Electrical, Communication, and Computer Engineering (ICECCE2020)*, 1-5. https://doi.org/10.1109/ICECCE49384.2020.9179434

[24] Lachgar, M. & Abdali, A. (2015). DSL and code generator for accelerating iOs apps development. *Third IEEE World Conference on Complex Systems (WCCS2015)*, 1-8. https://doi.org/10.1109/ICoCS.2015.7483269

Authors' contacts:

Ayoub Korchi
(Corresponding author)
SIGER Laboratory, Faculty of Science and Technology,
Sidi Mohamed Ben Abdellah University,
Fez, 36000, Morocco
ayoub.korchi@usmba.ac.ma

Mohamed Karim Khachouch
SIGER Laboratory, Faculty of Science and Technology,
Sidi Mohamed Ben Abdellah University,
Fez, 36000, Morocco
mohamedkarim.khachouch@usmba.ac.ma

Younes Lakhrisi
SIGER Laboratory, Faculty of Science and Technology,
Sidi Mohamed Ben Abdellah University,
Fez, 36000, Morocco
younes.lakhrissi@usmba.ac.ma

ISSN 1846-6168 (Print), ISSN 1848-5588 (Online)
https://doi.org/10.31803/tg-20.....

Categorization of paper
Received: y-m-d, Accepted: y1-m1-d1

14pt
14pt

Article Title Only in English (Style: Arial Narrow, Bold, 14pt)

14pt

Ivan Horvat, Thomas Johnson, Marko Marić (Style: Arial Narrow, Normal, 10pt)

14pt

Abstract: Article abstract contains maximum of 150 words and is written in the language of the article. The abstract should reflect the content of the article as precisely as possible. TECHNICAL JOURNAL is a trade journal that publishes scientific and professional papers from the domain(s) of mechanical engineering, electrical engineering, civil engineering, multimedia, logistics, etc., and their boundary areas. This document must be used as the template for writing articles so that all the articles have the same layout. (Style: Arial Narraw, 8pt)

8pt

Keywords: keywords in alphabetical order (5-6 key words). Keywords are generally taken from the article title and/or from the abstract. (Style: Arial Narraw, 8pt)

10pt
10pt

1 INTRODUCTION (Article Design)

(Style: Arial Narrow, Bold, 10pt)

10pt

(Tab 6 mm) The article is written in Latin script and Greek symbols can be used for labelling. The length of the article is limited to eight pages of international paper size of Letter (in accordance with the template with all the tables and figures included). When formatting the text the syllabification option is not to be used.

10pt

1.1 Subtitle 1 (Writing Instructions)

(Style: Arial Narrow, 10pt, Bold, Align Left)

10pt

The document format is Letter with margins in accordance with the template. A two column layout is used with the column spacing of 10 mm. The running text is written in Times New Roman with single line spacing, font size 10 pt, alignment justified.

Article title must clearly reflect the issues covered by the article (it should not contain more than 15 words).

Body of the text is divided into chapters and the chapters are divided into subchapters, if needed. Chapters are numbered with Arabic numerals (followed by a period). Subchapters, as a part of a chapter, are marked with two Arabic numerals i.e. 1.1, 1.2, 1.3, etc. Subchapters can be divided into even smaller units that are marked with three Arabic numerals i.e. 1.1.1, 1.1.2, etc. Further divisions are not to be made.

Titles of chapters are written in capital letters (uppercase) and are aligned in the centre. The titles of subchapters (and smaller units) are written in small letters (lowercase) and are aligned left. If the text in the title of the subchapter is longer than one line, no hanging indents.

10pt

Typographical symbols (bullets), which are being used for marking an item in a list or for enumeration, are placed at a beginning of a line. There is a spacing of 10pt following the last item:

- Item 1
- Item 2
- Item 3

10pt

The same rule is valid when items are numbered in a list:

1) Item 1
2) Item 2
3) Item 3

10pt

1.2 Formatting of Pictures, Tables and Equations

(Style: Arial Narrow, 10pt, Bold, Align Left)

10pt

Figures (drawings, diagrams, photographs) that are part of the content are embedded into the article and aligned in the centre. In order for the figure to always be in the same position in relation to the text, the following settings should be defined when importing it: text wrapping / in line with text.

Pictures must be formatted for graphic reproduction with minimal resolution of 300 dpi. Pictures downloaded from the internet in ratio 1:1 are not suitable for print reproduction because of unsatisfying quality.

10pt

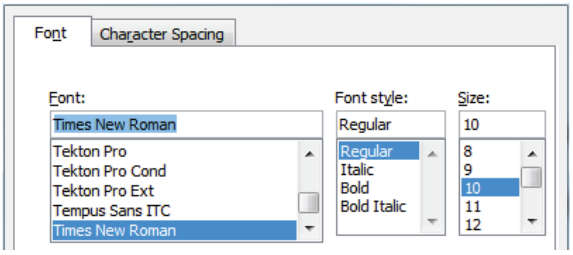

Figure 1 Text under the figure [1]
(Style: Arial Narraw, 8pt, Align Centre)

10pt

The journal is printed in black ink and the figures have to be prepared accordingly so that bright tones are printed in a satisfactory manner and are readable. Figures are to be in colour for the purpose of digital format publishing. Figures in the article are numbered with Arabic numerals (followed by a period).

Text and other data in tables are formatted - Times New Roman, 8pt, Normal, Align Center.

When describing figures and tables, physical units and their factors are written in italics with Latin or Greek letters, while the measuring values and numbers are written upright.

10pt

Table 1 Table title aligned centre
(Style: Arial Narraw, 8pt, Align Centre)

	1	2	3	4	5	6
ABC	ab	ab	ab	ab	ab	ab
DEF	cd	cd	cd	cd	cd	cd
GHI	ef	ef	ef	ef	ef	ef

10 pt

Equations in the text are numbered with Arabic numerals inside the round brackets on the right side of the text. Inside the text they are referred to with equation number inside the round brackets i.e. ".... from Eq. (5) follows ...." (Create equations with MathType Equation Editor - some examples are given below).

10pt

$$F_{\text{avg}}(t, t_0) = \frac{1}{t}\int_{t_0}^{t_0+t} F\left[q(\tau), p(\tau)\right] \mathrm{d}\tau, \tag{1}$$

$$\cos\alpha + \cos\beta = 2\cos\frac{\alpha+\beta}{2}\cdot\cos\frac{\alpha-\beta}{2}, \tag{2}$$

$$(\boldsymbol{AB})^{\mathrm{T}} = \boldsymbol{B}^{\mathrm{T}}\boldsymbol{A}^{\mathrm{T}}. \tag{3}$$

10pt

Variables that are used in equations and also in the text or tables of the article are formatted as *italics* in the same font size as the text.

10pt

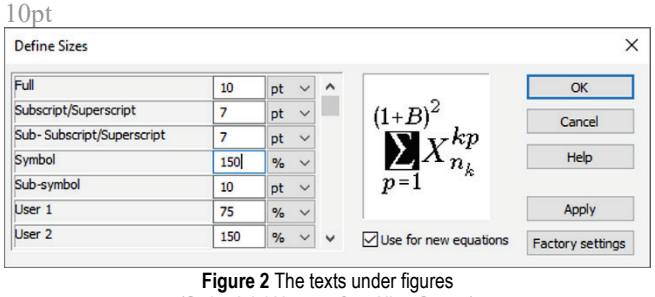

Figure 2 The texts under figures
(Style: Arial Narraw, 8pt, Align Centre)

10pt

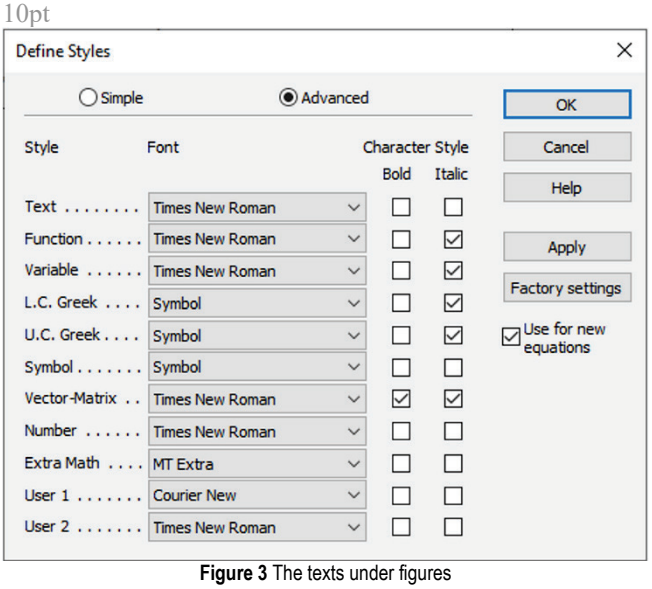

Figure 3 The texts under figures
(Style: Arial Narraw, 8pt, Align Centre)

Figures and tables that are a part of the article have to be mentioned inside the text and thus connected to the content i.e. " … as shown in Fig. 1…" or "data from Tab. 1…" and similar.

10pt

2 PRELIMINARY ANNOTATION

10pt

Article that is offered for publication cannot be published beforehand, be it in the same or similar form, and it cannot be offered at the same time to a different journal. Author or authors are solely responsible for the content of the article and the authenticity of information and statements written in the article.

Articles that are accepted for publishing are classified into four categories: original scientific papers, preliminary communications, subject reviews and professional papers.

Original scientific papers are articles that according to the reviewer and the editorial board contain original theoretical or practical results of research. These articles need to be written in such a way that based on the information given, the experiment can be repeated and the results described can be achieved together with the author's observations, theoretical statements or measurements.

Preliminary communication contains one or more pieces of new scientific information, but without details that allow recollection as in original scientific papers. Preliminary communication can give results of an experimental research, results of a shorter research or research in progress that is deemed useful for publishing.

Subject review contains a complete depiction of conditions and tendencies of a specific domain of theory, technology or application. Articles in this category have an overview character with a critical review and evaluation. Cited literature must be complete enough to allow a good insight and comprehension of the depicted domain.

Professional paper can contain a description of an original solution to a device, assembly or instrument, depiction of important practical solutions, and similar. The article need not be related to the original research, but it should contains a contribution to an application of known scientific results and their adaptation to practical needs, so it presents a contribution to spreading knowledge, etc.

Outside the mentioned categorization, the Editorial board of the journal will publish articles of interesting content in a special column. These articles provide descriptions of practical implementation and solutions from the area of production, experiences from device application, and similar.

10pt

3 WRITING AN ARTICLE

10pt

Article is written in the English language and the terminology and the measurement system should be adjusted to legal regulations, standards and the International System of Units (SI) (Quantities and Units: ISO 80 000 - from Part 1 to Part 14). The article should be written in third person.

Introduction contains the depiction of the problem and an account of important results that come from the articles that are listed in the cited literature.

Main section of the article can be divided into several parts or chapters. Mathematical statements that obstruct the reading of the article should be avoided. Mathematical statements that cannot be avoided can be written as one or

more addendums, when needed. It is recommended to use an example when an experiment procedure, the use of the work in a concrete situation or an algorithm of the suggested method must be illustrated. In general, an analysis should be experimentally confirmed.

Conclusion is a part of the article where the results are being given and efficiency of the procedure used is emphasized. Possible procedure and domain constraints where the obtained results can be applied should be emphasized.

AI and AI-assisted tools do not qualify for authorship under TG/TJ's authorship policy. Authors who use AI or AI-assisted tools during the manuscript writing process are asked to disclose their use in a separate section of the manuscript. The publishing agreement process works as usual, with the authors keeping the copyright to their own work.

10pt

4 RECAPITULATION ANNOTATION

10pt

In order for the articles to be formatted in the same manner as in this template, this document is recommended for use when writing the article. Finished articles written in MS Word for Windows and formatted according to this template must be submitted using our The Paper Submission Tool (PST) (https://tehnickiglasnik.unin.hr/authors.php) or eventually sent to the Editorial board of the Technical Journal to the following e-mail address: tehnickiglasnik@unin.hr

The editorial board reserves the right to minor redaction corrections of the article within the framework of prepress procedures. Articles that in any way do not follow these authors' instructions will be returned to the author by the editorial board. Should any questions arise, the editorial board contacts only the first author and accepts only the reflections given by the first author.

10pt

5 REFERENCES (According to APA)

10pt

The literature is cited in the order it is used in the article. No more than 35 references are recommended. Individual references from the listed literature inside the text are addressed with the corresponding number inside square brackets i.e. "… in [7] is shown …". If the literature references are web links, the hyperlink is to be removed as shown with the reference number 8. Also, the hyperlinks from the e-mail addresses of the authors are to be removed. In the literature list, each unit is marked with a number and listed according to the following examples (omit the subtitles over the references – they are here only to show possible types of references):

9pt

[1] See http://www.bibme.org/citation-guide/apa/

[2] See http://sites.umuc.edu/library/libhow/apa_examples.cfm

[3] (Style: Times New Roman, 9pt, according to APA)

[4] Amidzic, O., Riehle, H. J. & Elbert, T. (2006). Toward a psychophysiology of expertise: Focal magnetic gamma bursts as a signature of memory chunks and the aptitude of chess players. *Journal of Psychophysiology, 20*(4), 253-258. https://doi.org/10.1027/0269-8803.20.4.253

[5] Reitzes, D. C. & Mutran, E. J. (2004). The transition to retirement: Stages and factors that influence retirement adjustment. *International Journal of Aging and Human Development, 59*(1), 63-84. Retrieved from http://www.baywood.com/journals/PreviewJournals.asp?Id=0091-4150

[6] Jans, N. (1993). *The last light breaking: Life among Alaska's Inupiat Eskimos*. Anchorage, AK: Alaska Northwest Books.

[7] Miller, J. & Smith, T. (Eds.). (1996). *Cape Cod stories: Tales from Cape Cod, Nantucket, and Martha's Vineyard*. San Francisco, CA: Chronicle Books.

[8] Chaffe-Stengel, P. & Stengel, D. (2012). *Working with sample data: Exploration and inference.* https://doi.org/10.4128/9781606492147

[9] Freitas, N. (2015, January 6). People around the world are voluntarily submitting to China's Great Firewall. Why? Retrieved from http://www.slate.com/blogs/future_tense/2015/01/06/tencent_s_wechat_worldwide_internet_users_are_voluntarily_submitting_to.html (Style: Times New Roman, 9pt, according to APA)

10pt

10pt

Authors' contacts:

8pt

Full Name, title
Institution, company
Address
Tel./Fax, e-mail

8pt

Full Name, title
Institution, company
Address
Tel./Fax, e-mail

Note: Gray text should be removed in the final version of the article because it is for guidance only.

TEHNIČKI GLASNIK / TECHNICAL JOURNAL – GODIŠTE / VOLUME 18 – SPECIJALNI BROJ / SPECIAL ISSUE SI1

PROSINAC 2024 / DECEMBER 2024 – STRANICA / PAGES 1-120

Sveučilište Sjever

SVEUČILIŠTE SJEVER / UNIVERSITY NORTH – CROATIA – EUROPE

ISSN 1846-6168 (PRINT) / ISSN 1848-5588 (ONLINE)

TEHNICKIGLASNIK@UNIN.HR – HTTP://TEHNICKIGLASNIK.UNIN.HR